Control of embryonic stem cell fate: the role of phosphoinositide 3-kinase signalling and Zscan4

Kumpfmueller, Benjamin

Award date:
2011

Awarding institution:
University of Bath

Control of embryonic stem cell fate: the role of phosphoinositide 3-kinase signalling and Zscan4

Submitted by

Benjamin Kumpfmueller

For the degree of Doctor of Philosophy (PhD)

University of Bath Department of Pharmacy and Pharmacology

October, 2011

Acknowledgements

I want to truly thank Prof. Melanie Welham for her guidance and excellent supervision throughout my PhD journey. Without her support and encouragement this work would not have been possible.

I also want to thank Prof. Julian Chaudhuri for being a great co-supervisor, his input was greatly appreciated.

This journey was accompanied by many past and present laboratory members of her group, which made boredom a rare event. I have to thank our senior post-docs Heather Bone and Mike Storm for creating a creative and enjoyable work atmosphere. My special thanks goes to future doctor Yolanda Sanchez Ripoll, who brought the Spanish sunshine and temperament to our lab. Furthermore, I am very grateful for the help of Michael Buchholz from the Biology and Biochemistry department, assisting me with the protein purification work.

I am also indebted to Dr. Hitoshi Niwa for accepting me for half a year in his laboratory at the CDB RIKEN in Japan. This special time was an inspiration and beautiful memories remain. Thanks to everybody who made this exciting time possible, especially to Masaki and Kenjiro whose company also outside the lab was always a pleasure.

Of course, a huge thanks goes to my parents, who always supported and nurtured my interests.

Abstract

Embryonic stem (ES) cells have the remarkable ability to differentiate into all cells comprising the three germ layers of the developing embryo. It is this pluripotency that makes them attractive for use in regenerative medicine. However, in order to harness this potential, we must understand the molecular mechanisms regulating the ability of ES cells to self-renew and thereby generate identical pluripotent daughter ES cells. The Welham laboratory has previously described a requirement for PI3K signalling in maintaining self-renewal of murine ES (mES) (Paling et al., 2004; Storm et al., 2007). To identify the molecular mechanisms involved in regulating mES cell self-renewal downstream of PI3K signalling, an Affymetrix microarray screen was carried out prior to the start of this PhD. For the screen, mES cells were grown in the presence of LIF and treated with the reversible PI3K inhibitor LY294002 (LY) or a DMSO control for 24, 48 and 72 hours. A total of 646 statistically significant transcriptional changes were detected and subsequently divided into 12 clusters using k-means clustering.

Experiments using pharmacological inhibitors suggest that genes within the same cluster are regulated by common mechanisms. To identify potential candidates involved in regulation of mES cell pluripotency, further analyses concentrated on transcription factors and genes with unknown functions. In our microarray data Zscan4c, a member of a SCAN-domain containing Zinc finger protein family, is one of the earliest down-regulated probe-sets. Loss-of-function experiments using siRNA approaches highlight a role for Zscan4 downstream of PI3Ks in regulation of ES cell self-renewal. Immunohistochemical staining of cells overexpressing Zscan4c showed nuclear accumulation of the protein. This, together with the fact that Zscan4c was mainly detectable in the nuclear protein fraction, strengthens a role of Zscan4c in transcriptional regulation. Potential Zscan4c protein interaction partners were identified by applying a combined immunoprecipitation (IP) - mass spectrometry strategy. Interestingly, the majority of potential Zscan4c interacting proteins identified are associated with functions related to transcriptional regulation and DNA damage response, all characteristics linked with Zscan4. Furthermore, the Class I_A PI3K catalytic isoforms were genetically activated in mES cells, and liberation of the requirement for LIF was found upon over-expression of an activated p110α catalytic subunit.

Table of Contents

Table of Figures

Table of Tables

Abbreviations

APS	Ammonium Persulphate
ADP	Adenosine Diphosphate
APC	Adenomatous polyposis coil
ATP	Adenosine Triphosphate
BIO	6-bromoindirubin 3’-oxime
BMP	Bone morphogenic protein
BSA	Bovine Serum Albumin
cDNA	Complementary DNA
CKI	Casein kinase I
ChiP	Chromatin immunoprecipitation
CHIR	CHIRON99021
DAPI	4',6-diamidino-2-phenylindole
DMEM	Dulbecco’s Modified Eagle Medium
DMSO	Dimethylsulphoxide
DNA	Deoxyribonucleic Acid
DNA-PK	DNA-dependent protein kinase
Dox	Doxycycline
E	Stage of embryonic development, indicating days post coitum
EC	Embryonal Carcinoma
ECL	Enhanced Chemiluminescence
EDTA	Ethylenediaminetetraacetic acid disodium salt
EGF	Epidermal Growth Factor
EpiSC	Epiblast Stem Cell
ERK	Extracellular regulated kinase
ESC	Embryonic Stem Cell
FACS	Fluorescence Activated Cell Sorter
FBS	Foetal bovine serum
Fgf	Fibroblast Growth Factor

Gapdh	Glyceraldehyde-3-phosphate dehydrogenase
GFP	Green Fluorescence Protein
GMEM	Glasgow Minimal Essential Medium
GOI	Gene of Interest
Grb2	Growth Factor Receptor bound protein 2
GSK-3	Glycogen synthase kinase 3
GTP	Guanosine Triphosphate
hESC	Human Embryonic Stem Cell
HRP	Horse Radish Peroxidase
ICM	Inner Cell Mass
Id	Inhibitor of differentiation
IGF	Insulin-like growth factor
IL	Interleukin
iPSC	Induced pluripotent stem cells
IRES	Internal Ribosomal Entry Site
JAK	Janus Kinase
kDa	Kilo Daltons
Klf	Kruppel-like family
Klf4	Krupple-like factor 4
KO SR	Knockout Serum Replacement
LIF	Leukemia inhibitory factor
LIFR	LIF Receptor
MAPK	Mitogen activated protein kinase
MEK	Mitogen-activated extracellular signal-regulated kinase
mRNA	Messenger RNA
MTG	Monothioglycerol
mTOR	Mammalian target of rapamycin
mESC	Murine Embryonic Stem Cell
MCS	Multiple Cloning Site

NEAA	Non-essential amino acids
NTC	Non Targeting Control
PBS	Phosphate Buffered Saline
PCR	Polymerase Chain Reaction
PD	PD0325901
PDK1	3-phosphoinositide-dependent protein kinase 1
PH	Pleckstrin Homology
PI3K	Phosphoinositide 3-kinase
PI(3)P	Phosphatidylinositol-3-phosphate
PMSF	Phenylmethylsulphonylfluoride
POU	Pit Oct Unc
PTEN	Phosphatase and tensin homologue
qPCR	Quantitative PCR
RT-PCR	Reverse Transcription PCR
SDS-PAGE	Sodium Dodecyl Sulphate-Poly acrylamide gel electrophoresis
S.E.M.	Standard Error of the Mean
Shp2	Src-homology 2 containing phosphatase 1
shRNA	Short-hairpin Ribonucleic acid
siRNA	Short interfering Ribonucleic acid
Smad	*Caenorhabditis elegans* protein Sma, *Drosophila* mothers against
Stat3	Signal Transducer and Activator of Transcription 3
S6K1	p70 ribosomal S6 kinase (S6K)
TAE	Tris-acetate EDTA
TBS	Tris Buffered Saline
TBST	TBS plus 0.05%
TEMED	Tetramethylethylenediamine
Tet	Tetracycline
tTA	Tetracycline-sensitive transactivator
2i	2 inhibitors, GSK-3 and MEK

3i	3 inhibitors, GSK-3, MEK and FGFR
4-OHT	4-hydroxitamoxifen

Chapter 1: Introduction

1.1 Stem Cells and their characteristics

Stem cells are unspecialised cells which have two features, self-renewal and differentiation potential, making them very unique and fascinating. They have the ability to differentiate into other more specialised cell types and, depending on the type of stem cell, they have different constraints in their abilities to differentiate. Their potency, or ability to differentiate, is dependent on stem cell origin and reflects their different purposes. Embryonic stem (ES) cells are pluripotent, meaning they are able to give rise to all cell types of the adult animal. Adult stem cells are, in contrast, limited in their lineage progression and are usually replenishing cells of damaged or aged tissue. The other defining characteristic of stem cells is their self-renewal capacity. Self-renewal of a stem cell is its division giving rise to two daughter cells, with at least one being identical to its parental cell. It can be also described as proliferation with the suppression of differentiation (Burdon et al., 2002; Smith, 2001).

Due to their properties, ES cells have the potential to be used in several fields including, regenerative medicine for cell-based therapies, drug development and toxicity screening and as an *in vitro* system to study early embryo development (Figure 1.1).

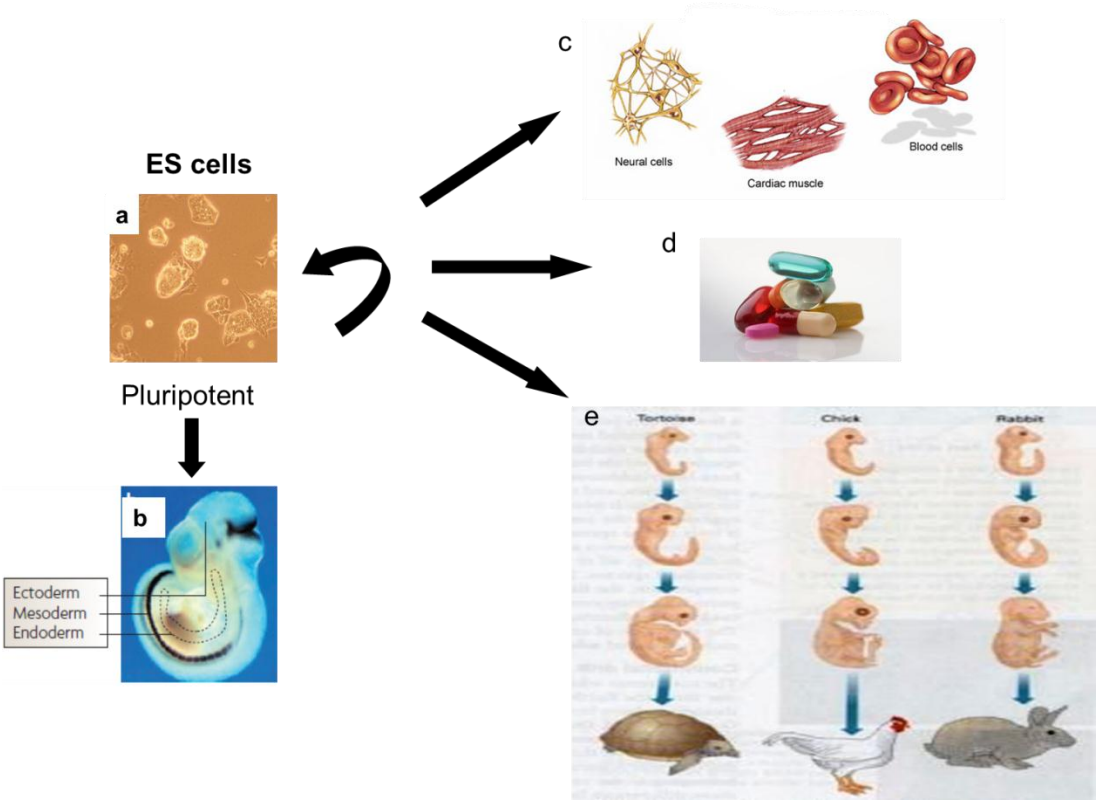

Figure 1.1 Properties and applications of ES cells. ES cells have self-renewal capacity (a), which is their ability to give rise to at least one daughter cell identical to the parental cell. ES cells are also pluripotent (b), they have the ability to give rise to all cell types of the adult animal. Due to these properties, ES cells can be used in regenerative medicine (c), drug development and toxicity screening (d) and as an in vitro model to study early development (e). Image (b) from Tam and Loebel, 2007, (c) from www.stemcellresearchfoundation.org, (d) from http://yxhealth.com/nutrition/ho-to-take-medicines and (e) Modified from Advance Biology by Michael Kent (OUP, 2000).

1.2 History of embryonic stem cells

The first evidence that supported the existence of embryonic stem cells dates back to 1970 when it was observed that grafting of early mouse embryos into adult mice produced teratocarcinomas (Solter et al., 1970; Stevens, 1970). The teratocarcinomas formed contained a proportion of undifferentiated cells, which could be propagated in culture and retained a differentiation potential giving rise to derivatives of all three germ layers (Martin and Evans, 1975). These undifferentiated cells were named embryonal carcinoma cells (EC) cells. The fact that teratocarcinomas, and hence EC cells, could only be derived from grafts containing epiblast suggested that EC cells were derived from the epiblast (see section 1.3) (Diwan and Stevens, 1976). EC cells resemble epiblast cells in their developmental potential and phenotype, are self-renewing and pluripotent, and some EC cells were shown to be able to contribute to the developing embryo (Brinster, 1974). However, EC cells are tumourigenic and cytogenetically abnormal, and most of them did not have a significant differentiation potential. Embryonic stem cells were first derived in 1981 from blastocyst co-culture with mitotically inactivated fibroblast, so called feeders (Evans and Kaufman, 1981; Martin, 1981). ES cells were similar to EC cells in morphology and even in the ability to produce teratocarcinomas when injected into an adult mouse (Figure 1.2). However, they maintained a normal karyotype, opposite to EC cells that are normally aneuploid. Moreover, ES cells injected into a developing blastocyst are able to contribute to various tissues in chimeras including the germ line (Bradley et al., 1984). The first human ES cells were derived in 1998 by Thomson (Thomson et al., 1998).

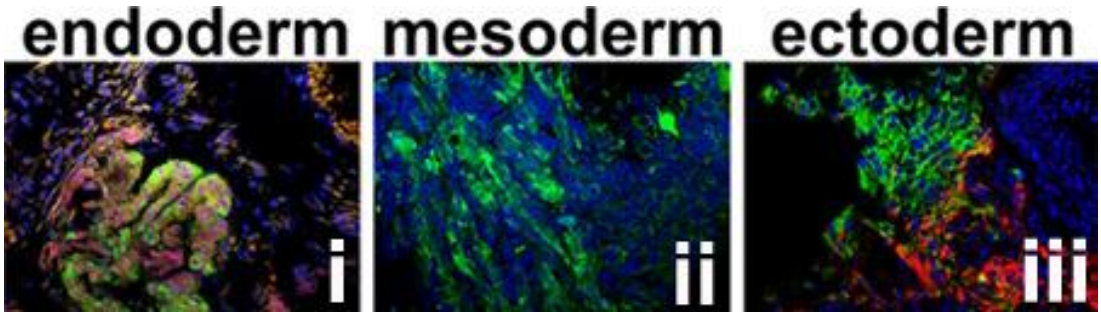

Figure 1.2 Immunohistochemistry stainings of teratomas. (i) endoderm (α-fetoprotein-positive, green; FOXA2-positive, red), (ii) mesoderm (α-actinin-positive cardiac myocytes, green), (iii) ectoderm (TuJ1-positive neuronal cells, green; glial fibrillary acidic protein-positive cells, red). Adapted from (Gonzalez et al., 2009).

1.3 Preimplantation mouse development

After fertilization, mitotic cell divisions in the zygote occur giving rise to 8 cells after two days of embryonic development (Figure 1.3). Remarkably the size of the 8 cells is similar to the initial fertilized egg. The 8-cell stage is followed by compaction and polarization of the cells in the embryo. At this point cells will become either inner or outer cells. The morula, which consists of 16 cells, is then formed. After 3.5 days of fertilization the blastocyst is formed. At the blastocyst state two different populations of cells can be observed, the trophoblast cells, which are the outer cells, and will give rise to extraembyonic tissue, including the placenta, and cells in the inner cell mass (ICM), which will form the embryo proper and yolk sack (Rossant and Tam, 2004). These distinct cell populations are characterized by the expression of different markers; Cdx2 and Eomes (Strumpf et al., 2005) in the case of trophectoderm or Oct4 and Nanog in the ICM (Chambers et al., 2003; Chazaud et al., 2006; Mitsui et al., 2003). ES cells can be isolated from the ICM and they can give rise to all cells of the adult tissue. The blastocysts also have a cavity, the blastocoel (Figure 1.3), which originates from fluids secreted by the trophectoderm.

After 4.5 days of fertilization the blastocyst implants into the uterine lining through the trophectoderm. At this stage the ICM of the blastocyst has transformed into the epiblast and the hypoblast or primitive endoderm (Gardner and Beddington, 1988). The primitive endoderm is formed between the epiblast and the blastocoel. Epiblast cells and primitive endoderm express different markers. Epiblast cells express Nanog and the primitive endoderm cells express Gata4 and Gata6 (Chazaud et al., 2006).

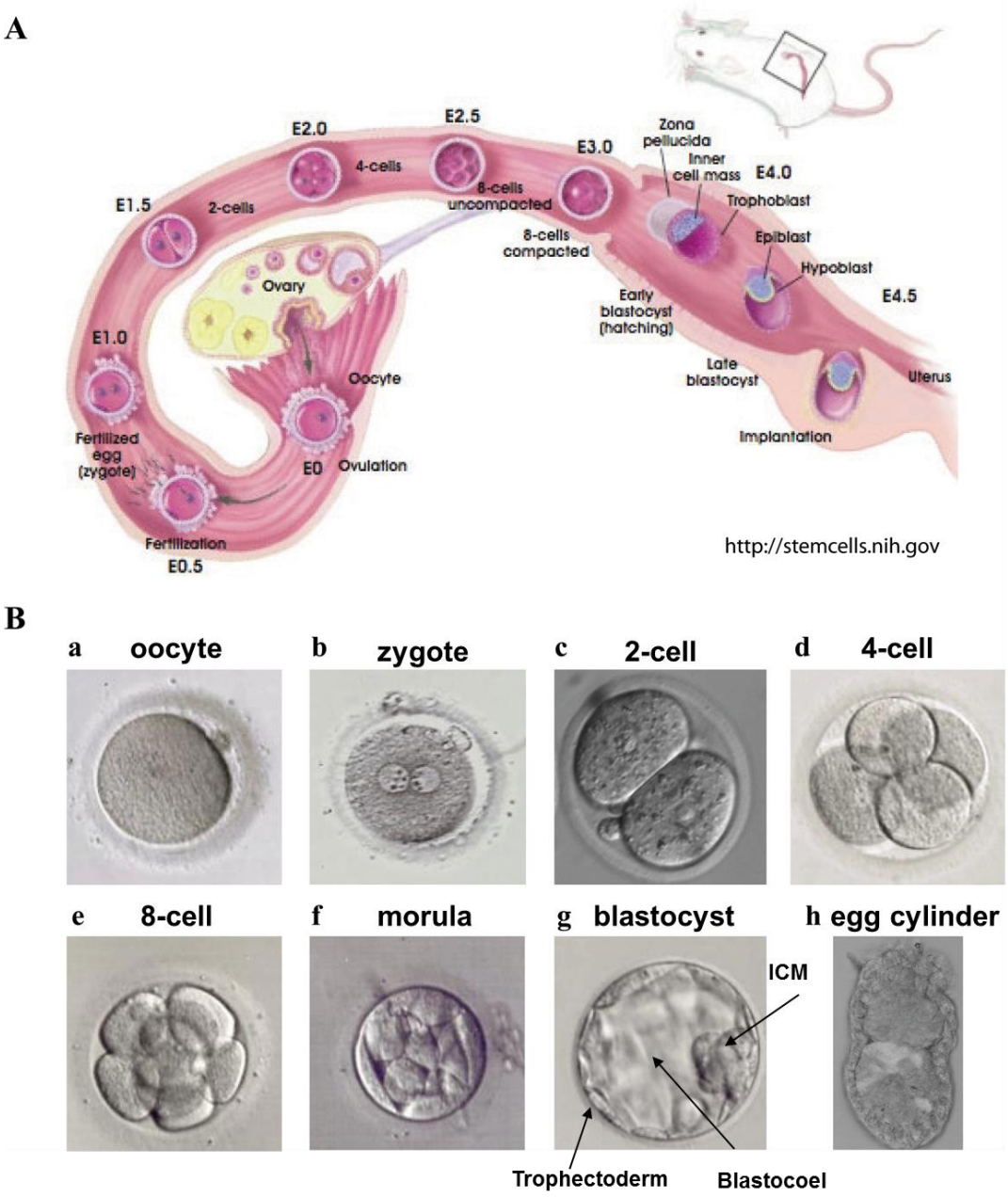

Figure 1.3: Mouse early embryonic development. (A) illustrates spatial and temporal stages of embryonic development. Pre-implantation embryonic development proceeds from fertilisation at the beginning of the fallopian tubes to implantation of the late blastocyst in the uterus (Diagram taken from www.stemcells.nih.gov). (B) Bright field images of different stages of development. (a) oocyte, (b) zygote, (c) 2-cell stage, (d) 4-cell stage, (e) 8-cell stage, (f) morula, (g) blastocyst and (h) egg cilinder. Images in (B) from http://www.ramsem.com/images/clip_image002.jpg.

1.4 Derivation of embryonic stem cells

ES cells are derived from the transient epiblast compartment of the blastocyst, the ICM (Figure 1.4). Different methods can be used to establish ES cell lines from the ICM. For example, the ICM can be isolated by laser dissection or immunosurgery, or mES cell lines can be created via blastocyst outgrowth and subsequent propagation of self-renewing colonies. ES cell derivation is improved by inducing diapause, which is achieved by injecting tamoxifen (Evans and Kaufman, 1981; Kawase et al., 1994). Under natural circumstances, diapause is a state of arrested development occurring in pregnant female mice still lactating their first litter. The implantation of the embryos of the second litter is, therefore, delayed until the preceding litter has been weaned (Brook and Gardner, 1997; Smith, 2001). It has been observed that ES cells can be derived more easily from some strains of mouse than others. The 129 mouse strain has the highest percentage of successful derivation, followed by C57BL/6, CBA and NOD. Derivation of ES cells from CBA and NOD mice has traditionally proved to be very difficult. However, more recently successful derivation of germline-competent ES cells from CBA and NOD strains has been achieved by culturing in 2i media plus LIF. The 2i is a basal media with 2 inhibitors, one is a MAPK inhibitor and the other is a GSK-3 inhibitor (Nichols et al., 2009; Ying et al., 2008). It is possible to keep ES cells self-renewing in 2i media without LIF, although addition of LIF enhances cloning efficiency. Derivation of germline-competent ES cells from rats has also been achieved for the first time by using 2i media (Buehr et al., 2008; Li et al., 2008b). These successes were the result of intensive research, deciphering self-renewal mechanisms which will, hopefully lead to the establishment of further species-specific ES cell lines. Furthermore, these findings might contribute to the knowledge required for the optimal culture of hES cells.

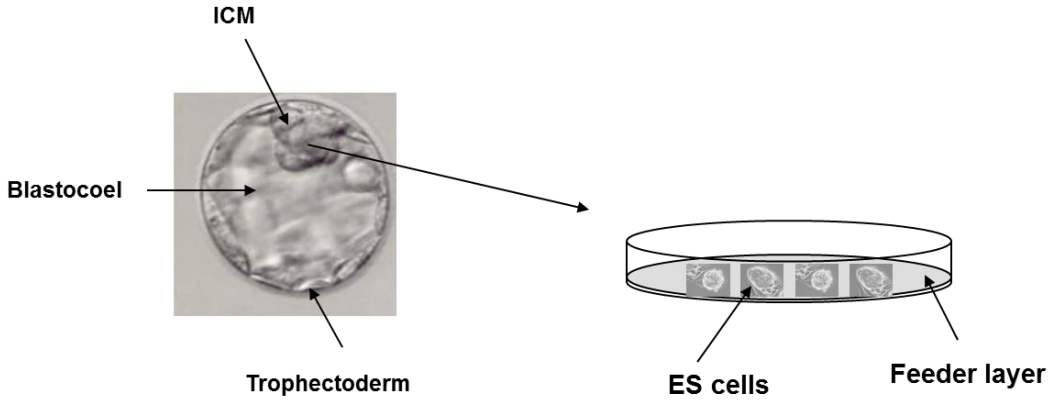

Figure 1.4 ES cells derivation. ES cells can be derived by plating the Inner cell mass (ICM) of the blastocyst onto a feeder layer of mitotically inactivated fibroblasts.

1.5 Murine embryonic stem cell self-renewal

Self-renewal of a stem cell (described in section 1.1) is a very complex process regulated by a variety of extrinsic and intrinsic factors, some of which will be described in this section.

1.5.1 Self-renewal markers of murine ES cells

A wide range of different markers have been identified by stem cell researchers aiding in defining the undifferentiated state of ES cells. To assess a panel of these markers can help to determine the undifferentiated ES cell state. Markers facilitate the characterisation of different ES cell subpopulations but to assess their ability to differentiate into different lineages requires more stringent tests like teratoma or chimera formation.

Alkaline phosphatase (ALP) is a hydrolase enzyme removing phosphate groups from a wide range of molecules, including alkaloids and proteins. The name reflects its optimal working conditions in an alkaline environment. ALP is expressed at a low level in all tissue types, but is elevated in some disease-related states such as liver

damage or bone growth alterations (Fernandez and Kidney, 2007). The inner cell mass of the blastocyst was also reported to have a high activity of ALP (Johnson et al., 1977). Undifferentiated, self-renewing mES cells also exhibit alkaline phosphatase activity, which is lost upon differentiation. Therefore, staining for alkaline phosphatase activity can be used to detect self-renewing ES cell colonies in the so called Alkaline phosphatase assay (Pease et al., 1990).

Rex1, also known as Zfp42, encodes for an acidic zinc finger protein expressed in undifferentiated ESCs and identified to be downregulated following retinoic acid induced differentiation (Hosler et al., 1989). Rex1 is restrictedly expressed in the ICM and is regulated, beside other factors, via Oct4 (Ben-Shushan et al., 1998; Toyooka et al., 2008). In later pluripotent cell populations, for instance the epiblast and primitive ectoderm (PrE), Rex1 levels are reduced (Toyooka et al., 2008). ES cells cultured in vitro in the presence of LIF contain different subpopulations, among them Oct4 positive/Rex1 positive cells and Oct4 positive/Rex1 negative cells. The Rex1 positive cell population has a higher differentiation potential and contributes more efficiently to chimera formation (Toyooka et al., 2008). Despite this observation, Rex1 is dispensable for the maintenance of mESCs and is not absolutely required for normal mouse embryo development. However, it is a suitable marker of mESC pluripotency, as its expression is downregulated rapidly upon differentiation (Rogers et al., 1991), but as it has no functional significance should be regarded as a marker solely, like alkaline phosphatase activity (Masui et al., 2008).

Three other well-known pluripotency markers are the transcription factors Nanog, Oct3/4 and Sox2. These pluripotency core factors hold key functional properties and are therefore discussed in more detail as part of the intrinsic factors of pluripotency section 1.5.3.

1.5.2 Extrinsic factors

1.5.2.1 Leukaemia inhibitory factor (LIF) Signalling

Maintenance of undifferentiated ES cells traditionally required their co-culture with feeder cells, secreting the soluble factor LIF. LIF belongs to the IL6 family of cytokines and can support mESC growth and self-renewal in presence of serum without feeders (Smith et al., 1988; Williams et al., 1988). Furthermore, when feeder cells contain a non-functional Lif locus, they are unable to sustain ESC self-renewal (Stewart et al., 1992). LIF signalling is mediated either through gp130 homodimers or via heterodimers consisting of gp130 and the LIF receptor (Yoshida et al., 1994). Janus-associated tyrosine kinases (JAKs) are recruited to the intracellular domain of gp130, where they phosphorylate tyrosine residues, creating binding sites for signal transducer and activator of transcription 3 (STAT3) (Boulton et al., 1994; Burdon et al., 1999a). STAT3 binds with its SH2 domains, which allows in consequence the phosphorylation of STAT3 by JAKs. Phosphorylated STAT3 homodimerises and translocates to the nucleus where it modulates transcription of target genes (Figure 1.5).

The molecular mechanisms by which LIF signalling suppresses differentiation have been delineated in great detail (Boeuf et al., 1997; Burdon et al., 1999a; Niwa et al., 1998). STAT3 activation was shown to be required, as inhibition of STAT3 activation by mutant STAT3, unable to dimerise, failed to sustain self-renewal (Niwa et al., 1998). Furthermore, artificial STAT3 activation is sufficient to maintain the undifferentiated state of ES cells (Matsuda et al., 1999). STAT3 homodimers act as transcription factors activating mediators of ES cell self-renewal. The proto-oncogene c-myc was reported to be a direct transcriptional target of STAT3 and overexpression of c-myc has been reported to lead to LIF-independent ES cells (Cartwright et al., 2005). Another downstream target of LIF is Klf4. When Klf4 is overexpressed during embryoid body (EB) differentiation, Oct-4 levels were higher than control levels, consistent with the idea of Klf4 promoting ESC self-renewal (Li et al., 2005). Both, c-myc and Klf4, were part of the original four reprogramming factor cocktail used to create induced pluripotent stem cells (iPS) cells (Takahashi and Yamanaka, 2006). In the light of this finding, a role of these two transcription factors in regulating pluripotency is strengthened, though precise mechanisms remain unclear.

Gene inactivation studies targeting gp130 in mice indicate that the LIF signalling axis is not necessary for normal development of the early embryo prior to gastrulation (Ware et al., 1995; Yoshida et al., 1996). It is unknown how or if the gp130/STAT3 signalling plays an important role *in vivo,* analogous to the maintenance of mES cell self-renewal in the cell culture. A role for LIF signalling was discovered during diapause in embryo development. Embryos lacking gp130 are unable to re-enter normal development after diapause arrest and exhibit an inability to maintain the epiblast (Nichols et al., 2001). Therefore, LIF signalling appears to be essential for extending the epiblast lifespan during diapause and this function might relate to the *in vitro* function of gp130 signalling in ES cell maintenance (Smith, 2001). It could be reasoned that only species exhibiting diapause have the ability to generate ES cells and therefore hES cells are functionally unresponsive to LIF (Daheron et al., 2004; Thomson et al., 1998). However, more recent studies indicate that hES cells might reflect a later developmental stage (Najm et al., 2011; Tesar et al., 2007). Furthermore, hES cells which are brought closer to a more naïve state of pluripotency, exhibit LIF responsiveness (Buecker et al., 2010; Hanna et al., 2010).

Besides the Jak/STAT3 pathway, two other signalling pathways are activated by LIF, the Mitogen Activated Protein Kinase (MAPK) and PI3K pathway. Both pathways play a role in stem cell fate choice, PI3K signalling activation promotes self-renewal through activation of Akt and GSK-3 inhibition, while MAPK activation induces differentiation through activation of Erk (Figure 1.6) (Burdon et al., 1999b; Niwa et al., 2009; Paling et al., 2004).

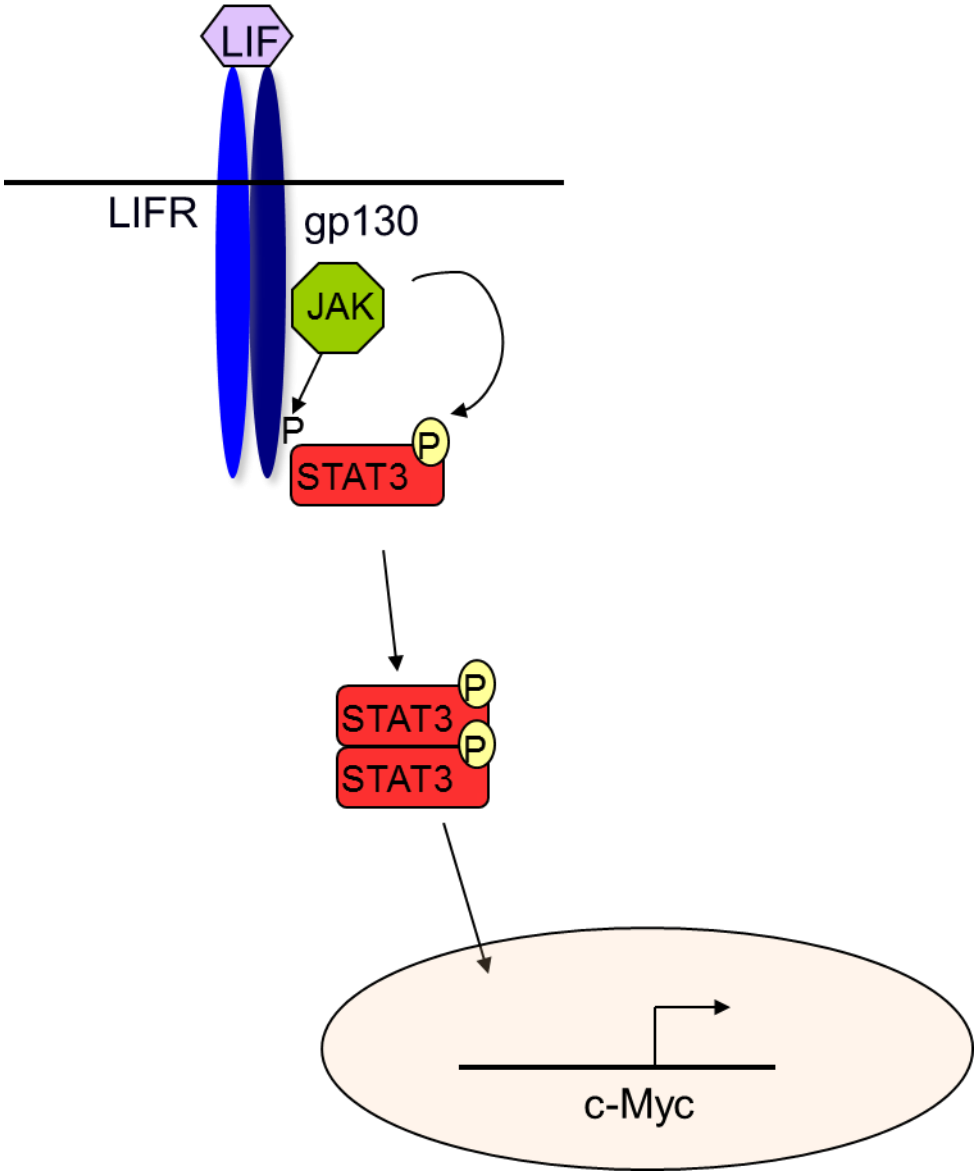

Figure 1.5 LIF/STAT3 signalling. LIF binding to the receptor leads to recruitment of JAK to the gp130 receptor where it phosphorylates tyrosine residues creating docking sites for recruitment of STAT3 through its SH2 domain. STAT3 is then phosphorylated by JAK and phosphorylated STAT3 forms homodimers and translocates to the nucleus where it modulates transcription of target genes, for example c-myc. Modified from Cartwright et al., 2005.

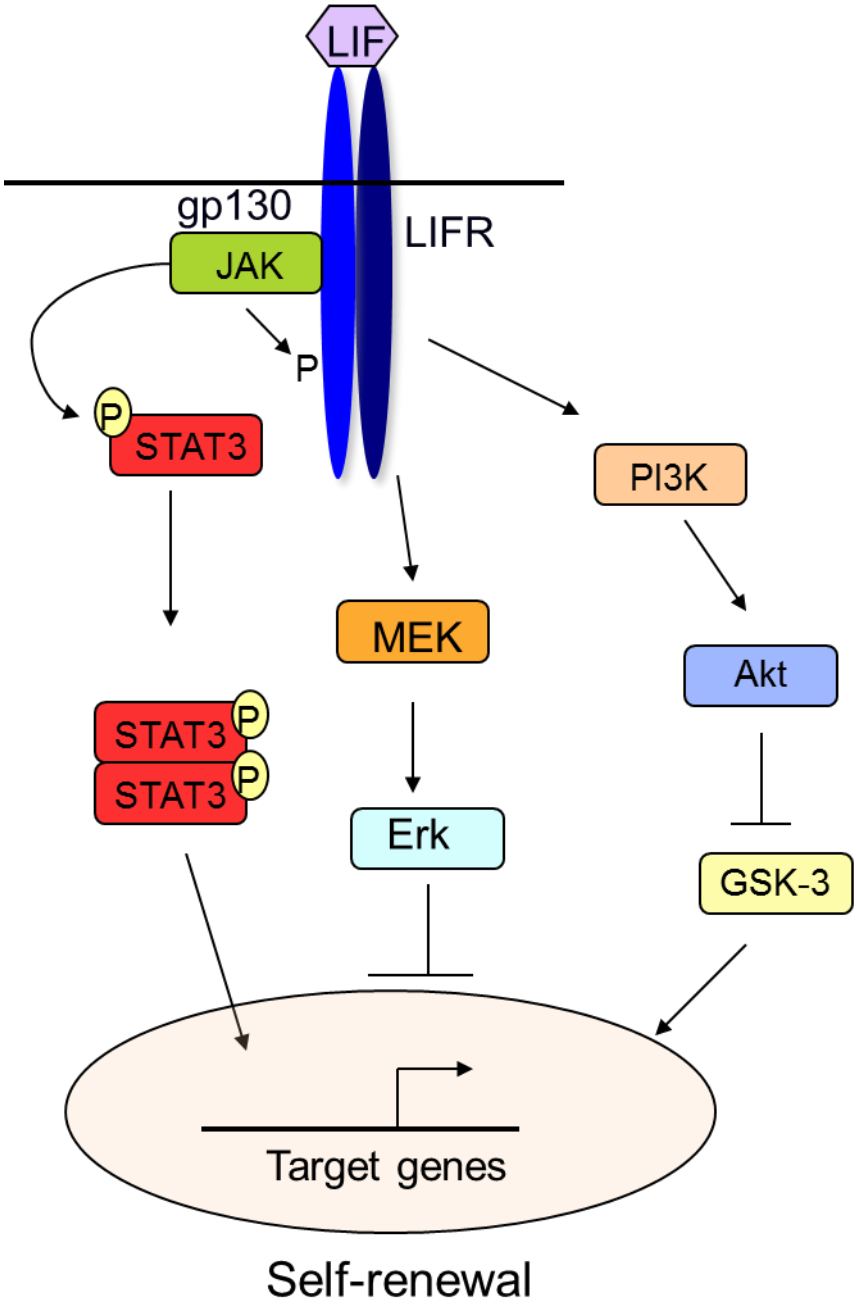

Figure 1.6 Signalling pathways activated by LIF. LIF binding to the receptor leads to activation of JAK/STAT3, PI3K pathways, MAPK. The two first pathways promote self-renewal while MAPK induces differentiation. Adapted from Niwa et al., 2009 (Niwa et al., 2009).

1.5.2.2 Bone morphogenetic protein (BMP) signalling

In feeder free culture systems, ESC maintenance requires the presence of serum in addition to LIF. LIF alone without serum is not sufficient to maintain ESC self-renewal, and subsequently results in neuronal differentiation. Therefore, other serum containing factors are involved in regulating mES cell pluripotency. Bone morphogenetic proteins (BMPs), known to inhibit neuronal differentiation, were identified as factors able to support self-renewal under serum free conditions in the presence of LIF (Ying et al., 2003).

BMPs bind to transmembrane serine/threonine kinase receptors. Cellular responses to BMPs are mediated by the formation of heteromeric complexes of type I and type II receptors (Shi and Massague, 2003) and in undifferentiated ESCs the two different types of BMP receptors, BmprIa (type I) and BmprII (type II) are both expressed (Qi et al., 2004). Ligand binding mediates signalling through SMADs to induce expression of Id (Inhibitor of differentiation) proteins, which are known to inhibit basic helix-loop-helix transcription factors needed for differentiation (Ruzinova and Benezra, 2003) (Figure 1.7). Constitutive expression of Id1, 2, or 3 is enough to free ES cells from BMP or serum dependence and allows self-renewal in LIF alone (Ying et al., 2003). ES cells not expressing Bmpr1a or Smad4 cannot be established from the blastocyst, contributing to the evidence that this pathway is important for self-renewal (Qi et al., 2004). Serum used in the standard *in vitro* culture environment induces Id genes via multiple pathways, among them is Integrin, which is bound by extracellular matrix molecules for instance fibronectin (Benezra, 2001; Norton, 2000).

The SMAD proteins take their name from the drosophila homolog protein, mothers against decapentaplegic (MAD) and the *Caenorhabditis Elegans* protein SMA (Attisano and Wrana, 2002). Forced expression of SMAD3/4 or constitutively activated BMP receptors cause differentiation into lineages other than neuronal, highlighting that a careful regulation of this pathway is necessary (Ying et al., 2003). In ES cells BMP signalling is multifaceted as upon LIF withdrawal BMP signalling switches to promote differentiation to non-neural lineages (Ying et al., 2003).

The LIF and BMP pathway act together to support mES cells self-renewal. While the BMP pathway seems to primary block TFs important for differentiation into

neuronal lineages, LIF acts through STAT3 to restrain mesoderm and endoderm differentiation (Ying et al., 2003) (Figure 1.8).

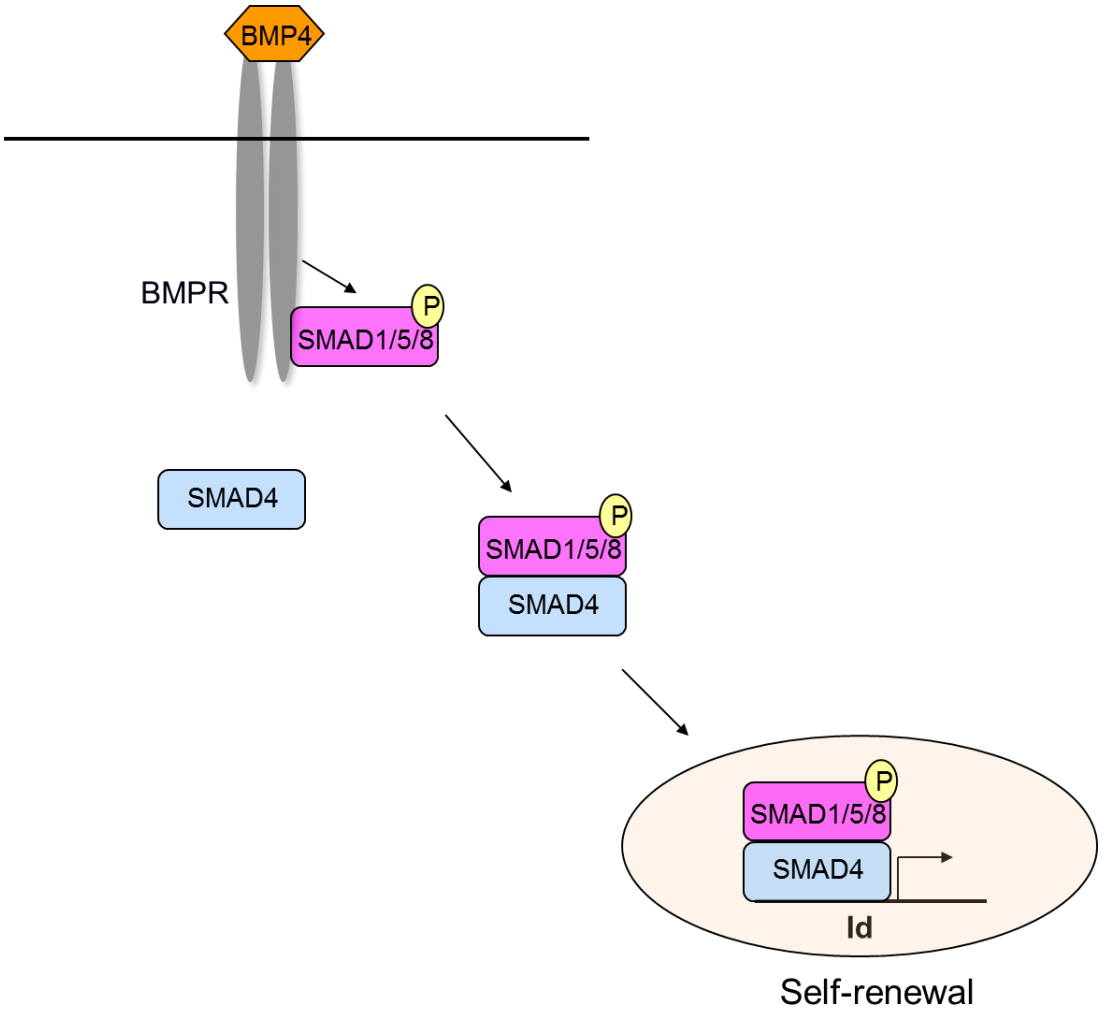

Figure 1.7 BMP signalling. BMP4 binding to the receptor results in Smad1/5/8 phosphorylation, phosphorylated Smad1/5/8 heterodimer with Smad4 and translocate to the nucleus where activate Inhibitor of differentiation (Id) proteins. (After Ying et al., 2003).

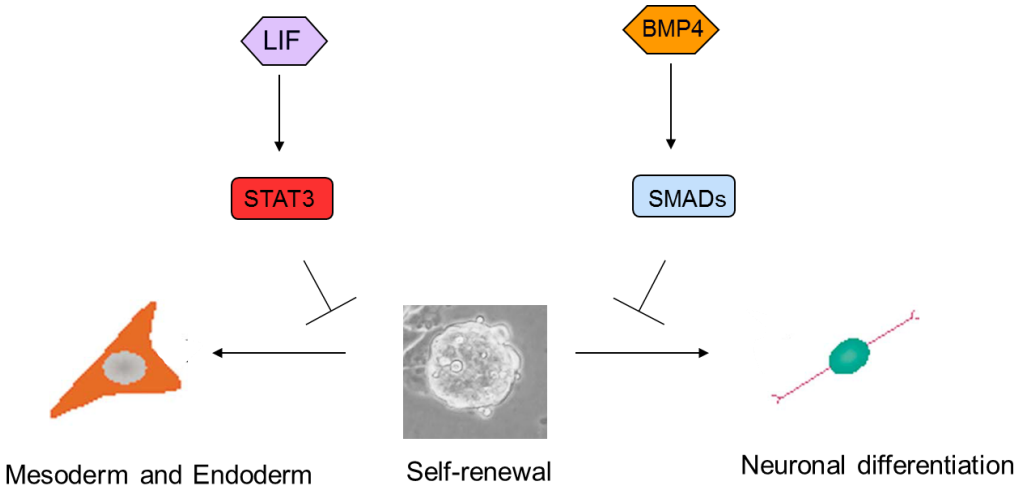

Figure 1.8 LIF and BMP cooperation to support self-renewal. LIF and BMP pathways cooperate to support self-renewal by restricting ES cell lineage commitment. LIF acts through STAT3 to inhibit mesoderm and endoderm differentiation while BMP through SMADs restrict neuronal differentiation (Modified from Ying et al., 2003).

1.5.2.3 MAPK signalling

The MAPK/Erk pathway is activated by extracellular stimuli, usually growth factors, and subsequently signals through a protein phosphorylation cascade to downstream effectors that regulate a large number of cellular processes. When this important pathway is dysregulated, it can result in the development of serious diseases like cancer (reviewed in (Crabbe et al., 2007)). During the signalling process from the cell membrane to the nucleus several steps lead to phosphorylation and activation of Erk1/2. Briefly, after activation of a receptor tyrosine kinase, SH2 domain containing proteins, including Shp2 and the adapter protein Grb2, bind to phosphorylation sites on the receptor. The protein SOS, named after its homologue Son of Sevenless in *Drosophila*, is able to bind to the membrane-bound protein Ras. Inactive Ras is bound to the nucleotide Guanosine diphosphate (GDP). SOS catalyses the exchange of GDP for Guanosine triphosphate (GTP) activating RAS, which in turn activates a chain of kinases, Raf, MEK (MAPK Erk Kinase) and finally Erk1/2. Phosphorylated Extracellular signal-regulated protein kinases, Erk1 and Erk2, can activate transcription factors of the AP-1 family, translocate to the nucleus and activate its targets (Figure 1.9). Erk1 and Erk2 have been demonstrated to be involved in regulating mESC self-renewal.

MAP kinases Erk1/2 are activated through the SH2 domain-containing tyrosine phosphatase-2 (Shp-2) as a consequence of LIF signalling. This is somewhat surprising, as Erk1/2 signalling negatively regulates self-renewal. The promotion of differentiation by Erk1/2 signalling was shown by creating gp130 mutant ES cells unable to bind Shp-2 (Burdon et al., 1999b). Extracellular signal stimulation did not activate the Erk pathway and low concentrations of LIF, normally unable to sustain self-renewal, were able to maintain mES cell pluripotency (Burdon et al., 1999b). The differentiation supporting effect of Erk signalling through Shp-2 is underlined by the enhanced self-renewal of ES cells overexpressing catalytically inactive Shp-2 mutant forms (Burdon et al., 1999b). Moreover, Shp-2 null ESCs are able to self-renew long-term, but are constrained in their ability to differentiate normally. They are impaired in their ability to differentiate into hematopoietic lineages, cardiac muscle cells, epithelial and fibroblast cells (Qu and Feng, 1998). Consistent with this observation, Grb2-null ESCs lack the ability to differentiate into endoderm as a consequence of a disturbed Ras/Erk signalling (Cheng et al., 1998). Signalling through Grb2/MEK was also claimed to be able to downregulate Nanog, shown by

introducing a constitutively active Mek mutant into ES cells or addition of the tyrosine phosphatase inhibitor, sodium vanadate, leading to Nanog repression and primitive endoderm differentiation (Hamazaki et al., 2006). Furthermore, treatment of ESC with the MEK inhibitor PD098059, inhibiting the activation of Erk1/2, did not block but rather enhanced self-renewal (Burdon et al., 1999b). This observation translates also to the embryo, where inhibition of Erk1/2 signalling promotes naïve pluripotency of the epiblast (Nichols et al., 2009). Epiblast cells expanded under Erk inhibition conditions could be expanded clonally and had high homogenous expression of pluripotency associated genes Nanog and Oct4 (Nichols et al., 2009).

Fibroblast growth factors (FGFs) are also able to trigger MAPK signalling by binding to FGF receptors, resulting in the activation of its receptor tyrosine kinase. It is peculiar that undifferentiated ES cells secrete FGF4, as this pathway is implicated in differentiation. Mouse ES cells treated with FGF receptor inhibitors or lacking FGF4 are unable to form neural or mesodermal lineages and are intractable to neuron differentiation by BMP induction. In accordance with this finding is the evidence for a requirement for Erk1/2 signalling during neural specification downstream of the FGF receptor (Stavridis et al., 2007). Absence of FGF4 does not prohibit differentiation entirely since FGF4 null ES cells can still form complex teratomas, but with a lower frequency than FGF4 heterozygous ES cells, possibly due to upregulation of other FGFs (Kunath et al., 2007). Differentiation defects resulting from the lack of FGF4 could be rescued by addition of recombinant FGF4, adding further evidence to suggest that the effect is caused by autocrine FGF4 signalling (Kunath et al., 2007). It is reasoned that Erk signalling promotes ESCs to a state allowing them to exit self-renewal by facilitating the response to differentiation signals (Kunath et al., 2007; Stavridis et al., 2007). Only a relatively short time window of sustained Erk1/2 activity is required to pass the threshold and allow neuronal fate lineage specification (Stavridis et al., 2007).

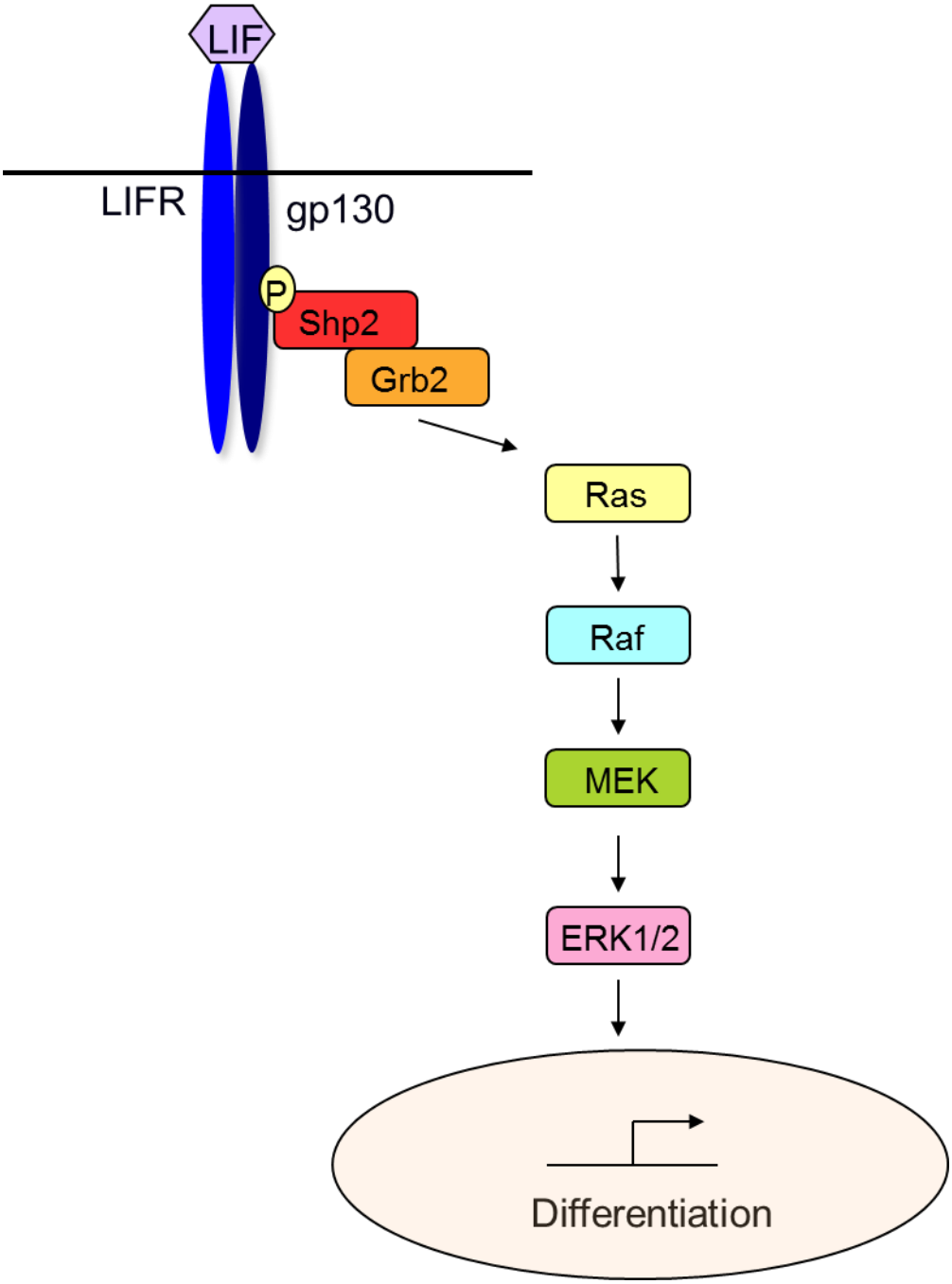

Figure 1.9 LIF/MAPK signalling pathway. Following activation of a tyrosine kinase receptor, Shp2 and Grb2 are recruited to the receptor through their SH2 domain. Subsequently, Ras is activated and in turn initiate a cascade of phosphorylation events resulting in activation of a chain of kinases, Raf, MEK, and Erk1/2. (After Burdon et al., 1999b).

1.5.2.4 GSK-3 in the Wnt-β-catenin signalling pathway

Glycogen synthase kinase-3 (GSK-3), isoforms GSK-3α and GSK-3β, are constitutively active serine/threonine protein kinases first discovered because of their ability to phosphorylate and inactivate the enzyme glycogen synthase (Embi et al., 1980; Woodgett and Cohen, 1984). GSK-3 is highly conserved from yeast to mammals and the mammalian class expresses two GSK-3 isoforms, α and β, which are encoded by distinct genes. They share 97% amino acid sequence identity within their catalytic domains, but outside the kinase domain the identity differs significantly. GSK-3 is implicated in numerous signalling pathways, including the Wnt/β-catenin pathway and plays key roles in a wide range of cellular processes (reviewed in (Woodgett, 2001; Wu and Pan, 2010)).

The canonical Wnt signalling pathway leads to the stabilization of β-catenin after activation by Wnt proteins (Figure 1.10). In the absence of Wnt a multi-protein destruction complex forms, consisting of APC (adenomatous polyposis coli), AXIN, GSK-3β, CKIα (casein kinase Iα), and β-catenin. The destruction complex targets β-catenin for proteasomal degradation. When Wnt proteins bind the Frizzeled (FZD) receptors located at the cell membrane, GSK-3-dependent β-catenin phosphorylation is suppressed via the protein Dishevelled, resulting in β-catenin stabilisation. Stabilized β-catenin is able to enter the nucleus, where it interacts with transcriptional regulators. LEF1 (Lymphoid Enhancing Factor-1) and TCFs (T cell factors) are known interactors, which, in association with β-catenin, upregulate target gene expression. Because GSK-3-mediated phosphorylation of the destruction complex acts as a switch in regulating β-catenin stability, pharmacological inhibition of GSK-3 can mimic the activation of the Wnt pathway, leading to stabilized β-catenin (reviewed in (Clevers, 2006; MacDonald et al., 2009)).

Wnt signalling was implicated in the self-renewal of ES cells by inhibition of GSK-3 with the small molecule inhibitor, BIO (Sato et al., 2004). Interestingly, this group claimed that both human and mouse ESCs maintain self-renewal upon BIO treatment. Consistent with this notion they showed expression of pluripotency associated transcription factors Oct3/4, Rex1 and Nanog. This was the first report of a self-renewal signalling pathway common to mouse and human ES cells, though it is conflicting with some more recent studies. A report by our group describes the discovery of a panel of compounds inhibiting GSK-3 selectively, leading to

enhanced self-renewal in mouse ESCs in presence of LIF and serum (Bone et al., 2009). In contrast, when the same specific GSK-3 inhibitors were added to hESC cultures, under chemically defined feeder-free culture conditions, ES cells differentiated towards definitive endoderm (Bone et al., 2011). Also, other groups reported mixed involvement of Wnt signalling in self-renewal (Hao et al., 2006; Ogawa et al., 2006; Sato et al., 2004; Singla et al., 2006) and differentiation (Dravid et al., 2005; Gadue et al., 2006; Lindsley et al., 2006). Wnt3a conditioned media was described to be able to support self-renewal and growth of mESCs in absence of LIF or feeder cells (Singla et al., 2006), while WNT5A and WNT6 were found to potently inhibit mES cell differentiation (Hao et al., 2006). However, β-catenin knock-out ESCs are not majorly impaired in their self-renewal abilities (Anton et al., 2007) and still express Sox2 and Nanog at levels comparable to wild type ESCs. This is surprisingly, as Wnt3a is suggested to support self-renewal via β-catenin, underlined by the finding that constitutively active β-catenin mimics the effect of Wnt3a (Ogawa et al., 2006). In the same study it was shown that other unidentified factors in the Wnt3a conditioned media were able to activate STAT3 at a low level and consequently it was demonstrated that low levels of LIF could act in synergy with Wnt3a to maintain self-renewal. Differences in the Wnt contribution to stem cell fate might arise from experimental setups, off-target effects of GSK-3 inhibitors and/or later developmental stages of ES cell lines used. The commonly used GSK-3 inhibitor BIO was for instance reported to activate a STAT3 reporter assay (Ogawa et al., 2006) and furthermore to have off-target effects, inhibiting Erk phosphorylation (Bone et al., 2009). Interestingly, in recent reports GSK-3 inhibition helped to convert hES cells to a more naïve state of pluripotency (Hanna et al., 2010), similar to mouse ESCs. This might indicate that the differences implicated by the above mentioned studies arise as a result of signalling pathway deviances because of developmental stage variations under *in vitro* cell culture conditions.

GSK-3 can be also inhibited via the PI3K-dependent signalling pathway through activation of Akt. As the PI3K pathway is a focus of this study, it will be explained in more detail in the section 1.6.

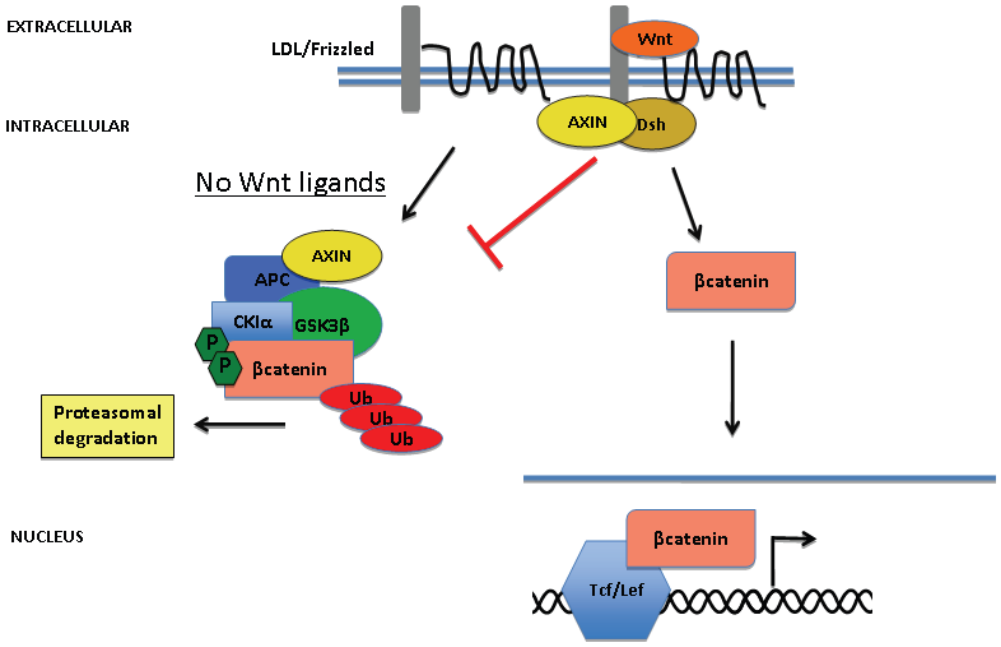

Figure 1.10 The canonical Wnt pathway. In the absence of Wnt, the destruction complex formed by Axin, APC, CKIα, GSK-3β and β-catenin, targets β-catenin for proteosomal degradation. Upon Wnt binding to the Frizzled receptor, the destruction complex is disrupted via Dishevelled (Dsh) and GSK-3 dependent phosphorylation of β-catenin is suppressed leading to β-catenin stabilisation. Stabilised β-catenin translocates to the nucleus where interacts with Tcf and Lef promoting expression of target genes (Taken from Atwood, 2011, Inechweb.org).

1.5.3 Intrinsic factors of pluripotency

1.5.3.1 Oct4 and Sox2

Two years after the identification of LIF, Oct4 (octamer-binding transcription factor 4), also known as Pou5f1, was discovered as a member of the POU-domain containing transcription factors (Scholer et al., 1989). The POU (Pit Oct Unc) domain is named after the first letters of genes that share the sequence homology, Pit1, Oct1/2 which are mammalian genes, and the *C. elegans* gene Unc-86. Oct4 can bind via its POU domain to the octamer DNA motif, 5'-ATGCAAAT-3', and alter target gene expression (Ryan and Rosenfeld, 1997). Oct4 is specifically expressed in germ cells, eggs, preimplantation embryos, the ICM, and the epiblast of post-implantation embryos (Okamoto et al., 1990; Rosner et al., 1990; Scholer et al., 1990). Oct4 deficient embryos develop to the blastocyst stage but die shortly after implantation with the inner cell mass not being pluripotent (Nichols et al., 1998). When Oct4 null ESCs are cultured *in vitro* they only develop trophectoderm-like cells and cannot contribute to inner cell masses (Nichols et al., 1998). Suppression of Oct4 expression in mouse and human ESCs results in the differentiation toward the trophoblast lineage (Niwa et al., 2000). However, artificial over-expression of Oct4, via inducible transgenes, is not able to maintain self-renewal and pluripotency in the absence of LIF (Niwa et al., 2000). Furthermore, reduced expression of Oct4, by less than 50% of wild-type levels, results in differentiation and the expression of trophectodermal markers (Figure 1.11). Expression levels above 150% of wild-type result in differentiation towards primitive endodermal and mesodermal lineages (Niwa et al., 2000). Thus, expression of Oct4 needs to be carefully balanced, as deviations greater than 50% from normal diploid expression levels alter both cell fate and lineage commitment (Niwa et al., 2000).

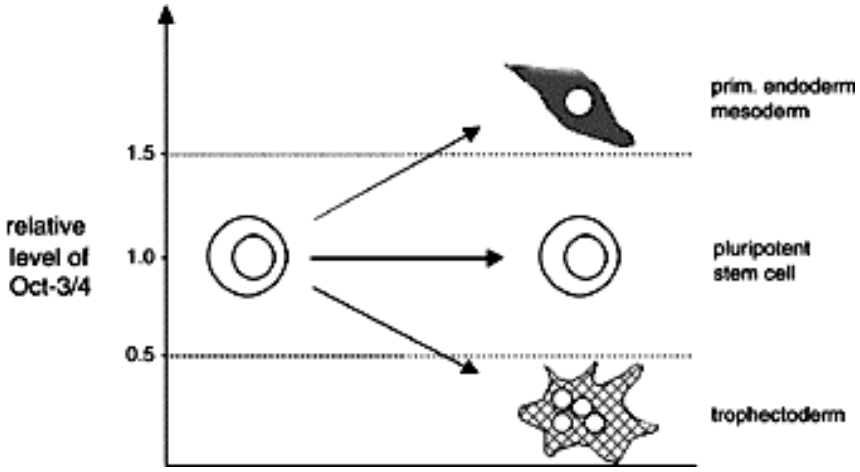

Figure 1.11 Relative expression levels of Oct-3/4 determine stem cell fate. To maintain mES cells undifferentiated Oct-3/4 levels must remain within plus or minus 50% of normal diploid expression. An increase above this threshold triggers differentiation to primitive endoderm. If Oct-3/4 levels fall below, this causes dedifferentiation into the trophectoderm lineage. (Niwa et al., 2000)

1.5.3.2 Nanog

Nanog, named after Tír na nÓg, the land of the ever young of a Celtic mythology, was discovered by two groups in 2003 (Chambers et al., 2003; Mitsui et al., 2003). It was discovered independently by functional expression cloning (Chambers et al., 2003) and through *in silico* differential expression analysis (Mitsui et al., 2003) around the same time. Both groups were able to show that overexpression of Nanog is sufficient to maintain ESC self-renewal independently of LIF/Stat. Nanog is a divergent homeodomain-containing transcription factor, which is commonly believed to be a key factor in the transcriptional network of pluripotency (Boyer et al., 2005; Loh et al., 2006; Wang et al., 2006). Furthermore, Nanog is essential for early embryonic development and plays a conserved role in pluripotency across a range of species including mammals, birds and fish (Chambers et al., 2003; Lavial et al., 2007; Mitsui et al., 2003; Wang et al., 2011). Nanog starts to be expressed at the morula stage and is expressed at a high level until the early blastocyst stage,

whereupon it declines before implantation. Still, it is detectable in primordial germ cells during their migration to the genital ridges, but is downregulated in later germ cell development (Chambers et al., 2007; Yamaguchi et al., 2005). In a second wave of transcription Nanog is re-expressed in the posterior region of the post-implantation egg cylinder, which might protect the egg cylinder epiblast from precocious commitment during gastrulation (Chambers et al., 2007; Hart et al., 2004).

Subsequently, Austin Smith's group has published that Nanog null ES cells, generated by genetic deletion of the Nanog locus, can self-renew permanently in the absence of LIF (Chambers et al., 2007). Despite the ability to self-renew long term, these cells are more susceptible to differentiation compared to wild type ESCs. The group hypothesised that Nanog acts to safeguard self-renewal by countering the effects of differentiation inducers and preventing progression to lineage commitment (Chambers et al., 2007). When Nanog levels are low, cells might have the opportunity to escape self-renewal. Nanog null ES cells were able to differentiate into all three germ layers *in vitro* and *in vivo*, but maturation of primordial germ cells was disturbed in the genital ridge (Chambers et al., 2007). These results indicate that Nanog might be more important for the establishment of pluripotency and to a lesser extent for the maintenance of pluripotency. Consistent with this idea is the importance of Nanog during embryo development. Nanog null blastocysts are indistinguishable from normal embryos (Mitsui et al., 2003). However, at E5.5 Nanog null embryos consist entirely of disorganized extraembryonic tissues with no discernible epiblast or extraembryonic ectoderm (Mitsui et al., 2003). ICMs of Nanog null blastocysts were isolated by immunosurgery but failed to proliferate when cultured on gelatin coated dishes and differentiated into parietal endoderm-like cells (Mitsui et al., 2003).

Surprisingly, despite its central role in establishing pluripotency, Nanog was not one of the four original factors necessary for the generation of iPS cells (Takahashi and Yamanaka, 2006). However, when reprogrammed cells were selected for reactivation of Nanog, instead of the first used Fbx15, the efficiency of full reprogramming was greatly increased (Okita et al., 2007). In a more recent paper, Nanog is shown to be required in the final phase of reprogramming (Silva et al., 2009). At this stage the ectopic expression of the reprogramming factors has

probably already activated expression of endogenous Nanog, necessary to reach true pluripotency (Silva et al., 2009).

1.5.3.3 The transcriptional network of pluripotency

The previously introduced transcription factors Oct4, Sox2 and Nanog are central players in assembling the pluripotency network maintaining ES cell self-renewal. The targets of each transcription factors have been assessed using chromatin immunoprecipitation (ChIP) and microarray technologies. A substantial binding site overlap of the three transcription factors was found in mouse and human ES cells genes and their targets frequently encode other homeodomain transcription factors important during development (Boyer et al., 2005; Loh et al., 2006). Interestingly, Oct4, Sox2 and Nanog co-occupied promoters of both active and inactive genes, as well as their own promoters. Actively transcribed genes includes those genes with a role in maintaining pluripotency of ES cells including the transcription factors Nanog, Oct4, Sox2 and Stat3, as well as components of the Wnt and TGF-β signalling pathways such as Dkk1 and Lefty2. Among the inactive genes are those encoding transcription factors with a developmental role. The fact that inactive genes were also co-occupied by Polycomb Repressive Complexes, which are related to transcriptional gene silencing, suggest that Oct4, Sox2 and Nanog repress expression of developmental genes while promoting expression of genes involved in maintaining ES cell identity (Boyer et al., 2005). Boyer *et al* proposed that Oct4, Sox2 and Nanog form a core transcription factor circuit with autoregulatory and positive feedback loops that promote pluripotency and repress developmental processes (Figure 1.12). Using a transcription factor network with positive and negative regulation can be a good mechanism for maintaining the right levels of gene expression that stabilize a particular cell state (von Dassow et al., 2000). Furthermore, it is possible to explain how small changes of network components can trigger transition from one state to another by using systems biology models (Kauffman, 2004). Extracellular signals feed into the core network and consequently influence the regulation of their targets (Niwa, 2007; Niwa et al., 2009).

More recent studies (Chen et al., 2008; Cole et al., 2008; Heng et al., 2010; Kim et al., 2008) investigated the binding sites of others pluripotency-associated

transcription factors and observed that the regulatory regions of Oct4 are bound by multiple transcription factors including Sox2, Nanog, Smad1, Stat3, Tcf3, Dax1, Nac1, Zfp281, Esrrb, Nr5a2, Klf4, Tcfp21l1 and Oct4 itself. These transcription factors are thought to act as enhancers and a correlation between the number of transcription factors bound to a promoter and its transcriptional status have been observed. Genes actively transcribed have more transcription factors bound than silenced genes (Chen et al., 2008; Kim et al., 2008). For example, Oct4 and Nanog promoter regions are occupied by 14 and 9 transcription factors respectively.

Several studies have shown that the transcription factor network is linked to the epigenetic and non-coding RNA networks (Barrero and Izpisua Belmonte, 2011; Loh et al., 2007; Marson et al., 2008; Zhang et al., 2011). For instance, Oct4 upregulates the expression of Jmjd1a and Jmjd2c that encode for histone H3 lysine 9 demethylases, which promote maintenance of ES cell pluripotency because histone H3 lysine 9 demethylases prevent the increase of repressive methylation in gene promoters (Loh et al., 2007). Oct4 can also upregulate expression of components of the Polycomb Repressive Complex 2 (PRC2) such as Jarid2 and Mtf2 that modulate trimethylation on the histone H3 lysine 27 residue, promoting repression of lineage-specific genes and thus contributing to maintenance of self-renewal (Zhang et al., 2011). Furthermore, Oct4, Sox2 and Nanog have been shown to promote the expression of microRNAs (miRNAs) such as the clusters mir302 and mir290 (Marson et al., 2008), which have been proposed to repress important cell cycle regulators including Cdkn1a, Rbl1 and Lats2 (reviewed in (Ng and Surani, 2011), resulting in the shortened G1 phase typical of ES cells. mir302 and mir290 are negatively regulated by Let-7 miRNA (Melton et al., 2010), which is repressed by the RNA-binding protein Lin28, and the core pluripotency transcription factor have been shown to upregulate Lin28 expression (Barrero and Izpisua Belmonte, 2011).

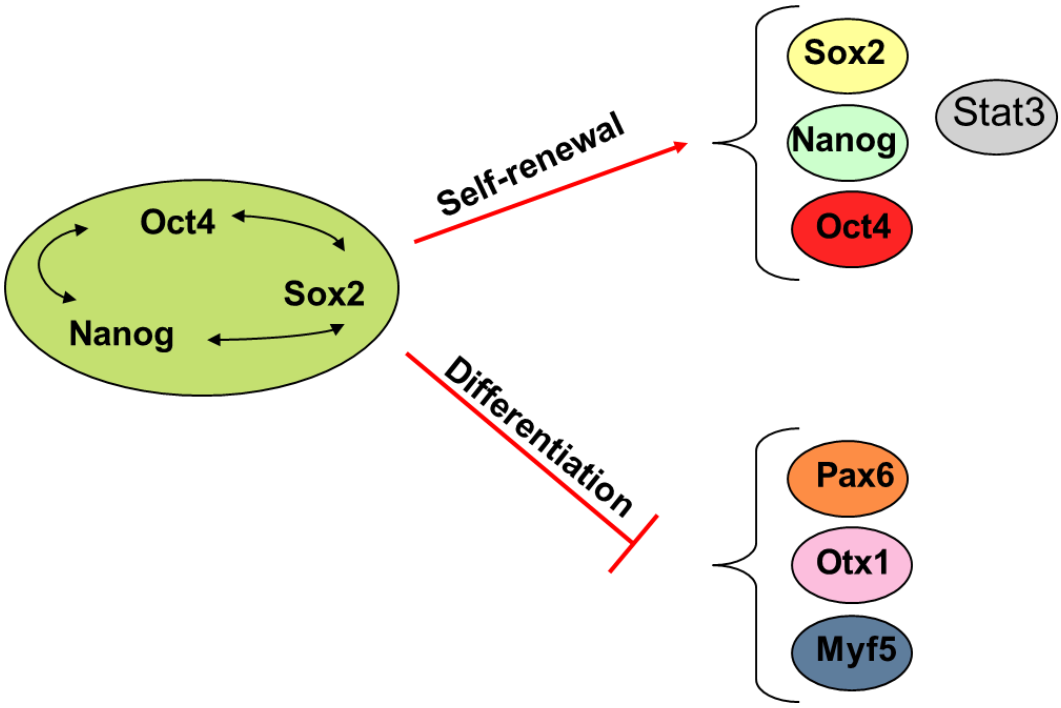

Figure 1.12 Core pluripotency transcriptional factor network. Oct4, Sox2 and Nanog form a core transcription factor circuit with autregulatory and positive feedback loops that induce expression of genes that promote self-renewal, Sox2, Nanog, Oct4, Stat3 and others and repress the expression of genes that promote differentiation such as Pax6, Otx1 and Myf5. (After Boyer et al., 2005).

1.6 Phosphoinositide 3-Kinases (PI3Ks)

1.6.1 Structure and function of PI3Ks

Phosphoinositide 3-kinases (PI3Ks) are a family of lipid kinases which play many important roles in the regulation of various cellular processes including proliferation, growth, cell differentiation, migration and immune function (Crabbe et al., 2007; Engelman et al., 2006). Members of the PI3K family of enzymes phosphorylate the D3 hydroxyl group of the inositol ring of phosphoinositides (Figure 1.13 A). This facilitates the recruitment of proteins containing pleckstrin homology domains (PH domains) and other phosphoinositide-binding domains to the plasma membrane, triggering a cascade of signalling events. The ability of phosphoinositides to act as important second messengers was first reported in the early 1980s (reviewed in (Berridge and Irvine, 1984; Berridge and Irvine, 1989)), linking extracellular signalling from growth factor receptors to downstream target genes. The different types of PI3Ks respond to diverse signals and favour specific inositol substrates over others. This results in a manifold of second messenger variations (Figure 1.13 B), with potentially multiple functional outputs. The PI3K pathway is an extremely complex signalling pathway, involving many activators, inhibitors, effectors, and second messengers. Because of its many loops and branches it is far from being completely understood, but it is essential for many cellular functions and associated with a wide range of diseases when dysregulated (Balla, 2006; Vanhaesebroeck et al., 2010).

PI3Ks have been divided into three classes (I-III) (Vanhaesebroeck et al., 1997), of which class I is the focus in this study and therefore exemplified in more detail. Class I PI3Ks exhibit a higher susceptibility to the pharmacological broad spectrum inhibitors wortmannin and LY294002 and are the best studied class to date. Class I PI3Ks are further subdivided into classes I_A and I_B depending on their activation mechanism. Class I_A consists of three catalytic subunits p110α, p110β, p110δ and of five respective regulatory subunit p85α, p55α, p50α, p85β or p55γ, while class I_B assemble the catalytic isoform p110γ with one of two regulatory subunits (p84/87 or p101) (Crabbe et al., 2007; Vanhaesebroeck et al., 2005). Interestingly, genetic deletion of either the p110α and p110β catalytic subunits results in embryonic

lethality, indicating non-redundant and essential regulatory roles of PI3Ks in early development (summarized in Table 1).

Table 1: Class I_A PI3Ks subunit composition and viability of mice with targeted PI3K catalytic sub-unit genetic deletions.

Catalytic Subunits	KO of Catalytic Subunit	Regulatory Subunits	Gene name
p110α	Embryonic lethal (E10.5)	p85α	Pik3r1
p110β	Embryonic lethal (blastocyst stage: around E.3.5)	p55α	
p110δ	Viable	p50α	
		p85β	Pik3r2
		p55γ	Pik3r3

In contrast to the broadly expressed isoforms, p110α and p110β, the other class I PI3Ks isoforms p110δ and γ exhibit a more restricted pattern of expression. P110δ is largely expressed in cells of the immune system, playing a major role in the lymphohaemopoietic system (Vanhaesebroeck et al., 1997). Transgenic mice expressing a catalytically inactive form of p110δ show impaired B and T cell immune responses (Okkenhaug et al., 2002). P110δ was also shown to be required for normal B cell function and development (Clayton et al., 2002; Jou et al., 2002). Expression of p110γ, the only class I_B PI3K isoform, is confined to the haematopoietic system, heart, endothelium and brain. Its function is associated with regulating inflammatory and cardiovascular processes (reviewed by (Ruckle et al., 2006)). Knock-out of either p110δ or p110γ does not affect viability or fertility of mice, therefore it is unlikely that these isoforms play an important role during early embryonic development (Clayton et al., 2002; Jou et al., 2002; Ruckle et al., 2006).

A

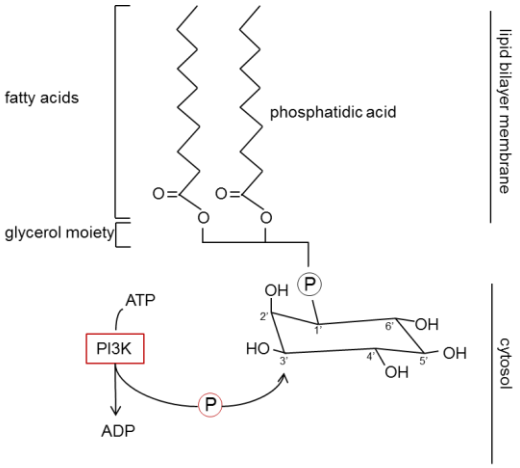

B

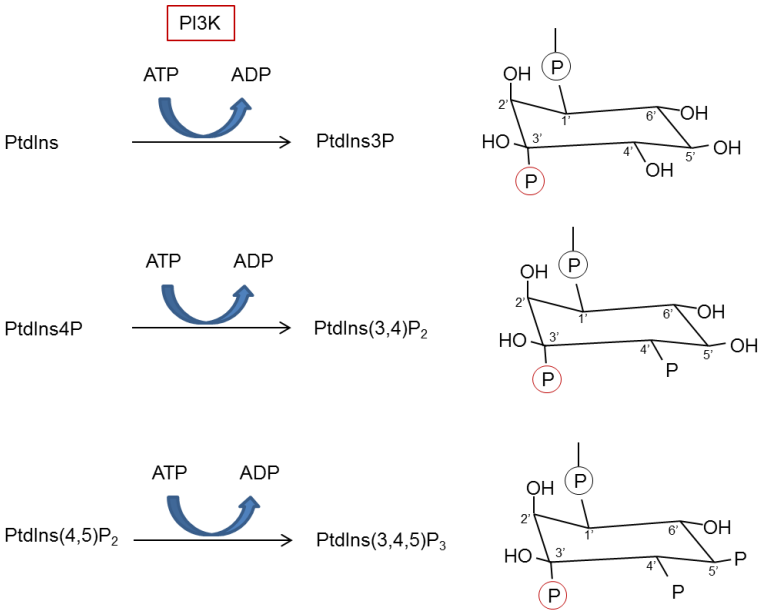

Figure 1.13 Reactions catalysed by PI3Ks. (A) PI3K phosphorylates the D3 position of the inositol ring of phosphatidyl inositols (PtdIns) by adding the γ-phosphate of ATP. The PtdIns are anchored with their fatty acid side chains in the lipid bilayer of the cell membrane and are able to activate various signalling pathways once they are activated by phosphorylation. (Vanhaesebroeck and Waterfield, 1999). (**B**) Three reactions catalysed by PI3K activities *in vitro* and their structural phosphoinositide products are shown (Hawkins et al., 2006).

PI3Ks can be activated by multiple factors, usually involving extracellular stimuli such as growth factors, neurotransmitters, hormones or antigens (Wymann and Pirola, 1998). Class I_A PI3Ks are primarily activated downstream of tyrosine kinase-linked receptors, while Class I_B PI3Ks are activated by G protein-coupled receptors. There is also evidence that the class I_A enzyme p110β can be regulated by a heterotrimeric G protein subunit complex (Yart et al., 2002). Both, class I_A and I_B kinases can bind the small GTPase Ras, and there is evidence to suggest that Ras can activate PI3Ks when associated with GTP (Rodriguez-Viciana et al., 1994). After activation, PI3Ks preferentially phosphorylate phosphatidylinositol (4,5) bisphosphate (PIP_2) to produce the important second messenger phosphatidylinositol (3,4,5) triphosphate (PIP_3). *In vitro* PI3Ks have also been shown to phosphorylate PI and PI(4)P (Irvine, 1992). PIP_3 is anchored with its fatty acid chains in the lipid membrane of the cell (Figure 1.13 A) and serves to amplify the PI3K signal transduction by interacting with partners of the signalling pathway. PI3K effector proteins contain the conserved Pleckstrin Homology (PH) domain allowing them to bind the second messenger products, which in turn recruits them to the inner cell membrane (Katan and Allen, 1999).

One known effector recruited in this way is the phosphoinositide-dependent protein kinase 1 (PDK1). PDK1 can in turn interact and phosphorylate other proteins, for instance Akt (also known as Protein Kinase B, PKB) (Alessi et al., 1997; Komander et al., 2004) (Figure 1.14). The mutual ability of Akt and PDK1 to interact with PIP_3 is likely to be important for regulating Akt activation (Anderson et al., 1998; Currie et al., 1999; Filippa et al., 2000). In accordance with this is a report that ES cells expressing a mutant form of PDK1, which is unable to bind PIP_3, could not activate Akt substantially (McManus et al., 2004). Structural studies suggest that a major conformational change is induced by the binding of Akt to PIP_3, which is likely to play an important role in Akt activation by PDK1 (Mora et al., 2004). Importantly, binding of PIP_3 to the PDK1 PH domain has no direct repercussion on the activity of the PDK1 kinase domain, but rather acts through activation of Akt by direct interaction of Akt with PDK1 (Currie et al., 1999; Stephens et al., 1998).

After recruitment to the cell membrane Akt can be activated by phosphorylation of the Thr308 and Ser473 residues (Alessi et al., 1996). The phosphorylation sites lie in two distinct regions of the enzyme. While Ser473 is located in the "hydrophobic motif" on the carboxy terminal side of the catalytic domain, Thr308 lies in the so called 'T-loop' of the kinase domain. In PDK1 knock-out cells activation of the Thr308 site is impaired and as a consequence downstream phosphorylation of GSK-3 is abolished. Interestingly, phosphorylation at the Ser473 site was not affected after genetic deletion of PDK1. Preincubation of cells with the broad PI3K inhibitor LY294002 reduced the level of Ser473 phosphorylation to below basal levels, indicating the involvement of another phosphoinositide dependent protein kinase, PDK2 (Hresko et al., 2003; Williams et al., 2000). Another explanation could be the previously described function of a PDK1-interacting fragment (PIF), that in combination with PDK1 can phosphorylate Ser473 of Akt, as well as Thr308 (Balendran et al., 1999). In respect of these findings, it is still unclear whether the activity arises from PDK1 in combination with PIF or PDK2. Activated Akt can in turn phosphorylate Ser21 and Ser9 of GSK-3 α and β leading to its inactivation. GSK-3 is known to regulate a number of cellular processes including glycogen synthesis, protein synthesis, cell cycle and apoptosis.

PDK1 is also implicated in activating other members of the AGC family kinases, for instance p70 ribosomal S6 kinase (S6K) and p90 ribosomal S6 kinase (RSK) (Figure 1.14) (reviewed in (Alessi et al., 1996; Belham et al., 1999; Williams et al., 2000)). The AGC group is named after the protein kinase A, G, and C families (PKA, PKC, PKG) and includes in total 16 families. These kinases have a strong preference for phosphorylation of Serine and Tyrosine residues located in close proximity to the basic amino acids Lysine and Arginine. PDK1 plays a central role in mediating extracellular signals downstream of PI3Ks by phosphorylating key regulatory proteins, orchestrating multiple cellular functions, including cell cycle, apoptosis, protein and glycogen synthesis (Hanada et al., 2004; Hennessy et al., 2005).

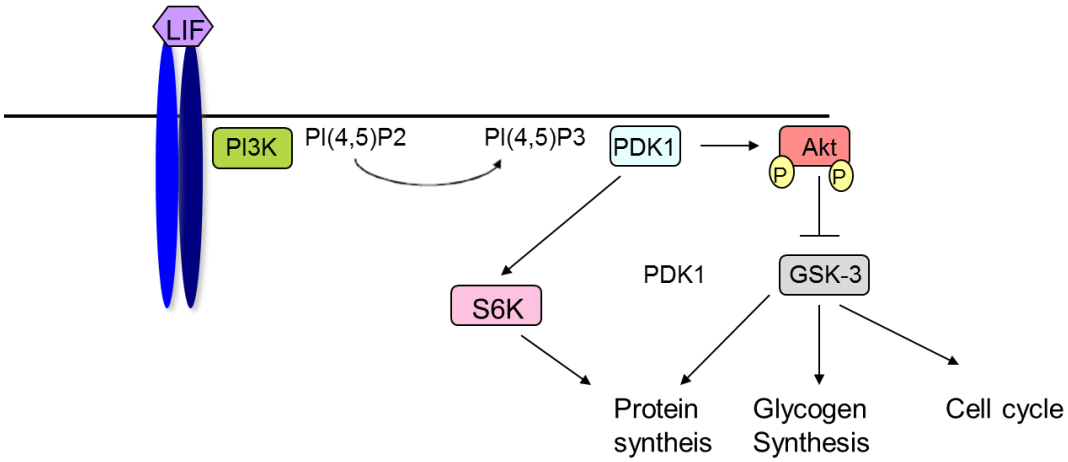

Figure 1.14 PI3K signalling. Following LIF binding PI3K is activated and phosphorylates PI(4,5)P2 in the membrane to form PI(3,4,5)P3, PDK1 is recruited to the membrane where it phosphorylates Akt at Thr308 and Ser473. Activated Akt in turn phosphorylates and inactivates GSK-3. PDK1 can also phosphorylate S6K promoting protein synthesis.

1.6.2 Regulation of PI3K activity

With the involvement of PI3Ks in a wide range of fundamental cellular functions, regulation mechanisms have to be accurately in place, as dysregulation is likely to result in serious consequences and diseases. A constitutively active class I_A p110α isoform, as a result of genetic mutations, is involved in proliferation and progression of various human tumours (Samuels et al., 2004; Vanhaesebroeck et al., 2001). Furthermore, activating mutations of PI3K pathway components are found in 40% of all human colorectal cancers (Parsons et al., 2005). Unbalanced regulation of p110γ or p110δ isoform activity can also lead to a disturbance of inflammatory responses (Crabbe et al., 2007).

There are two important main negative regulators of the PI3Ks pathway, acting through reversing the phosphorylation of PIP_3 induced by PI3Ks. One of them is the SH2-containing inositol 5-phosphatase (SHIP) and the other one is the phosphatase and tensin homolog (PTEN). While SHIP dephosphorylates the D5 position of the

phosphoinositol ring, PTEN mediates the removal of the phosphate group from the D3 position. Both dephosphorylation events reduce the availability of the second messenger $PI(3,4,5)P_3$. Consequently, recruitment of effector proteins to the cell membrane and signalling cascade events are reduced. PTEN-null cells exhibited constitutively active Akt in the wake of increased PIP_3 levels (Stambolic et al., 1998). In accordance with PTEN antagonizing the effect of PI3Ks it is a well-recognized potent tumour suppressor in a range of tissue types and is commonly mutated in multiple cancers (Li and Sun, 1997; Whang et al., 1998).

The regulatory subunit p85, whose SH2 domains bind phosphotyrosine in specific recognition motifs, positively regulates activation of p110 isoforms in association with receptor-tyrosine kinases (Dhand et al., 1994). It has also been suggested to act as a negative regulator when prevalent as monomers, by binding to activated receptor domains averting the binding of the heterodimeric p85-p110 complex (Brachmann et al., 2005; Geering et al., 2007).

1.6.3 Role of PI3Ks in ESCs

1.6.3.1 Self-renewal

The requirement of PI3Ks for maintaining mES cell self-renewal was shown for the first time by inhibition of PI3Ks using the broad spectrum inhibitor LY294002 or a dominant negative p85 subunit of PI3K (Paling et al., 2004). Both forms of inhibition lead to a loss of self-renewal of mES cells, even in the presence of LIF, implicating the importance of PI3Ks for the regulation of self-renewal. ESC differentiation could be rescued by MEK inhibition with U0126, and it was suggested that increased Erk activity is the cause of differentiation resulting from PI3Ks inhibition (Paling et al., 2004). Furthermore, Nanog RNA and protein levels decreased upon treatment with LY294002, and the reduction was reported to be reversible by GSK-3 inhibition with the small inhibitor BIO (Storm et al., 2007). GSK-3 inhibition also rescued the differentiation of ESCs induced by LY294002 (Storm et al., 2007) and by expressing a myristoylated mouse p110 subunit it was shown that activation of PI3Ks can lead to phosphorylation and therefore inhibition of GSK-3 (Popkie et al., 2010). Surprisingly, inhibition of MEK/Erk signalling was

unable to reverse the decrease in Nanog expression, questioning increased Erk activity as the main reason for differentiation observed when PI3Ks were inhibited.

The importance of the PI3Ks pathway in self-renewal of mESCs was further strengthened by the finding that expression of a myristoylated, and therefore constitutively active, form of Akt can sustain self-renewal in absence of LIF (Watanabe et al., 2006). In another study around the same time, Akt was also identified as being able to maintain self-renewal in the absence of LIF by using a combination of cDNA library screens and microarray (Pritsker et al., 2006). Furthermore, overexpression of suggested Akt downstream target genes, TBX3 and Nanog, results in LIF independency (Niwa et al., 2009). With Akt being an important downstream effector of PI3Ks, this might support the advocated role of PI3K signalling to self-renewal by inhibition of GSK-3 through Akt (Storm et al., 2007). Other indications implicating PI3Ks in self-renewal comes from the finding that the small molecule pluripotin supports self-renewal by activating PI3K signalling, while suppressing Erk signalling (Chen et al., 2006).

PI3K have also been shown to be involved in regulating self-renewal in human ES cells (Armstrong et al., 2006). In this study, hES cells were induced to differentiate by forming embryoid bodies and subsequent transcriptional and protein changes were analysed. Components of the PI3K/Akt signalling pathway were reported to be decreased upon differentiation. Furthermore, inhibition of the PI3K pathway using specific inhibitors resulted in loss of pluripotency, suggesting an important contribution of the PI3K signalling pathway in hES cell maintenance (Armstrong et al., 2006). In addition, a combination of GSK-3 inhibition, while stimulating the PI3K pathway by overexpressing the PI3K stimulator Eras, or potentially via overexpression of a PI3K transgene, was proposed to be sufficient for feeder free ESC proliferation (Smith, 2009).

1.6.3.2 Proliferation

In mES cells PI3Ks have been reported to be involved in cell-cycle control, activation of ES cell proliferation and tumourigenicity (Jirmanova et al., 2002). A role for PI3Ks in control of mES cell proliferation was suggested after the finding that mES cells lacking the phosphatase PTEN exhibited a decrease in the time required to complete a cell division cycle (Sun et al., 1999). As previously mentioned, PTEN is a phosphatase that dephosphorylates the second messenger $PI(3,4,5)P_3$ and therefore acts as a negative regulator of PI3K signalling. PTEN-null ES cells were able to proliferate in reduced levels of serum suggesting activation of PI3K activity by serum-containing factors. This group also proposed reduced levels of the G1 cyclin-dependent kinase inhibitor, $p27^{KIP1}$as the mechanism of action for the enhanced growth rate. Reduced expression of $p27^{KIP1}$ could originate from inhibition of FOXO family transcription factors via phosphorylation by Akt (Stahl et al., 2002). Akt is also implicated in increasing cell survival by phosphorylation of Bad, a member of the Bcl2 family of pro-apoptotic proteins and indeed in PTEN-null ESCs levels of phosphorylated Bad were elevated (Sun et al., 1999). Furthermore, deleting both alleles of Akt-1 in the PTEN-null background reversed the growth advantage of the PTEN knockout, highlighting Akt as a major effector in PTEN knockout cells (Stiles et al., 2002).

Among the multiple downstream effectors of the PI3K pathway is mTOR (mammalian target of rapamycin), which appears to be a major player in regulating mES cell proliferation (Murakami et al., 2004; Takahashi et al., 2005). Inducible ablation of mTOR or inhibition by the specific mTOR inhibitor rapamycin leads to a decrease in mES cell proliferation. The mTOR protein kinase is 290 kDa in size and phosphorylates serine and threonine residues. The identified downstream substrates include p70 ribosomal S6 kinase (S6K) (Brown et al., 1995) and 4E-BP1 (eukaryotic initiation factor binding protein 1) (Gingras et al., 1999). PI3Ks can activate mTOR through relieving a negative regulator protein complex of tuberous sclerosis complex 1 and 2 (reviewed in (Marygold and Leevers, 2002)) and can therefore be regarded a strong candidate for a downstream target of the PI3K signalling in ES cells (Takahashi et al., 2005).

The PI3K pathway can not only be activated by exogenous factors, but also endogenously by a constitutively active Ras form, termed ERas (ES cell-expressed Ras). ERas is uniquely expressed in mES cells and is a Ras-like protein identical to oncogenic Ras mutants. ERas was also reported to regulate proliferation as deletion of ERas resulted in a loss of proliferation (Takahashi et al., 2003). Importantly, over-expression of p110α was able to rescue the proliferation defects of ERas null ES cells. In addition, inhibition of the p110α catalytic subunit of PI3Ks with the specific inhibitor PIK-75, or inhibition of PI3Ks with the broad specificity inhibitor LY294002, results in a reduced proliferation rate (Jirmanova et al., 2002; Kingham and Welham, 2009). Taking these findings together, PI3K signalling seems to play an important role in ES cell proliferation. Figure 1.15 shows a schematic overview of the signalling pathways regulated by PI3Ks in ES cells.

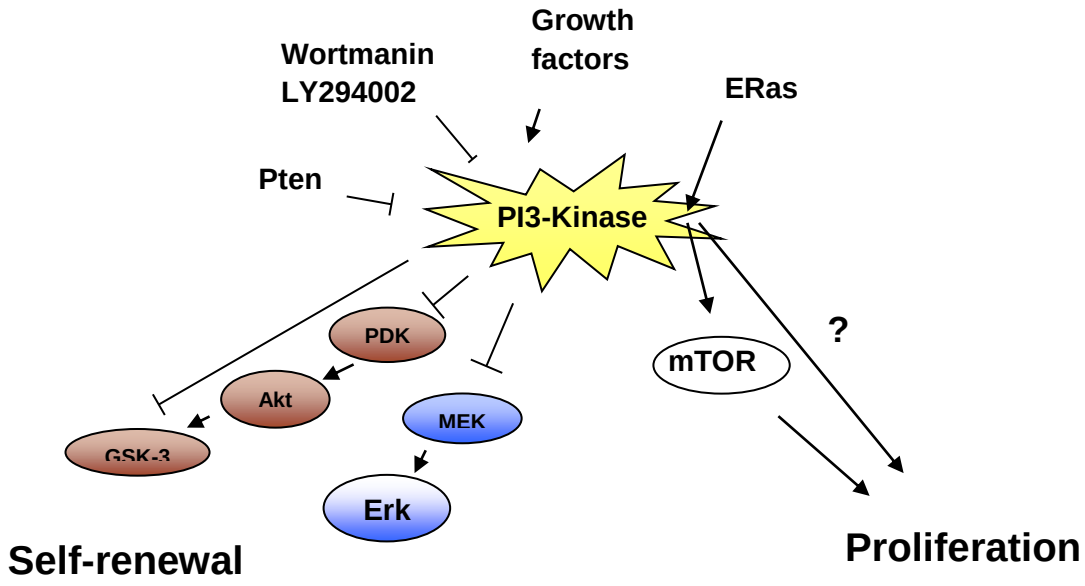

Figure 1.15 Role of PI3K in regulating self-renewal and proliferation of mES cells. PI3K is implicated to be involved in maintaining mES cells pluripotent by inhibition of Erk phosphorylation, responsible for differentiation. GSK-3 signalling, known to enhance self-renewal on inhibition, is also reduced by PI3K in mES cells. Furthermore, PI3K was postulated to play a role in proliferation of mES cells.

1.6.3.3 PI3Ks inhibitors and application opportunities

The Phosphatidylinositol-3 kinase family of enzymes are involved in multiple important cellular functions such as cell growth, survival, proliferation, migration, differentiation and intracellular trafficking. When these basic cellular functions are anomalous, diseases are likely to occur, so it does not come as a surprise that PI3Ks are implicated in various diseases. Dysregulation can contribute to diseases including diabetes, inflammation, and also autoimmune diseases (Engelman et al., 2006; Hennessy et al., 2005; Rommel et al., 2007). Inhibition of PI3Ks with pharmacological inhibitors was subsequently considered as an elegant way of disease treatment. Despite containing several structural elements most, if not all, PI3K inhibitors target the ATP binding pocket of the catalytic subunit.

The two infamously most studied PI3K inhibitors are Wortmannin, a metabolite of the plant pathogen *Penicillium funiculosum* (Wiesinger et al., 1974) and LY294002, developed by Lilly Research Laboratories (Vlahos et al., 1994). Wortmannin forms a covalent interaction with the catalytic lysine residue within the ATP-binding pocket of PI3Ks, thus inhibition is irreversible (Wymann et al., 1996). The other early inhibitor, LY294002, is, in contrast, a reversible ATP competitive inhibitor, but less potent than wortmannin (Vlahos et al., 1994). Both inhibitors are broad spectrum inhibitors and are therefore not selective for particular PI3Ks isoforms, making it impossible to unravel individual isoform contributions. In addition, a high toxicity when tested *in vivo* ruled out any potential therapeutic use, but as the earliest PI3Ks inhibitors available, they provided key tools to investigate PI3K signalling (Hennessy et al., 2005).

The co-crystallisation of broad selectivity inhibitors binding to the ATP pocket of the catalytic p110 isoform helped to understand the steric composition of this process (Walker et al., 2000). Computer modelling based on the obtained structure revealed a conformational change as a result of inhibitor binding to the entrance to the ATP binding pocket (Knight et al., 2006; Walker et al., 2000). This leads to the formation of hydrogen bonds between inhibitor and binding site, which are similar to the ones formed with ATP. Furthermore, affinity increases when inhibitors access deeper into the hydrophobic ATP binding pocket (Knight et al., 2006). This knowledge helped to understand and develop novel, more specific PI3Ks inhibitors

with reduced toxicity. A number of PI3Ks inhibitors are at the moment in different stages of clinical trials to assess their therapeutic potential. For instance, ZSTK474 is an inhibitor of PI3K γ (IC_{50} at 6nM), PI3K α (IC_{50} of 17nM), and PI3K β (53nM) (Marone et al., 2008), and is currently in a phase I clinical trial study for treatment of Neoplasms (http://clinicaltrials.gov/ct2/show/NCT01280487). Another example is Perifosine, which acts as an Akt inhibitor and as a PI3K inhibitor and is in a phase III trial for colorectal cancer (http://www.clinicaltrial.gov/ct2/show/NCT01097018). Furthermore, Perifosine is in another phase III clinical trial for multiple myeloma (http://www.clinicaltrial.gov/ct2/show/NCT01002248).

In this study selective inhibitors for the p110 alpha, beta and delta isoforms were used and are briefly described below. A summary of the structures of all PI3K inhibitors used in this study is shown in Table 2.2. Two p110α inhibitors, compound 15e and PIK-75, with distinct chemical structures have been used. The synthesis of compound 15e was published in 2006 (Hayakawa et al., 2006) and this study showed an inhibition of A375 cell proliferation with an IC_{50} of 580nM. Besides the original study, information on compound 15e is sparse and its potential effects on other PI3K-related kinases and mTOR are not available to date. PIK-75 in contrast was screened for kinase selectivity and inhibits p110α with an IC_{50} of 5.8nM, while other isoforms are only affected at higher doses; p110β (IC_{50}=1300nM), p110γ (IC_{50}=76nM), p110δ (IC_{50}=510nM) (Knight et al., 2006). Like most p110α inhibitors PIK-75 also inhibits DNA-dependent protein kinase (DNA-PK) quite potently, possibly resulting from a structural similarity in the active site, which is somewhat surprisingly as these kinases share limited sequence identity (Knight et al., 2006). The off target effect of PIK-75 on mTOR is, in this context, rather minor as it lingers in the μM range and is therefore not in the typical applied concentration span of PIK-75. For the p110β isoform, inhibitory compounds of the Thrombogenix series have been developed, including TGX-121 (Robertson et al., 2001) and TGX-221 (Jackson et al., 2004). TGX-221 is more potent than TGX-121, and contributed to deciphering the role of the beta isoform during platelet activation upon fluid sheer stress (Jackson et al., 2005). In 2001, the ICOS Corporation discovered IC87114, the earliest isoform selective inhibitor, exhibiting a 100–1000-fold selectivity for the p110δ isoform over other class I PI3Ks (Sadhu et al., 2001). The selectivity of this

inhibitor is remarkable regarding the high conservation of the residues that line the ATP binding pocket of the class I PI3Ks and its discovery was the first lead for the generation of other selective inhibitors (Knight and Shokat, 2007; Marone et al., 2008). IC87114 contributed to uncover essential roles of p110δ in neutrophil polarisation and their attenuation in specific directional movement (Sadhu et al., 2001), also an involvement in allergic airway inflammation and hyperresponsiveness in a murine asthma model was shown (Lee et al., 2006).

PI3K isoform selective inhibitors are undoubtedly extremely valuable to determine the precise isoform function in the respective environment, but inhibitors targeting multiple known and accurately described pathways, also promise to be an interesting disease treatment option. Once the biological signalling cascades of a disease are correctly profiled, the adequate selective or multi-selective inhibitor can be chosen. An example for a multi-selective inhibitor would be the Piramed compound PI-103, that inhibits p110α and mTor with equipotency. This inhibitor alone stops aggressive glioma cell lines, *in vitro* and *in vivo*, from proliferating (Fan et al., 2006). This effect is comparable to the combination of single specific p110α and mTor inhibitors and therefore unlikely to be an off-target effect (Fan et al., 2006). The success in recent years to develop and validate novel PI3Ks inhibitors will hopefully soon lead to novel treatments of cancer and inflammatory diseases. A structural understanding of the inhibition mechanism is key to solving the remaining challenges of targeting the PI3Ks family pharmacologically (reviewed in Crabbe et al., 2007).

1.7 Pluripotent Cell Types

Harvesting pluripotent cell types, able to differentiate into all three germ layers, was originally only possible using embryonic sources. More recently, researchers tried to establish stable pluripotent cell types from alternative cell sources, applying their acquired knowledge. Tremendous success, beyond common expectations, has been achieved in the recent years and has led to various pluripotent cell types being available for study today. Now there are pluripotent cells established from the germ cell lineage (Ko et al., 2009; Matsui et al., 1992), from post-implantation embryos (Brons et al., 2007; Tesar et al., 2007) and from reprogrammed somatic cells (Takahashi et al., 2007; Takahashi and Yamanaka, 2006). Interestingly, beside stable and fully pluripotent cell types, various metastable and partially reprogrammed states have been identified. Under appropriate culture conditions these states can often be pushed to naïve pluripotency, revealing an unexpected high plasticity (Chou et al., 2008).

1.7.1 Embryonic Germ Cells and Spermatogonial Stem Cells

Pluripotent cell lines can be established from various stages of the germ lineage. In 1992, it was reported for the first time that embryo-derived mouse unipotent primordial germ cells (PGCs) can be converted into embryonic ES-like cells, which were subsequently termed embryonic germ (EG) cells. PGCs are isolated from E8.5-12.5 embryos and can be turned into EG cells when maintained long-term in media supplemented with steel factor, LIF and basic fibroblast growth factor (bFGF) on feeder cells (Matsui et al., 1992; Resnick et al., 1992). In vitro EG cell lines established under these conditions have similar differentiation capacity to ES cells and express genes associated with pluripotency. Furthermore, they fulfill the true hallmarks of pluripotency, giving rise to teratomas when injected into immunocompromised mice and being able to contribute to chimaeras including the germline (Labosky et al., 1994; Matsui et al., 1992). It is noteworthy that PGCs cannot contribute to chimaeras when transplanted directly from the embryo (Matsui et al., 1992). The authors also observed that additional growth factors were only required in the initial derivation of EG cells, once established cells could be maintained in conventional ES cell medium. This might imply that establishment of

EG cells is some sort of reprogramming event triggered by the specific culture growth factor environment, which can result in several unique stem cell ground states (Chou et al., 2008).

In contrast to EG cells, Spermatogonial stem cells (SSCs) are harvested from neonatal mouse testis by dissociating and culturing testis cells in the presence of glial cell line-derived neurotrophic factor (GDNF), epidermal growth factor (EGF), bFGF, and LIF (Kanatsu-Shinohara et al., 2003). In these cultures morphological ESC-like colonies were observed and upon closer examination ES cell markers like Nanog and SSEA1 were detected. These cells were named multipotent germ-line (mGS) cells and are truly pluripotent, as assessed by teratoma formation and generation of chimeras (Kanatsu-Shinohara et al., 2004). Once more, the specific culture growth factor environment seems to be essential for the establishment of mGS cells, as direct transfer of neonatal testis cells into ES cell culture medium fails to produce pluripotent mGS colonies. The establishment of pluripotent cells from the testis of adult mice was reported by selecting for cells that showed GFP expression which was placed under the control of the Stra8 promoter, a marker of spermatogonia (Guan et al., 2006). GDNF was not necessary for ES-like colonies to appear, which is somewhat surprising and not fully understood yet. Another group was also able to generate functional multipotent adult stem cells (MASCs) from adult spermatogonial progenitor cells (SPCs) (Seandel et al., 2007). Orphan adhesion-type G-protein-coupled receptor (GPR125) positive germline progenitor cells were shown to give rise to MASCs upon long-term culture, which are capable of differentiating into derivatives of the three embryonic germ lines and contribute to chimeras. In 2009, Ko and colleagues reported advances in obtaining germline-derived pluripotent stem (gPS) cells from adult germ cells (Ko et al., 2009). They developed a robust and reproducible protocol for establishing gPS cells by defining precise culture conditions and plated cell numbers. Their findings should facilitate further the investigation of the molecular reprogramming mechanisms underlying this conversion and will also allow other influences, such as genetic background or dynamics of the process, to be studied.

To use adult cell sources for the direct generation of multipotent cell types is quite fascinating, as this promises to be an easily accessible autologous stem cell source

which does not require the destruction of embryos (Kanatsu-Shinohara and Shinohara, 2006). This idea was further nurtured by the generation of pluripotent stem cells from adult human testis (Conrad et al., 2008), though this study has so far not been reproduced and is, therefore, highly criticised (Ko et al., 2010). It remains to be seen if it will be possible to transfer the findings from mouse to human, but it is likely that cells of the germ lineage are more susceptible to spontaneous reprogramming events as they already express pluripotency-associated genes.

1.7.2 Induced Pluripotent Stem Cells

For a long time researchers have been seeking an easy way by which to create patient specific pluripotent cells, hence making it possible to use them for treatment without immunorejection. To produce this desired cell type, reprogramming, describing the process of altering the epigenetic status of a somatic cell, is required. Epigenetic marks have to be erased to reset the somatic cell programme and reopen the differentiation potential of the cell. This type of cell was initially produced via cell fusion (Tada et al., 2001) or nuclear transfer (Gurdon et al., 1958), but both approaches have their limitations. Reprogramming somatic cells by fusing them with ES cells is possible, but results in hybrid cells that maintain a tetraploid DNA content, and are therefore not useful for applications (Cowan et al., 2005; Tada et al., 2001). Somatic cell nuclear transfer (SCNT) is a process where the nucleus of a somatic cell is transferred to an enucleated unfertilized oocyte and therefore reset to pluripotency by factors of the egg cytoplasm. Reprogramming by SCNT in mammals was successful for the first time in 1997 with the generation of "Dolly" (Wilmut et al., 1997). Despite this achievement, SCNT is hindered by the obstacles of very low efficiency and the requirement of fresh oocytes, the latter raising the ethical issue surrounding the potential to produce cloned human embryos.

In 2006, Takahashi and Yamanaka showed that somatic mouse fibroblast cells could be reprogrammed into induced pluripotent stem cells (iPSCs) by simply overexpressing four transcription factors: Oct4 (POU5F1), Sox2, Krüppel-like factor 4 (Klf4), and cMyc (Takahashi and Yamanaka, 2006). This was a true breakthrough discovery changing the whole stem cell field in an instant. The use of induced

pluripotent stem cells holds the potential to overcome all previously mentioned barriers and iPSCs are therefore believed to be the future for regenerative medicine and other stem cell based applications. The "gold rush" was not stoppable anymore after two publications showed that this discovery is transferable to the human system (Takahashi et al., 2007; Yu et al., 2007). It came as something of a surprise that Nanog, an important transcription factor for ES cell self-renewal, appeared to be dispensable for iPS cell generation (Takahashi and Yamanaka, 2006), even though Thomsons's group managed to generate human iPS cells by replacing Klf4 and c-Myc with Lin28 and Nanog (Yu et al., 2007). A possible explanation could be that Nanog is not required for the initial steps of reprogramming, but appears to be essential at later stages for reaching the naïve state of pluripotency (Silva et al., 2009). In this case, four factor reprogramming in absence of Nanog activates endogenous Nanog expression, which in return helps to transit from intermediate states to the ground state of pluripotency. Transition might be achieved in a way that Nanog recruits core factor protein complexes or helps to reform the epigenome allowing regions that are required for the transition to be accessed (Silva et al. 2009).

The initial studies used retroviruses to transfect somatic cells with the reprogramming factors, creating the problem of random integration of the factors into the genome and the risk of reactivation during development. This is especially a problem as c-myc and Klf4 are well known oncogenes and indeed the first chimeric mice generated with iPS cells developed tumours (Okita et al., 2007). A wide variety of different reprogramming techniques have been established since to tackle these hurdles and to develop easier platforms for studying reprogramming mechanisms. Integration-free reprogramming was achieved with transient and non-integrative plasmids (Gonzalez et al., 2009; Okita et al., 2008; Yu et al., 2009b), adenoviruses (Stadtfeld et al., 2008b), transgene post-reprogramming excisable systems (Kaji et al., 2009; Woltjen et al., 2009) and by direct delivery of reprogramming proteins into somatic cells (Kim et al., 2009a; Zhou et al., 2009). With the availability of this huge reprogramming toolbox, the molecular mechanisms underlying the change from differentiated to the bona fide pluripotent state began to be revealed.

To reach a true pluripotent state a cell has to overcome several barriers, a process that requires time with current standard protocols. At least 1-2 weeks are necessary

for the first morphological ES-like colonies to emerge. It is tantalising that only a few cells expressing all four factors go on to form iPS colonies. A panoply of theories to explain this phenomenon have been suggested and are still under evaluation. Fluctuation in transgene expression can be excluded as all known methods to produce iPS cells, including polycistronic vectors and secondary iPS systems, exhibit this observation. The theory that there is only a small minority of cells in the total population susceptible for reprogramming is unlikely, as a wide range of cell types have now been used, including terminally differentiated and adult stem cells (Aoi et al., 2008; Stadtfeld et al., 2008a). Nevertheless, there are inter cell type specific differences, for instance keratinocytes exhibited a 100-fold higher reprogramming success rate than fibroblasts (Aasen et al., 2008). In an interesting experiment a donor pre‑B-cell population was transfected and single cells were plated in separate well and as expected a low percentage of cells were successfully reprogrammed after 2 weeks. In the following 16 weeks positive wells (containing at least a few pluripotent cells) reached more than 90%. This paper argues for a stochastic reprogramming event given enough time any cell might be susceptible to move to a pluripotent state. The kinetics of this process are argued to be accelerated by a faster proliferation rate, and therefore increased stochastic probability, as well as by cell division independent mechanisms, as for instance Nanog can increase reprogramming kinetics by activating intrinsic mechanisms, leaving proliferation rate unaltered (Hanna et al., 2009). There is accumulating evidence that there are several epigenetic barriers to be overcome and it is reasoned that only a minority of cells are able to overcome all of them and are therefore fully reprogrammed (Plath and Lowry, 2011; Takahashi, 2010).

The time course of the reprogramming process can be divided into different phases, each exhibiting typical attributes distinguishable by phenotypic, transcriptional and chromatin changes (Figure 1.16) (reviewed in (Plath and Lowry, 2011)). In the early phase of reprogramming, ectopic expression of transcription factors leads to a morphological change into smaller, and more rapid proliferating cells. Somatic genes start to be downregulated while proliferation genes are upregulated. Also the epigenome of the cells are changing, for instance promoter regions of pluripotency-associated genes show increased H3K4 dimethylation (Mikkelsen et al., 2008). It is

noteworthy that most cells, despite expressing all necessary transgenes, drop out already in the first phase of reprogramming (Plath and Lowry, 2011). The intermediate phase of reprogramming is marked by the appearance of cells tightly clustering together exhibiting an epithelial character. ESC marker genes are upregulated, but they are still dependent on transgene expression. Partially reprogrammed ES-like cells often stall at this stage, not reaching a *bona fide* iPSC state. These trapped ES-like cells are termed pre-iPSCs and are a great tool for studying late stages of reprogramming, as it is possible to create clonal populations that can be propagated and driven to mature iPSCs under appropriate conditions (Mikkelsen et al., 2008; Silva et al., 2008). In the late phase, proper ES-like colonies are obvious, key ES cell regulators are transcribed and the core transcription network of pluripotency forms, leading to transgene independence. Full reprogramming is also evident on the chromatin level, where repressive marks are lost and in mouse iPSCs the X chromosome is reactivated. For human iPS cells, X chromosome reactivation was to date not reported (Tchieu et al., 2010), even in conditions favouring X inactivation during hES cell derivation it seems to be not achievable, indicating a later time of development (reviewed in (Plath and Lowry, 2011)). Interestingly, some studies reported that reprogrammed cells were easier to differentiate back to the cell type of their derived origin and it is therefore speculated that they retain an 'epigenetic memory' (reviewed in (Barrero and Izpisua Belmonte, 2011)). Continuous culture of iPS cells seems to reduce epigenetic differences and some studies report that at later passage murine iPS cells are almost indistinguishable from mES cells. Despite these reports there are increasing numbers of studies that raise concerns regarding multiple differences between iPS and ES cells, possibly arising from incomplete reprogramming (reviewed in (Blasco et al., 2011)). It might be misleading to directly compare these studies, as there are likely to be differences between the iPS cell generation and the selection of iPS cell lines considered as being fully reprogrammed. Furthermore, there are significant differences between ES cell lines themselves, so care should be taken when judging whether the differences between iPS cell lines fall into or are clearly distinct from these variations. Apparent differences should be followed and their potential progression to a functional level has to be assessed. Two recent manuscripts argue for a more general genomic instability of human pluripotent lines affecting both hiPS and hES cell lines, though despite both being highly plastic, general differences

shine through (Laurent et al., 2011; Taapken et al., 2011). The process of reprogramming led to deletions including tumour suppressor genes, while long-term culture of iPS and hESCs was accompanied by novel genomic aberrations including copy number variations (CV) of oncogenic genes. These worrying observations have to be followed-up and could result possibly from the non-ideal culture conditions of human pluripotent cell lines. It is of essence to solve these issues, because a common genomic instability would hit stem cell research at its foundation, especially as duplications in regions comprising pluripotency-related genes could cause serious issues in regard of regenerative medicine applications, where pluripotent precursors have to be eliminated to avoid the risk of cancer formation (Laurent et al., 2011).

Remaining issues of concern are how to choose the best iPS and ES cell lines and if they are identical at a functional level. There is no absolute gold standard to solve this problem especially as the best and most stringent test, the tetraploid complementation assay, where pluripotent cells entirely account for the animal, is not ethically applicable for humans (Zhao et al., 2009). It will probably be necessary to decide the most appropriate pluripotent cell type for each application and assess their safety risk carefully.

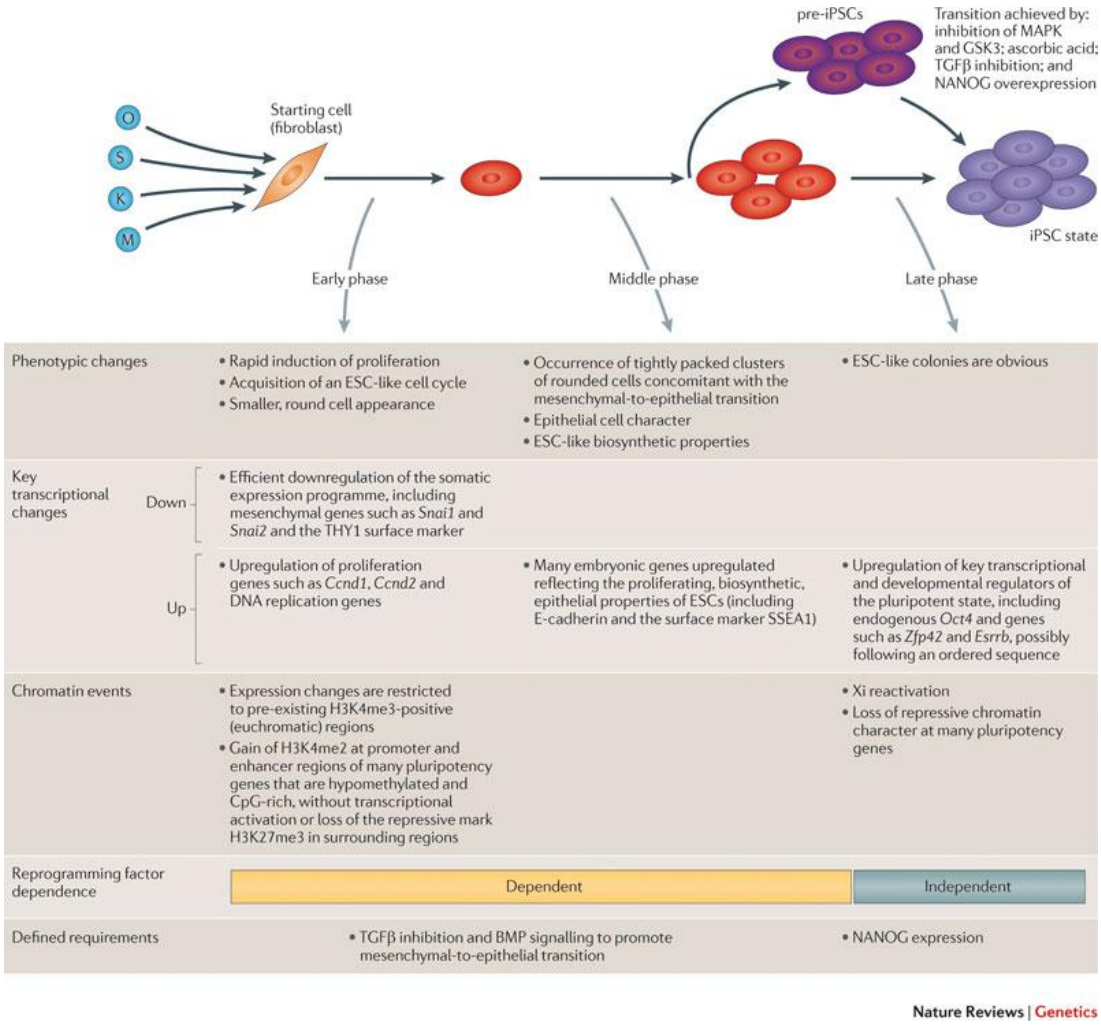

Figure 1.16 The reprogramming process consists of multiple steps. Different events happening during early, middle and late phases of reprogramming mouse embryonic fibroblasts to induced pluripotent stem cells (iPSCs) by the four reprogramming factors (Oct4, Sox2, Klf4, and c-myc) are shown. It is more delicate to separate events happening in the early and middle phase of reprogramming compared to those that occur at the later stage. Image obtained from (Plath and Lowry, 2011).

1.7.3 Epiblast Stem Cells

Epiblast Stem Cells (EpiSCs) are a pluripotent cell type first derived by dissecting and maintaining the epiblast of post-implantation embryos (E5.5-6.5) in special culture conditions (Brons et al., 2007; Tesar et al., 2007). In both studies culture conditions similar to hES cell culture systems succeeded in maintaining the long-term pluripotency of epiblast-derived cells. The presence of Activin A and FGF2 seemed to be optimal for EpiSC self-renewal and similar to hES cells it was necessary to propagate them in clumps rather than following trypsin dissociation. Furthermore, like hES cells, EpiSCs grow as large flattened colonies as opposed to the round domed mES cell colonies. Survival after plating at clonal density was low, but some cells were able to form EpiSC colonies which could again be clump passaged without limit. Pluripotency was proved by teratoma formation after injection into immunocompromised mice, *in vitro* differentiation assays and detection of pluripotency marker gene expresion. Despite being able to form all three germ layers, EpiSCs very poorly contributed to chimeras following morula aggregation or blastocyst injection. Only in one of the two studies were chimeras obtained (2/385) but none of them contributed to the germline (Brons et al., 2007). This could be due to incompatibility between the EpiSCs and the cells of the ICM resulting from a developmental asynchrony limiting the ability of EpiSCs to colonise the host embryo. As these cells apparently cannot form functional gametes they cannot be termed naïve or truly pluripotent, even though a functional core transcription factor network equivalent to ES cells is in place.

The mechanisms to integrate the signals from the surface (extrinsic) to the core (intrinsic) differ between EpiSCs and mES cells and are in fact more similar between EpiSCs and hES cells. EpiSCs appear to be a distinct cell type that is confirmed by analysis of different markers and might reflect the later stage of development from which they are derived. This could become of major interest regarding the similarity to hES cells and raises the possibility that hES cells are also representative of a later developmental stage, meaning that true hES cells are not established yet, but are instead human EpiSCs. Two years after the initial discovery of the EpiSCs, Austin Smith's group showed that mES cells and EpiSCs are interconvertible (Guo et al., 2009). Conversion of ES cells to EpiSCs was achieved by simply transferring mES cells to serum-free N2B27 medium supplemented with Activin A and Fgf2 (bFGF).

The reversion is possible by overexpression of Klf4 or Nanog in media containing inhibitors of Mek/Erk signalling plus LIF (Guo et al., 2009; Silva et al., 2009). In culture conditions considered to be optimal for mES cell (Ying et al., 2008), EpiSCs did not convert spontaneously to naïve pluripotency in the absence of transgene overexpression (Guo et al., 2009). In a more recent paper Najm et al. report the derivation of mES and EpiSCs from pre-implantation mouse embryos (Figure 1.17). A medium optimised for maintaining both ES and EpiSCs was able to support the outgrowth of preimplantation embryos, leading to two distinct morphological colony types (Najm et al., 2011). The round, tight ES colonies and flat EpiSC-like colonies were separated after 16 days and expanded in either media supporting ES or EpiSCs. Interestingly, the divergence appeared to be early as conversion of morphology was never observed (Najm et al., 2011). This raises the question of whether distinct pluripotent cell types relate to each other which might support the hypothesis that the closest *in vivo* counterpart of ES cells are early germ cells (Zwaka and Thomson, 2005).

A direct way of creating EpiSCs from somatic cells was achieved by reprogramming fibroblasts with the four factors, Oct4, Sox2, Klf4 and c-Myc and simultaneously applying EpiSC culture conditions (Han et al., 2011). This study demonstrated the importance of the culture environment being able to determine the cell fate during reprogramming. Cells undergoing reprogramming appear to be very plastic and therefore it might be possible to force cells to a new identity simply by modulating culture conditions. This also becomes of interest regarding transdifferentiation events which could possibly be triggered by forcing closely related cell fates to one or another in specific culture conditions, if necessary with the help of activating specific transcription factors.

In a study performed in Rudolf Jaenisch's laboratory, it was demonstrated for the first time that human fibroblasts, as well as hESCs, can be driven to a naïve state very similar to mouse ESCs or mouse iPS cells (Hanna et al., 2010). This was achieved by overexpressing the transgenes Oct4, Klf4, and Klf2, in addition to culture in LIF and inhibitors of mitogen-activated protein kinase (Erk1/2) and glycogen synthase kinase 3β (GSK-3β) pathway. They showed that these naïve cells were similar to mESCs on a transcriptional level and also on an epigenetic level as

both X-chromosomes were inactivated, a feature that is lost in most if not all derived hES cells (Lengner et al., 2010). On the basis of this study it can be speculated that so far established hES lines are more likely to be hEpiScs or primed hES cells. Further work will be needed to create permanently stable naïve human pluripotent cells, ideally without the use of transgenes. Once this goal is reached, a powerful tool to be used in basic and applied research will be available to tackle human health and development questions, eventually opening up new opportunities for patient-specific treatments.

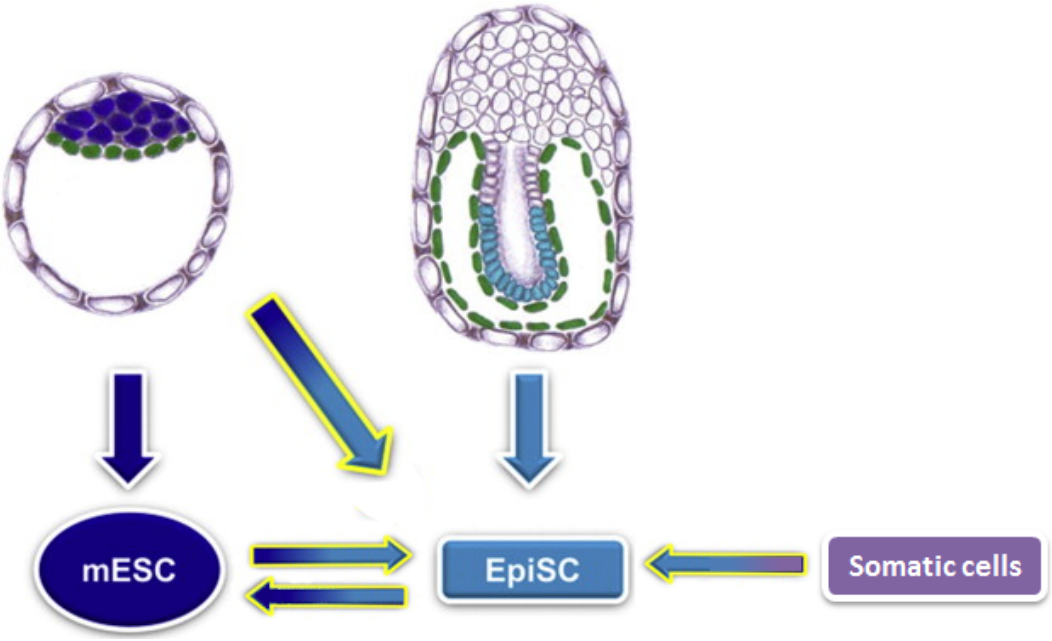

Figure 1.17 Pluripotent stem cell states. Mouse embryonic stem (ES) cells and epiblast stem cells (EpiSCs) are distinct, pluripotent states that can be isolated from pre- and post-implantation embryos respectively. Furthermore, epiblast like stem cells could be established by reprogramming somatic cells in EpiSC culture conditions (Han et al., 2011). Human ES cells differ from mouse ES cells, and share similarities with EpiSCs, yet are derived from pre-implantation human embryos (Najm et al., 2011). Figure adapted from (Najm et al., 2011).

1.8 ZSCAN4

Zscan4 is a novel gene family discovered in this study to be regulated downstream of PI3Ks. In this section the Zscan4 family is introduced, as it was a major focus of this study.

1.8.1 Structure and composition of the Zscan4 family

Zscan4 is a relatively novel gene family consisting of nine members that have been found to be specifically expressed in two-cell embryos and ES cells (Falco et al., 2007). In their 2007 article they identified the Zscan4 family by analysing data of large scale EST and DNA microarray studies. Zscan4 regulation by Zfp206, a putative transcription factor which also regulates other genes important for ES cell differentiation, had previously been reported (Zhang et al., 2006b). Both, Zscan4 and Zfp206 are SCAN domain-containing Zinc finger proteins, which is a common feature in transcription factors. The SCAN domain is a leucine rich region that plays a role in protein-protein interactions. Its name is an artificial word derived from the first letters of the four proteins initially found to contain this domain (SRE-ZBP, CTfin-51, AW-1, Number 18 cDNA) (Williams et al., 1995) and also known as LeR (leucine rich region) (Pengue et al., 1994). Zinc finger domains are best known for their sequence specific DNA binding function, but are also reported to be involved in protein-protein and RNA binding. Because of their high DNA binding specificity it is even possible to design Zinc finger nucleases targeting precise regions of the genome. Therefore, they can be used as a tool for manipulating the genome of higher organisms for which no species specific embryonic stem cells are available (Perez et al., 2008; Urnov et al., 2010). Three of the Zscan4 family members were reported to be pseudogenes by Falco et al. (Figure 1.18). Another third, Zscan4c,d,f are full length proteins consisting of 506aa and more than 94% conserved to each other. They contain a SCAN domain and four Zinc finger domains (Falco et al., 2007). Zscan4A, B and E are shorter versions and were published to encode only for the SCAN part of the protein, though Zscan4B and E appear to be almost full length (505aa) in a recent database search. This will be discussed further as part of the results chapter four.

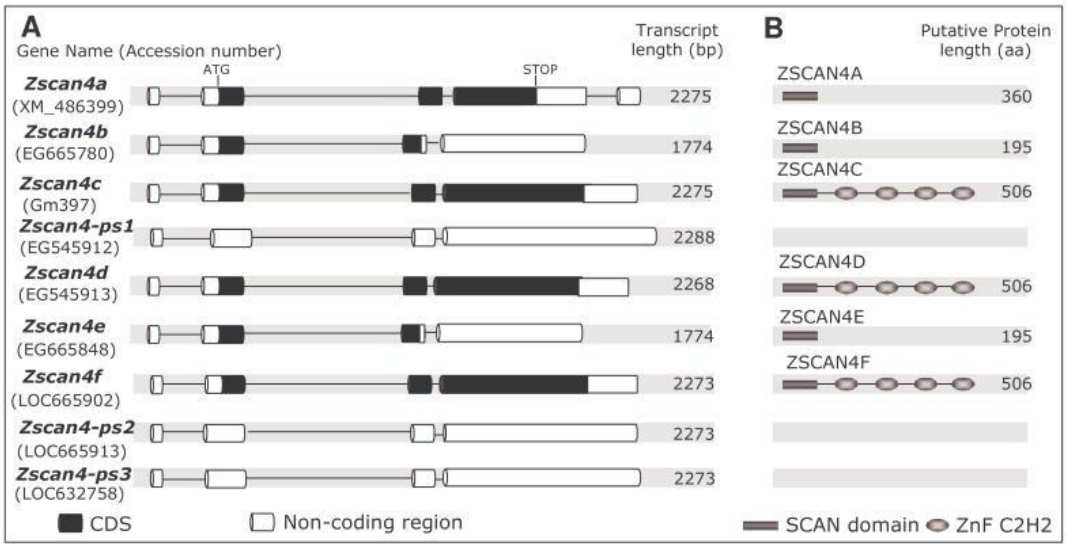

Figure 1.18 The Zscan4 family. (A) The Zscan4 family consists of nine paralog members. Three of them are full length proteins, while the other two thirds are shorter versions or pseudo genes. (B) Predicted protein domains of the Zscan4 family members are shown. Full length proteins contain a SCAN domain and four zinc fingers. (Falco et al., 2007)

1.8.2 Regulation of Zscan4

Zscan4 exhibits a very restricted pattern of expression with a strong peak in the late 2 cell stage during mouse embryonic development. This was shown by profiling the expression of Zscan4 during preimplantation development stages by whole-mount in situ hybridization (WISH) and qRT-PCR analysis (Falco et al., 2007). Interestingly, Zscan4 was undetectable at the blastocyst stage where ES cells are normally derived from. Zscan4 transcripts were re-expressed in mES cells but only by a small fraction of cells within a self-renewing ES cell colony (Falco et al., 2007). This curious expression pattern was reconfirmed in a successive publication by the same group in 2010 (Zalzman et al., 2010). In this study the Zscan4c promoter region was used to drive expression of the Cre-recombinase (CreERT2 fusion enzyme) gene which can translocate to the nucleus in the presence of tamoxifen. Once in the nucleus, it excises a neomycin resistance cassette leading to irreversible activation of LacZ

expression. Using these pZscan4-CreERT2 cells cultured in the presence of tamoxifen, they were able to estimate that every day 3% of the Zscan4 negative cells become Zscan4 positive, whereas 47% of the Zscan4 positive cells lost Zscan4 expression, leading to the equilibrium of 5% positive cells at any given time (Zalzman et al., 2010). These data were obtained via X-gal staining and by flow cytometry after green fluorescent substrate CMFDG (5-chloromethylfluorescein-di-β-galactopyranoside) staining. How this expression pattern is regulated remains to be unravelled but seems to be extremely important for the correct physiological function of Zscan4.

1.8.3 Function of Zscan4

Knock-down of Zscan4 transcript by siRNA injection into the male pronucleus of zygotes leads to a delay in the progression from the 2-cell to the 4-cell stage of embryonic development by about 24h (Falco et al., 2007). This finding is underpinned by another set of experiments in which Zscan4 siRNA was injected into one of the blastomeres of early 2-cell stage embryos. About a third of the treated blastomeres experienced a delay in the division progression compared to the untreated control blastomer. Besides the developmental delay, a functional impairment was also observed. Zscan4 knock down blastocysts neither implanted when transferred to the uterus of pseudopregnant mice nor proliferated normally *in vitro* (Falco et al., 2007). In their following publication they describe an implication of Zscan4 in regulating telomere elongation and genomic stability in mES cells (Zalzman et al., 2010). They show that knock-down of Zscan4 increases karyotype instability, exemplified by chromosome deletions and fusions, a phenotype that can be rescued by overexpression of exogenous Zscan4. Furthermore, mES cells with knocked-down levels of Zscan4 transcript have shorter telomeres, reduced proliferation and go into culture crisis with apoptosis after several passages. Their data also suggests that Zscan4 localizes at the telomeres leading to telomere extension most likely by a recombination process. An increase in telomere sister chromatid exchange (T-SCE) events in Zscan4-induced cells was measured by a telomere chromosome orientation FISH (CO-FISH) assay. The precise molecular recombination mechanism is unclear to date but seems to go in hand with an upregulation of meiosis-specific homologous recombination genes induced by

Zscan4 (Zalzman et al., 2010). Interestingly, sister chromatid exchange (SCE) events in non-telomeric regions, commonly associated with genetic instability, are decreased upon Zscan4 overexpression and increased after knock-down of Zscan4 transcript. This finding further strengthens the important role of Zscan4 in guarding genomic stability of mESCs.

In brief, Zscan4 is a key regulator for maintaining ES cell genetic stability making long term ES cell culture possible. Zscan4 achieves this by positive telomere regulation via recombination mechanisms (Zalzman et al., 2010). The described telomere elongation appears to be independent of telomerase activity and might be therefore related to a telomere elongation mechanism referred to as alternative lengthening of telomeres (ALTs), which is based on homologous recombination (Bryan et al., 1995). Beside this, Zscan4 has most likely other functions and appears to also act as a transcription factor activating and repressing specific target genes (Nishiyama et al., 2009). Furthermore, stem cells and cancer cells share many features in common, and as multiple types of cancers also rely on ALT mechanisms, it can be speculated that a similar molecular machinery underlies this common phenomenon. A potential role of Zscan4 in these cancer types remains to be investigated.

1.9 Aims

The goal of current stem cell research is to increase our understanding of ES cell behaviour, so that one day it will be possible to use their full therapeutic potential, without the risk of unwanted side effects. We are far from a complete knowledge of ES cell behaviour and, therefore, basic studies unravelling the functional mechanisms controlling ES cell fate decisions are essential for reaching this ultimate goal. To use ES cells in future regenerative medicine applications it is necessary to expand them in sufficient numbers. This can be challenging as culture conditions have to be optimal, so that propagated cells do not lose their pluripotent phenotype, while also maintaining genomic stability. The PI3K signalling pathway is a focus of our laboratory and it has been reported by, us and others, to be important for ES cell self-renewal (Niwa et al., 2009; Paling et al., 2004; Storm et al., 2007). The overall aim of this study was to gain further knowledge of the role played by PI3K-dependent signalling in maintaining ES cell identity.

- The first aim of this study was to identify novel regulators of ES cell identity downstream of PI3Ks, based on the list of transcriptional changes obtained by a microarray screen performed prior to the start of this study (Chapter 3). In this microarray screen, mES cells were cultured over a defined time-course in the presence or absence of the broad-spectrum pharmacological PI3K inhibitor LY294002.

- The second aim was to unravel the mechanisms of action of the novel regulators identified by aim 1. Zscan4 was identified as a PI3K downstream target important for maintaining ES cell identity. Over-expression and protein interaction studies were performed to gain further knowledge about its function in mES cells (Chapter 4).

- A third aim focussed on investigating the role of Class I_A PI3K catalytic subunit isoforms in regulation of ES cell identity. This aim was addressed by activation of individual Class I_A PI3K catalytic subunits using a genetic approach (Chapter5).

Chapter 2: Materials & Methods

2.1 Cell lines and tissue culture

2.1.1 Cell lines

2.1.1.1 E14tg2A murine embryonic stem cell line

The E14tg2a murine embryonic stem cell line (clone R63) was a kind gift of Dr. Owen Witte, UCLA, California (Era and Witte, 2000). The R63 cell line stably expresses the tetracycline transactivator encoded by the plasmid pCAG20-1.

2.1.1.2 R1/ pTet-On Advanced embryonic stem cell line

The R1/ pTet-On Advanced murine embryonic stem cell line constitutively expresses the tetracycline-controlled transcriptional transactivator, Tet-On Advanced (Urlinger et al., 2000). The R1/ pTet-On Advanced murine embryonic stem cell line was a kind gift of Dr. Giusi Manfredi, University of Bath, UK.

2.1.1.3 Rex1-Gfp-BSD/Oct3/4-Ecfp-pac murine ES cells (OCRG9 cells)

OCRG9 is a knock-in ES cell line, which contains fluorescent proteins in the Rex1 and Oct3/4 loci to visualize expression of these genes (Toyooka et al., 2008). Cells contain an Oct3/4-ECFP fusion gene and IRES (internal ribosome entry site)-puromycin resistance cassette, which allows for the selection of Oct3/4 positive cells with puromycin. In the Rex1 (also called Zfp42) locus an eGFP and IRES-blasticidin resistance cassette was inserted (Toyooka et al., 2008).

2.1.1.4 EB5 murine embryonic stem cell line

EB5 is a germ line-competent ES cell line derived from E14tg2a, generated by introducing an Oct3/4 knockout vector carrying IRESBSDpA (Niwa et al., 2002; Ogawa et al., 2004). EB5 cells can be selected for Oct3/4 positive cells with blasticidin.

2.1.1.5 Induced pluripotent stem cell line

The induced pluripotent stem cell line used was a kind gift from Dr. Shinya Yamanaka. The iPS cells were established as described in (Okita et al., 2007).

2.1.2 Tissue culture techniques

2.1.2.1 Embryonic stem cell culture

Murine embryonic stem cell lines were routinely cultured on tissue culture plates (Nunc) coated with 0.1% (w/v) porcine gelatin (Sigma) in knock-out (KO) Dulbecco's Modified Eagle Medium (Invitrogen, Scotland) in the presence of 15% (v/v) knock-out serum replacement (Invitrogen), 0.1mM mercaptoethanol, 2mM glutamine and 0.1mM non-essential amino acids. Knockout DMEM plus supplements is referred to as complete KO DMEM media from here on. Alternatively, mES cells were cultured in Glasgow Minimal Essential Medium (GMEM) in presence of 10% (v/v) Hyclone serum (Perbio, Hyclone, UK). Cultures were supplemented with either 1000 units/ml LIF (Chemicon, UK) or 4µl/ml recombinant LIF conditioned media from HEK293LIFV5 cell line generated by stable expression of a V5 epitope-tagged LIF plasmid in HEK293 cells. To passage, cells were washed twice with phosphate buffered saline (PBS) then dissociated with Trypsin/EDTA (Invitrogen) for 5 minutes at 37°C. Dissociated cells were resuspended in complete KO DMEM media, centrifuged at 1000 revolutions per minute (rpm) for 5 minutes and supernatant was removed. After resuspending in complete knockout medium, the concentration of cells in the single cell suspension was determined using a Neubauer haemocytometer. Cells were plated at densities of 0.5×10^6 cells / 10cm dish for passage every two days or 0.2×10^6 cells/dish for over the weekend. Cultures were maintained in humidified incubators at 37°C and 5% (v/v) CO_2. Tissue culture consumables which were used in this study are summarised in Table 2.1.

Table 2.1 Tissue culture consumables

Product	Supplier	Cat. Number
Growth medium		
Glasgow Minimal Essential Medium (GMEM) (GMEM)	Invitrogen, Paisley, UK	21710-025
Knockout Dulbecco's Modified Eagle Medium (DMEM)	Invitrogen	10829-018
Serum		
Knockout Serum Replacement	Invitrogen	10828-028
ES screened Fetal Bovine Serum (FBS) (Hyclone)	Perbio, Hyclone, UK	SH30070.03E
Medium supplements		
ESGRO LIF	Chemicon, Hampshire, UK	ESG1106
200mM L-Glutamine	Invitrogen	25030-024
2-mercaptoethanol (2-ME)	Bio-Rad, Hemel Hempstead, Hertfordshire	161-0710
100x Non-essential amino acids (NEAA)	Invitrogen	11140-050
Monothioglycerol	Sigma	M6145
Sodium Pyruvate	Fisher Scientific	11360
Tetracycline Hydrochloride	Sigma	T7660
Penicillin/streptomycin	Invitrogen	15140-122
Other reagents		
Porcine Gelatine	Sigma	G1890-110G
10x Hanks Balanced Salt Soolution (HBSS)	Invitrogen	14060-040
DMSO	Sigma	D2650
Trypsin-Ethylenediaminetetraacetic acid (EDTA)	Fisher Scientific	25300-062
Phosphate Buffered Saline (PBS)	Invitrogen	14200-067
Tissue culture plastic ware		
15ml centrifuge tubes	Greiner Bio-one (GBO) Gloucestershire, UK	188271
50ml centrifuge tubes	GBO	227261
NUNC cryovials	Fisher Scientific	CRY-960-070B
NUNC tissue culture dish 60 x 15mm	Fisher Scientific	TKT-110-010S
NUNC tissue culture dish 92 x 17mm	Fisher Scientific	TKT-110-070A
NUNC T175 Tissue Culture Falsks	Fisher Scientific	TKT-130-130R
NUNC T75 Tissue Culture Falsks	Fisher Scientific	TKT-130-330J
3ml Pasteur Pipettes	GBO	612398
Petri (non-tissue culture treated) dishes 60 x 15mm	GBO	628160
10ml Single-wrapped Sterile Pipettes	GBO	607180
25ml Single wrappedSterile Pipettes	GBO	760180
150mm unplugged glass pipettes	Fisher Scientific	FB50251

2.1.2.2 Freezing and Thawing mES cells

Ice-cold Glasgow Minimal Essential Medium (GMEM) (Invitrogen), supplemented with 2mM glutamine, 50µM ß-mercaptoethanol, 0.1mM non-essential amino acids, 1mM sodium pyruvate (Invitrogen) and 10% (v/v) Foetal Bovine Serum (FBS) was used for resuspending mES cell pellets, obtained using the routine culture protocol. Cold freezing media plus 10% (v/v) dimethylsulphoxide (DMSO) was added drop-wise to a final concentration of 1 x 10^6 cells/ml. Cells were aliquoted into cryovials (1 ml per vial) and placed at -80°C overnight before being transferred for long term storage in liquid nitrogen.

For recovery, cells were thawed rapidly in a 37°C water bath, gently resuspended in KO DMEM and pelleted at 1000rpm in a Jouan CR412 centrifuge. Cell pellets were resuspended in complete KO DMEM media plus 1000 U/ml LIF, plated and further cultured in humidified incubators at 37°C with 5% CO_2 (v/v) .

2.2 Inhibitors used in the study

Details of pharmacological inhibitors used in this study to assess roles of PI3Ks on gene regulation and mES cell identity (Table 2.2).

Table 2.2 Pharmacological Inhibitors

NAME	STRUCTURE	DESCRIPTION	SOURCE
LY294002	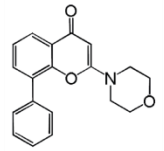	LY294002 is a selective phosphatidylinositol 3-kinase (PI3K) inhibitor, inhibiting class IA PI3Ks. IC50: PI3K 1.4 μM p110α 9.3 μM, p110β 2.9 μM, p110δ 6.0 μM, p110γ 38 μM mTOR 8.9 μM Vlahos, C.J., et al. (1994) J Biol Chem 269 5241-5248.	Calbiochem & Sigma
PI-103	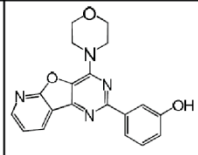	PI-103 is a potent, cell-permeable, ATP-competitive inhibitor of phosphatidylinositol 3-kinase (PI3K) family members with selectivity toward DNA-PK, PI3K (p110α), and mTOR. IC50: DNA-PK 2nM, p110α 8nM, mTORC1 20nM, p110δ 48nM, mTORC2 83nM, p110β 88nM, and p110γ 150nM. Fan, Q., et al. (2006) Cancer Cell 9 341-349.	Generous gift from Tom Crabbe & Cayman Chemical
PIK-75	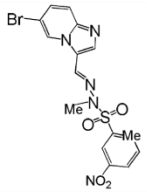	PIK-75 is an imidazopyridine that selectively inhibits p110α with an IC50 value of 5.8 nM.2 It inhibits p110γ and p110β considerably less effectively with IC50 values of 0.076 μM and 1.3 μM, respectively. Knight, Z.A., et al. (2006) Cell 125 733-747.	Generous gift from Peter Shephard, Auckland, NZ & Cayman Chemical
Compound 15e	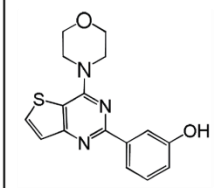	Specific inhibitor of phosphoinositide 3-kinasep110α isoform (IC50=2nM). p110β isoform (IC50=16nM) p110γ isoform (IC50=0.66μM) Inhibits proliferation of A375 melanoma cells (IC50=0.58μM). Hayakawa, M., et al. (2006). Bioorg Med Chem, 14(20) 6847-6858.	Alexis Biochemicals, Nottingham, UK
IC87114	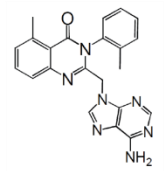	A potent, cell-permeable, ATP-competitive and selective inhibitor of PI 3-K isoform p110δ (IC50 = 60 nM). Inhibits p110α and p110β only at higher concentrations (>1 μM). IC87114 does not inhibit other PIK-related kinases such as ATM, ATR, DNA-PK, and mTOR even at concentrations up to 100 μM. Chaussade, C., et al. (2007). Biochem. J. 404, 449.	Generous gift from Tom Crabbe & Cayman Chemical
TGX-121	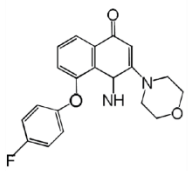	IC50: PI3K 0.05 μM p110β 0.05 μM p110γ 5 μM Robertson, A. D., et al. (2001). Pat., I WO/2001/053266. Kuang, R. R., et al. (2006). Eur J Med Chem 41(4) 558-65	Generous gift from Tom Crabbe
TGX-221	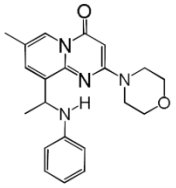	Potent, selective, and cell permeable inhibitor of p110β. Inhibition appears to occur at the ATP binding site based on the observed increase in IC50 from 5 to ~50 nM at ATP concentrations of 50 μM and 1 mM, respectively. TGX-221 inhibits PtdIns-(3,4)-P2 production in platelets with an IC50 of 50 nM. Jackson, S.P., et al. PI 3-kinase p110β (2005). Nat Med 11(5) 507-514.	Generous gift from Peter Shephard, Auckland, NZ & Cayman Chemical
Rapamycin	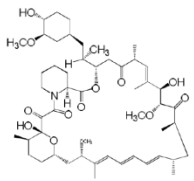	Rapamycin specifically interacts with the cytosolic FK-binding protein 12 (FKBP12) to form a complex which inhibits the mammalian target of rapamycin (mTOR) pathway by directly binding to mTOR Complex 1 (mTORC1) Inhibition of p70 S6K activity in 3T3 cells IC50 50 pM Kuo C.J., et al. (1992). Nature, 358(6381) 70-3.	Calbiochem

2.3 Biochemical and functional techniques

Biochemical consumables used in this study are summarised in Table 2.6.

2.3.1 Bradford protein quantification assay

A Bradford assay (Bradford, 1976) was performed to determine protein concentrations of cell lysates. This assay utilises an absorption shift of the Coomassie brilliant blue dye at 595nm when bound to arginine and hydrophobic residues in a protein. To generate a standard curve, BSA was added to 1ml aliquots of 1:10 diluted Bradford reagent (Biorad) at a final concentration of 0, 2, 4, 6, 8, 10 or 12μg/ml. 1-5μl of the protein extract samples were added to 1ml of 1 in 10 Bradford reagent and mixed well. 100μl of each sample was added to the wells of a 96 well tray and the optical density at 595nm was determined on a Versamax microplate reader (Molecular Devices). A standard curve was constructed from the BSA standards and sample protein concentrations were extrapolated. The same amount of protein (10-20μg) was taken from each sample, diluted with lysis buffer, and boiled in SDS sample buffer (5x sample buffer; 10% SDS (w/v), 50% glycerol (v/v), 200mM Tris-HCl pH 6.8, 5% (v/v) 2-mercaptoethanol and 2% (w/v) bromophenol blue.

2.3.2 Protein resolution and immunoblotting

2.3.2.1 Sodium dodecyl sulphate polyacrylamide gel electrophoresis (SDS-PAGE)

SDS-PAGE is a technique used to separate protein samples according to their molecular size using a gel electrophoresis system. Samples were boiled in a buffer containing 2-mercaptoethanol which denatures protein structure and disrupts (reduces) disulphide bonds. The ionic detergent SDS is another component of the buffer, and binds linear proteins at a rate of 1.4g SDS per 1g protein. This leads to a roughly equal charge to mass ratio for different proteins, allowing proteins to be separated by polypeptide size alone. Samples were loaded into individual wells of the upper stacking gel, which is a non-restrictive large pore matrix. The stacking gel is prepared with Tris/HCl buffer pH 6.8, at this pH glycine is only weakly ionised and moves slowly. NaCl, also present in the buffer, is fully ionised and moves faster.

The level of protein ionisation is in between those of Glycine and NaCl, hence the proteins move in between the boundaries of NaCl and Glycine. This leads to a focusing of the proteins at the small porous resolving gel, where the glycine becomes highly ionised because of the higher pH of 8.8. Glycine will start to migrate much faster, which relieves the boundary, and proteins will separate according to their size (Laemmli, 1970).

Mini Protean III Gel Electrophoresis Apparatus (Bio-Rad) was used to prepare gels and perform electrophoresis according to the manufacturer's guidelines. The percentage of acrylamide used in the resolving gel was dependent upon the size of the target proteins (Table 2.3).

Table 2.3 Resolving power of gels with different acrylamide percentages

% acrylamide	Size of target protein (kDa)
7.5	40-200
10.0	25-200
12.0	15-100

The resolving gel was prepared at the desired percentage of acrylamide (Table 2.4) and ~4.5ml was poured into the gel casting apparatus. The resolving gel was overlaid with water and allowed to polymerise, before the water was removed by aspiration. The stacking gel (1.67ml acrylamide, 6ml milli-Q H_2O, 1.25ml 1M Tris-HCl pH6.8, 0.15ml 10%(w/v) SDS, 50µl 10% (w/v) ammonium persulphate and 20µl TEMED) was poured on top and a fifteen well comb was inserted to create the wells. The comb was removed after solidifying of the gel and the wells were washed with milliQ water. The gel was placed into a gel tank filled with 1x SDS-PAGE running buffer (25mM Tris base, 192mM glycine, 0.1% (w/v) SDS) and samples were then loaded into the wells. SDS-PAGE broad range molecular weight marker (Biorad)

was also loaded into a separate well. Samples were run with a constant voltage of 80mV through the stacking gel and at 180mV to resolve.

Table 2.4 Acrylamide resolving gel compositions

Acrylamide (%)	Bis/Acryl (ml)	Milli-Q H2O (ml)	1M Tris-HCl pH 6.8 (ml)	10% (w/v) SDS (ml)
6.0	3.0	6.35	5.6	0.25
6.5	3.25	6.1	5.6	0.25
7.0	3.5	5.85	5.6	0.25
7.5	3.75	5.6	5.6	0.25
8.0	4.0	5.35	5.6	0.25
10	5.0	4.35	5.6	0.25
12	6.0	3.35	5.6	0.25
15	7.5	1.85	5.6	0.25
50µl 10% (w/v) ammonium persulphate and 20µl TEMED were added to each mix				

2.3.2.2 Immunoblotting by Semi-Dry Transfer

Immunoblotting was used to transfer the proteins from SDS-PAGE gels onto nitrocellulose paper. Therefore, gels were placed onto a piece of nitrocellulose, sandwiched between four buffer-soaked (39mM glycine, 48mM Tris base, 0.0375% (w/v) SDS, 20% (v/v) methanol) 3MM Whatman paper. This stack was placed between the lower (positive) and the upper (negative) electrode of the transfer apparatus. Immunoblotting was performed with a current of 0.8mA per cm^2 for 60 minutes. Ponceau S was used to check protein transfer, equal loading and to mark the molecular weight standards. After washing in TBS (20mM Tris-HCl pH7.5, 150mM NaCl) blots were blocked for 1 hour in blocking solution (5% (w/v) Bovine serum albumen (BSA), 1% (w/v) ovalbumin, 0.05% (w/v) sodium azide in TBS) or Advance blocking solution (200mg ECL advance blocking agent /10ml TBS)) and rinsed afterwards with TBS. Blots were incubated overnight with primary antibody (see Table 2.5) diluted in blocking buffer before being washed once in TBS, three times with TBS Tween (TBST) (0.05% Tween in TBS) for 15 minutes and a final TBS wash.

Horseradish peroxidase (HRP) labelled secondary antibody were then applied and blots were incubated for 1 hour. Blots were washed as before with an additional final TBS wash. Enhanced Chemiluminescence Western blotting detection reagent (Amersham) was applied for 1 minute. Blots were wrapped in Clingfilm and placed in an autoradiography cassette. ECL signal was detected with Kodak X-AR5 film.

For reprobing blots with a different antibody, the blots were stripped in stripping buffer (6.25% (v/v) 1M Tris-HCl pH 7.5, 2% (w/v) SDS, 0.77% (v/v) ß-mercaptoethanol) at 55°C for 45 minutes. After stripping blots were washed thoroughly in TBS and blocked in blocking buffer for 1 hour. Rinsed blots were reprobed as mentioned.

Table 2.5 Antibodies used for immunoblotting

Antibody	Source	Blocking	Dilution	Diluent	Supplier	Cat. No.
Primary antibodies						
α-Nanog	Rabbit	ECL Adv.	1:5000	ECL adv.	Abcam	# ab21603
α-Oct4	Rabbit	ECL Adv.	1:1000	ECL adv.	Santa Cruz	# sc-9081
α-p110α	Rabbit	5% BSA	1:1000	1% BSA	Santa Cruz	# sc-7174
α-p110β	Rabbit	5% Milk	1:1000	1% Milk	Santa Cruz	# sc-7175
α-pAkt (Ser 473)	Rabbit	5% BSA	1:1000	1% BSA	Cell Signaling	# 9271
α-Akt	Rabbit	5% BSA	1:1000	1% BSA	Cell Signaling	# 9272
α-phospho-S6	Rabbit	5% BSA	1:1000	1% BSA	Cell Signaling	# 2211
α-S6	Rabbit	5% BSA	1:1000	1% BSA	Cell Signaling	# 2708
α-Ctbp2	Rabbit	5% BSA	1:1000	1% BSA	Abcam	# ab113265
α-Lsd1	Rabbit	5% BSA	1:1000	1% BSA	Abcam	# ab17721
α-V5	Mouse	ECL Adv.	1:5000	ECL adv.	Abcam	# 27671
α-GFP	Rabbit	5% BSA	1:1000	1% BSA	MBL	# 598
α-TBP	Rabbit	5% BSA	1:1000	1% BSA	Abcam	# ab51432
α-Shp-2	Rabbit	5% BSA	1:2000	1% BSA	Santa Cruz	# sc-280
α-Gapdh	Mouse	5% Milk	1:1000	1% Milk	Abcam	# ab9484
Secondary antibodies						
Mouse-HRP	Goat	-	1:10000	TBST	Dako	# P0447
Rabbit-HRP	Goat	-	1:20000	TBST	Dako	# P0778

2.3.3 Cytosolic/nuclear protein extraction

For the separation of cytosolic and nuclear protein fraction two different methods were used. The NE-PER nuclear and cytoplasmic extraction reagents (PIERCE Biotechnology, #78833) were used according to the manufacturer's protocol. For the GFP-Nanotrap (Chromotek) the following protocol was used. ESCs were harvested after trypsinisation in 50ml tubes (4 x T175 flasks per tube) by centrifugation at 1000 x *g* for 5 minutes at 4°C. Cytosolic extraction was performed after washing the cell pellet twice in cold PBS by resuspending pellets in 6ml cold cytosolic lysis buffer (20mM HEPES, 10mM KCl, 1mM EDTA, 10% glycerol, pH 7.9) and incubation on ice. Cells were then pulled 10 times through a 27G (0.4mm) needle and centrifuged at 16300 x *g* for 5 minutes at 4°C. The supernatant contained cytosolic proteins and was kept on ice until further use. The pellet containing the nuclear fraction was washed twice in 500µl cytosolic extraction buffer and centrifuged at 16300 x *g* for 5 minutes at 4°C. Nuclear proteins were extracted by addition of 2ml of nuclear extraction buffer (20mM HEPES, 10mM KCl, 400mM NaCl, 1mM EDTA, 20% glycerol, pH 7.9) per nuclear pellet and incubated on a rotator for 1 hour at 4°C. Extracts were then centrifuged (16300 x *g* for 15 minutes at 4°C) and the supernatant, containing nuclear proteins, was collected. All buffers contained fresh protease and phosphatase inhibitors (1mM phenylmethylsulfonylfluoride (PMSF), 1µg/ml aprotinin, 1µg/ml leupeptin, 1µg/ml pepstatin, 5µg/ml anipain, 157µg/ml benzamidine, 5mM β-glycerophosphate, 5mM NaF 1mM Na_3VO_4).

2.3.4 Immunoprecipitation with GFP-Nanotrap (Chromotek)

Cytosolic and nuclear cell extracts were prepared as described in 2.3.3. Cytosolic and nuclear fractions containing soluble protein were cleared by ultra-centrifuging for 30 minutes with 60,000 x *g* at 4°C in a Beckman Coulter ultra-centrifuge. A subsequent buffer exchange to IP buffer (50mM Na_2HPO_4, 150mM NaCl, pH 7.4) was performed using Amicon centrifugal filters with a 10kDa cut-off according to the manufacturer's protocol. Prior to immunoprecipitation (IP) lysates were pre-cleared with hydrated agarose or sepharose beads for 1h at 4°C on a rolling shaker. IPs were performed with 500µl GFP-Trap-A beads (Chromotek) for 1-3 hours on a rolling shaker at 4°C, followed by three washes with IP buffer. Bound protein was

eluted with 200mM glycine at pH 2.5 and 1M Tris-base (pH 10.4) was added for neutralization. The eluates were centrifuged at 1000rpm for 1 minute and the supernatant without beads was transferred to Amicon centrifugal filters with a 3kDa cut-off for concentration, according to the manufacturer's protocol. SDS loading buffer was added to samples and samples were boiled for 5 minutes before running on an SDS-PAGE gradient gel.

2.3.5 Immunochemistry

To obtain confocal images, ESCs were cultured on Lumox (Sarstedt) or chamber cover glass (NUNC) trays. Following the culture period, cells were fixed with 4% (w/v) paraformaldehyde (PFA) for 15 minutes at room temperature. Cells were permeabilised in PBST (PBS containing 0.2% Triton X-100), incubated with PBS containing 2%(v/v) FCS for 20 minutes to block non-specific binding and incubated with primary antibody overnight at 4°C. Dilution ratios of primary antibodies used are: 1:500/1:100 for anti-Nanog antibody, 1:500 for anti-V5 antibody, 1:200 for Oct-4 antibody, 1:2000 for E-cadherin antibody, 1:250 for anti-pericentrin antibody. After washing with PBS, the cells were incubated with respective secondary Alexa-Fluor antibodies (1:500) for 30 minutes at room temperature. Cells were then washed and counterstained for 10 minutes with 0.5μg/ml DAPI (4',6-diamidino-2-phenylindole) (Sigma) or 0.5μg/ml Hoechst (Sigma), washed again and mounted in MOWIOL. Images were captured using a Leica TCS SP5 confocal microscope system (Leica Microsystems) or a Zeiss 10 Meta confocal microscope.

2.3.6 Flow cytometry

2.3.6.1 Cell cycle analysis

For cell cycle analysis, Zscan4c-Tet-off Clones were grown in presence and absence of 1μg/ml tetracycline for 48h. Cells were fixed in ice-cold 70% (v/v) ethanol and occasionally stored at -20°C for up to 2 weeks until further use. Cells were rehydrated in PBS + 1% (w/v) BSA at 4°C for 10 minutes and stained with the DNA dye 7-AAD (25 μg/ml) at 4°C for 90 minutes. Zscan4c was labelled with 5μg/ml anti-V5 antibody and a FITC conjugated secondary antibody. Zscan4c expression and 7-AAD staining was monitored by flow cytometry of 10000 events on a FACSCanto™ flow cytometer and analysed using FACS Diva software.

2.3.6.2 Detection of GFP-positive ESCs

Flow cytometry was used in this study to detect ES cells expressing GFP, on two different occasions. Firstly, to quantify the percentage of eGFP-Zscan4c positive cells after induction of expression with 1μg/ml doxycycline for 72h. Secondly, Rex1-GFP expression was measured as a read-out for self-renewal in OCRG9 ES cells following treatment with specific PI3K inhibitors. Prior to flow cytometry, cells were trypsinised as described in 2.1.2.1 and washed twice in cold FACS buffer (1% (v/v) FCS, 0.02%. (w/v) sodium azide in PBS) Approximately $0.5x10^6$ cells were resuspended in 500μl FACS buffer supplemented with Propidium iodide (1:5000) and transferred to FACS tubes. Dead cells stained with propidium iodide were excluded from the analysis and 10000 live events were counted on a FACSCanto™.

2.3.6.3 Gating for GFP-positive cells

Gate for GFP-positive cells was set by using wild-type cells. Propidium iodide was used to analyse live cells.

Table 2.6 Biochemical consumables

Product	Supplier	Cat. Number
Preparation of cell extracts		
Aprotinin	Roche Biochemicals, Burgess Hill, UK	236624
Bromophenol blue	BD electran	44305
Bradford Reagent	Bio-Rad	500-006
GFP-Trap®	Chromotek	gt-250
Glasgow's Modified Eagle Medium	Invitrogen	21710-025
200mM Glutamine	Invitrogen	25030-024
Glycerol	Sigma	G5150
1M HEPES	Invitrogen	15630-056
Leupeptin	Sigma	G5150
Nonidet P40	VWR, Leicestershire, UK	560092-L
Pepstatin	Sigma	P5318
Phosphate buffered saline (PBS)	Invitrogen	18912-014
PMSF	Sigma	H0891
Protein Sepharose A	Amersham/GE Healthcare, Buckinghamshire, UK	17-0780-01
Protein Sepharose G	Amersham/GE Healthcare	17-0618-01
Sodium chloride	Sigma	S7653
SDS	VWR, Leicestershire, UK	442444-H
Sodium fluoride	Sigma	S6521
Sodium Molybdate	VWR, Leicestershire, UK	102542-Q
Sodium Vanadate	Sigma	S6508
Soybean Trypsin Inhibitor	Sigma	T9003
Trizma (Tris) base	Sigma	T8404
Protein resolution and immunoblotting		
30% Acrylamide:Bis 37.5:1	Bio-Rad	161-0158
Ammonium persulphate	Sigma	A7460
Bovine Serum Albumin (BSA)	Roche Biochemicals	735-108
ECL	Amersham/GE Healthcare	RPN-2106
ECL Advance	Amersham/GE Healthcare	RPN-2135

Glycine	Sigma	G8790
Methanol	Fisher	M-4056-17
2-mercaptoethanol	Bio-Rad	161-0710
Nitrocellulose	Amersham/GE Healthcare	RPN203D
Ovalbumen	Sigma	A5378
Ponceau S	Sigma	P7170
Sodium azide	Fischer	S-2380-48
TEMED	Sigma	T9281
3MM Whatman paper	VWR	3030917
Immunochemistry		
α-Ecadherin	Takeichi Lab, CDB RIKEN, Japan	
α-Nanog	R&D Systems, Minneapolis, USA	MAB1997
α-Nanog	Abcam	ab21603
α-Oct4	Santa Cruz	sc-9081
α-pericentrin	Covance, New Jersey, USA	PRB-432C
α-V5	Abcam	27671
α-rat IgG (594)	Invitrogen	A-11007
α-mouse IgG (488)	Invitrogen	A-11029
α-rabbit IgG (555)	Invitrogen	A-21429
Chambered coverglass	NUNC	155409
Lumox 24-well trays	Sarstedt, Nümbrecht, Germany	440592
Paraformaldehyde	Sigma	15812
Pertex Mounting Media	Cell Path	SEA-0104-00A
Dapi	Sigma	D9542
Hoechst	Sigma	23491-52-3
Flow cytometry		
7AAD	Sigma	A9400
FACs tubes	BD Biosciences	6297461
Propidium iodide	Sigma	81845

2.3.7 Functional assays

2.3.7.1 Self-renewal Assay (Alkaline Phosphatase assay)

The undifferentiated state of ES cells can be characterized by high levels of expression of Alkaline Phosphatase (AP) (Pease et al., 1990; Scutt and Bertram, 1999).

ES cells were plated at $1.5x10^3$ cells per well of a 6-well NUNC tissue culture plate coated with 0.1% (w/v) porcine gelatin in GMEM media with 10% (v/v) serum and 1000U/ml LIF (Chemicon). For some experiments, limited LIF concentrations were used, these are indicated accordingly. Cells were washed twice with PBS and fixed with 100% methanol for 10 minutes. Methanol was aspirated and dishes were allowed to air dry. Fixed colonies were incubated for 20 minutes with a solution of 0.1M Tris-HCl pH 9.2, 200µg/ml Naphthol AS-MX and 1mg/ml Fast Red TR Salt. Self-renewing colonies expressing alkaline phosphatase stained red, while differentiated colonies remain unstained. Dishes were washed twice with dH_20 and allowed to air dry. Colonies were counted according to their staining and morphology. Non-self-renewing colonies were either unstained (white) or light red with a flattened morphology, while self-renewing colonies were tight round and stained bright red or exhibited a stained red core with a white border. All colonies were assessed in each well and scored according to the extent of staining and appearance.

2.3.7.2 XTT cell metabolism assay

The XTT assay was used to measure the metabolic activity of ESCs. The assay was adapted from earlier studies on activated T cells and from studies investigating viability and proliferation of tumour cell lines (Roehm et al., 1991; Scudiero et al., 1988). The colorimetric assay is based on the cleavage of the yellow tetrazolium salt XTT, sodium 3'-[1-[(phenylamino)-carbonyl]-3,4-tetrazolium]-bis(4-methoxy-6-nitro) benzene-sulfonic acid hydrate yielding to a highly coloured water soluble formazan product. The cleavage is catalysed by the dehydrogenase enzymes of metabolically active cells. The bioreduction of XTT is potentiated when used in combination with the electron coupling agent phenazine methosulfate (PMS).

Prior to the performance of the assay, murine Zscan4c Tet-off ES cells were plated in presence and absence of 1μg/ml tetracycline on a NUNC flat bottomed 96-well plate at a density of 200 cells per well in GMEM plus 10% (v/v) Hyclone serum, or in complete KO DMEM medium, supplemented with 1000U/ml LIF. 50μL PMS-XTT solution was added per well after d5 or d6 of culture and incubated for 4 hours. The absorbance at 490nm was read on a Versamax microplate reader.

Table 2.7 Functional assay consumables

Product	Supplier	Cat. Number
Self-renewal assay		
Naphthol AS-MX	Sigma	N4875
Fast red TR salt	Sigma	F2768
XTT dye reduction assay		
XTT Salt	Sigma	X4626
Phenazine methosulfate (PMS)	Sigma	P5812

2.3.7.3 Embryoid body differentiation assay

The embryoid body formation assay protocol is based on earlier studies on embryonic stem cell differentiation to hematopoietic lineages (Keller et al., 1993; Kennedy et al., 1997). ESCs were trypsinised and resuspended at a concentration of $1x10^4$ cells/ml in Iscove's Modified Dulbecco's Medium (IMDM) and mixed in a ratio of 1:1 with 2% (v/v) methylcellulose in IMDM. The mix was supplemented with 450μM MTG, 50μg/ml L-ascorbic acid, 10μg/ml recombinant human insulin, 200μg/ml transferrin and 15% (v/v) FCS. After vortexing, the mix was aliquoted into 30mm non-adherent petri dishes and further cultured in humidified incubators at 37°C with 5% CO_2 (v/v) for up to six days.

2.4 Molecular Techniques

2.4.1 RNA extraction

2.4.1.1 RNeasy Mini Kit (Qiagen)

RNA was extracted using Qiagen RNeasy kits according to the manufacturer's protocol. In addition, on-column DNase treatment with an extended (> 30 minutes) digestion time was performed to remove genomic DNA. Cell lysates were homogenized by passing them at least 5 times through a blunt 20-gauge needle (0.9mm diameter) fitted to an RNase-free syringe before transfer to the RNeasy spin columns. RNA was eluted in 30µl RNase-free water and quantified with a spectrophotometer.

2.4.1.2 TRIzol Method for RNA Isolation

Cells were washed twice with PBS and 1ml TRIzol reagent was added per $1x10^6$ cells. Sterile cell scrapers were used to harvest RNA and lysate was transferred to sterile RNase-free 1.5ml tubes. 200µl of Chloroform were added per tube and mixed vigorously. Tubes were centrifuged at 14000rpm at 4°C for 15 minutes. Upper aqueous phase was transferred to a new RNase free 1.5ml tube. For RNA precipitation an iso-volume of 2-Propanol was added and after 10 minutes incubation at room temperature the mix was centrifuged for 10 minutes at 14000rpm at 4°C. After a 75% (v/v) ice cold Ethanol wash, the RNA pellet was allowed to air dry and resuspended in RNase free H_2O. RNA samples obtained with the TRIzol method were further DNase treated to remove contaminating genomic DNA. Therefore, 1µg or 0.5µg RNA was incubated with 1U DNase (Promega) in DNase buffer (400mM Tris-HCl pH8.0, 100mM $MgSO_4$, 10mM $CaCl_2$) (Promega) at 37°C for 30 minutes. DNase was heat inactivated at 65°C for 10 minutes with 1µl DNase stop solution (20mM EDTA pH8.0).

2.4.2 cDNA synthesis

DNase treated RNA samples (0.5-2µg RNA) were incubated at 65°C for 5 minutes with 0.5µl of 500µg/ml Oligo dT (Promega) then kept on ice for at least 1 minute. RT-PCR was performed using first strand buffer (Invitrogen), 5mM DTT (Invitrogen), 2U/µl Rnasin plus (Promega), 0.5mM dATP, 0.5mM dTTP, 0.5mM dGTP, 0.5mM dCTP (Invitrogen) and 10U/µl Superscript III (Invitrogen). Samples were incubated at 42°C for 50 minutes for elongation, then at 70°C for 15 minutes to denature. The resulting cDNA was usually diluted 1:10 in sterile water and used as template for PCR analysis, cloning or stored at -20° for later use.

2.4.3 Quantitative real-time PCR (qRT-PCR)

Quantitative RT-PCR was performed on a Roche Molecular Biochemical LightCycler to quantify gene specific expression using appropriate primers (Table 2.9). SYBR Green dye was used, which intercalates with double stranded DNA, resulting in an increase in fluorescence. Based on this principle, online monitoring and quantification of double stranded PCR product is possible using the Lightcycler. A master mix composed of 0.5µM primers, 3.5mM $MgCl_2$, 1µl SYBR Green and sterile water to 8µl was added to pre-chilled capillaries, prior to addition of 2µl of diluted cDNA sample. The capillaries were then centrifuged at 4000rpm for 20 seconds at 4°C. An amplification program with 40 cycles was run and melting curves were analysed to check the size of desired PCR product. For LightCycler program used see Table 2.8. LightCycler software (v4.0) uses monitored amplification slopes to calculate PCR efficiencies which are further used to calculate the relative quantification values normalized to the one of a calibrator. Gapdh or β-actin were used for normalisation.

Table 2.8 LightCycler program

Stage	Temperature	Duration	Cycles
Hot start	95°C	10 minutes	
Inition elongagion	95°C	30 seconds	
Denaturation	95°C	10 seconds	40 cycles
Annealing	Primer dependent (Table 2.9)	5 seconds	
Elongation	72°C	16 seconds	
Melting curve	65-95°C	0.1°C/sec	

Table 2.9 Primers used for quantitative RT-PCR

Gene annotation	Primer Sequences		Annealing Temperature
AF067061	sense	5'-TGTTTCAGCAAACGAGCAAAGC	58°C
	anti-sense	5'-CCTGAGCAAGCTGGAGGGTTG	
β-actin	sense	5'-TAGGCACCAGGGTGTGATGG	62° C
	anti-sense	5'-CATGGCTGGGGTGTTGAAGG	
Baz1a	sense	5'-ATAGAACAGGGCATTGAACG	64°C
	anti-sense	5'-CATCAGGAACAGCCTTGAGC	
Gapdh	sense	5'-ACCACAGTCCATGCATCAC	58°C
	anti-sense	5'-TCCACCACCCTGTTGCTGTA	
Klf4	sense	5'-CCAGCAAGTCAGCTTGTGAA	58C
	anti-sense	5'-GGGCATGTTCAAGTTGGATT	
LOC327811	sense	5'-GAATTTGGCTGCCGACTGTACC	64°C
	anti-sense	5'-GCTTCCCACCAGTATCCACG	
Nanog	sense	5'-CTCTTCAAGGCAGCCCTGAT	60°C
	anti-sense	5'-CCATTGCTAGTCTTCAACCAC	
Nanog *	sense	5'-CCAGGTTCCTTCCTTCTTCC	58°C
	anti-sense	5'-GGTGAGATGGCTCAGTGGAT	
Oct3/4	sense	5'-GCGTTCTCTTTGGAAAGGTGTTC	58°C
	anti-sense	5'-CTCGAACCACATCCTTCTCT	
Oct3/4 *	sense	5'-TGCCATCACTGCCACCCAGAAGACTG	58°C
	anti-sense	5'-TGAGGTCCACCACCCTGTTGCTGTAG	
Rex1	sense	5'-CGTGTAACATACACCATCCG	55°C
	anti-sense	5'-GAAATCCTCTTCCAGAATGG	
Shp-1	sense	5'-TGTCTACCTGCGGCACC	61°C
	anti-sense	5'-AGAGGTTCTCATCTGGACC	
Tbx3 *	sense	5'-AGGAGCGTGTCTGTCAGGTT	58°C
	anti-sense	5'-GCCATTACCTCCCCAATTTT	
Yipel2	sense	5'-ACTCATTTCCAAGTCCTTCC	60°C
	anti-sense	5'-GATGCTATCAGGTCAGTCCC	
Zscan4	sense	5'-TTGAAGCCTCCTGTCATGGTCC	61°C
	anti-sense	5'-TCCATTTCATTTCCACTACAGC	
1700061G19Rik	sense	5'-AATCTATACTCGTGGAAAGG	54°C
	anti-sense	5'-CAGGGAAGCAAAGTGGCAGG	

* primers used at Laboratory for Pluripotent Cell Studies, CDB Riken

2.4.4 Blunt end PCR for cloning

Phusion® Hot Start High-Fidelity DNA polymerase (Finnzymes, F540) was used to amplify products from ES cell cDNA or 100ng plasmid, which were used as a template for PCR in a total reaction volume of 50µl. Reactions were performed using a Techne Touchgene gradient PCR machine (Table 2.10). DNA was run on an agarose gel, stained with Ethidium bromide, and correct amplicon size was verified under UV light. PCR products were excised, purified with Qiagen gel extraction kit (Qiagen, 28704) and used for ligation reactions.

Table 2.10 Blunt end PCR program

Stage	Temperature	Duration	Cycles
Hot start	94°C	5 minutes	
Denaturation	94°C	1 minute	
Annealing	Primer dependent	1 minute	30 cycles
Elongation	72°C	1 minute	
Final elongation	72°C	10 minute	
Hold	4°C		

2.4.5 Agarose gel electrophoresis

Agarose gels were used to separate DNA by electrophoresis. Gels were prepared by dissolving the appropriate quantity of agarose ((1-4% (w/v) as required) by boiling in TAE buffer (50x TAE buffer: 2M Trizma base, 50mM Na_2 EDTA (pH8.0) adding glacial acidic acid to pH7.6). Once cooled, the gel was poured into a gel tray sealed with masking tape and a well forming comb inserted. After the gel had set, the comb and tape were removed and gel was submerged in an electrophoresis tank containing 1x TAE buffer. Samples were prepared by adding 6x gel loading dye (30% (v/v) glycerol, 0.05% (w/v) Xylene/Cyanol, 0.05% (w/v) bromphenol blue) to them. Samples were loaded into individual wells of the agarose gel and run at 70-90V until sufficient separation was achieved. The gel was then placed into a 0.5µg/ml ethidium bromide 1x TAE solution for 15 minutes and visualised under UV light. Image was taken in a Syngene UV transluminator using Genesnap software.

2.4.6 Transient siRNA transfection

Small interference RNAs (siRNA) were transiently transfected into mESCs to knockdown the expression of target genes. Richard Jorgensen and Carolyn Napoli were the first stumbling over the RNA interference (RNAi) phenomenon when trying to create a purple Petunia flower in 1986. Jorgensen proposed an "RNA-based information superhighway in plants" (Jorgensen et al., 1998). Work in the nematode worm *c. elegans* helped to understand the mechanisms of RNA interference (Fire et al., 1998) and the post-transcriptional gene silencing mechanism was later utilized in mammalian cells (Elbashir et al., 2001).

RNAi is a post-transcriptional process of sequence-specific gene silencing, which is initiated by sequence homologous double-stranded RNA (dsRNA) (Elbashir et al., 2001). The RNA is cleaved into smaller siRNA fragments of 21 to 25 nucleotides in size by a dsRNA-specific endonuclease belonging to the family of RNAse III-like enzymes, and is also called Dicer (in Drosophila) (Bernstein et al., 2001; Elbashir et al., 2001). The RNA induced silencing complex (RISC) is a multiprotein complex that incorporates one strand of a small interfering RNA (reviewed in (Fuchs et al., 2004)). The RISC complex that has bound this template siRNA is able to recognize complementary messenger RNA and degrades it, leading to a subsequent knockdown of targeted protein levels (Martinez et al., 2002).

2.4.6.1 Endoribonuclease-prepared siRNA (esiRNA)

Endoribonuclease-prepared siRNA was prepared according to the method first reported by Kittler (Kittler et al. 2004). Primers were designed to generate a PCR product of 200-400bp within the region of the gene of interest incorporating a T7 promoter sequence (5'-CGTAATACGACTCACTATAGGG) at the 5'. PCR was carried out to generate cDNA using Hotstart Taq (Invitrogen) over 35 cycles. Ambion MEGAscript kit was used to generate dsRNA from cDNA in 10µl reactions according to the manufacturers protocol (1µl 10 x transcription buffer, 4µl 75mM ATP, GTP, CTP, and UTP mix, 4µl PCR product, 1µl T7 RNA polymerase enzyme mix). Reaction was incubated at 37°overnight and annealing was performed in a thermal cycler as follows: 90°C for 3min, ramp to 70°C with 0.1°C/sec, 70°C for 3

min, ramp to 50°C with 0.1°C/sec, 50°C for 3 min, ramp to 25°C with 0.1°C/sec. 10µl dsRNA was then digested in 90µl dsRNA digestion buffer (pH 7.9 20mM Tris-HCl, 0.5mM EDTA, 5mM MgCl2, 1mM DTT, 140mM NaCl, 2.7mM KCl, 5% (v/v) glycerol) plus 4µl Rnase III and incubated at RT room temperature for 4-5 hours. A 2-4µl aliquot was run in 4% agarose (v/v) along with a 25bp DNA ladder marker to check the size range of digestion products. esiRNA RNA was then purified using BioRad MicroBio-spin chromatography columns to remove remaining DNA template, unincorporated nucleotides and longer dsRNAs. Purified esiRNA was resuspended in pH7.5 0.1mM Tris and stored at -80°C.

2.4.6.2 Commercial small interference RNA (siRNA)

Commercially available chemically synthesized siRNAs, specific to our genes of interest, were obtained from Dharmacon. Dharmacon Smartpool siRNAs, targeting 4 different regions of specifc gene transcript, were in general used in the performed loss-of function experiments.

2.4.6.3 Transfection of mES cells with siRNA

siRNA/esiRNA was added in desired concentrations to 1.5ml tubes and made up to 50µl with KO SR DMEM. In a second tube, Lipofectamine2000 (Invitrogen) was added (final concentration 1:500) and also made up to 50µl with KO SR DMEM. After 5 minutes the contents of both tubes were mixed and left on bench for 20 minutes to allow for the formation of Lipofectamine-siRNA complexes. In the meantime, a single cell suspension was prepared, as described in 2.2.1 and added after 20 minutes to the Lipofectamine-siRNA mix. This cell mixture was then plated onto gelatin-coated multi-well cell culture dishes. Transfected cultures were maintained in humidified incubators at 37°C and 5% (v/v) CO_2 over-night and medium was changed the following day. On day 3 after transfection RNA and/or Protein were harvested and expression of specific genes was analysed as described in sections 2.3.2 and 2.4.3.

2.4.7 Purification of plasmid DNA

2.4.7.1 Phenol chloroform extraction

The DNA containing solution was extracted with an equal volume of buffer saturated phenol:chloroform (1:1) and centrifuged for 1 minute at maximum speed in a microcentrifuge. The aqueous phase (top phase) was removed carefully to a clean tube and extracted with an equal volume of chloroform. This was centrifuged for 1 minute and aqueous phase was removed. DNA was precipitated by ethanol precipitation.

2.4.7.2 Ethanol precipitation of DNA

0.1 volume of 3M sodium acetate (pH 5.2) and 2 volumes of 100% ethanol were added to the solution from which the DNA was to be precipitated. The mixture was placed at -20°C for at least 30 minutes, before the precipitated DNA was pelleted in a microcentrifuge at 4°C for 10 minutes at full speed. Ethanol was aspirated off and the pellet was washed in 70% (v/v) ethanol. Pellets were dried at room temperature and then resuspended in TE (10mM Tris-HCl pH 8.0, 0,1mM EDTA pH 8.0) or dH_2O and stored at -20°C.

2.4.7.3 Small-scale plasmid preparation

Alkaline lysis protocol

A single bacterial colony was picked and transferred to 3ml 2YT broth containing appropriate antibiotics. The culture was grown with vigorous shaking at 37°C overnight. 1ml of culture was transferred to an Eppendorf tube and pelleted for 1 minute at full speed. The pellet was resuspended in 100µl solution I (50mM glucose, 10mM EDTA, 25mM Tris-HCl pH8.0). Then 200µl of lysis solution II (0.2M NaOH, 1% (w/v) SDS) was added and the suspension incubated on ice for 5 minutes. 150µl of cold solution III (3M potassium acetate, 2M acetic acid) was added and mixture was incubated on ice for further 5 minutes after vortexing. Then debris was pelleted at full speed in a microcentrifuge at 4°C for 10 minutes. The supernatant was moved to a clean tube and the plasmid DNA was extracted using

phenol:chloroform extraction followed by ethanol precipitation (as described in sections 2.4.7.1 and 2.4.7.2).

Macherey-Nagel Nucleospin protocol

3ml of overnight bacterial culture was pelleted at 11000xg for 30 seconds and the pellet was resuspended in 250µl cell buffer A1. Then 250µl cell lysis buffer A2 was added and mixture was incubated for 5 minutes at room temperature. After addition of 300µl stop buffer A3, lysates were clarified by centrifuging for 10 minutes at 11000g. Supernatant was loaded in Nucleospin column and centrifuged at 11000g for 1 minute. Two washing steps followed with 500µl buffer AW and 600µl buffer A4, after each step columns were centrifuged for 1 minute at 11000g. Column silica membrane was dried by centrifuging for 2 minutes at 11000g and DNA was eluted with 50µl of preheated (70°C) elution buffer AE.

2.4.7.4 Large-scale plasmid preparation

For large-scale plasmid preparation QIAGEN midi plasmid preparation kits were used, according to the manufacturer's guidelines. Briefly, 100ml of 2YT broth containing appropriate antibiotics were inoculated with a bacterial starter culture carrying the plasmid of interest. After culturing overnight, bacteria were pelleted in a Beckman M5 centrifuge with a JA-14 rotor at 5000rpm for 10 minutes. The supernatant was discarded and the pellet was resuspended in 4ml buffer P1. Then 4ml of lysis buffer P2 were added and the solution was carefully mixed by inverting the tube and placed on ice for 15 minutes. Chilled stop buffer P3 was added (5ml) and mixture was centrifuged for 30 minutes at 15500rpm in the JA-20.1 rotor at 4°C. QIAGEN column 100 was equilibrated with 4ml QBT buffer before supernatant was moved to column. After washing twice with 10m QC buffer, DNA was eluted with 5ml of buffer QF. The DNA was then extracted by ethanol precipitation (2.4.7.2).

Table 2.11 Plasmids used in this study

Plasmid	Derivation	Use
pcDNA3.1-Zscan4c-V5-His (TOPO)	Mammalian expression plasmid with Zscan4c-V5-His driven by the CMV promoter. Generously donated by Dr. Michael Storm.	Used as template for cloning Zscan4c-V5-His
pPyCAGIZ	Episomal expression vector containing the zeocin resistance gene. Constructed by Dr. Hitoshi Niwa.	Episomal supertransfection of Zscan4c-V5-His
pUHD10-3neo	Response plasmid pUHD10-3 with neomycin resistance gene	Inducible expression of Zscan4c-V5-His under influence of tTA expressed by pCAG20-1 (Tet-off system)
pTRE-Tight-eGFP	Tet-on advanced expression vector containing eGFP. Kind gift of Michael Buchholz.	Doxycycline inducible expression of eGFP-Zscan4c.
pGEM-Teasy-Hygromycin	Vector containing NotI excisable Hygromycin resistance gene under SV40 promoter. Kind gift of Michael Buchholz.	Excised Hygromycin cassette was used for co-transfection with pTRE-Tight.
pET15b	Bacterial expression vector that possesses an His-Tag at the N-terminus.	Expression and purification of Zscan4c-His protein.
pPBCAGcHAIN	PiggyBac transposon vector, containing CAG promoter and IRES-Neomycin for selection.	Overexpression of transgenes of interest, with piggyBac transposon/transposase system.
pCAG-PBase	Transposase expressing helper plasmid.	Co-transfection with piggyBac vector.
pPyCAG-GS-eGFP-IP	Vector containing GS linker and eGFP.	Used for creating c-terminal GS linker eGFP fusion proteins
pPyCAG-myrp110α-IP	Vector containing myr-p110α. From Dr. Yamanaka.	Cloning myr-p110α into piggyBac vector.

2.4.8 Manipulation of DNA

2.4.8.1 Restriction enzyme digest

New England Biolabs (NEB) restriction enzymes were used and are provided with the appropriate 10x buffer and if required with a 10x BSA stock. Digests were typically performed in a 10 or 20µl reaction volume containing 10% (v/v) restriction enzyme and 10% (v/v) enzyme buffer, 1-5µl of DNA to be cut and water to make up to 10 or 20µl of total reaction volume. Digests were incubated at 37°C for 1 hour to overnight.

2.4.8.2 Ligation

Ligations of DNA fragments were performed with NEB T4 DNA ligase in a 10 or 20µl total reaction volume. 1µl 10xT4 DNA ligase buffer, 100ng digested vector, DNA insert in a molar ratio of 3:1 (insert : vector), distilled water to 9ul and 1ul T4 DNA ligase were mixed in a 1.5ml eppendorf tube and incubated at 16°C for at least 1 hour.

2.4.8.3 Sequencing

DNA plasmids were prepared by the miniprep method (2.4.7.3) and sent together with sequencing primers to the Biochemistry Department of Oxford University for sequencing. Sequence analysis was performed with ApE plasmid Editor v1.17 or Clone Manager 9 Professional.

Table 2.12 Primers used for cloning in this study

Sequence (5'-3')	Orientation	T.	Use
AATGTCGACTAATACGACTCACTATAGGG	**sense**	53°C	SalI T7 primer used for cloning Zscan4c-V5-His into episomal vector and pUHD10-3.
AATGTCGACTAGAAGGCACAGTCGAGG	**anti-sense**	53°C	SalI BGH primer used for cloning Zscan4c-V5-His into episomal vector and pUHD10-3.
TTATGGCTTCACAGCAGGCA	**sense**	55°C	Creation of eGFP-Zscan4c fusion protein. Cloning into pTRE-tight-eGFP digested with Sma1 and Not1.
TTAATTGCGGCCGCTCAGTCAGATCTGTGGTAAT	**anti-sense**	55°C	Creation of eGFP-Zscan4c fusion protein.
CGTTACATATGGCTTCACAGCAGGCA	**sense**	53°C	Zscan4c NdeI primer for cloning into pet15b.
TCAGTGGATCCTCAGTCAGATGTGTGGT	**anti-sense**	53°C	Zscan4c BamHI primer for cloning into pet15b.
TCGACCACCATGGGGAGCAGCAAGAGCAAGCCCAAGG	**sense**	-	Myr self-annealing primers, for cloning into piggyBac vector with xhoI.
TCGACCTTGGGCTTGCTCTTGCTGCTCCCCATGGTGG	**anti-sense**	-	Myr self-annealing primers, for cloning into piggyBac vector with xhoI.
ATACTCGAGATGCCTCCTGCTATGGCAGA	**sense**	54°C	Cloning of p110β from Fantom cDNA F630002D04.
ATAGCGGCCGCCTAGGACCTGTAGTCTTTCC	**anti-sense**	54°C	Cloning of p110β from Fantom cDNA F630002D04.
ATACTCGAGATGCCCCCTGGGGTGGACTG	**sense**	54°C	Cloning of p110δ from Fantom cDNA F830107C10.
ATAGCGGCCGCCTACTGTCGGTTATCCTTGG	**anti-sense**	54°C	Cloning of p110δ from Fantom cDNA F830107C10.
ATACTCGAGCCACCATGGGGAGCAGCAAGAGCA	**sense**	54°C	Cloning myr-p110α into piggyBac vector.
ATAGCGGCCGCTCAGTTCAAAGCATGCTGCT	**anti-sense**	54°C	Cloning myr-p110α into piggyBac vector.
ATACTCGAGCCACCATGGGGAGCAGC	**sense**	54°C	For creation of myr-p110x-gfp fusions. XhoI site.
TATTCTAGAGGACCTGTAGTCTTTCC	**anti-sense**	54°C	For creation of myr-p110β-gfp fusions. XbaI site, stop codon deleted.
TATTCTAGACTGTCGGTTATCCTTGG	**anti-sense**	54°C	For creation of myr-p110δ-gfp fusions. XbaI site, stop codon deleted.
TATTCTAGAGTTCAAAGCATGCTGCT	**anti-sense**	54°C	For creation of myr-p110α-gfp fusions. XbaI site, stop codon deleted.

2.4.9 Expansion of plasmid DNA

2.4.9.1 Preparation of competent *E. coli* strain DH5α

Bacteria from a frozen stock of the *E. coli* DH5α were streaked out onto a fresh 2YT agar plate (16g Bactotryptone, 10g yeast extract, 10g NaCl, 15g bacto-agar made up to 1l and autoclaved). This plate was incubated inverted at 37°C overnight and the following day a colony was picked and transferred to a 4ml LB (10g tryptone, 5g, yeast extract, 10g NaCl) and cultured at 37°C overnight . The overnight culture was added to 1l pre-warmed LB medium and grown in a shaking incubator to an OD_{600} of 0.5. Culture was then placed at 4°C for 30 minutes and subsequently centrifuged with a swing-out rotor at 5000g for 5 minutes at 4°C. Supernatant was discarded and pellet was resuspended in 100ml of ice cold 0.1M $CaCl_2$. After at least 1 hour of incubation on ice, the mixture was added to 100% glycerol so that the final concentration was 17.5% (v/v). The mixture was aliquoted and snap frozen in a dry-ice/ethanol bath and stored at -80°C.

2.4.9.2 Transformation of *E. coli* strain DH5α

Competent cells were thawed at room temperature and placed on ice for about 10 minutes. DNA was added to a concentration of less than 100ng per 200μl of cells and incubated on ice for 20 minutes. Cells were heat shocked at 42°C for 45 seconds and returned on ice for 1 minute. 4 volumes of LB medium were added and cells were placed in a water bath at 37°C for one hour. Required amounts were plated onto 2YT agar plates containing for selection necessary antibiotics and plates were incubated inverted at 37°C for 16-18 hours.

2.4.10 Electroporation

After trypsinisation murine ES cells were washed three times with sterile PBS w/o Ca^{2+} and Mg^{2+} and resuspended at a concentration of ~$1x10^7$ cells per 0.8ml. 0.8ml were transferred into electroporation cuvette and 20µg linearized DNA plasmid was added. Electroporation was performed at 3µF/800V with a Bio-Rad Gene Pulser. Episomal vectors were electroporated as circular DNA with a pulse at 960µF/200V. The pulsing cuvette was transferred onto ice for 5 minutes, before cells were seeded in ES cell medium supplemented with 1% (v/v) Hyclone FCS at a concentration of $2x10^6$ cells/90mm plate. The next day, medium was changed and appropriate drugs required for selection also added.

When colonies were clearly visible (7-10 days after electroporation), colonies were picked. Therefore, medium was aspirated and plates were washed with PBS and 5ml of PBS were added to dish. 10µl of trypsin-EDTA were added to each well of a round bottom 96-well plate. Colonies were picked with a pipette and placed into prepared trypsin-EDTA wells. 100µl of ES medium was used to resuspend the colonies by gentle pipetting and cells were transferred to individual wells of cell culture trays. Clones were then expanded for screening and freezing.

2.4.11 Screening clones for tetracycline regulated expression

G418 (Tet-off) resistant clones were expanded in the presence of 1µg/ml tetracycline) and hygromycin (Tet-on) resistant clones were expanded in absence of doxycycline. Cells were washed 2x with PBS, trypsinised and plated out at $5x10^4$ cells/ml in presence or absence of 1µg/ml tetracycline/doxycycline in 48-well plates. Protein samples were taken at various time intervals up to 72 hours later by direct addition of Laemmli Lysis Buffer (2% (w/v) SDS, 10% (v/v) Glycerol, 60mM Tris pH6.8, 0.1M DTT, Bromophenol blue). Samples were placed on ice immediately, before boiling for 5 minutes. Samples were freeze/thawed at least once to shear genomic DNA, and subjected to SDS-PAGE to determine expression of the protein of interest. Following immunoblotting with the anti-V5 (Tet-off) or anti-GFP (Tet-on) epitope tag antibodies, clones showing the most robust and inducible expression

of the protein of interest were selected, expanded, frozen down (2.1.2.2) and stored in liquid nitrogen for further use.

2.4.12 PiggyBac transposon/transposase system

The piggyBac (PB) transposon/transposase system is host-factor independent and only requires inverted terminal repeats at both ends of the transgene and the transient expression of the transposase enzyme which catalyses the insertion/excision (Fraser et al., 1996). It has been used successfully in ES cells and for the establishment of iPS cells (Cadinanos and Bradley, 2007; Kaji et al., 2009; Woltjen et al., 2009).

One day before transfection $2x10^4$ cells/well were plated in 12-well cell culture trays. The following day, 1μg of piggyBac vector containing the transgene under a CAG promoter (pPB-X) and 1μg transposase expressing helper plasmid (pCAG-PBase) were mixed in 25μl of GMEM without serum. 25μl Lipofectamine2000 dilution (2μl Lipofectamine2000 plus 23μl GMEM) was added and the mix was incubated at room temperature for 10 minutes. Then 450μl GMEM plus FCS were added and mixture was transferred to one well of the prepared 12-well plate. After 3 hours of incubation, mixture was aspirated and 1ml fresh ES cell media (GMEM + FCS) was added per well. The successive day, medium was changed and appropriate antibiotics for selection were added. After three days of culture, mESCs were replated into 6-well cell culture plates at a density of $1x10^4$ cells/well and $2x10^3$ cells/well in selection media. When colonies were clearly visible, they were expanded and frozen as described (2.1.2.2).

Chapter 3: Screening for Novel Regulators of Pluripotency downstream of PI3Ks

3.1 Introduction

The class IA phosphoinositide 3-kinase (PI3K) family of lipid kinases regulate a variety of physiological responses and were previously reported to play an important role in proliferation and maintenance of self-renewal in mESCs (Jirmanova et al., 2002; Kingham and Welham, 2009; Paling et al., 2004; Takahashi et al., 2003; Watanabe et al., 2006). Nanog, one of the major players in regulating ESC self-renewal, was identified as a molecular target downstream of the PI3K pathway, and appears to be regulated in GSK-3 dependent manner (Storm et al., 2007).

The aim of this part of the study was to identify novel genes involved in PI3K-dependent regulation of mESC behaviour, initially based on a microarray screen previously performed in our laboratory. With this approach it was hoped to further delineate the molecular mechanisms of PI3K involvement in self-renewal of ESCs, a process that gained major attention through the establishment of iPS cells. With the rapid development of microarray technology in the last decade, it is now possible to perform global analyses on the expression of thousands of genes within the same sample simultaneously. Thus, RNA samples of mES cells treated with the PI3K inhibitor LY294002 over a defined time-course of 72h were used to perform expression profiling with Affymetrix GeneChips. Using filtering of greater than 1.5-fold change in expression and an analysis of variance significance level of $p < 0.05$, a dataset was defined comprising 646 probe sets that detect changes in transcript expression (469 down and 177 up) on inhibition of PI3Ks. An initial hierarchical clustering of the 646 probe sets suggested that the dataset falls into 12 groups. This was used to cluster the data using k-means (k=12), and the corresponding heatmap is shown in Figure 3.1A. The 20 genes showing the most statistically significant changes in gene expression are shown in Figure 3.1B. Expression patterns of genes of interest (see below for selection criteria) were validated by qRT-PCR and in 14 out of 16 cases, highly comparable expression patterns were measured by both microarray and qRT-PCR. In the other two cases, expression was similar, indicating a high degree of agreement between the two approaches. Figure 3.1C shows quantitative RT-PCR validation examples for Zscan4 and Shp-1.

A

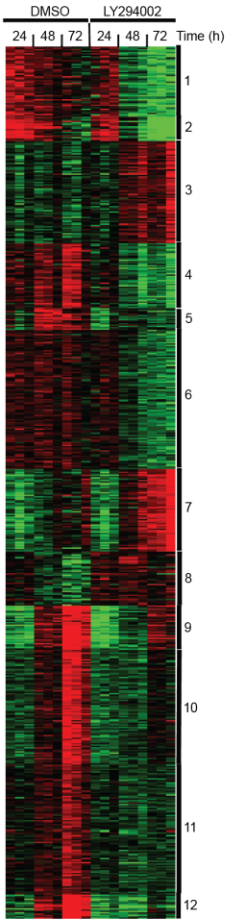

B

Affy Probe set ID	ANOVA	FC 24h	FC 48h	FC 72h	Gene Symbol	Cluster
1423066_at	3.10885E-09	1.10	1.72	1.83	Dnmt3a	8
1437486_at	4.62218E-09	-1.24	-1.87	-1.96	Rai3	4
1435113_x_at	4.77352E-09	-1.16	-1.77	-1.63	Stmn3	10
1447896_s_at	2.15408E-08	-1.09	-1.48	-1.62	2010109N14Rik	10
1436392_s_at	2.24768E-08	-1.44	-2.47	-2.00	Tcfap2c	10
1437435_at	4.09194E-08	-1.30	-2.17	-2.45	1700061G19Rik	4
1448371_at	4.15148E-08	-1.24	-2.94	-4.05	Mylpf	11
1450626_at	4.35211E-08	1.01	-2.17	-3.29	Manba	1
1423852_at	5.21738E-08	-1.20	-2.88	-2.90	Tmem46	10
1429366_at	6.46628E-08	-1.17	-3.01	-3.49	Lrrc34	12
1449276_at	7.22575E-08	-1.04	-1.33	-1.57	1700029P11Rik	6
1429388_at	7.80077E-08	-1.30	-1.73	-1.82	Nanog	11
1438664_at	9.01738E-08	1.06	1.77	2.08	Prkar2b	3
1449410_a_at	1.00977E-07	-1.09	-1.41	-1.66	Gas5	6
1416239_at	1.20857E-07	-1.36	-2.09	-1.95	Ass1	4
1436520_at	1.27845E-07	-1.29	-2.08	-2.23	AI450948	9
1429524_at	1.37450E-07	-1.62	-4.17	-2.19	Myo1f	12
1428529_at	1.82608E-07	-1.08	-1.32	-1.59	2810026P18Rik	6
1426808_at	2.35460E-07	-1.60	-6.49	-5.74	Lgals3	12
1437073_x_at	3.32457E-07	1.12	1.52	1.57	AV025504	8

C

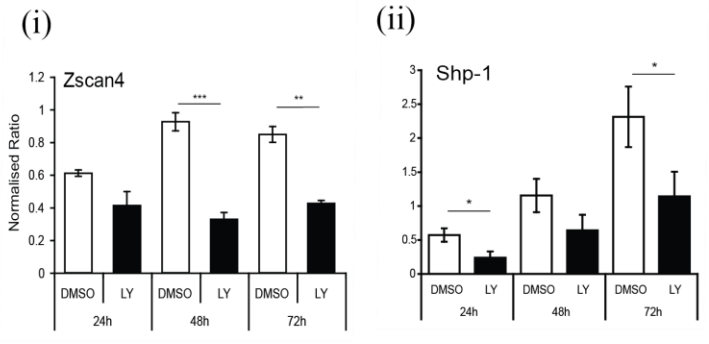

Figure 3.1 Clustering and gene ontology analyses of gene expression changes occurring in embryonic stem (ES) cells upon inhibition of phosphoinositide 3-kinases (PI3Ks). (A) k-means clustering of 646 probe sets into 12 clusters. **(B)** Probe sets with the 20 highest significance scores in the dataset are presented. The Affymetrix probe set ID is shown along with the ANOVA value and FC in expression between controls and LY294002-treated samples at each time point. **(C)** ES cells were cultured in the presence of leukemia inhibitory factor plus or minus 5μM LY294002 for the times indicated. Expression of Zscan4 and Shp-1 was analysed by quantitative reverse transcription polymerase chain reaction, and target gene expression was normalised relative to β-actin levels. The averages and ±SEM of duplicate samples from each of three independent biological replicates are shown: *, $p < .05$; **, $p < .005$; ***, $p < .0005$, in a Student's t test.

Microarray screen was performed prior to the start of this study by M. Storm and partners of the FunGenEs consortium (www.fungenes.org). (Storm et al., 2009).

3.2 Microarray analyses and data mining

Microarray-based expression analyses are a powerful technology with huge potential to accurately detect transcriptional changes and provide detailed genome-wide molecular signatures of cellular states. The downside of this type of analysis is the large amount of data generated, which makes it very difficult to identify key functional regulators of the investigated biological processes. Therefore, it is necessary to apply computational analyses and data mining to aid the identification of targets that are of interest and to address the challenge of understanding specific biological phenomena. Analysis of microarray datasets encounters a number of challenges for data mining, the biggest of which is probably the finding of false positive probe set changes and, therefore, it is important to develop robust methods and validate the established models. A thorough selection of genes is crucial and can be done by attributing selection criteria, most strongly related to predicted classes. The clustering of genes showing similar patterns of expression, for example according to hierarchy, can reveal some interesting trends and help to determine key components of the genetic signature.

3.2.1 Selection of Genes of interest

To focus further functional analyses on the most promising candidates that could be playing a role in regulating mES cell self-renewal, downstream of PI3K signalling, additional selection criteria were applied to the significant probe set changes of the Affymetrix GeneChip expression analyses described. Briefly, the following criteria were applied; (a) significant downregulation within 24-48h of PI3K inhibition; (b) predicted to function as transcription factors; (c) predicted or known to be signalling pathway components; (d) genes with unknown function and (e) genes with expression restricted to early development. A preliminary loss-of-function screen, using esiRNAs generated to our target genes (Kittler et al. 2004) (2.4.6.1), was performed on 21 genes obtained with the described selection criteria (M. Storm, unpublished data). A list of seven genes (summarized in Table 3.1), namely AF067061, 1700061G19Rik, Ypel2, Baz1a, Shp-1, LOC327811 and Zscan4c, was established based on the outcome of the pre-screen, which had indicated their ability to reduce ES cell self-renewal. AF067061 belongs to the 2-cell-stage gene family and its precise function is to date unclear. 1700061G19Rik, appears to have

sequence identities with acyl-CoA synthetases of other species, suggesting it is most likely involved in lipid metabolism. Ypel2 encodes a putative zinc-binding protein found in association with mitotic spindles or the centrosome, highlighting a potential function in cell division (Hosono et al., 2004). YPEL family proteins have been shown to be present in effectively all eukaryotes and are therefore likely to play important roles in the maintenance of life. Baz1a encodes a protein with a bromodomain adjacent to a zinc finger domain. The bromodomain is a structural motif that is found in proteins involved in chromatin remodelling to regulate transcription. They commonly act in complexes with other proteins and frequently possess histone acetyltransferase activity (Bochar et al., 2000; Jones et al., 2000). Shp-1 encodes a protein tyrosine phosphatase which has been reported to be part of a signalling complex downstream of the stem cell factor receptor c-kit (Paulson et al., 1996). It is known to be involved in the control of cellular proliferation and survival in other cell types (Bone et al., 1997) and was therefore considered to be a promising candidate. LOC327811, now annotated as Gm4340, is full-length protein coding and predicted to be THO complex 4-like, though nothing is reported about its exact function to date. The THO complex plays a role in transcription elongation as well as in the further formation and assembly of the mature messenger ribonucleoproteins (mRNP). Binding of the THO complex to specific mRNA export factors recruits these export factors to the mRNA during transcription (Ho et al., 2002; Zenklusen et al., 2002). Possibly, LOC327811 could be part of a similar mechanism due to its predicted structure. Zscan4c, also known as Gm397, is a member of the Zscan4 family. This family of proteins comprise a SCAN domain, which is a Leucine rich element and a highly conserved motif specific to vertebrates, and four zinc finger domains, usually responsible for DNA interaction (Falco et al., 2007). Other members of the family of the SCAN domain containing zinc finger proteins (SCAN-Zfps) act as transcription factors and have been previously described to be involved in cell survival and differentiation (Edelstein and Collins, 2005). A more detailed description of the Zscan4 family is given in section 1.8.

Table 3.1 Summary of Genes of Interest (GOI)

Gene annotation	UnigeneID	gene characteristics	postulated function
AF067061	236546	Member of 2-cell-stage gene family	not known
1700061G19Rik	78625	sequence identities with acyl-CoA synthetases	lipid metabolism
Ypel2	77864	zinc-binding protein family	cell division
Baz1a	452855	bromodomain adjacent to a zinc finger domain	chromatin remodeling
Shp-1	5777	protein tyrosine phosphatase	signaling molecule
LOC327811/ Gm4340	1138251	THO complex 4 - like	not known
Zscan4c	245109	SCAN domain + 4 Zinc finger domains	transcription factor

3.2.2 Identification of signalling pathways downstream of PI3Ks involved in regulation of genes of interest

PI3K signalling normally suppresses activity of GSK-3 via Akt, and therefore PI3Ks activity can be mimicked partly by artificial inhibition of GSK-3. It was demonstrated previously that PI3K-dependent inhibition of GSK-3 activity is involved in the regulation of Nanog gene and protein expression (Storm et al., 2007). To investigate if other genes identified by the microarray screen are regulated in a similar manner, the pharmacological inhibitors BIO and LY294002 were used for the inhibition of GSK-3 and PI3Ks respectively, both separately and in combination, to determine whether genes are regulated in a GSK-3-dependent manner (Figure 3.2 A). Based on these findings, it was of interest to determine if there was a relationship between common pathways regulating GOIs and their respective expression clusters. As expected, expression of all our genes of interest dropped significantly on inhibition of PI3Ks, confirming robustness of the Affymetrix dataset (Figure 3.2 B). Zscan4, AF067061, LOC327811, and Baz1a are all members of Cluster 1 and importantly their expression patterns after treatment with PI3K and GSK-3 inhibitors follows a similar trend. Interestingly, inhibition of GSK-3 was not able to overcome the effect of PI3K inhibition, suggesting that regulation of these genes is independent of GSK-3 (Figure 3.2 B). In contrast, inhibition of GSK-3 was able to overcome the effects of PI3K inhibition on expression of Shp-1 and 1700061G19Rik (clusters 11 and 4, respectively), restoring the expression back to control levels in the presence of LIF alone. Consistent with this finding is the previous report that Nanog (also member of cluster 11) protein expression is regulated in an identical manner (Storm et al., 2007), reflecting the GSK-3 dependency of all three genes of interest.

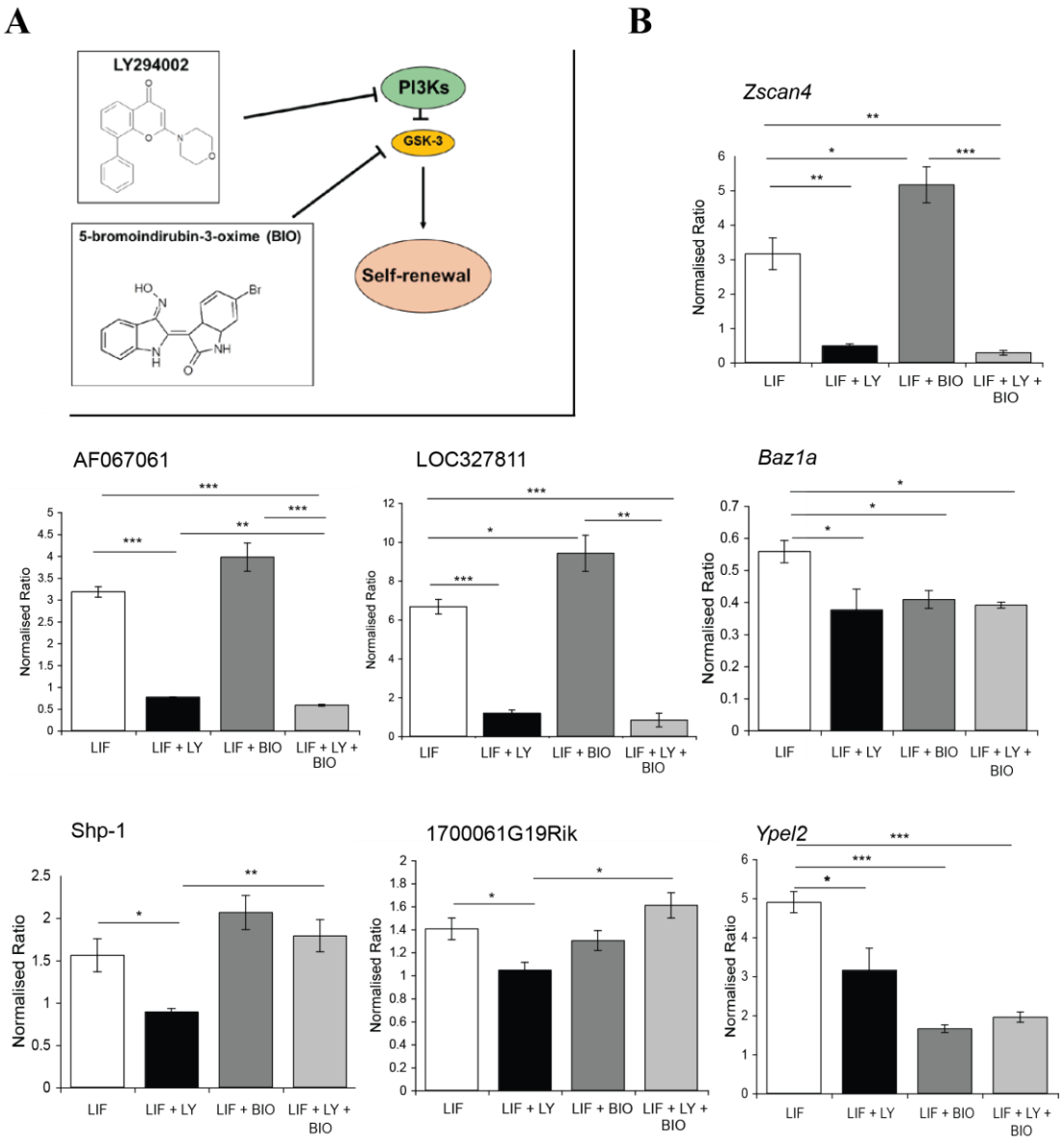

Figure 3.2 Glycogen synthase kinase 3 (GSK-3)-dependent and independent mechanisms are involved in the control of expression of phosphoinositide 3-kinase target genes. (**A)** Schematic diagram of the action of PI3Ks on GSK-3 activity and the inhibitors used to determine downstream gene regulation. (**B)** E14tg2a embryonic stem cells were cultured in the presence of LIF plus or minus 5μM LY294002, plus or minus 2μM of the GSK-3 inhibitor BIO for 72 hours. Expression of selected genes was analysed by quantitative reverse transcription polymerase chain reaction, and target gene expression was normalised relative to β-actin levels. The averages and ±SEM of duplicate samples from each of two independent biological replicates are shown: *, $p < .05$; **, $p < .005$; ***, $p < .0005$, in a Student's t test.

Expression of Ypel2, mapping to cluster 10, was inhibited by either LY294002 or BIO, whereas addition of both together had no additive effect, suggesting a more complex pattern of regulation.

GSK-3α/β double-knockout (DKO) ESCs show constitutively activated Wnt/β-catenin signalling (Doble et al., 2007) and were used to further confirm GSK-3 dependency of regulation of selected genes. Zscan4 and AF067061 expression, earlier suggested to be GSK-3 independent, were also downregulated after inhibition of PI3K with LY294002 in GSK-3 DKO cells, confirming a GSK-3 independent regulation mechanism (Figure 3.3 A). Expression of both genes was also affected following treatment with the p110α selective inhibitor PIK-75, indicating regulation via this PI3K isoform, which will be discussed in more detail in section 3.4.1. Nanog and 1700061G19Rik, both from the regulation cluster 11 and postulated to be regulated by GSK-3, were neither downregulated by broad inhibition of PI3Ks with LY294002, nor by the more selective PIK-75 inhibitor, affirming an upstream regulation by GSK-3 (Figure 3.3 B).

A summary of the inspected genes, including their cluster mapping, heatmap and their postulated regulation mechanisms are shown in Figure 3.4. Overall, these data suggest that PI3K signalling regulates changes in gene expression via both GSK-3-dependent and independent processes.

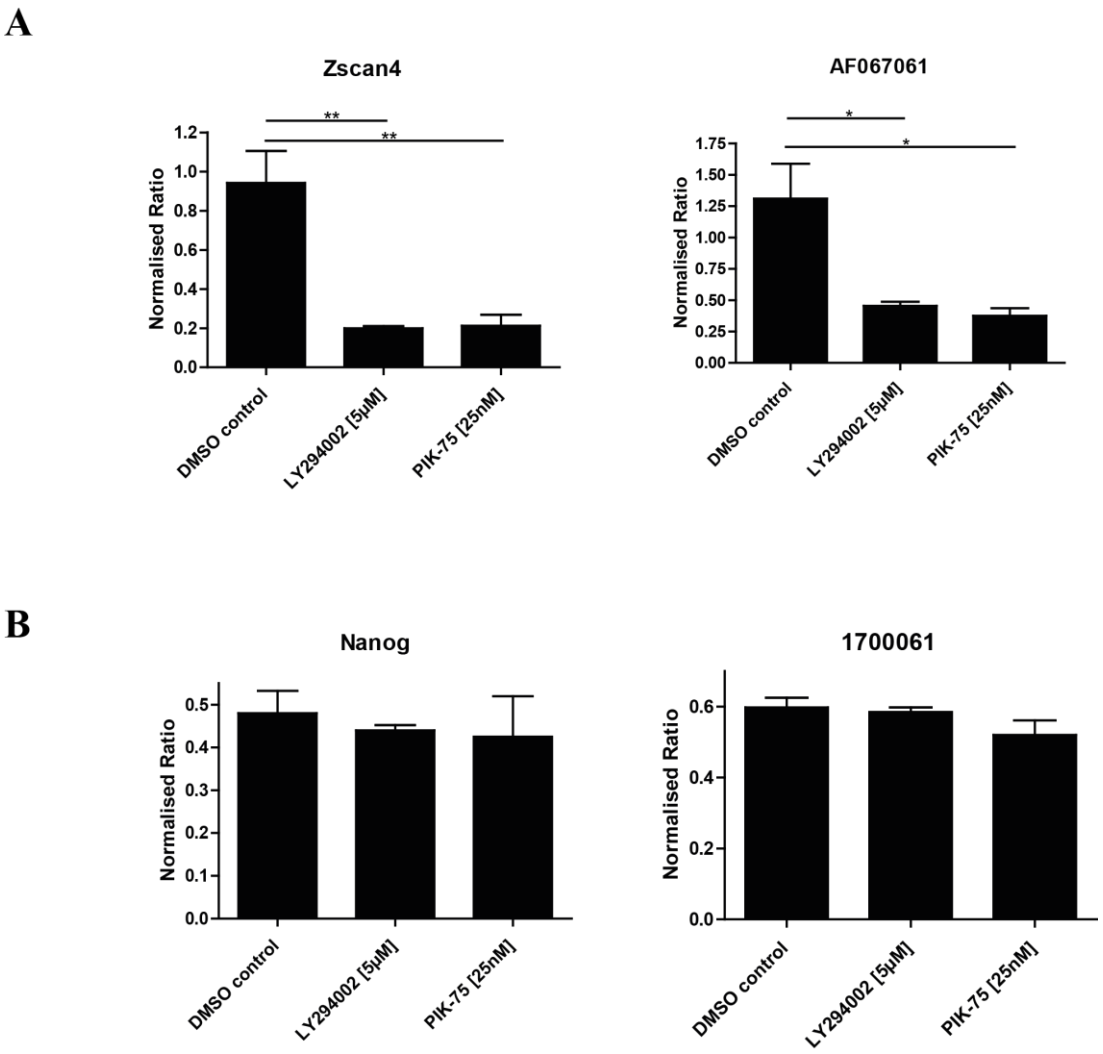

Figure 3.3 Regulation of phosphoinoside 3-kinase target genes in GSK-3 double knock-out (DKO) mES cells. GSK-3 DKO mES cells were cultured in the presence of LIF plus or minus 5μM LY294002 and plus or minus 25nM of the p110α specific inhibitor PIK-75 for 72 hours. Expression of selected genes was analysed by quantitative reverse transcription polymerase chain reaction, and target gene expression was normalised relative to β-actin levels. **(A)** Gene members of Cluster 1 and **(B)** Cluster 11 are pictured. The averages and ±SEM of duplicate samples from each of two independent biological replicates are shown: *, $p < .05$; **, $p < .005$, in a Student's t test.

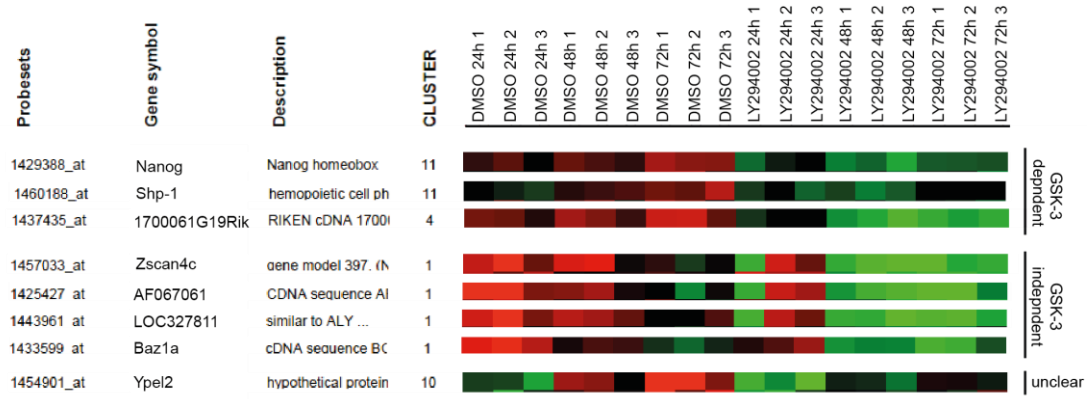

Figure 3.4 Overview of genes of interest and their regulation. This figure shows a summary of the analysed genes for GSK-3-dependent and independent regulation. Gene names, correlating probe sets of the affymetrix microarray screen, heatmap of the probe set changes, and their respective cluster are pictured.

3.3 Functional Analysis of PI3K-Target Genes in Control of ES Cell Fate

Several known regulators of self-renewal, i.e. Nanog, Tbx-3, Essrb, Klf2 and 4, were among the probe sets in the dataset that significantly changed, suggesting their regulation downstream of PI3Ks. A main aim of these studies was to determine the biological function of our selected genes of interest, in respect of their ability to maintain ES cell identity. An siRNA loss-of-function strategy was our first choice to investigate a potential role of our candidates in control of mES cell fate. RNA interference has been used by other groups to successfully identify genes that were previously not associated with maintaining mES cell self-renewal (Ivanova et al., 2006).

Two different types of siRNA, endoribonuclease-prepared siRNA (esiRNA) (Kittler et al., 2004) for initial screening and commercially available siRNA from Dharmacon, were used for gene silencing experiments. Both methods showed comparable results following transient transfection, though Dharmacon siRNA appeared to be more robust. This is possibly because in-house preparation of

esiRNAs on a small scale resulted in higher batch to batch variations. Dharmacon siRNAs of two different types were used, Smartpool siRNA, which is a pool of four single siRNAs targeting different regions of the same mRNA, and Dharmacon siRNA targeting only a single site of the specific mRNA. The use of a variety of different siRNA sources, targeting different regions of the same mRNA, reduces the risk of false positive findings, which might occur when siRNAs downregulate unexpected off-targets. Off-target effects upon use of siRNAs occur for instance by the binding of siRNA to mRNA with incomplete complementarity, which leads to undesired silencing of these genes, baring the risk of false positive data. Products like Smartpool siRNA ensure efficient knock-down, as all four siRNAs target the same gene, whereas off-target effects should be lower, but broader because the number of complementary binding sequence homologies are higher. Non-targeting Dharmacon siRNA was selected as a control and to establish siRNA toxicity effects, not associated specifically with silencing of targets. The homeodomain transcription factor Nanog, widely accepted as a key regulator of self-renewal, was selected as a postive control during siRNA experiments (Figure 3.5 A) (Chambers et al., 2003; Mitsui et al., 2003).

This study focused on elucidating the function of Zscan4, AF067061, Ypel2, Baz1a and 1700061G19Rik using siRNAs targeting each of these genes and subsequently assessing their loss-off-function effect by a clonal assays, based on alkaline phosphatase staininng. In this self-renewal assay, differentiated colonies remain unstained, exhibiting a flattened morphology, while self-renewing colonies are dome shaped and stain violet. Differentiated and undifferentiated colonies are scored, which allows for quantification of the loss-off-function effect of the targeted gene. Despite achieving up to 80% reduction in expression of AF067061, and Baz1a, using Smartpool siRNAs (Dharmacon), no consistent significant effects on self-renewal in the presence of LIF and serum were observed (Figure 3.5 B). This was also observed for 1700061G19Rik, and Ypel2, but caution has to be taken, as knockdown efficiency was below 50%. No significant change in total number of colonies was observed upon siRNA knockdown. However, transient knock-down of Zscan4 resulted in a reduction of self-renewal ability compared to control (see 3.3.1).

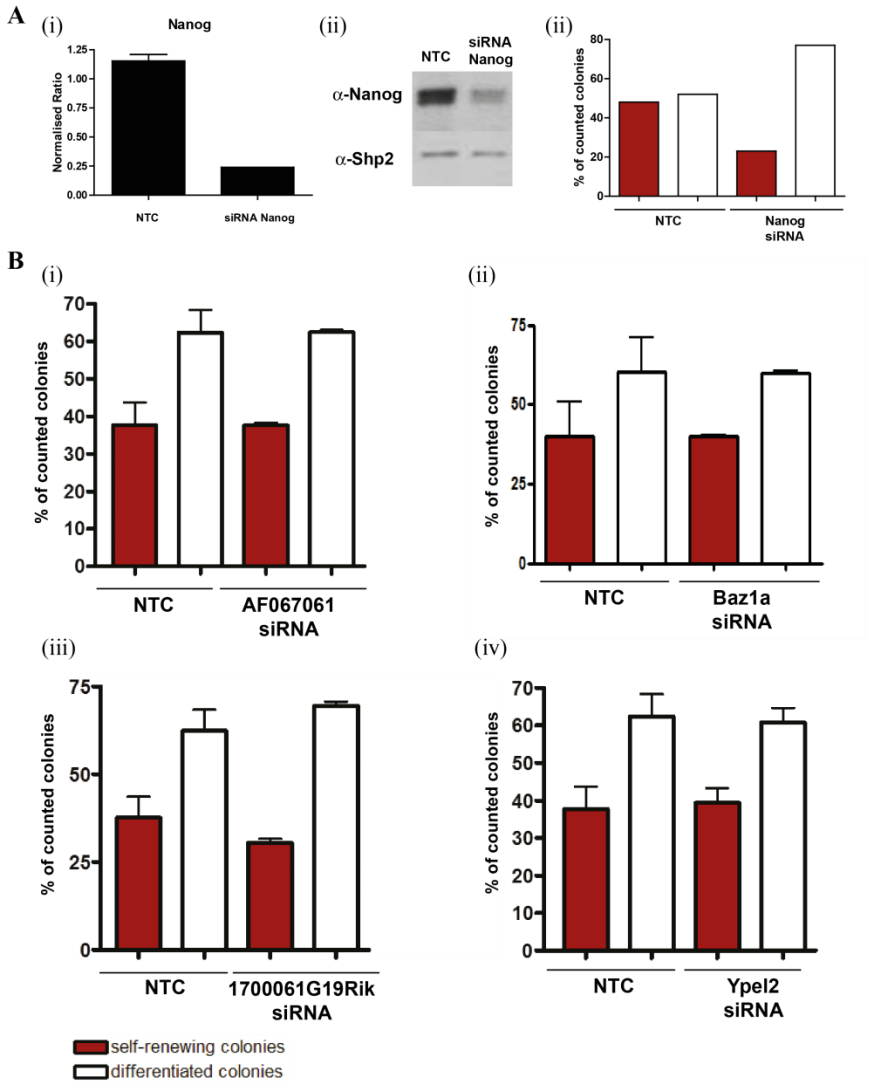

Figure 3.5 siRNA-mediated knockdown of Nanog, AF067061, Baz1a, 1700061G19Rik, and Ypel2. (A) Knockdown of Nanog was used as a positive control. (i) Subsequent analysis of Nanog transcript expression was analysed by quantitative RT-PCR. (ii) Nanog protein expression was analysed by immunoblotting. 20µg of protein/sample were immunoblotted using Nanog antibodies. All blots were stripped and reprobed with anti-Shp2 antibodies to assess loading. (NTC = Non Targeting Control). (iii) SiRNA-mediated Nanog expression knockdown leads to more differentiated colonies upon AP staining; a representative experiment is shown. (B) Knockdown of (i) AF067061, (ii) Baz1a, (iii) 1700061G19Rik and (iv) Ypel2 did not significantly reduce the ability of embryonic stem (ES) cells to self-renew, as assessed by the alkaline phosphatase ES cell colony staining assay. Values correspond to the average ±SEM from three independent biological experiments, and significance was determined using a Mann-Whitney test.

3.3.1 Identification of Zscan4 involved in regulating self-renewal of mESCs

Transient knockdown of Zscan4 with Smartpool siRNAs led to a consistent and significant reduction in the percentage of self-renewing colonies, compared to non-targeting siRNA, shown in Figure 3.6 A. Zscan4 transcripts were decreased by approximately 80% compared to normal levels, after lipofection of Dharmacon targeting siRNA, assessed by quantitative RT-PCR (Figure 3.6 B). A single siRNA targeting the 3' untranslated region of Zscan4c also led to a reduction in alkaline phosphatase positive, self-renewing colonies, although this was less marked than with the siRNA pool. Comparable results were obtained with in-house generated esiRNAs (experiments performed by M. Storm; not shown). Consistent with this reduction in the number of alkaline phosphatase positive colonies, knockdown of Zscan4 also led to reduction in expression of markers of pluripotency, including Nanog, Oct4, and Rex1 (Fig. 3.6 B). The loss of these pluripotency associated genes was typically in the range of 30-40%, while the reduction of alkaline phosphatase positive self-renewing colonies was in the range of 10-20%.

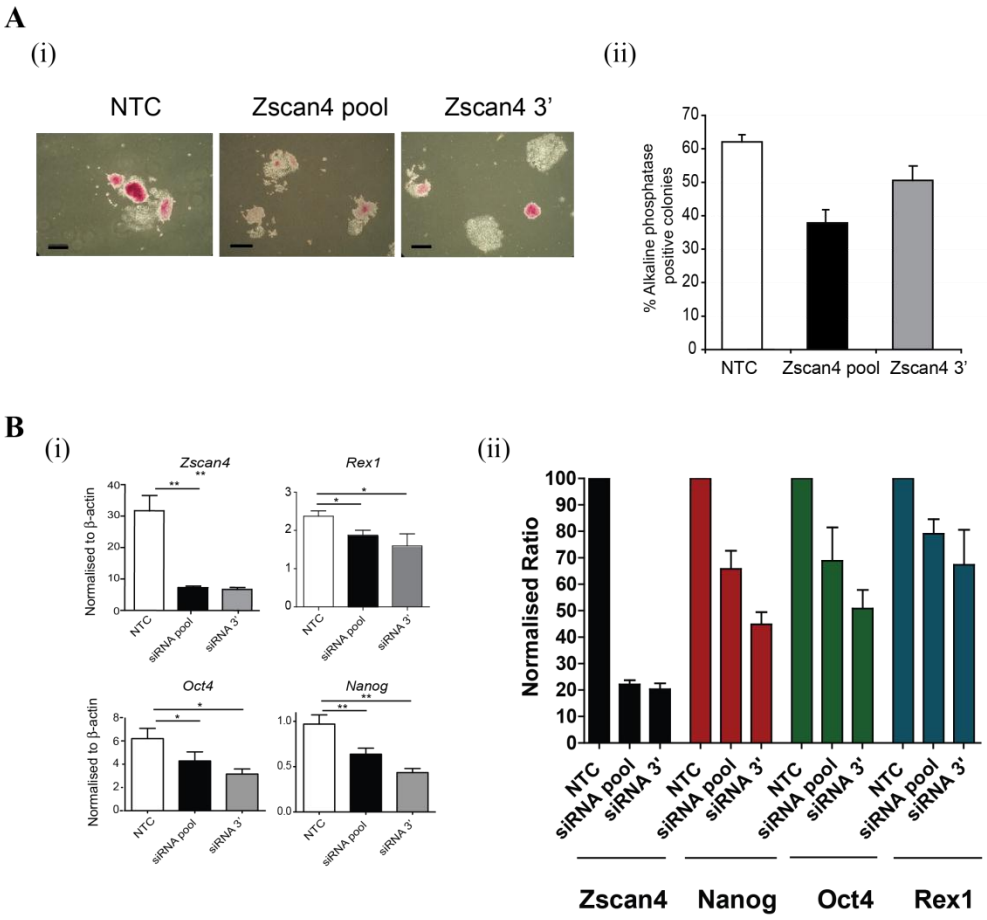

Figure 3.6 siRNA-mediated knockdown of Zscan4 reduces the ability of embryonic stem (ES) cells to self-renew. Smartpool siRNA targeting the Zscan4 family (pool), a single siRNA targeting the 3' untranslated region of Zscan4 (siRNA 3') or NTC siRNA, were transiently transfected into E14tg2a ES cells. A concentration of 50nM for each siRNA was used. Three days post-transfection cells were replated at low density and self-renewal measured after a further 4 days. **(A) (i)** Photographic images of representative colonies are shown (scale bar is 200μm) and **(ii)** the percentage of self-renewing, alkaline phosphatase positive colonies presented, with the values corresponding to the average ±SEM of three independent experiments. **(B) (i)** Knockdown of Zscan4, Rex1, Oct4, and Nanog transcripts was monitored by quantitative reverse transcription polymerase chain reaction and target gene expression was normalised relative to β-actin levels. Values correspond to the average ±SEM from three independent biological experiments, and significance was determined using a Student's t test. *, $p < 0.05$; **, $p < 0.01$. **(ii)** Data of (B)(i) normalised to NTC = 100.

3.3.2 Behaviour of Zscan4 upon differentiation

With the finding that Zscan4 plays a potential role in the regulation of ES cell pluripotency, it was of interest to examine how Zscan4 expression behaves in the transition from a pluripotent to a differentiated state. Zscan4 was previously published to be exclusively expressed in 2-cell stage embryos, with to date no transcripts of Zscan4 detected in any other *in vivo* cell type (Falco et al., 2007). Its re-expression in pluripotent embryonic stem cells, comes therefore as a surprise, with their *in vivo* counterpart, the inner cell mass cells of the blastocyst, not expressing Zscan4 at a detectable levels (Falco et al., 2007).

ES cells cultured in presence of serum and LIF under feeder-free conditions, expressed Zscan4, as measured with quantitative RT-PCR (Figure 3.7 B). For induction of differentiation either simple LIF withdrawal or an embryoid body (EB) differentiation assay were performed (Figure 3.7 A). EBs are cell aggregates, which allow the initiation of differentiation of pluripotent ES cells, and because of the three dimentional culture environment cells begin to a limited extent to recapitulate embryonic development (Martin and Evans, 1975). After induction of differentiation by embryoid body formation, Zscan4 levels drop dramatically compared to starting levels, to about 6.75% after four days and 1.25% after six days (Figure 3.7 B (i)). Concurrent with the drop of Zscan4 levels, was the expected drop of Nanog expression, reflecting the differentiation induction, though the decline appeared to be slower as on day 4 levels had dropped only to ~23% and on day 6 to ~2% of the respective starting levels (Figure 3.7 B (ii)). A similar decline of Zscan4 expression could be detected at the protein level, when differentiation was induced by withdrawal of LIF, leading to a complete deprivation of Zscan4 protein after 4 days (Figure 3.7 C).

GSK-3 is implicated in playing an important role in maintaining ESC self-renewal, shown by the use of pharmacological inhibitors and by genetic deletion of the two isoforms, α and β, of GSK-3 (Bone et al., 2009; Doble et al., 2007; Sato et al., 2004). Inhibition, as well as deletion, of GSK-3 enhances mouse ESC self-renewal and pluriopotency and therefore it was of interest to determine whether Zscan4 expression is affected by either of these two forms of reducing GSK-3 activity. To assess the long-term effect of GSK-3 inhibition by pharmacological inhibitors, mESCs were cultured in presence of the GSK-3 inhibitors BIO or 1M for 14 days.

Long-term inhibiton of GSK-3 almost doubled the expression of Nanog (Figure 3.7 B (ii)) compared to control, indicating an increase in self-renewal. Zscan4 expression also rose upon GSK-3 inhibition, but it is noteworthy that inhibition with the more specific GSK-3 inhibitor, 1M, resulted in an augmented elevation by about 225% compared to control, whereas the less specific inhibitor BIO increased expression by only 24%, which were statistically insignificant. It could be speculated that lower potency or off-target effects of BIO, such as inhibition of Erk (Bone et al., 2009), could influence regulation of Zscan4, and indeed preliminary experiments showed a reduction of Zscan4 when Erk was inhibited with the inhibitor U0126 (Figure 3.7 D). In addition to the small molecule inhibitor approach, GSK-3 DKO mES cells were analysed for the expression of Zscan4 protein, in comparision to E14tg2a wild-type control cells. The findings of these experiments support the inhibitor data, as Zscan4 protein levels are markedly higher in mES cells with ablated GSK-3 loci. Nevertheless, these cells still respond to LIF withdrawal, in respect of a complete loss of Zscan4 expression over 4 days (Figure 3.7 C). These findings are of interest with regard to the PI3K cascade being critical in regulating GSK-3 activity via Akt mediating phosphorylation of Ser9/20 of GSK-3 β/α respectively, leading to GSK-3 inactivation (Welham et al., 2011).

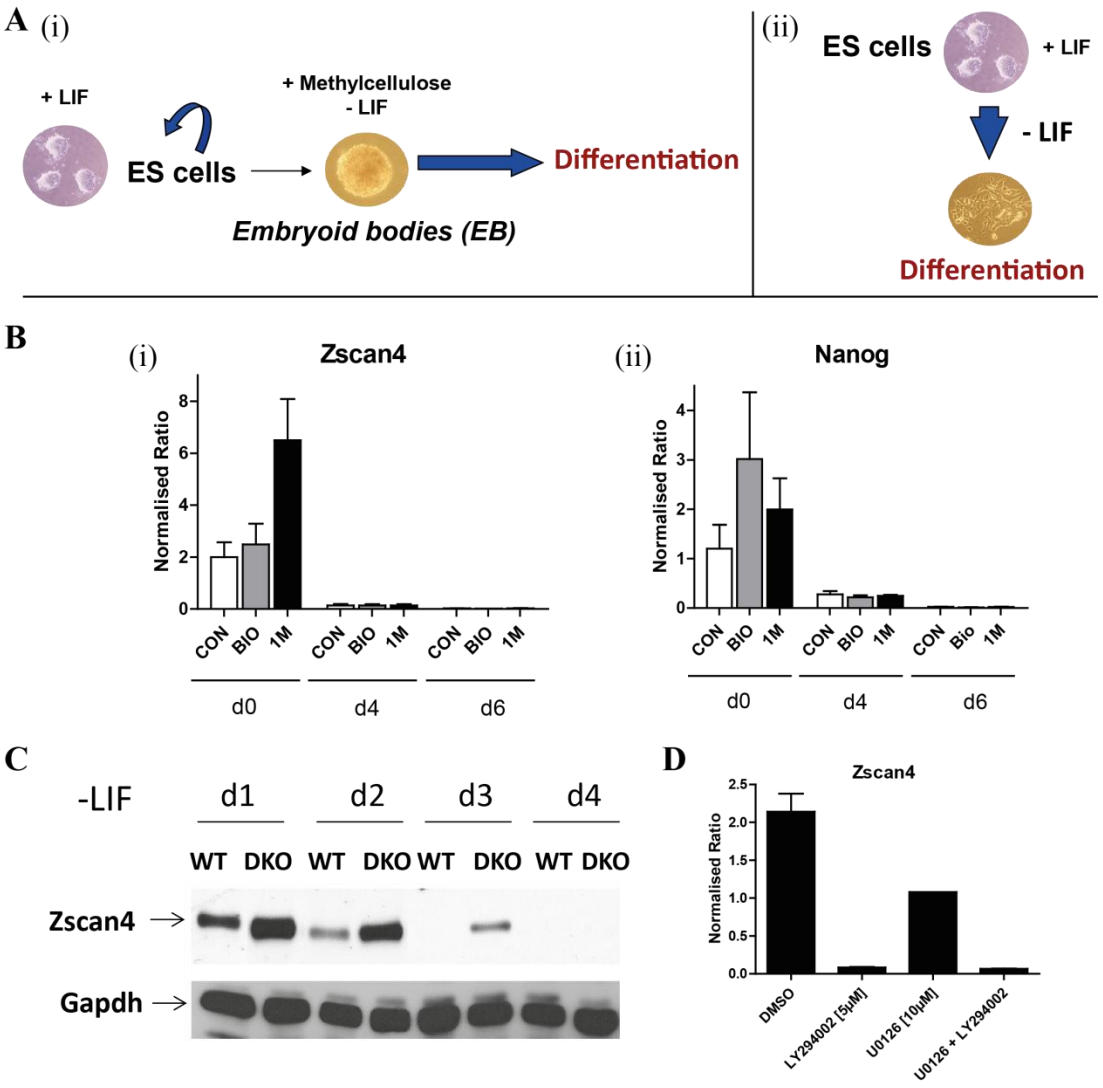

Figure 3.7 Monitoring expression of Zscan4 upon induction of differentiation. **(A)** Illustration of differentiation by (i) the embryoid body (EB) formation assay in presence of methylcellulose and absence of LIF or (ii) induction of differentiation in monolayers by LIF withdrawal. **(B)** E14tg2a embryonic stem cells were cultured in the presence of LIF as a control and in the presence of the GSK-3 inhibitors BIO (0.5μM) or 1M (2 μM) for 14 days. RNA of day 4 (d4) and day 5 (d5) EBs was extracted and (i) Zscan4 and (ii) Nanog expression was analysed by quantitative reverse transcription polymerase chain reaction. Target gene expression was normalised relative to β-actin levels. The averages and ±SEM of duplicate samples from each of two independent biological replicates are shown. **(C)** Immunoblot of E14tg2a and GSK-3 DKO lysates of mES cells grown over a 4-day LIF withdrawal time-course. Blots were probed with a Zscan4 antibody then reprobed with a Gapdh antibody to check for equal loading. **(D)** Quantitative RT-PCR of Zscan4 expression upon treatment with PI3Ks inhibitor LY294002 and/or MEK inhibitor U0126. (n=1).

3.3.3 Zscan4 expression in iPS cells

The notion that induced pluripotent stem (iPS) cells gain expression of Zscan4 during their reprogramming is of special interest (Takahashi and Yamanaka, 2006). With the recent publication reporting that Zscan4 plays a role in genome maintenance (Zalzman et al., 2010), it can be considered that Zscan4 is a key regulator in pluripotent stem cells, controlling both their genomic stability and their self-renwal ability (Welham et al., 2011). How and when exactly Zscan4 is re-expressed during ES cell derivation from inner cell mass cells of the blastocyst, not expressing Zscan4, as well as during iPS cell generation, remains to be elucidated. To verify expression of Zscan4 in iPS cells and to compare the levels with mES cell levels, quantitative RT-PCR was performed on samples taken of each. Both, mES and iPS cells express Zscan4 at comparable levels (Figure 3.8 A), and also Nanog levels are in a similar range, which is entirely consistent with the literature (Figure 3.8 B).

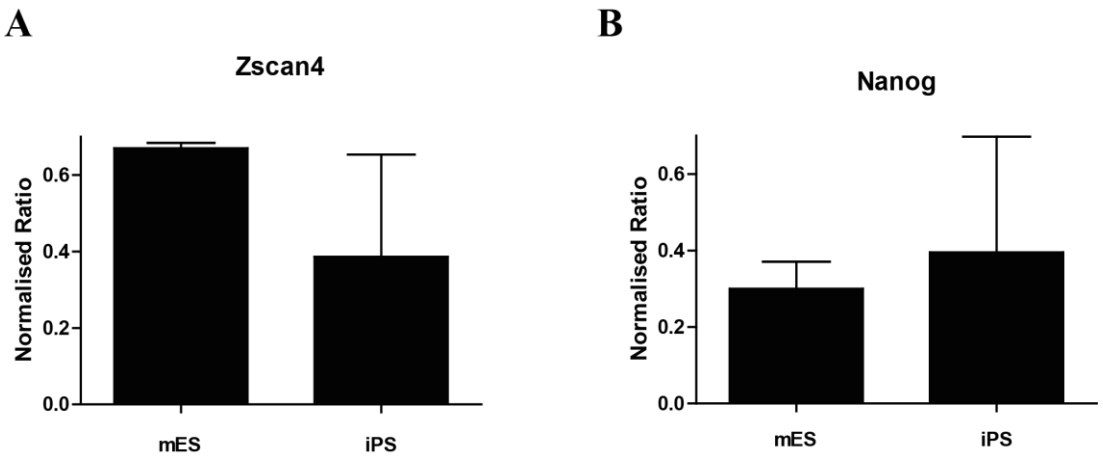

Figure 3.8 Zscan4 expression in mouse iPS cells. Quantitative RT-PCR was conducted to detect expression of Zscan4 and Nanog in E14tg2a mESCs and mouse iPS cells. The averages of duplicate samples and standard deviations from each of two independent biological replicates are shown.

3.4 PI3Ks catalytic isoforms in mES cells

PI3Ks have been implicated in the regulation of both ESC proliferation and self-renewal (Kingham and Welham, 2009; Paling et al., 2004; Takahashi et al., 2003). It is noteworthy that PI3Ks of the class IA sub family, which are predominantly linked with mESC fate, are already expressed from as early as the one cell stage of development and remain expressed through to the blastocyst stage of murine preimplantation embryo development (Riley et al., 2005). With Zscan4 being regulated downstream of PI3Ks, one aim of this part of the study was to investigate whether its regulation is coupled to a specific isoform of PI3Ks. Recent advances in the development of selective, cell-permeable, small molecule inhibitors provide a useful toolbox to study the different catalytic subunits of PI3Ks. These inhibitors typically interact in a reversible manner with the ATP binding pocket of the PI3K catalytic isoforms, competing directly with the substrate ATP. From the repertoire of available inhibitors we selected a few specific inhibitors to investigate the regulation of Zscan4 downstream of the p110α, β and δ isoforms.

Two structurally distinct p110α inhibitors, namely PIK-75 and Compound 15e, were used to determine a possible role for p110α in the regulation of Zscan4. PIK-75 was characterised as a selective p110α inhibitor and was reported to inhibit p110α with an IC_{50} of 5.8nM (Knight et al., 2006). Besides inhibition of p110α, PIK-75 also inhibited DNA-PK with an IC_{50} of 2nM, but not mTORC1 (IC_{50}=1μM) or mTORC2 (IC_{50}=10μM) at the typically applied concentration of 25nM (Dagia et al., 2010; Hers, 2007; Kim et al., 2009b; Marone et al., 2008). The other selective p110α inhibitor, compound 15e, inhibits the catalytic alpha isoform with an IC_{50} of 2nM, while off-target effects of other isoforms are at higher concentrations (IC_{50}: p110β=16nM; p110γ=660nM). It was identified to inhibit growth of various cancerous cell lines like A375 melanoma cells (IC_{50}=0.58μM), U87MG human glioblastoma cells (IC_{50}=1.10.μM), A2780 human ovarian cells (IC_{50}=0.27μM), and might be a potential anti-tumour compound (Folkes et al., 2008; Hayakawa et al., 2006).

To assess the contribution of the p110β isoform to regulation of Zscan4, TGX-121 and the more potent TGX-221 inhibitors were used (Jackson et al., 2004; Robertson et al., 2001). TGX-221 was used previously to assess PI3K signalling and helped to elucidate a function of p110β in platelet activation, defining p110β as an important new target for antithrombotic therapy (Jackson et al., 2005). TGX-121 was described to have an IC_{50} of 50nM, while the more potent TGX-221 had an IC_{50} in the range of 5-50nM, depending on the ATP concentrations of 50μM and 1mM (Jackson et al., 2005). For TGX-121 undesired inhibition of p110γ is described with an IC_{50} of 5μM (Robertson et al., 2001), and TGX-221 also inhibits p110α (IC50= 5μM) and p110γ (IC50= 10μM) (Jackson et al., 2005).

IC87114 was the first isoform-selective PI3K inhibitor described and was shown to be highly specific for the p110δ isoform (Sadhu et al., 2001). In cell studies IC87114 was used to inhibited p110δ to establish a selective role in neutrophil polarization and directional migration at doses of 5-10μM (Sadhu et al., 2003). IC_{50} values of ~60nM for p110δ, and >1μM for p110α+β, were determined using PI3K lipid kinase assays on multiple preparations of recombinant protein (Chaussade et al., 2007). IC87114 is a very "clean" inhibitor, not targeting ATM, DNA-PK, ATR, and mTOR, even at high concentrations of 100μM (Chaussade et al., 2007).

A brief summary, including the chemical structures of all PI3K inhibitors used in this study are summarised in Table 2.2. Furthermore, a simple illustration shows the p110 specific inhibitors and their targets in Figure 3.9 A. Drawbacks of small chemical inhibitors are possible off-target effects, mostly on structural similar proteins, and it is therefore important to consider these carefully. Furthermore, IC_{50} values are often obtained in cell-free assays, and a change of conditions can result in different values. For example, when ATP-competitive inhibitors are tested in kinase assays the IC_{50} varies, depending on the ATP concentration. In addition, there are many other factors that can cause variability, for instance inhibitor stability under cell culture conditions, cell permeability, differences in cell types, just to mention a few.

3.4.1 Contribution of specific PI3Ks isoforms in regulating Zscan4

Murine ESCs were incubated with the pharmacological inhibitors, PIK-75, TGX-121, TGX-221 or IC87114, for 48h in the presence of serum and LIF to inhibit the respective p110 isoforms (Figure 3.9 A). The broad spectrum PI3K inhibitor, LY294002, was used as positive control. Inhibitors were applied in typical concentrations for mESCs, based on the experience of work conducted in the Welham laboratory (Kingham and Welham, 2009). Quantitative RT-PCR analyses revealed a significant downregulation of Zscan4 expression upon treatment with LY294002, as expected from the microarray data. Interestingly, PIK-75 was the only specific catalytic isoform inhibitor to induce downregulation of Zscan4 expression, indicating regulation occurs solely through p110α. Neither of the two p110β inhibitors, TGX-121 or TGX-221, nor the delta inhibitor IC87114 appeared to alter Zscan4 expression (Figure 3.9 B).

Potential cumulative effects resulting from the combination of the different isoform specific inhibitors were assessed over a time-course of 3-5 days (Figure 3.10). The dramatic negative effects of PIK-75 (-90%) and LY94002 (-83%) on Zscan4 expression were maintained over the entire time-course, when assessed with quantitative RT-PCR. On average levels of Zscan4 dropped upon p110α inhibition by ~90% and after LY294002 treatment by ~83%. Furthermore, inhibition with PIK-75 was dominant in all the combinations of inhibitors tested. Inhibition of the p110β and p110δ isoforms alone did not affect Zscan4 levels, but the combination of both did show some cumulative effects, especially at the later time points (Figure 3.10 B, C). Inhibition of one of the PI3K isoforms alone might not be enough to decrease PIP_3 levels sufficiently to reduce Zscan4 expression. Dual inhibition of p110β and p110δ might decrease total PIP_3 levels to an extent that leads to a reduction of Zscan4 expression. When all three PI3Ks inhibitors were used simultaneously the decrease in Zscan4 expression compared to PIK-75 treatment alone was 7.5% stronger, indicating some cumulative effects.

By using another structural different p110α inhibitor, further strength was added to these previous findings. When mESCs were cultured in presence of Compound 15e for 48h at a concentration of 600nM, Zscan4 expression was reduced, similar to the levels observed after LY294002 treatment (Figure 3.11 A).

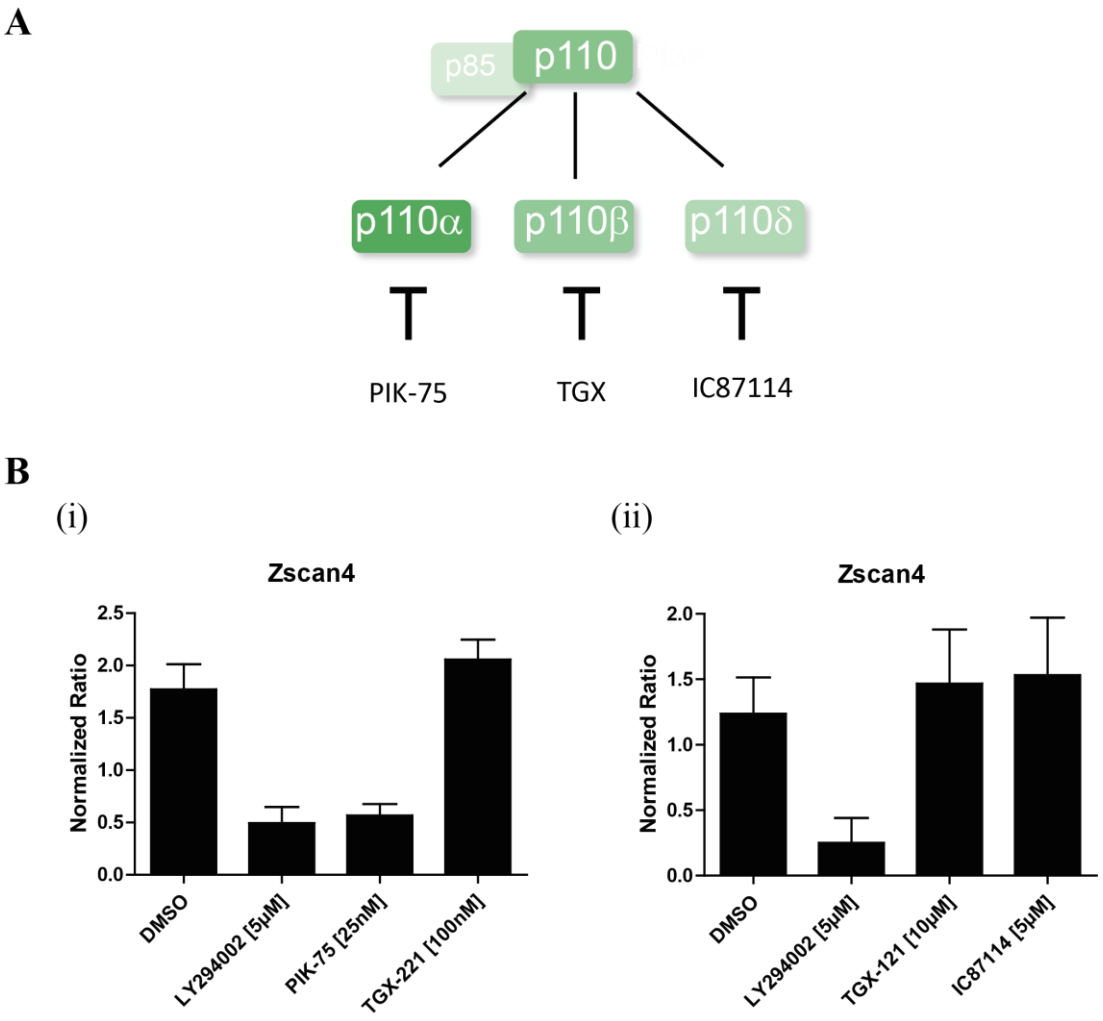

Figure 3.9 Contribution of specific PI3Ks isoforms to regulation of Zscan4 expression. (A) Schematic diagram of specific p110 PI3K catalytic isoform inhibitors used. **(B) (i)** E14tg2a ESCs were cultured in the presence of LIF plus DMSO as control, 5μM LY294002, 25nM PIK-75, 100nM TGX-221, **(ii)** 10μM TGX-121 or 5μM IC877114 for 48h. Expression of Zscan4 was analysed by quantitative reverse transcription polymerase chain reaction, and expression was normalised relative to β-actin levels. Error bars represent standard deviation of duplicate samples from each of two independent biological replicates.

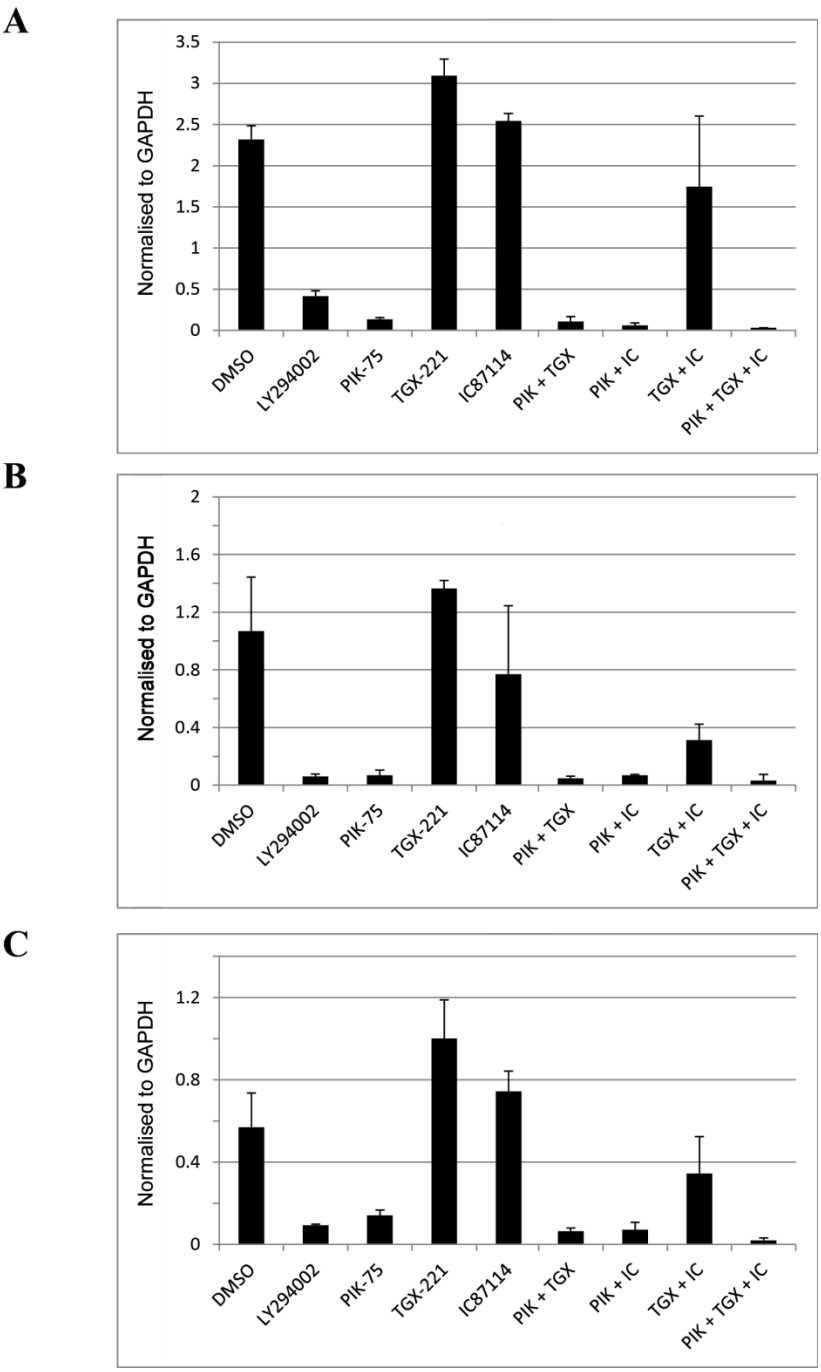

Figure 3.10 Time-course of Zscan4 expression after treatment with PI3K isoform selective inhibitors. OCRG9 mES cells were cultured in the presence of LIF and were treated with the PI3Ks inhibitors, 10μM LY294002, 25nM PIK-75, 100nM TGX-221, 5μM IC87114, or combinations of these inhibitors as indicated. RNA samples were taken after **(A)** three **(B)** four and **(C)** five days. Expression of Zscan4 was analysed by quantitative reverse transcription polymerase chain reaction, and expression was normalised relative to Gapdh levels. The averages of triplicate samples from one biological replicates are shown.

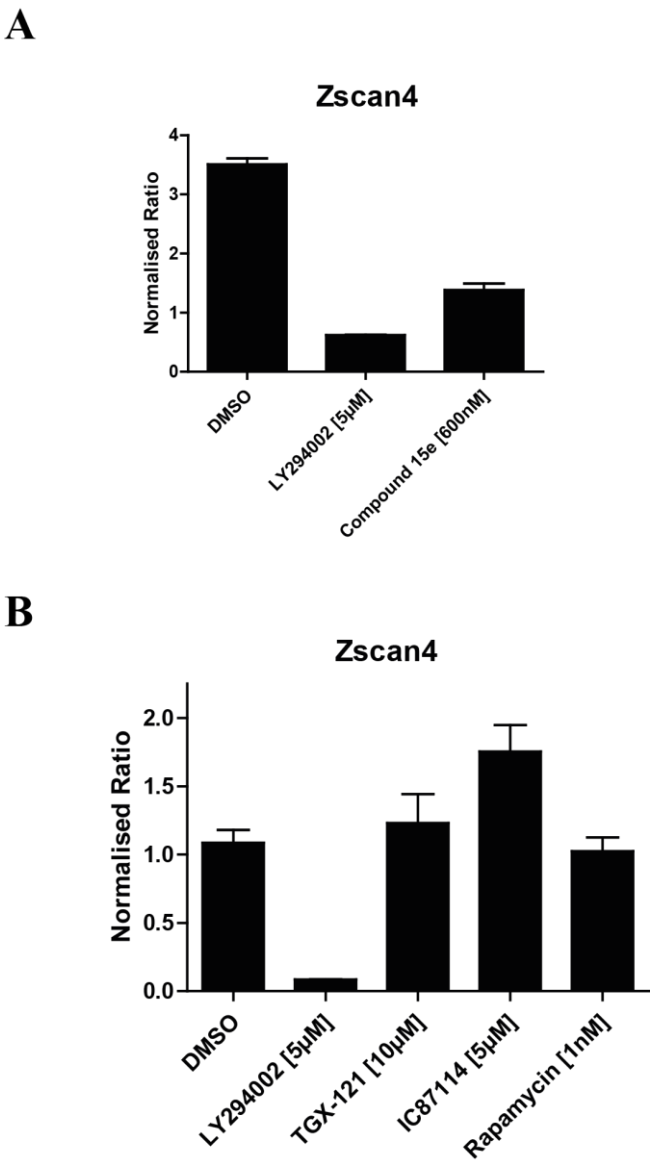

Figure 3.11 Regulation of Zscan4 by the p110α catalytic subunit of PI3K (A) E14tg2a cells were treated with 5μM LY294002 or 600nM Compound 15e and samples were assessed by Q-PCR for the expression of Zscan4. **(B)** RNA was extracted 48h after inhibitor treatment as indicated, quantitative RT-PCR was performed and Zscan4 expression normalised relative to β-actin levels. Graphs show standard deviation and are representative of three experimental repeats.

In adipocytes, PIK-75 was reported to be able to block activation of the mTOR pathway as measured by phosphorylation of S6 ribosomal protein (Knight et al., 2006). To eliminate the possibility that a potential off-target effect of PIK-75 might be the cause for the Zscan4 alteration, mTOR was inhibited directly with the specific inhibitor Rapamycin. ESCs cultured in presence of Rapamycin for 48h did not exhibit any change in Zscan4 expression, ruling out that the downregulation seen with PIK-75 arises from mTOR inhibition (Figure 3.11 B).

To further explore the mechanisms regulating Zscan4, a gain-of-function approach was applied to complement the loss-of-function studies described in the preceding section. To achieve this, the PI3K pathway needed to be artificially activated, and this was accomplished by creating myristoylated versions of the catalytic p110 isoforms (further details are given in 5.2). The myr-p110 transgenes were overexpressed under the control of the CAG promoter (Niwa et al., 1991) in OCRG9 mESCs, utilising the piggyBac transposon system (2.4.12). Colonies over-expressing myr-p110 isoforms were expanded after selection with respective antibiotics. Three independent clones over-expressing myr-p110α were analysed with quantitative RT-PCR for the expression of Zscan4. OCRG9 control mESCs and respective myr-p110α clones were cultured in presence and absence of LIF for 4 days, before analysis. In line with the loss-of-function approach, activation of the PI3K p110α pathway led to a significant upregulation of Zscan4 (Figure 3.11). Expression of Zscan4 was upregulated on average around 70-fold in presence of LIF compared to control. Interestingly, Zscan4 expression was also maintained at high levels in the absence of LIF in myr-p110α expressing cells (Figure 3.12).

Taken together, these date provide strong evidence that p110α is the main PI3K catalytic isoform responsible for the regulation of Zscan4.

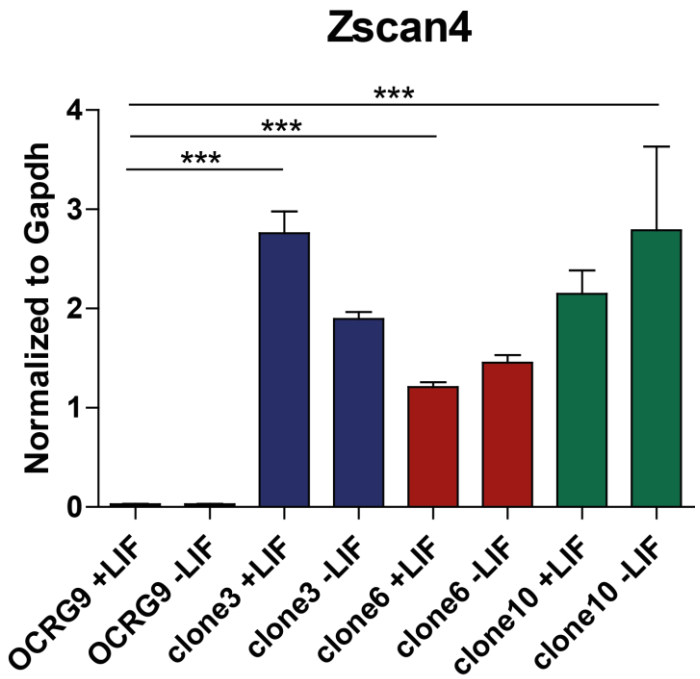

Figure 3.12 Influence of over-expression of activated p110α PI3K catalytic isoform on Zscan4 expression. Clones over-expressing a myristoylated version of the p110α catalytic subunit of PI3Ks were cultured in presence and absence of LIF. As a control parental OCRG9 ES cells were grown in presence and absence of LIF for 4 days. Expression of Zscan4 was analysed by quantitative RT-PCR and Zscan4 expression was normalised relative to Gapdh levels. The averages and S.E. of triplicate samples from each of three independent biological replicates are shown: ***, $p < 0.0005$, in a Student's t-test.

3.4.2 Contribution of specific PI3Ks isoforms in regulating Shp-1

The protein tyrosine phosphatase Shp-1 was also found to be important for ES cell self-renewal (work of Belinda Thompson reported in (Storm et al., 2009)). Isoform specific PI3Ks inhibitors were also used to examine regulation of Shp-1 expression. In contrast to Zscan4, the p110β catalytic isoform appeared to be dominant for the regulation of Shp-1, with some additional contribution of p110α (Figure 3.13 A). As for Zscan4, there was no change in Shp-1 expression when mTOR or the p110δ catalytic isoform were targeted (Figure 3.13 B).

A

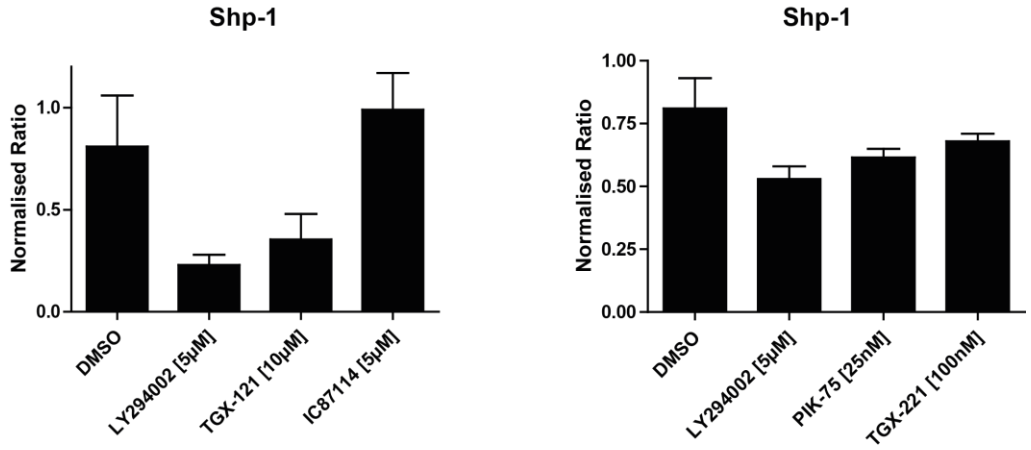

B

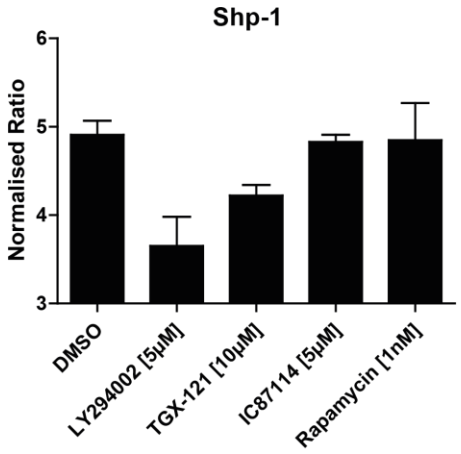

Figure 3.13 Catalytic Class IA PI3K isoform-mediated signalling regulates expression of Shp-1 (A) (B) RNA was extracted 48h after inhibitor treatment as indicated, quantitative RT-PCR was performed and Shp-1 expression normalised relative to β-actin levels. The data are the average of one biological experiment run in duplicates.

3.4.3 Effect of PI3K isoform selective inhibitors on mESC fate

Members of the class-IA PI3K family of lipid kinases regulate key signalling pathways in many cell types leading to a variety of physiological responses, including cell proliferation, self-renewal and survival (section 1.6). How the different catalytic isoforms couple to functional responses is a hot topic in current biomedical research, and a promising field for drug development. In ESCs PI3K activity has been linked with self-renewal (Paling et al., 2004), growth and tumorigenicity (Jirmanova et al., 2002; Takahashi et al., 2003) and previous work in our laboratory has provide some evidence that specific p110 catalytic isoforms are related to different functions in mESCs (Kingham and Welham, 2009).

To gain further insights into the mechanisms of PI3K function, OCRG9 mESCs were treated with catalytic isoform specific PI3K inhibitors described above (cross-ref section). OCRG9 ES cells contain an EGFP-IRES-blasticidin cassette in exon 4 of the Rex1 gene (Toyooka et al., 2008). This knock-in ES cell line can be used to track Rex1 expression by detecting the corresponding EGFP fluorescent protein levels. Rex1 (also known as Zfp42) is a well-recognized pluripotency marker, which is strongly expressed in the ICM and self-renewing mESCs, but downregulated upon differentiation (Rogers et al., 1991). To address whether PI3K isoforms affect Rex1 expression, ESCs were cultured with additional specific PI3K inhibitors, and subsequently EGFP expression was measured with flow cytometry (Figure 3.14). Broad inhibition of PI3Ks with LY294002 resulted in a drop in the proportion of EGFP positive cells by almost 70%, confirming previous reports of its ability to reduce self-renewal. PIK-75 was also able to reduce the proportion of cells expressing EGFP (Rex1) after treatment for 5 days, but the reduction observed was only 19% drop in comparison to controls. PI-103, described to inhibit p110α and mTOR, but with potential off-target effects on other PI3K-related enzymes, also led to a reduction in proportion of EGFP positive cells of 18%. Inhibitors for the p110β and p110δ isoforms, TGX-221 and IC87114, did not appear to change EGFP expression compared to untreated or vehicle controls. This came as a surprise as the p110β isoform was related previously to self-renewal in mESCs (Kingham and Welham, 2009). Further investigations are necessary to clarify the discrepancy between the experimental results, possibly a consequence of the inhibitor batch, stability of the inhibitor or the use of different cell lines. Combinations of the three

specific isoform inhibitors, PIK-75, TGX-221 and IC87114, further enhanced the decrease in the proportion of EGFP/Rex1 expressing cells to a total of 26%. It is noteworthy that the combination of the three specific inhibitors did not lead to a loss of self-renewal to the same level as LY294002 inhibition. There might be several potential reasons for this observation, such as incomplete inhibition of all three isoforms, different inhibitor stabilities, or additional off-target effects of LY294002. Large numbers of intracellular interacting targets have been found for LY294002, at doses close to typical used concentrations used for PI3Ks inhibition (Gharbi et al., 2007). One common target of PI3K inhibitors is the mTOR pathway, which was for this reason addressed with stimulation experiments (Figure 3.15). When ESCs were cultured in presence of the PI3K inhibitors and stimulated with LIF, only treatment with LY294002 at a concentration of 10μM, led to a strong reduction in phosphorylation of S6, a read-out for mTOR activity. PI-103, which is reported to inhibit p110α and mTOR, also resulted in a loss of S6 phosphorylation, but to a lesser extent. The inhibitors PIK-75, TGX-221, and IC81774 did not alter significantly mTOR activity, judged by S6 protein phosphorylation. It should be noted that these experiments were performed in standard cell culture conditions in the presence of serum, which can like, LIF, stimulate the mTOR pathway.

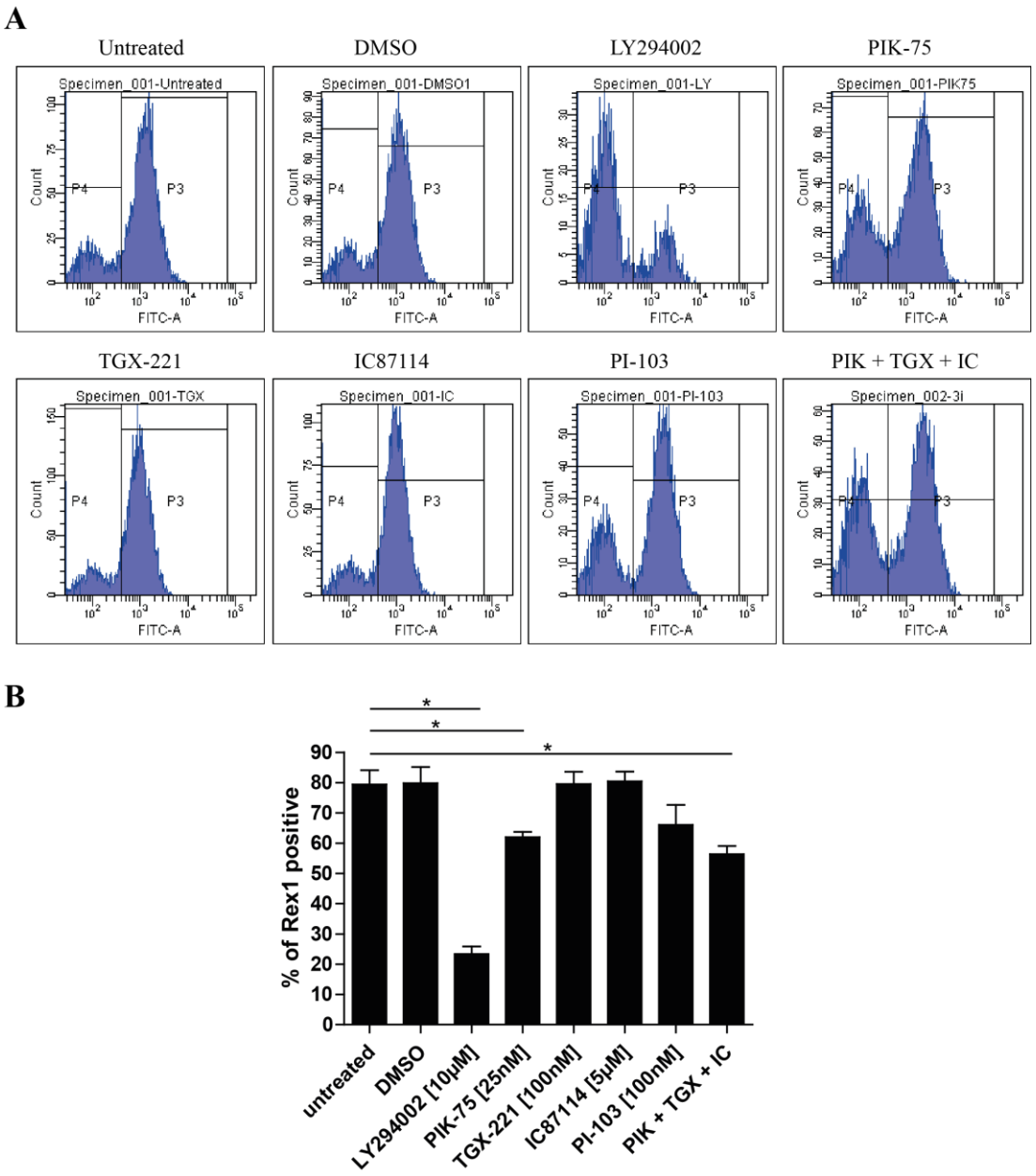

Figure 3.14 Effects of PI3K isoform selective inhibition on Rex1/EGFP expression in OCRG9 mES cells. OCRG9 cells were grown for 5 days in the presence and absence of PI3K inhibitors as indicated and fluorescence intensity was measured with flow cytometry. The Y-axis represents cell number, while the X-axis represents fluorescent intensity. **(B)** Summary of four independent experiments plotting the percentage of Rex1 (EGFP) positive cells upon inhibitor treatment on day 5. Values correspond to the average ±SEM from four independent biological experiments, and significance was determined using a Mann Whitney test.*, $p < 0.05$

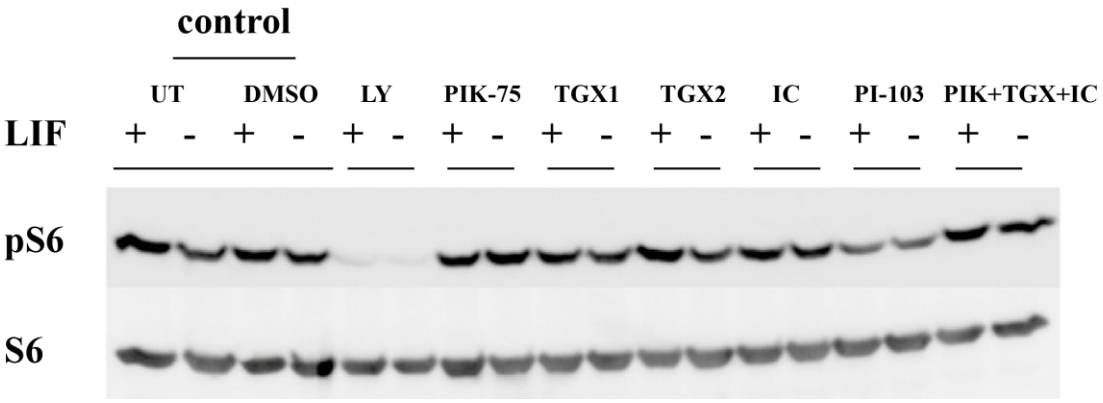

Figure 3.15 Identifying off-target effects of applied PI3Ks inhibitors on mTOR.

ES cells were cultured in the absence of LIF for 12h hours with the indicated inhibitors for the last 1 hour. Inhibitors were used at following concentrations: LY294002 (10μM), PIK-75 (25nM), TGX-221 (1: 100nM, 2: 200nM), IC81774 (5μM), PI-103 (100nM). Cells were treated with vehicle (DMSO), or left untreated (UT), as control. Then LIF was added to the culture (1000 Units/ml) and whole cell lysates were prepared at 10 minutes after addition of LIF for western blot analyses of total and phosphorylated (Ser235/236) forms of S6.

Cell density is an important parameter for maintaining optimal self-renewal and for survival in mESCs in culture. Autocrine signalling has been reported to play a role in self-renewal and therefore a reduction in cell or colony numbers might negatively impact self-renewal (Guo et al., 2006; Singla et al., 2008; Welham et al., 2007). In order to verify that our PI3K inhibitors don't affect cell-density or cell survival, colony size and numbers were assessed upon culture of mESCs with the respective inhibitors. After culture for five days, ESC colonies were fixed and stained with Leishman's reagent. Average colony size and number per condition were assessed after scanning and digital image analysis with NIST's Integrated Colony Enumerator (NICE) software (http://physics.nist.gov/nice) (Figure 3.16). For optimal automatic analysis scanned images were changed to grayscale (Figure 3.16 A i) and detected colonies were marked by NICE with a red cross (Figure 3.16 A ii, iii).

PIK-75 alone, or in combination with other PI3K selective inhibitors, markedly decreased colony size by about 75% compared to untreated or vehicle controls, which might account for some of the effects on self-renewal determined via Rex1 FACS analysis (Figure 3.16 B). This finding is not inconsistent with a previous report of PIK-75 leading to a reduction in ESC proliferation (Kingham and Welham, 2009). Interestingly, total colony numbers did not change after ESC culture with PIK-75 at 25nM for 5 days, as detected with NICE (Figure 3.16 C). Only the two broader PI3K inhibitors, LY294002 and PI-103, lead to a reduction in total colonies, probably occurring as a consequence of toxicity effects arising from off-targets. Overall, the p110α inhibitor PIK-75 exhibited the largest impact on ESC proliferation, which was possibly a major contributor to the effects seen on self-renewal.

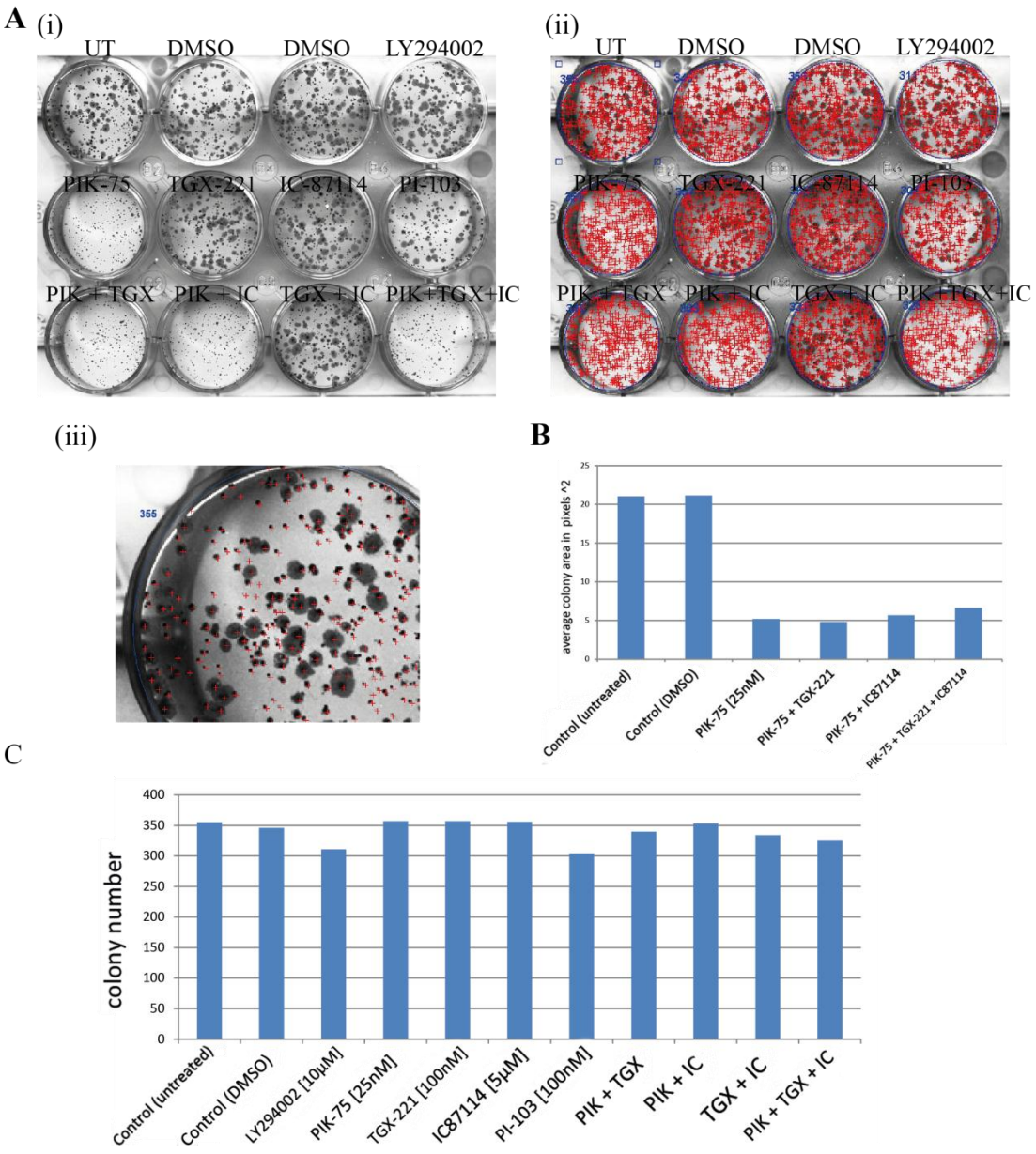

Figure 3.16 Effects of PI3K selective inhibitors on ES cell colony number and size (A) OCRG9 ES cells were plated at a density of 400 cells/well in a 12 well cell culture tray. PI3K selective inhibitors were added to the cell culture medium after allowing cells to attach. Following 5 days of culture emerged colonies were stained with Leishman's stain. **(i)** Scanned and for analysis purposes processed image of Leishman-stained d5 colonies. **(ii)** Colony size and numbers were assessed with NIST's Integrated Colony Enumerator (NICE) software (http://physics.nist.gov/nice). **(iii)** Close up of untreated (UT) condition, each colony count is highlighted by a red cross. **(B)** Colony size in square pixels assessed with NICE software of untreated and vehicle control verses p110α inhibition by PIK-75. **(C)** Colony numbers were automatically counted with algorithm of NICE. One representative out of three total experiments is shown.

3.5 Discussion and Summary

Prior to the start of this study, a microarray screen was performed in our laboratory to identify novel regulators of self-renewal downstream of PI3Ks (Storm et al., 2009). From the resulting dataset of this PI3Ks inhibition screen, candidate genes, AF067061, Baz1a, LOC327811, Shp-1, 1700061G19Rik, Ypel2, and Zscan4c, were chosen for further analysis.

3.5.1 Summary

- GSK-3-dependent and independent regulatory mechanisms were determined by inhibition of PI3Ks and GSK-3 with LY294002 and BIO. Further confirmation was gained by the use of GSK-3 DKO ES cells, and subsequent analysis of candidate gene expression via quantitative RT-PCR.

- Hierachical clustering of the significant probesets resulted in 12 separate groups. Genes regulated by common mechanisms fell into similar expression clusters, indicating a relationship between regulation and the clusters defined.

- Functional involvement of Zscan4 in ES cell identity was established by siRNA loss-of-function studies, and subsequent analysis of self-renewal markers and use of the clonal alkaline phosphatase assay.

- Zscan4 expression was shown to be lost upon differentiation, as assessed with embryoid body formation and LIF withdrawal experiments. Zscan4 levels were elevated at the transcriptional and protein levels upon long-term inhibition of GSK-3 with the specific GSK-3 inhibitor 1M or the use of GSK-3 DKO mES cells.

- In induced pluripotent stem cells, Zscan4 expression was comparable to expression in embryonic stem cells.

- Inhibition of the p110α PI3K catalytic isoform with the specific inhibitors PIK-75 and Compound 15e, resulted in a loss of Zscan4 expression, strongly suggesting a regulation of Zscan4 via this isoform. Additional evidence was

generated by artificial activiation of p110α leading to an increase of Zscan4 expression.

- Shp-1 was another gene identified by data mining the microarray screen and functional studies indicated its involvement in regulating self-renewal (Belinda Thompson (Storm et al., 2009)). In contrast to Zscan4, it appeared to be mainly regulated by the p110β isoform upon specific inhibitor treatment, with some contributions of the p110α isoform.

- Rex-1 expression, mirrored by GFP expression in OCRG9 knock-in mES cells, was significantly lower in comparison to control upon inibition of p110α with PIK-75, as assessed using flow cytometry.

- PIK-75 negatively affected proliferation of mESCs, leading to colonies that were smaller in size. Despite the reduction in size, colony numbers did not change when digital images were analysed.

3.5.2 Discussion

The characterization of the PI3K-dependent transcriptome in murine ES cells, facilitated the identification of novel molecular mechanisms potentially involved in regulating ES cell fate (Storm et al., 2009). The importance of the PI3K pathway in ES cell self-renewal was first reported by the group of Prof. M. Welham at the University of Bath (Paling et al., 2004). Further definition of the gene expression patterns regulated via PI3K helps to provide a clearer understanding of the underlying mechanisms maintaining ES cell pluripotency. Gene ontology analysis of the dataset revealed that the most over-represented functional group were transcription factors (Storm et al., 2009). Consistent with this notion is the widely accepted theory that a core trsancriptional regulatory circuitry is driving self-renewal of ESCs and its disturbance ultimately causes differentiation (Boiani and Schöler, 2005; Boyer et al., 2005; Kim et al., 2008; Loh et al., 2006). In line with previous research conducted in our laboratory, Nanog, a key component of the self-renewal core transcription factor network was susceptible to inhibition of PI3Ks by LY294002 (Storm et al., 2007). Other regulators of pluripotency, Tbx-3, Esrrb

(Ivanova et al., 2006) and Klf4 (Jiang et al., 2008; Li et al., 2005), were also downregulated, possibly as a cause of being regulated to some extent by Nanog (Loh et al., 2006). Interestingly, expression of Sox2 and Oct4, also belonging to the intrinsic core circuit of self-renewal, were not decreased over the 72h time-course of PI3K inhibition. Half a year after our publication, work of Niwa et al. described a parallel circuit downstream of LIF signalling, maintaing pluripotency of mouse ES cells. In this work, Tbx-3 was implicated as being regulated by the PI3K-Akt pathway downstream of LIF signalling, predominantly stimulating Nanog (Niwa et al., 2009). This work could explain why the levels of Sox2 and Oct4 were not reduced after 72h of LY294002 treatment, with LIF stimulating the second parallel pathway, integrating the signal via Jak/Stat3 into the core transcription factor network by Sox2 and Oct4. Such a functional hierarchy of transcription factors could be the evolutionary cause for increasing the robustness of the pluripotent state, which needs to be guarded from fluctuating environmental triggers inducing differentiation.
Significant changes in gene expression upon LY294002 treatment were clustered according to similar expression patterns into 12 groups by applying the k-means nonhierarchical method (Storm et al., 2009). We were interested in whether there was a correlation of expression patterns and regulation by pathways downsteam of PI3Ks. The Wnt signalling pathway was considered as it is an important downstream signalling pathway in ESCs (Sato et al., 2004; Storm et al., 2007; Ying et al., 2008). GSK-3 is known to negatively regulate Wnt signalling, by marking β-catenin through phosphorylation which leads to its degradation (Aberle et al., 1997; Rubinfeld et al., 1996). For this reason Wnt signalling can be mimicked by GSK-3 inhibition with pharmcological inhibitors, which were used in this study to investigate GSK-3-dependent or independent regulation. The hypothesis of a correleation between regulatory pathways and expression cluster was confirmed by the finding that all genes analysed from cluster 1, AF067061, Baz1a, LOC327811, and Zscan4c, appeared to be regulated downstream of PI3Ks independently of GSK-3. In contrast, others which were in the same or very similar expression clusters, including Nanog (Storm et al., 2007), Shp-1, and 1700061G19Rik, exhibited GSK-3-dependent regulation. This is of particular interest given the discovery that inhibition of GSK-3 is required for the ground state of ES cell pluripotency (Ying et al., 2008). These studies have shown that it is sufficient to maintain self-renewal of mESCs in a

serum-free minimal medium when GSK-3 and MEK were inhibited with two specific pharmacological inhibitors (Wray et al., 2010; Ying et al., 2008). This culture condition, was also termed '2i' conditions, and does not require any exogenous growth factors, but additional LIF was shown to have beneficial effects on clonogenic self-renewal of ES cells (Silva et al., 2008). Furthermore, it was shown that GSK-3 DKO cells could be propagated without loss of pluripotency solely by inhibition of MEK, which blocks the differentiation inducing effects of autonomously secreted FGF4 (Kunath et al., 2007; Stavridis et al., 2007). The population doubling times were reduced in these conditions, but could be restored by addition of LIF, showing that LIF-mediated signalling through STAT3 operates independent of GSK-3 inhibition (Matsuda et al., 1999; Niwa et al., 1998; Ying et al., 2008).

Zscan4, a gene that provoked our special interest because it belonged to a small group of genes that were detected to have a significant decrease in their expression within 24 hours of PI3K inhibition, appeared to be regulated via GSK-3-independent mechanisms. Evidence from experiments using the inhibitors LY294002 and BIO, to block PI3Ks and GSK-3 signalling, alone or in combination, demonstrated that GSK-3 inhbition was not able to overcome the effects of inhibiting PI3Ks on Zscan4 expression. In contrast, Nanog was previously shown to be reguated in a GSK-3-dependent manner (Storm et al., 2007). Additional experiments with GSK-3 DKO ESCs strenghtened these findings, as PI3K inhibition could reduce the transcriptional levels of Zscan4, but not the levels of GSK-3-dependent Nanog. However, it is noteworthy that Zscan4 expression was increased at the RNA and protein levels, when GSK-3 was inhibited with the specific 1M compound or by the use of GSK-3 DKO mES cells. This observation might be the cause of an increase in the overall self-renewal capacity of the ESC culture, rather than a direct cause of GSK-3 inhibition, as it is reported that GSK-3 inhibition in serum plus LIF conditions increases self-renewal (Bone et al., 2009). Furthermore, Wnt proteins in combination with LIF were shown to be sufficient for ESC self-renewal (Berge et al., 2011). In a recent report it was suggested that GSK-3 inhibition acts through relieving negative pressure of the T-cell factor 3 (Tcf3) on the pluripotency network. (Wray et al., 2011).

When an siRNA loss-of-function method was used on our selected candidate genes, knock-down of Zscan4 resulted in a loss of self-renewal, assessed by measuring alkaline phosphatase activity and expression of self-renewal associated marker genes. Besides the role we proposed for Zscan4 in regulating pluripotency, Zscan4 was recently reported to play a key role in telomere elongation and genome stability in murine ESCs (Zalzman et al., 2010). These two mechanisms of Zscan4 are not necessarily contradictory, as an increase in genomic instability is likely to result in alterations that could bring the metastable state of pluripotency out of balance, resulting in differentiation or apoptosis. In addition, there might be other functions of Zscan4 contributing to the mentioned effects, as roughly 500 significant up- and downregulated gene changes were detected upon its overexpression in ES cells (Nishiyama et al., 2009). Zscan4 can be regarded a master regulator of ES cells as ablation of Zscan4 drives ES cells into crisis, which might arise from multiple functions of Zscan4 ((Zalzman et al., 2010) and personal communication with Minoru Ko).

Expression of Zscan4 was previously reported to be restricted to early embryo development and ES cells (Falco et al., 2007; Zhang et al., 2006b). But there is a discrepancy in these reports, as Falco et al. described expression of Zscan4 to be transient with the highest expression in the late 2-cell embryos, while Zhang et al. report the peak of Zscan4 expression in the 3-4 cell stage. Falco et al. presents data of quantitative RT-PCR and whole mount in situ hybridization (WISH), whereas the other group only presented qRT-PCR results, but where the differences arise from is unclear at the moment. Interestingly, in both reports Zscan4 expression was very low or undetectable at the blastocyst stage, the biological *in vivo* counterpart of ES cells. This could be due to the fact that Zscan4 exhibits an extremely mosaic expression pattern, with only around 5% of cells being positive for Zscan4 in ESCs (Falco et al., 2007; Zalzman et al., 2010). On the other hand, it might be that the specific functions of Zscan4 are not required anymore after the 2-cell stage *in vivo*, but are transiently required for stable long-term culture of pluripotent cells under *in vitro* conditions. In light of this restricted expression of Zscan4 it is of interest that induced pluripotent cell types, reprogrammed from somatic cells, managed to reactivate Zscan4 expression to similar levels as in ESCs.

One of the few pieces of evidence regarding regulation of Zscan4 expression derives from a report identifying Zscan4 to be among a small set of ES cell and early embryo developmental specific transcripts, which are postively regulated by Zfp206 (Zhang et al., 2006b). Zfp206, recently renamed to Zscan10, is a putative SCAN-Zinc finger transcription factor that plays a role in regulating the pluripotency of mouse and human ES cells (Wang et al., 2007c; Yu et al., 2009a). Expression of Zfp206 was reported to be expressed predominantly in the ICM of blastocysts (Yoshikawa et al., 2006), which does not match with the finding of Zfp206 peaking at the 2-cell stage, with no further upregulation shown up to the ES cell level (Zhang et al., 2006b). It is noteworthy that the relatively homogenous ICM expression of Zfp206, as well as the absence of Zscan4 expression in the ICM was detected at the RNA level using in situ hybridization by the same group led by Minoru Ko, which should rule out inter-laboratory technical variations. Further evidence backing Zfp206 epxression in the ICM comes from studies detecting the protein levels of Zfp206 by immunohistochemistry, which located Zfp206 protein at the blastocyst stage in the nucleus of all cells, both trophectoderm and ICM (Wang et al., 2007c). While this data supports the findings of Zfp206 expression in the ICM, it highlights a discrepancy between the preferential localization of Zfp206 mRNA to the ICM and the additional protein detected in the trophectoderm. A possible explanation could be that Zfp206 is a relatively stable protein, remaining abundant in trophectoderm despite the loss of RNA. This could be of interest as Zscan4 levels were so far only traced at the RNA level during preimplantation development, and therefore a stable Zscan4 protein might result in Zscan4 function also at later than reported stages of development. Protein studies during preimplantation development, by either histochemistry or western blot could shed light on this possiblity.

How the homogenously expressed transcription factor Zfp206 can regulate the reported mosaic expression of Zscan4, with only a low percentage of Zscan4 positive cells in the total population, was not determined in the studies of Zhang et. al. Six different isoforms were reported for Zfp206, and it maybe that the different alternatively spliced products regulate their targets in a positive or negative way, resulting in a mosaic pattern. Zfp206 was also reported to be part of the core transcriptional regulatory network in ES cells, and is positively regulated by the transcription factors Oct4 and Sox2, but in turn also binds to the Oct4 promoter

regulating its expression. In addition, it was found that Zfp206 also interacts directly with both Oct4 and Sox2. Such protein complexes might regulate Zscan4 expression in a mosaic fashion and, depending on the composition, they might be able to bind to the Zscan4 promoter driving its expression. Noteably, homogenously expressed Oct4 has also been reported to regulate the heterogenously expressed transcription factor Nanog. Epigenetic cell cycle regulated mechanisms, were recently shown to contribute to the mosaic expression of Nanog (Villasante et al., 2011). Similar regulatory mechanisms could be also an explanation for the mosaic expression of Zscan4.

With the reports of restriced Zscan4 expression during early embryonic development and ESC culture, the behaviour of Zscan4 expression under differentiation inducing conditions were investigated. Differentiation was triggered by embryoid body formation or LIF withdrawal and, as expected, both methods led to loss of Zscan4 expression at the protein and RNA levels. Interestingly, Zscan4 appeared to be very sensitive to differentiation with expression dropping rapidly to almost undetectable levels around day 5. This decrease appeared to precede even the drop of Nanog expression, a relative sensitive marker of pluripotency, in comparison to Oct4 (Brill et al., 2009).

One major disparity between differentiated cell types and ES cells is that somatic cells are limited in their number of times they are able to divide, whereas ES cells can be propageted indefinitely while maintaining a relative stable karyotype (Cervantes et al., 2002; Suda et al., 1987). The phenomenon of this limited cell division ability of somatic cells was termed the ‘Hayflick limit’ and describes the number of times a normal cell population will divide before it stops (Hayflick, 1965; Hayflick and Moorhead, 1961). This limit has been found to correlate with the telomere length (Bodnar et al., 1998; Harley et al., 1990; Olovnikov, 1996; Watson, 1972). Telomeres are repetitve DNA sequence regions at the end of a DNA strand, which, together with associated proteins, protect the ends of the chromosomes (Blackburn, 2001; Blackburn and Gall, 1978). Because of the nature of DNA replication, with DNA polymerases only working in the 5' to 3' direction, one finds a leading and a lagging strand on the DNA molecule being replicated. On the lagging strand, short RNA primers are needed for the DNA polymerase to bind, which are later replaced with DNA fragments. However, at the very end of the DNA strand the

RNA primer cannot be replaced leading to loss of a short DNA fragment at each cell division (Watson, 1972). This shortening is also known as the end replication problem and oxidative stress contributes significantly to shortening of telomeres in cell culture conditions (von Zglinicki, 2000). The enzyme telomerase can counteract the shortening of telomeres, and indeed in ES cells telomerase activity is elevated (reviewed in (Hiyama and Hiyama, 2007)).

Interestingly, Zscan4 has been implicated in regulating telomere length and genomic stability by another mechansism, one that is more similar to the alternative lengthening of telomeres (ALT) phenomomenon (Zalzman et al., 2010). ALT regulates telomere length via recombination, however, the exact mechanism of this pathway is yet to be determined and it is normally associated with abnormal cell types like immortalized cells or cancerous cells (Bryan et al., 1995; Henson et al., 2002). Interestingly, a telomerase-independent lengthening of telomeres has been found in early stages of embryo development and it was postulated that a recombineering mechanism underlies this observation (Liu et al., 2007). At the blastocyst stage a strong upregulation of telomerase was described, mainly functioning to maintain the telomere length established by the ALT mechanism (Liu et al., 2007). This temporal restricted recombination event correlates well with the published Zscan4 function and expression during early development (Falco et al., 2007; Zalzman et al., 2010; Zhang et al., 2006b). With Zscan4 being the potential cause of ALT, which is reported to be involved in the maintenance of some forms of cancers (Bryan et al., 1997; Bryan et al., 1995), the possibility to alter expression levels of Zscan4 by, for instance small chemical inhibitors, could become of therapeutic interest.

Zscan4 was identified as a downstream target of PI3Ks by applying the broad spectrum inhibitor LY294002, which targets all PI3Ks isoforms, to murine ESCs (Storm et al., 2009). To investigate whether a specific PI3Ks isoform might play a prominent in the regulation of Zscan4 expression a more selective approach was needed. Selective PI3K catalytic isoform inhibitors, for the p110 alpha, beta and delta isoforms were used, and inhibition of p110α by PIK-75 resulted in a rapid drop of Zscan4 expression. This finding was complemented by overexpression of an activatived form of p110α, resulting in a strong increase in Zscan4 expression.

Therefore, p110α is proposed to be the major PI3K isoform involved in regulating Zscan4 expression. Expression of p110α plays also an indispensable role during embryo development, with an early expression already detectable at the zygote stage of mouse embryonic development and its transient knockdown results in a G2/M arrest, preventing the activation of Akt (Xu et al., 2009). Genetic homozygous deletion of p110α was reported to be embryonic lethal around E9.5, because of proliferative defects (Bi et al., 1999).

Unsurprisngly, inhibition of p110α with PIK-75 resulted in growth retardation, with a significant reduction of ES cell colony size. This is consistent with previous reports implicating the catalytic alpha isoform in growth and metabolism (Foukas et al., 2006; Kingham and Welham, 2009; Knight et al., 2006). In ES cells a specifically expressed Ras-like gene, termed Eras, was found to be important for the tumour-like growth properties of ES cells and was shown to act through activation of PI3Ks (Takahashi et al., 2003). Deletion of Eras causes proliferative defects, which can be rescued, at least in part, by over-expression of activated p110α (Takahashi et al., 2003). The ERas/PI3K pathway was shown to act via Akt, but the authors did not rule out other factors likely to be involved. Akt is a pathway that is strongly proposed to be important also for mES cell self-renewal, as artificial activation can lead to LIF independency (Pritsker et al., 2006; Watanabe et al., 2006). Furthermore, the PI3K/Akt pathway was implicated in the regulation of other important self-renewal regulators, like Tbx3 and Nanog (Niwa et al., 2009; Storm et al., 2007). In line with the importance of Akt for self-renewal, inhibition of p110α with PIK-75 leads to a reduction in phosphorylated Akt (Kingham and Welham, 2009), and was also found in this study to reduce Rex1-Gfp expression after 5 days in OCRG9 ES cells. Reduction of Rex1 expression could have been also caused by the lower cell density, which will lead to a lower concentration of paracrine and autocrine secreted factors known to be important for optimal self-renewal (Berge et al., 2011; Guo et al., 2006; Welham et al., 2007).

Taken together, these findings highlight the important role of Zscan4 in ES cell identity, and a proposed regulation via the PI3Ks catalytic alpha isoform opens up the possibility to alter Zscan4 expression levels.

Chapter 4: Further investigation of Zscan4 mechanisms of action

4.1 Introduction

Having identified Zscan4 as a novel contributor to mouse ES cell self-renewal, the aim of the next phase of this study was to further explore its mechanism of action. The very recent discovery of Zscan4 playing a role in maintaining genomic stability and telomere length, together with our findings, suggest that the Zscan 4 family may play a number of roles in ES cells, although its precise molecular mechanisms are not yet understood (Nishiyama et al., 2009; Zalzman et al., 2010).

To complement loss-of-function experiments (section 3.3.1) previously performed, an over-expression strategy was applied for studying potential functions of Zscan4. Zscan4c was found to be the predominant paralogous gene expressed in mES cells and was, therefore, the chosen family member for our expression studies (Falco et al., 2007). A variety of Zscan4c overexpressing cell lines were established and characterised as part of this investigation, including both constitutive and inducible expression systems. Studying Zscan4 at the protein level was of special interest, as at the time of experimental design no protein data and no murine anti-Zscan4 antibody was available. Creation of murine ES cell lines with an inducible eGFP-Zscan4c fusion protein allowed tracking of the protein and was used for identifying potential protein binding partners using a combined immunoprecipitation (IP) - mass spectrometry strategy. Protein interaction partners are a promising route towards elucidating mechanisms of Zscan4c.

4.2 The Zscan4 family

Zscan4 was found to be a gene family consisting of nine paralogous genes, which are tightly clustered in a 0.85Mb region on mouse Chromosome 7 (Falco et al., 2007). According to Falco et al. three of these nine genes are not transcribed and are, therefore, considered to be pseudogenes. Zscan4c is the predominant transcript in ES cells, whereas Zscan4d was found to be prominent at the late 2-cell stage (Falco et al., 2007). Inconsistent with this report, work from our group has shown that both Zscan4-ps2 and Zscan4-ps3 can be cloned out from mESC cDNA, challenging their previous classification (Storm et al., 2009). Since the first publication describing the Zscan4 family (Falco et al., 2007), the composition of the family has changed, implicated by a recent Ensembl database search (July 2011). Previously Zscan4c, d and f were the only transcripts encoding full-length protein of with 506 amino acids (aa) in length, while now pseudogene two (Zscan4-ps2-201) appears to encode a protein of 506aa in the database. For Zscan4f, an additional smaller isoform of 77aa was found in Ensembl. Zscan4b and e are now published in the Ensembl database to encode a protein consisting of 505aa, in contrast to the earlier report of 195aa. The other reported pseudogenes, Zscan4-ps1 and Zscan4-ps3, are not listed anymore in Ensembl. A summary of all Zscan4 members as found in Ensembl database from a search in July 2011 are listed in Table 4.1.

Table 4.1 Summary of Zscan4 family members (http://www.ensembl.org)

Name	Transcript ID	Length (bp)	Protein ID	Length (aa)	Biotype
Zscan4b-201	ENSMUST00000168158	1745	ENSMUSP00000127301	505	Protein coding
Zscan4c-001	ENSMUST00000131379	2301	ENSMUSP00000118506	506	Protein coding
Zscan4c-201	ENSMUST00000067210	2276	ENSMUSP00000066504	506	Protein coding
Zscan4d-201	ENSMUST00000165848	1992	ENSMUSP00000131258	506	Protein coding
Zscan4e-201	ENSMUST00000166753	1745	ENSMUSP00000125906	505	Protein coding
Zscan4f-001	ENSMUST00000145237	1829	ENSMUSP00000120149	506	Protein coding
Zscan4f-002	ENSMUST00000091440	2277	ENSMUSP00000089014	506	Protein coding
Zscan4f-003	ENSMUST00000141491	521	ENSMUSP00000122083	77	Protein coding
Zscan4-ps2-201	ENSMUST00000094850	2277	ENSMUSP00000092446	506	Protein coding

The protein sequences of the different Zscan4 paralogs were aligned to compare sequence similarities (Figure 4.1). As previously reported, sequences are highly similar to each other (Falco et al., 2007) and are in a range from 92 to 99%. Protein sequences were aligned to each other and the percentage of sequence similarity is shown in Table 4.2.

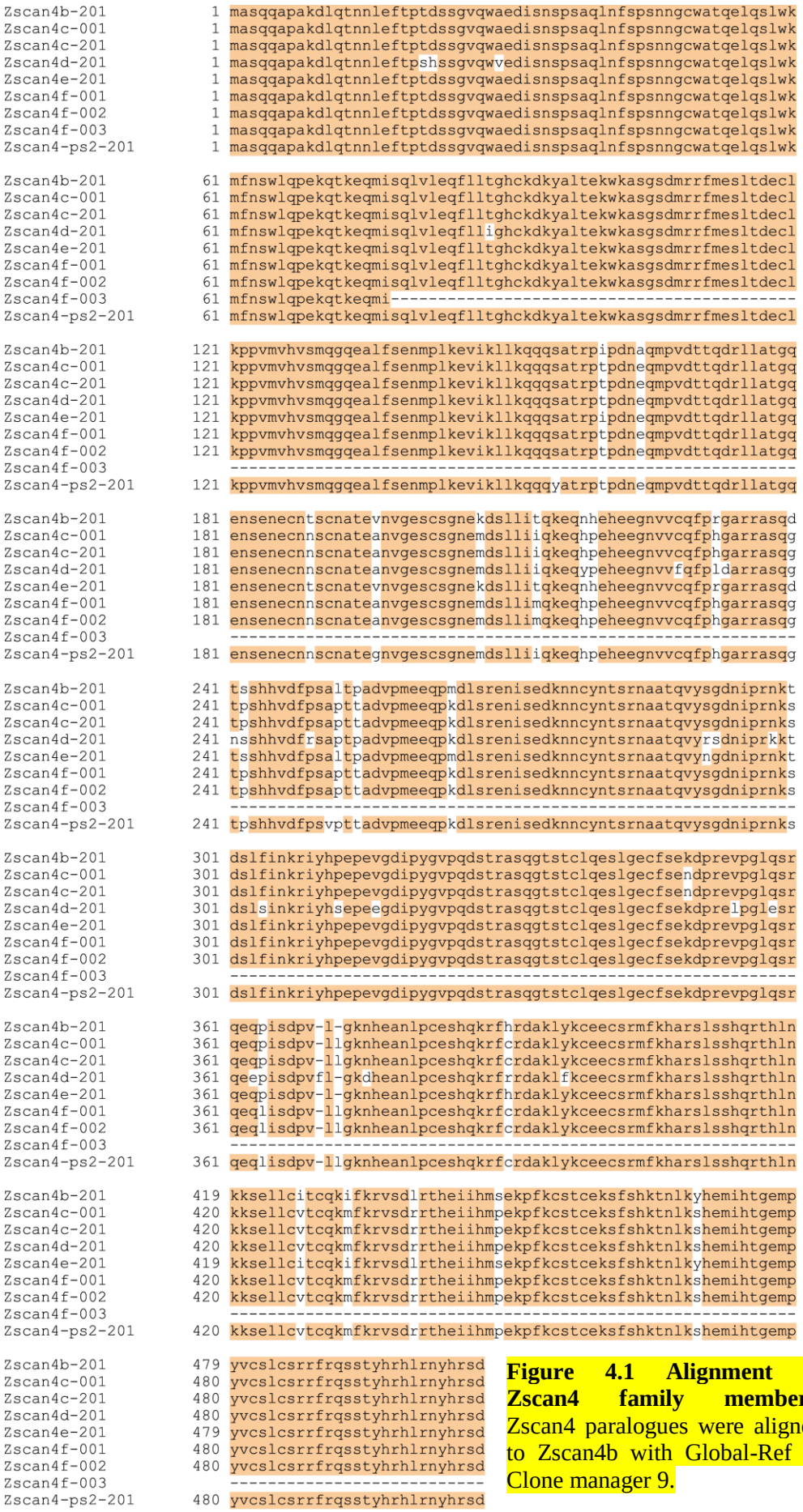

Figure 4.1 Alignment of Zscan4 family members. Zscan4 paralogues were aligned to Zscan4b with Global-Ref of Clone manager 9.

Table 4.2 Protein homology of Zscan4 family members

	Zscan4b	Zscan4c	Zscan4d	Zsan4e	Zscan4f	Zscan4f-003	Zscan4-ps2
Zscan4b	100%	95%	92%	99%	95%	15%	95%
Zscan4c	95%	100%	94%	95%	99%	15%	99%
Zscan4d	92%	94%	100%	92%	94%	14%	94%
Zsan4e	99%	95%	93%	100%	95%	15%	95%
Zscan4f	95%	99%	94%	95%	100%	15%	99%
Zscan4f-003	15%	15%	14%	15%	15%	100%	15%
Zscan4-ps2	95%	99%	94%	95%	99%	15%	100%

To show the evolutionary relation of the different Zscan4 family members a phylogenetic tree based on the Ensembl protein database sequences was created by using Neighbour-Joining phylogeny in Clone manager 9 professional (Figure 4.2). Zscan4d branches the earliest from the other paralogs, and Zscan4c and Zscan4f are the closest to each other. Interestingly, Zscan4c (40%) was the major transcribed isoform in ES cells, followed by significant levels of Zscan4f (24%) (Falco et al., 2007). The more distant Zscan4d family member was only expressed 5% in ES cells, whereas it was the predominant form (90%) in 2-cell stage embryos. How these expression levels are regulated is not currently known to and whether their sequence differences result in an alteration of their function still need to be investigated.

Figure 4.2 Phylogenetic tree of Zscan4 family members. Phylogenetic tree was calculated by exhaustive pairwise alignments of Zscan4 protein sequences and progressive assembly of alignments using Neighbour-Joining phylogeny. Multi-way alignment of Clone manager 9 professional was used.

4.3 Episomal supertransfection of Zscan4c

An episomal vector was used to over-express Zscan4c in mouse ES cells (Figure 4.3 A). The episomal approach is based on work performed by Gassman et al., and uses the polyoma virus replication system (Gassmann et al., 1995). Vectors that contain the polyoma viral origin of replication (ori), can be propagated without chromosomal integration in ES cells expressing the large T protein (Niwa et al., 1998). As the vector is not integrating into the cellular genome, unpredictable changes due to the chromosomal integration are avoided. Furthermore, the yield for establishing stable transfectants is at least 100-fold higher in comparison to conventional transfection protocols and was termed supertransfection (Niwa et al., 1998).

Zscan4c-V5-His was subcloned from the pcDNA3.1-Zscan4c-V5-His vector by PCR amplification and ligated into the episomal over-expression vector pPyCAGIZ. The episomal vector contains a Zeocin resistance cassette, which should allow for the selection of stable transfectants by addition of Zeocin. The pPyCAGIZ-Zscan4c vector was transfected by electroporation into E14/T mES cells expressing the large T protein and selection was applied 24h after transfection. Surprisingly, no colonies emerged upon selection with Zeocin in three independently performed experiments. This suggests that the high expression levels of Zscan4c potentially achieved with the episomal system cannot be tolerated by ES cells. High levels of Zscan4c might drive cells into crisis, omitting the formation of ES cell colonies. To investigate whether Zscan4c could be expressed from this vector, a transient transfection approach was taken. Cells were electroporated, but no selection was applied after transfection and protein samples were taken after 48 and 72 hours. Samples were analysed by immunoblotting with an anti-V5 antibody and Zscan4c-V5 was shown to be expressed 48h after transfection (Figure 4.3 B). Expression was lost 24 hours later, which could be the result of a loss of the vector or because of toxicity effects. Toxicity effects appear to be more reasonable, as a loss of the vector would have been avoided in the previous experiments due to the presence of Zeocin. It was reported that the pluripotency associated genes Tbx3 and Klf4 also failed to produce ES cell colonies when over-expressed with an episomal vector system (Niwa et al., 2009), indicating a tight dosage regulation of these genes.

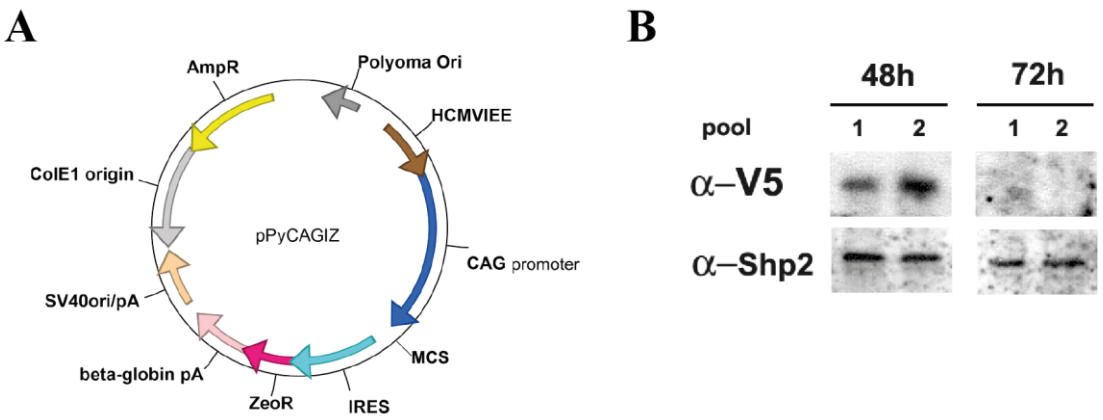

Figure 4.3 Episomal supertransfection of Zscan4c cloned in the pPyCAGIZ vector into E14/T ES cells. (A) cDNA encoding Zscan4c with a C-terminal V5-epitope tag, was subcloned into the pPyCAGIZ episomal expression vector containing the Zeocin resistance gene (ZeoR). This plasmid carries a polyoma origin with the F101 mutation, allowing episomal replication in ES cells. The plasmid also contains a Human cytomegalovirus immediate early enhancer (HCMVIEE), globin poly A signal (beta-globin pA), SV40 ori (simian virus 40 origin), ampicillin resistance gene (AmpR), and internal ribosome entry site (IRES). Zscan4c was subcloned into the Multiple Cloning Site (MCS), and expression is driven by the modified chicken beta-actin promoter (CAG). **(B)** Immunoblotting was performed on cell extracts following transient transfection with the pPyCAGIZ-Zscan4c plasmid. Expression of Zscan4c was detectable with an anti-V5 antibody 48h after electroporation of episomal expression vector into E14/T cells. Expression was lost after 72h. Blots were reprobed with a Shp2 antibody to demonstrate equal loading.

4.4 Inducible expression of Zscan4c

The tetracycline-OFF (Gossen and Bujard, 1992) and advanced tetracycline-ON (Urlinger et al., 2000) inducible expression systems were used to overcome the limitations of the episomal expression system (Figure 4.4). These systems contain a transcipritional activator protein (transactivator), which consists of a fusion protein of the Tet repressor and a VP16 activation domain. Tet-off and Tet-on transactivators can bind to the tetracycline response elements (TREs) consisting of multiple repeats of the bacterial tet operator sequence located within an inducible

promoter (CMV_{min}). In both systems, Tet-on and Tet-off, the transactivator activates gene expression, the difference arises form their response to tetracycline. In the Tet-off system the transactivator drives gene expression in the absence of tetracycline, whereas the Tet-on advanced system requires the presence of the tetracycline analogue doxycycline to induce expression of the gene of interest.
There are several advantages of a tetracycline inducible expression system over a constitutive active system.

- During the generation of stable cell lines the transgene can be switched off and therefore cell lines with proteins that are normally toxic for the host cells can be established.

- It is possible to alter the dose of transgene expression by titrating the amount of tetracycline. In this respect the tet-regulated systems are more versatile than, for example, the inducible Cre-lox system, in which protein expression is induced by site-specific recombination leading to a permanent transgene expression.

- The level of transgene expression is similar or greater than in a constitutive expression system using the same CMV promoter (Yin et al., 1996).

- The use of tetracycline or doxycycline does not induce cytotoxic effects at the required dose for expression induction. This is in contrast to other inducible systems where the inducing agents can have non-specific effects, as for instance steroids, heat shock, heavy metals, which can in turn interfere with experimental results (Saez et al., 1997).

- The tet-regulated expression systems are based on prokaryotic regulatory proteins binding specifically to their targets, circumventing pleiotropic effects (Harkin et al., 1999).

- Compensatory effects as a result of transgene over-expression are avoided during the establishment of stable cell lines.

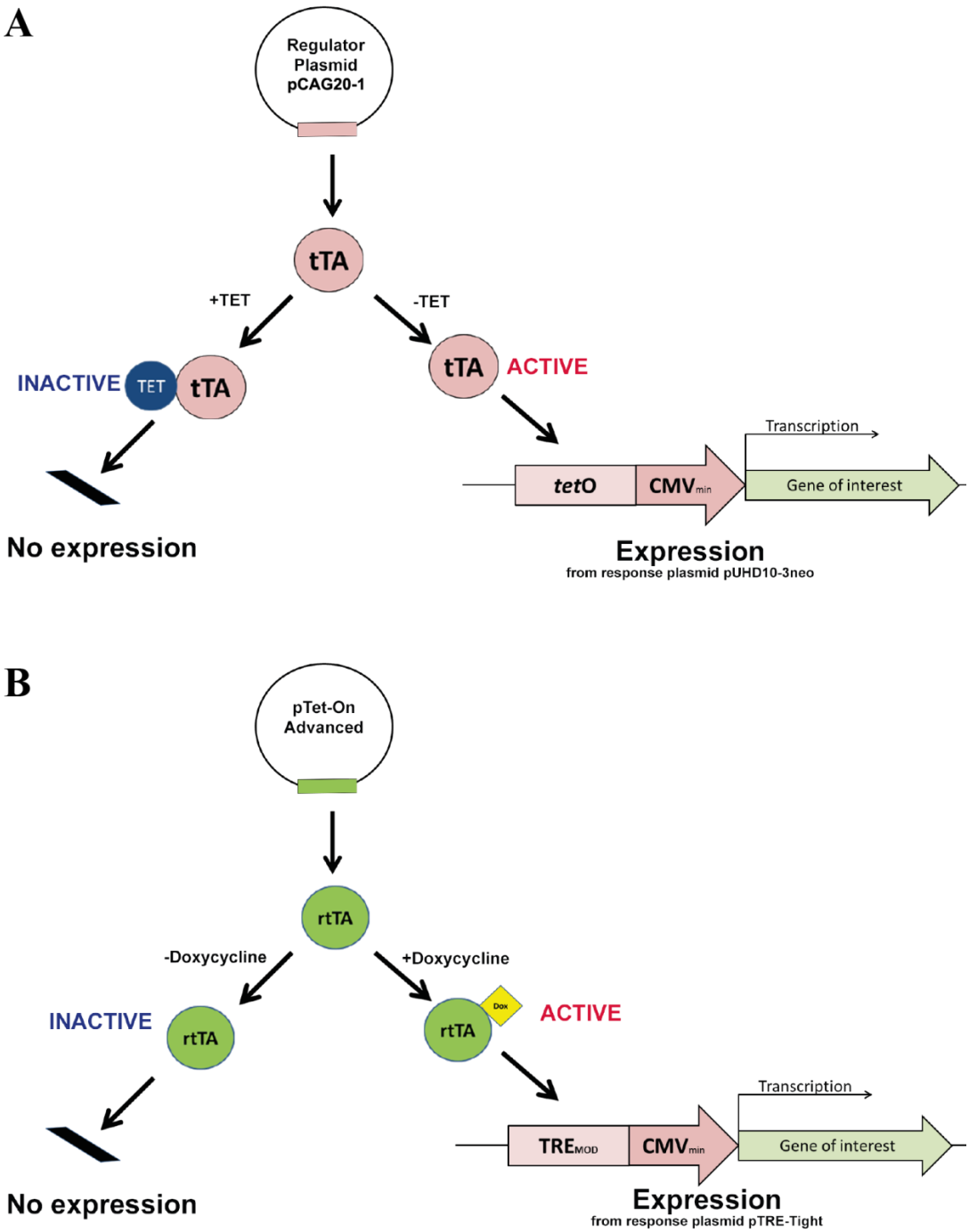

Figure 4.4 Mechanisms of tetracycline regulated Tet-off and Tet-on expression systems. (A) The Tet-off system uses a constitutively expressed regulatory plasmid pCAG20-1, which produces a transactivator (tTA). The transactivator binds to a tTA dependent promoter on the response plasmid pUHD10-3neo. The system is regulated by tetracycline that binds to tTA and prevents it from binding to the tTA-dependent promoter. When tetracycline is removed tTA binds to the hybrid promoter and drives expression of the Gene of Interest (GOI). **(B)** Tet-on advanced system from Clontech drives expression of GOI in the presence of doxycycline (Dox). Target cells constitutively express the Tet-on advanced transactivator (rtTA) that can bind to the pTRE-Tight expression vector only in presence of Dox.

4.4.1 Generation of ES cells expressing Zscan4c under the control of the Tet-off inducible system

For the generation of Zscan4c Tet-off inducible cell lines, Zscan4c, with a C-terminal dual V5-His epitope tag was PCR amplified from a pcDNA3.1vector containing the required insert (Storm et al., 2009). The fragment was blunt end ligated into the Tet-off response plasmid pUHD10-3, which was beforehand digested with XbaI and blunted (Figure 4.5A). Prior to transfection, the construct was sequenced to verify the correct sequence and orientation. To generate inducible Zscan4c-Tet-off mES cell lines the linearized construct was transfected by electroporation into E14tg2A (Clone R63) murine ES cells (Era and Witte, 2000). These cells contain the stable integrated pCAG20-1 vector, that constitutively expresses the tetracycline transactivator (tTA) driven by the CAG promoter. Following electroporation transfectants were selected in G418 and surviving clones were expanded (performed as described in 2.4.10/11). Clones were screened by immunoblotting for the induction of Zscan4c expression after withdrawal of tetracycline and high expressing clones were expanded, frozen and used for further analyses. Four clones with the highest degree of inducible expression (clones 7, 17, 43, 45) were selected for further analyses in the remainder of this study. Clones were routinely cultured in presence of 1μg/ml tetracycline to keep the transgene expression switched off. For induction of transgene expression tetracycline was removed.

As demonstrated by Figure 4.5B, Zscan4c-V5 protein was reproducibly and stably expressed when induced by removal of tetracycline. Zscan4c expression was maintained also upon LIF withdrawal (Figure 4.5 B (i)), and was detectable at a similar level over a time-course of 120 hours (Figure 4.5 B (ii)).

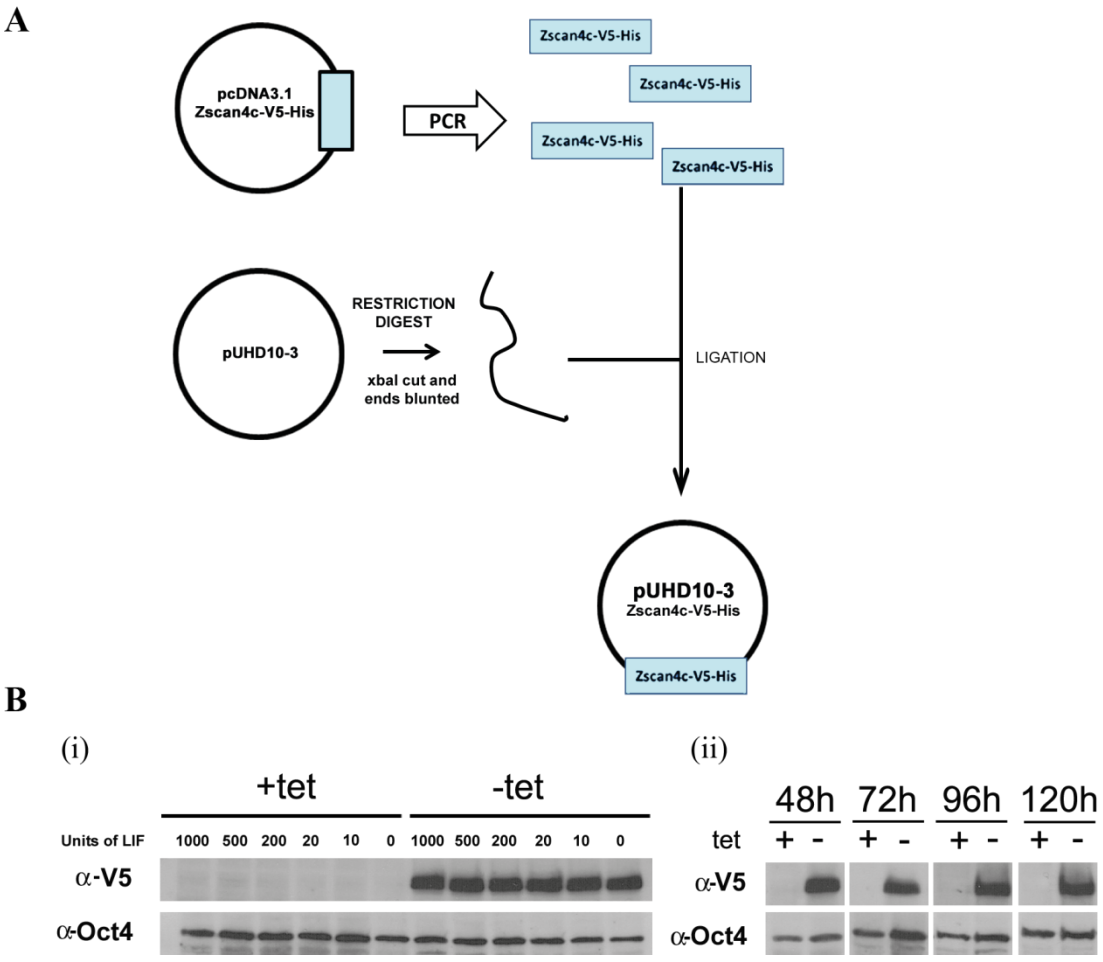

Figure 4.5 Generation of Zscan4c-Tet-off inducible mES cells. (A) Schematic showing how pUHD10-3-Zscan4c-V5-His expression vector was generated. Zscan4c-V5-His fragments were amplified from the respective pcDNA3.1 vector (a kind gift of Michael Storm) and ligated into the pUHD10-3 vector. **(B)** Immunoblots showing induction of Zscan4c-V5 protein (clone 43) upon withdrawal of tetracycline (tet**)** detected with anti-V5 antibody. **(i)** Expression after 24h of induction under different concentrations of LIF as indicated. **(ii)** Expression was maintained over a time-course of 120h. Immunoblots were stripped and re-probed with Oct-4 antibody.

4.4.1.1 Localisation of Zscan4c

At the time of the study, nothing was known about the protein localisation of the Zscan4 protein, as most work had been done at the RNA level (Falco et al., 2007). Establishment of the Zscan4c-V5 inducible cell lines allowed for immunostaining of cells for Zscan4c with an anti-V5 antibody. Immunostaining revealed a strong accumulation of Zscan4c-V5 protein in the nucleus of the cell (Figure 4.6A; red staining). The nucleus was counterstained with DAPI (in blue) and images were merged with the Zeiss LSM Image Browser (Version 4.2.0.121). Smaller amounts of Zscan4c-V5 protein were also observed in the cytosol. Additional confirmation was gained by immunoblotting protein lysates of cytosolic and nuclear fractions (Figure 4.6B). Nuclear and cytoplasmic separation was achieved using the NE-PER nuclear and cytoplasmic extraction reagents from PIERCE Biotechnology. The immunoblotting results were similar to the ones obtained by immunochemistry, though Zscan4c-V5 protein levels appeared to be slightly higher in the cytosolic fraction in comparison to immunostaining. This observation could result from an incomplete seperation of the cytosolic and nuclear proteins. This can be seen from the nuclear reprobe for the anti-TATA binding protein (TBP), which was also detected in the cytsolic fraction. Furthermore Gapdh, marking the cytosolic fraction was also detected to a lower extent in the nuclear fraction on the immunoblots, suggesting some contamination.

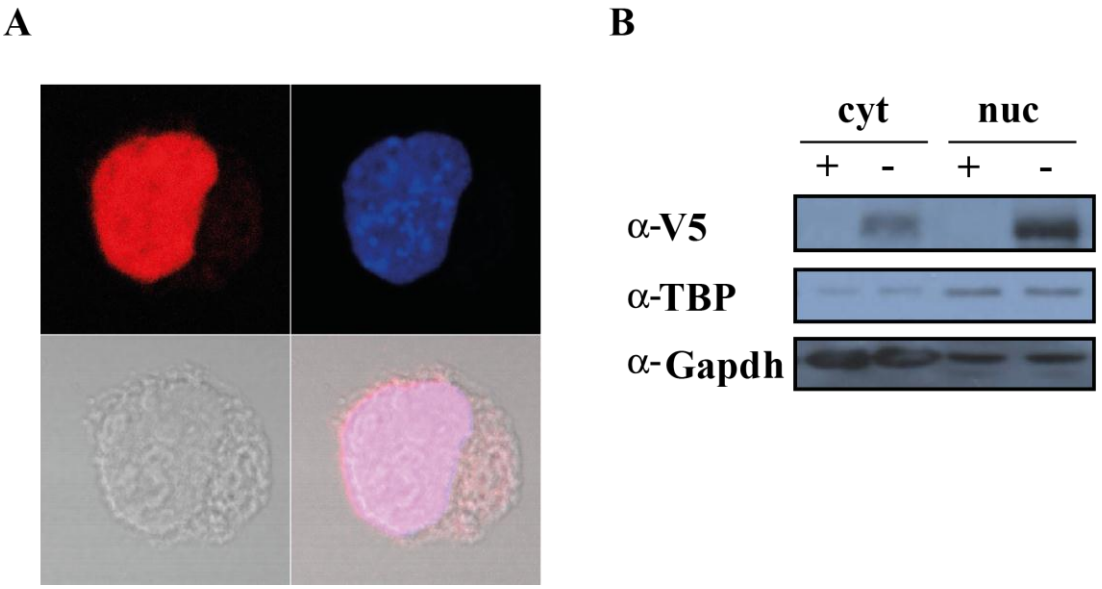

Figure 4.6 Nuclear accumulation of Zscan4c. (A) Localisation of Zscan4c-V5 protein was assessed with immunostaining of Tet-off inducible cell lines grown in the absence of tetracycline. Anti-V5 antibody was used to detect Zscan4c-V5 protein in clone 45 (red). Cell nuclei were counter-stained with DAPI (blue). **(B)** Zscan4c-Tet-off inducible mES cell lines were grown in the presence and absence of tet. Cytosolic and nuclear proteins were separated and immunoblotting was performed with anti-V5, anti-TBP (nuclear) and anti-Gapdh (cytosolic) antibodies. Immunostaining and immunoblot were performed of four independent Zscan4c-V5 inducible clones.

4.4.1.2 Heterogeneous expression of Zscan4c in Tet-off clones

Immunohistochemical staining for Zscan4c-V5 were performed on clones grown in the presence and absence of tetracycline (Figure 4.7). Upon removal of tetracycline, a highly heterogenous expression of Zscan4c-V5 protein (in red) was detected. Only a few cells expressed high levels of Zscan4c-V5, while the majority (>90%) appeared to be low or completely absent in ectopic Zscan4c expression. The precise reasons for this heterogenous expression are still not known, but as expression of the transgene is driven by the Tet-off CMV_{min} promoter a more homogenous expression was expected. A number of possibilities could explain these observatons. Based on previous results using the episomal expression system, the Zscan4 protein could be unstable or some regulatory mechanisms could act directly on the protein level, leading to a quick degradation and so loss of Zscan4 protein. Alternatively, it could be that the clones analysed by immunohistochemistry had integrated the transgene at a disadvantageous place in the genome, so that, for instance, epigenetic mechanisms hindered their homogenous expression. It is noteworthy that sub-cloning of Zscan4c Tet-off clones did not resolve the heterogenous expression. Possibly screening more clones by immunostaining, rather than immunoblotting, could resolve this issue. Another possibility could be that the constitutively transcribed transactivator is integrated at a unfavourable place or is being silenced. Other lab members using this same ES cell line (Bone and Paling unpublished observations) have also previously observed differing levels of transgene induction in the same ES cell population. This possibility could be ruled out by performing immunostaining for the Tet-off transactivator. Should silencing be contributing to heterogeneity in expression, transgenes could be integrated at a defined locus known to be favourable for homogenous and stable expression, as for example the Rosa26 locus (Masui et al., 2005).

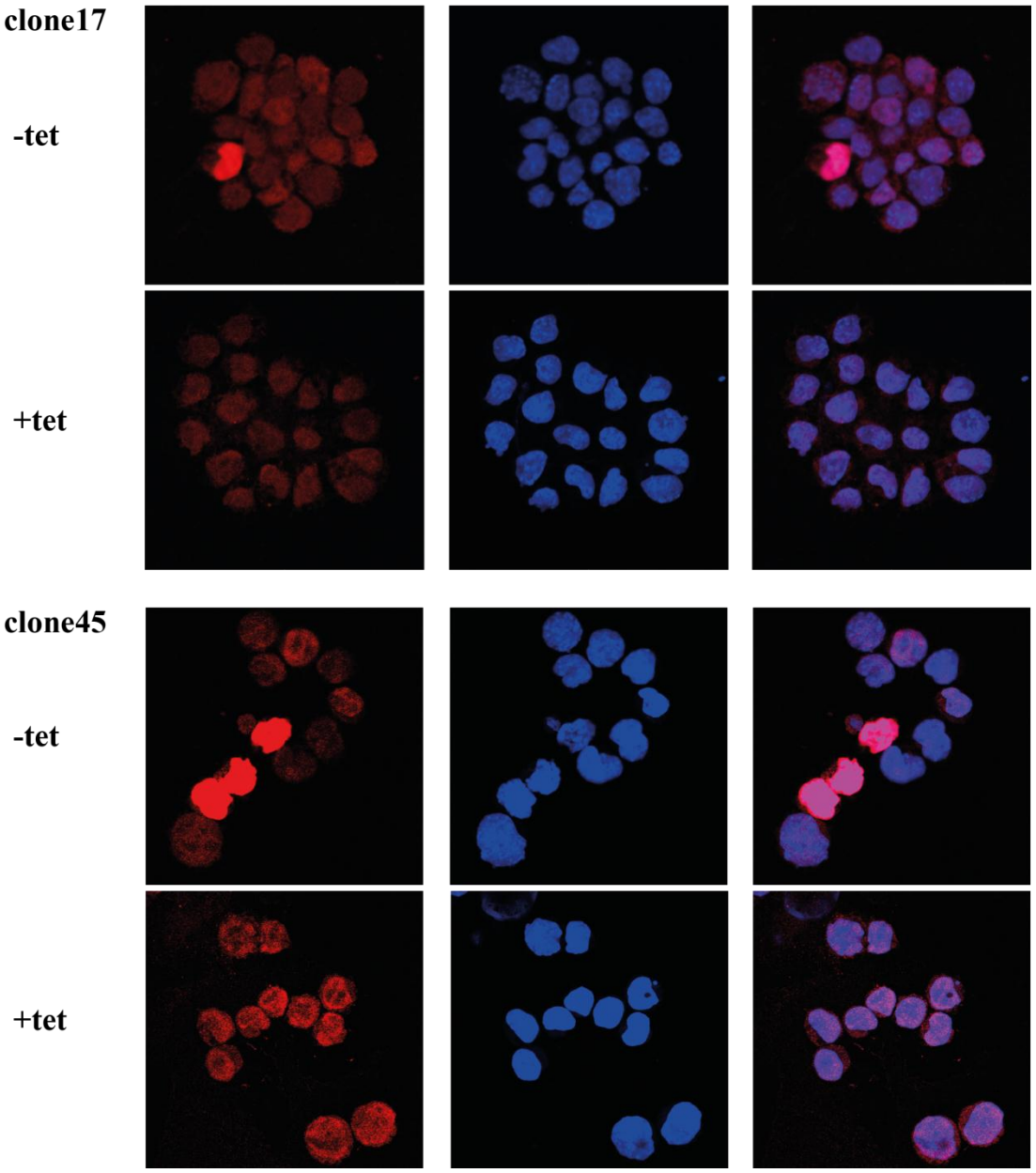

Figure 4.7 Heterogeneous expression of Zscan4c in Tet-off inducible cell lines. Zscan4c-Tet-off inducible cell lines were grown in the presence (+tet) or absence (-) of 1μg/ml tetracycline for 48 hours. Immunocytochemical staining with anti-V5 antibodies (red) detects a heterogeneous expression pattern upon induction of Zscan4c (-tet). Images show two representative independent clones, clone 17 and clone 45.

4.4.1.3 Zscan4c protein stability

Zscan4c protein stability was assessed to test whether heterogenous protein expression might have arisen from an unstable Zscan4c protein. Intracellular Zscan4c-V5 protein stability was investigated with experiments applying cycloheximide to block protein biosynthesis. Cycloheximide is produced by the bacterium Streptomyces griseus, from which it was originally isolated (Leach et al., 1947). It acts on eukaryotic but not prokaryotic protein assemby. Inhibition of protein biosynthesis occurs by interfering with the translocation step in protein synthesis. Elongation was shown to be blocked by binding of cycloheximide to the ribosome, where it inhibits eEF2-mediated translocation (Obrig et al., 1971). Cycloheximide is a useful tool to determine the half-life of a protein by treating the cells in time-course experiments followed by immunoblotting. Cycloheximide treatment can be used to assess the half-life of a protein without mistaken contributions from transcription or translation.

In the experimental setup used, murine Zscan4c-Tet-off clones were grown in the absence of tetracycline to induce Zscan4c-V5 expression, and cycloheximide was added to the cell culture to examine protein degradation. Protein whole cell lysates were taken at 0, 2, 4, and 6 hours after addition of cycloheximide, and immunoblotting was performed to compare Zscan4c-V5, Nanog and Oct4 protein levels. Zscan4c-V5 protein was stable over the chosen time-course, with a slight decrease at 6 hours. Zscan4c appears to be much more stable than Nanog protein, which vanished to almost undetectable levels after 6 hours of protein synthesis inhibition. Over 6 hours cycloheximide treatment, Oct4 protein stability was comparable to Zscan4c stability.

Zscan4c protein containing a His tag was also over-expressed in bacteria and subsequently purified using nickle columns (Figure 4.8). Protein stability of purified protein was also stable over the handling period of a few days, which rules out a potential degradation-sensitive amino acid sequence.

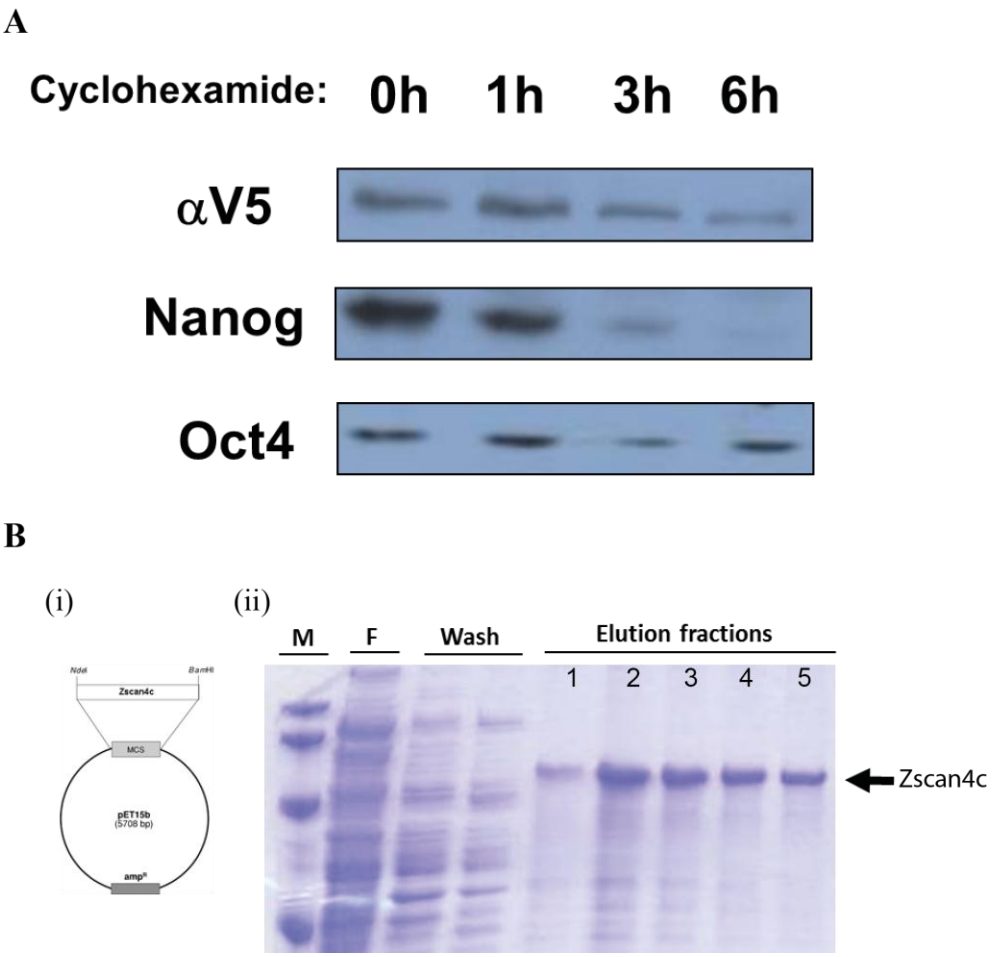

Figure 4.8 Assessment of Zscan4c protein stability. **(A)** Zcan4c-Tet-off ES clones were grown in absence of tetracycline and 10μg/ml cycloheximide was added for 1, 3 and 6 hours to block protein synthesis. Zscan4 protein stability was determined by immunoblotting of whole cell lysates with anti-V5 antibody. Blots were stripped and re-probed with an anti-Nanog and an anti-Oct4 antibody for comparison of protein stabilities. Results shown represent two independent biological experiments performed with separate clones. **(B) (i)** Zscan4c was subcloned into the bacterial expression vector pET15b. **(ii)** Zscan4c-pET15b was transformed into the bacterial strain Rosetta-gami B from Novagen and grown to an OD_{600} of ~0.6 before inducing expression by addition of 1mM IPTG. After 4 to 5 h induction with IPTG, the bacteria were harvested and lysates were purified by FPLC using nickel columns and an imidazole gradient (20mM to 500mM). Image shows a coomassie stained gel of a typical His-tagged Zscan4c purification. M= Marker, F= Flow through, Wash shows two representative samples taken throughout the imidazole gradient, Elution fractions (1-5) show samples of 1ml collected fractions at 500mM imidazole.

Taking these findings together, the heterogenous expression observed by immunochemical analyses are unlikely to arise from an unstable protein. Regulatory effects by other proteins cannot be completely ruled out as the protein synthesis of the regulators are also stopped by cycloheximide, although existing proteins in the cell at the time of cycloheximide addition should be still active.

4.4.1.2 Cell cycle analysis of Zscan4c in Tet-off clones

Murine embryonic stem cells proliferate very actively, with a generation time typically of less than 10 hours (Jirmanova et al., 2002), the cause of which is a reduction in the the duration of G1 phase (Savatier et al., 1994). Under normal culture conditions the majority of the population, around 70%, is in the S phase of the cell cycle (Savatier et al., 2002). This is in strong contrast to, for instance, embryonic fibroblasts where only ~25% of the population is in S phase and ~70% are in the G1 phase (Savatier et al., 2002). When ES cells are induced to differentiate, their cell cycle profile shifts substantially towards the G1 phase (Egozi et al., 2007; White et al., 2005).

With Zscan4 being specifically upregulated during the two cell stage of embryo development it was of interest to investigate whether ES cells expressing Zscan4c in the Tet-off clones experience a change in their cell cycle profile. Therefore, Tet-off clones were grown in the presence and absence of tetracycline for 48h. Subsequent Zscan4-V5 staining was performed with an anti-V5 antibody and a FITC-labeled secondary. Cell cycle analysis was performed with the 7-AAD DNA dye as described in 2.3.6.1. A classical cell cycle profile consists of two peaks separated by a lower intermediate population. The first peak represents the G_1 phase, in which each cell contains a single genome. In the intermediate phase are cells in the S phase of the cell cycle, replicating their DNA content. The second peak are cells containing two genomes just before their division (G_2 phase), and consequently take up double the amount of 7-AAD in comparison to cells of the G_1 phase. Zscan4c expression and 7-AAD staining were monitored by flow cytometry and an example of an experimental profile is shown in figure 4.9. Figure 4.9 A shows Zscan4c-Tet-off cells grown in presence of tetracycline in contrast to panel B which depicts cells grown in the absence of tetracycline and therefore express Zscan4c-V5 (in blue). Consistent with the observation of the immunochemistry, only a minority of cells of

the whole population express Zscan4c-V5 at a detectable level (Gate P2). As expected, two smaller peaks could be detected with the 7-AAD staining, marking G_1 and G_2 phase, flanking the broader intermediate population of the S phase (Figure 4.8A (i) and B (i)). Cells expressing Zscan4c-V5 (blue) after induction by removal of tetracycline did not appear to be enriched in a particular phase of the cell cycle Figure 4.8B (ii). It is unlikely that only cells in a particular cell cycle express Zscan4c-V5, nor that Zscan4c-V5 affects the cell cycle. A slight change of the cell cycle profile towards the G_2 peak of the whole population was noted after induction of Zscan4c in this particular experiment shown, but as in most of these cells Zscan4c was undetectable it is likely to be an artefact.

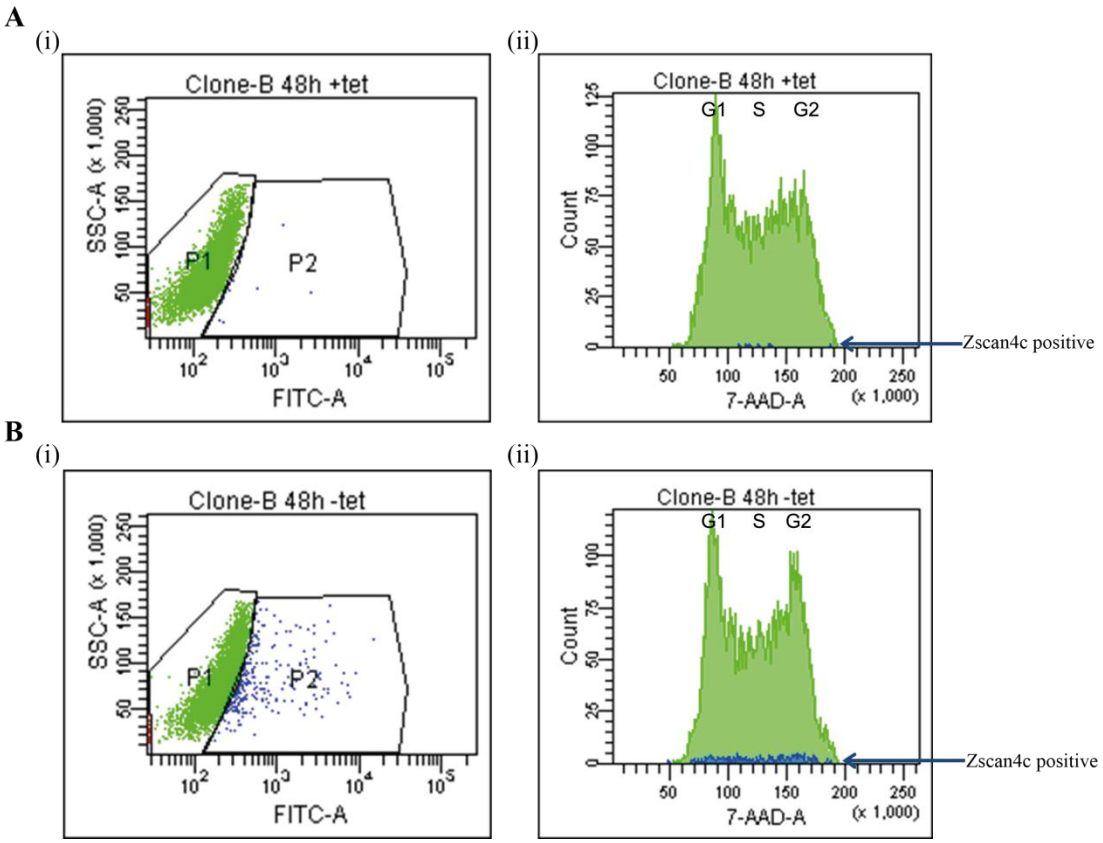

Figure 4.9 Cell cycle analysis of Zscan4c-Tet-off ES cell lines. Zscan4c-Tet-off Clones were grown +/- tet for 48h in the presence of serum and LIF before trypsinisation and fixation in ice-cold 70% (v/v) ethanol. Cells were rehydrated and stained with the DNA dye 7-AAD at 25 µg/ml. Zscan4c was labelled with an anti-V5 antibody and a FITC conjugated secondary antibody. Zscan4c expression (in blue) and 7-AAD staining (in green) was monitored by flow cytometry. G_1, S, and G_2 phase of the cell cycle are indicated in images (ii). Images show one representative experiment of three independent experiments performed with separate clones.

4.4.1.2 Effects of sub-optimal LIF concentrations on self-renewal

With Zscan4c found to play a role in maintenance of ES cell self-renewal (Chapter 3), it was of interest whether over-expression of Zscan4c in Tet-off clones can shelter cells from differentiation events. To determine the potential effect of Zscan4c over-expression, cells were grown for 5 days at clonal density in decreasing concentrations of LIF (1000, 500, 200, 20, 10, 0 Units/ml). Experiments were set up in the presence and absence of tetracycline for different Tet-off clones, as shown in Figure 4.10. ES cell colonies were fixed and stained for alkaline phosphatase activity, and scored into two categories, differentiated and self-renewing colonies.

Colonies negative in alkaline phosphatase activity increased upon LIF withdrawal to almost 100% at 0 units/ml. In comparision to plus tetracycline controls, no significiant benefical effects on self-renewal were observed upon over-expression of Zscan4c when LIF concentrations were reduced. This could be due to the very heterogenous expression of Zscan4c, with a minority of cells expressing high levels. On the other hand, over-expression of Zscan4c might not be enough to maintain self-renewal under sub-optimal growth conditions.

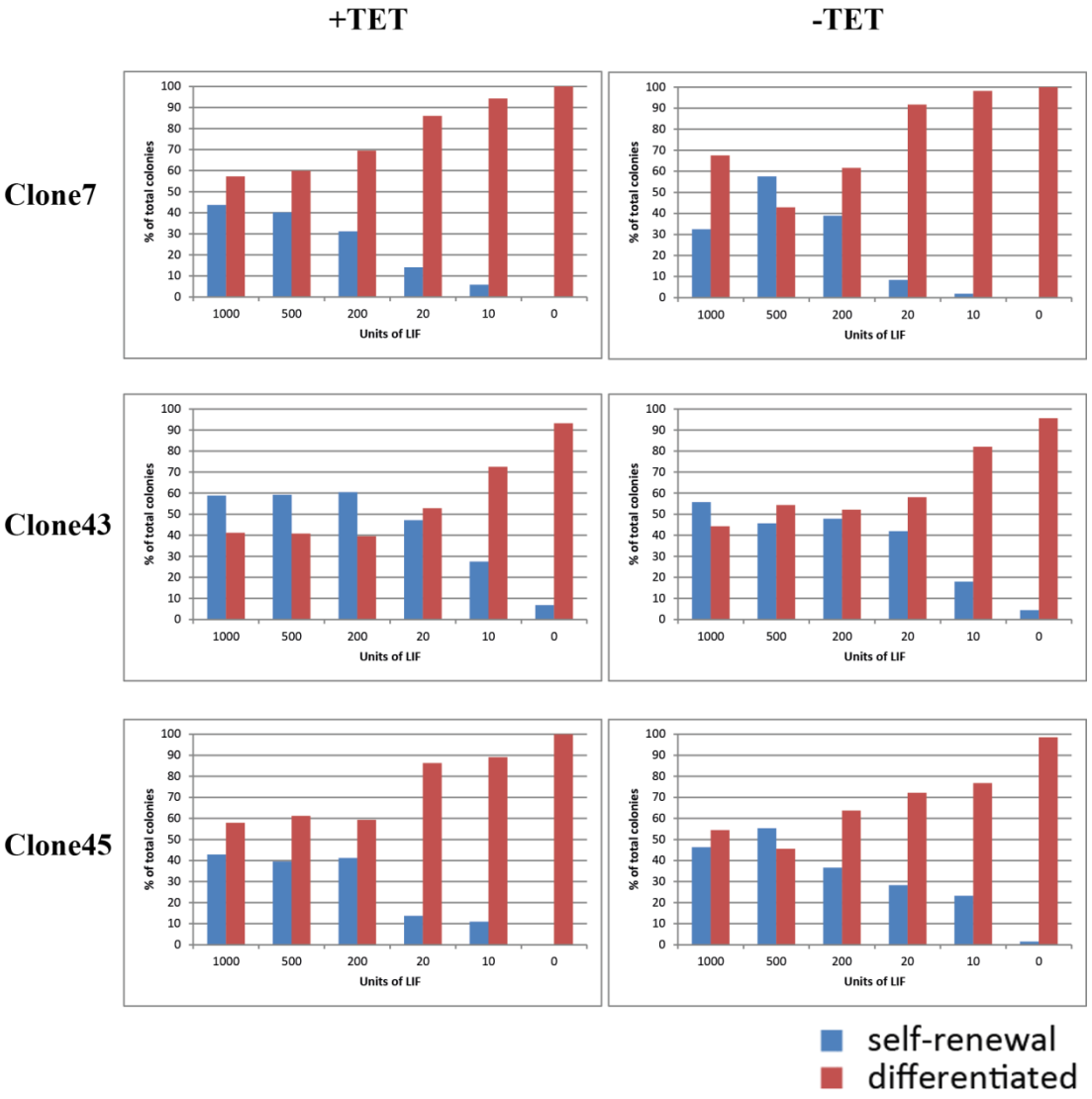

Figure 4.10 Effect of reduced LIF concentrations on self-renewal of transgenic mES cells expressing Zscan4c. Tet-off inducible Zscan4c ES cell clones were cultured in the presence and absence of tetracycline for 5 days. ES cell colonies were stained and scored for alkaline phosphatase activity, marking self-renewing colonies. The percentage of self-renewing (blue bars) and differentiated (red bars) colonies are shown for three independently analysed clones.

4.4.2 Tet-on advanced system

To overcome the limitations encountered with the Tet-off system, the Tet-on advanced expression system from Clontech Laboratories was chosen. According to the manufacturer's manual, the system has several advantages over other inducible mammalian gene expression systems. The expression is extremely tightly regulated, with virtually no residual binding of the Tet-on advanced transactivator to the TRE sequence, thus basal expression is extremely low. Cells do not need to be cultured permanently in the presence of doxycycline and concentrations required for induction of the Tet-on systems are far below cytotoxic levels. The induction of transgene expression after addition of doxycycline is very high and quick, and can be already detected within 30 minutes. It is worth noting that the Tet-on advanced system only works in presence of doxycycline and not with tetracycline.

4.4.2.1 Tet-on inducible eGFP-Zscan4c

The labeling of proteins with a fluorescent marker like eGFP allows us to track intracellular localisation of proteins easily by for instance confocal microscopy. Potential artefacts of antibody staining can be avoided by labeling proteins in this way. Furthermore, eGFP can be used to purify proteins or isolate protein complexes by immunoprecipitation technologies for instance the GFP Nanotrap from Chromotek. A version of Zscan4c that was N-terminal tagged with the enhanced green fluorescent protein (eGFP) (Figure 4.11 A i) was generated through a cloning strategy. This fusion protein (eGFP-Zscan4c) was used for inducible over-expression studies in the pTRE-Tight expression vector of the Clontech Tet-on advanced system. Stable transgenic cell lines were established by transfecting R1 ES cells (2.1.1.2), constitutively expressing the Tet-on transactivator, with linearised pTRE-Tight-eGFP-Zscan4c vector as described in 2.4.10. A linear hygromycin resistance cassette was co-transfected with the pTRE-Tight-eGFP-Zscan4c vector to allow for selection. Selection was performed in 300μg/ml Hygromycin B and emerging clones were picked, expanded and screened (2.4.11).

The correct karyotype (Mus musculus, 2N = 40) was assessed by counting DAPI stained metaphase chromosome spreads of confocal images (Figure 4.11 A ii).

Established eGFP-Zscan4c-Tet-on inducible clones were tested for the induction of fusion protein expression and an example is shown in Figure 4.11B. The time

necessary for induction and expression over 48h was assessed by immunoblotting. Doxycycline was added at a concentration of 1μg/ml to transgenic cell cultures and cell lysates were harvested after 0, 6, 12, 24, 36 and 48 hours. Nuclear and cytosolic proteins were prepared as described in 2.3.3 and nuclear fractions were run on SDS-PAGE gels to perform immunoblotting with an anti-GFP antibody (Figure 4.11B (i)). Nuclear reprobes were performed with an anti-TBP antibody to assess loading. After as little as six hours from addition of doxycycline, transgenic eGFP-Zscan4c protein was detectable and remained stably expressed over the 48 hour time-course. Induction of eGFP-Zscan4c was also detectable at the transcriptional level by quantitative RT-PCR with primers specifically binding the GFP sequence (Figure 4.11B (ii)). EGFP fluorescence was also detectable with confocal microscopy, one example of an eGFP-ZScan4c positive colony grown for five days and in presence of doxycycline for the last two of them, is shown in Figure 4.11B panel (iii). Induction of GFP was also determined over a defined time-course via fluorescent microscopy and correlated well with the previously described expression data derived using immunoblotting, indicating a robust expression of eGFP-Zscan4c.

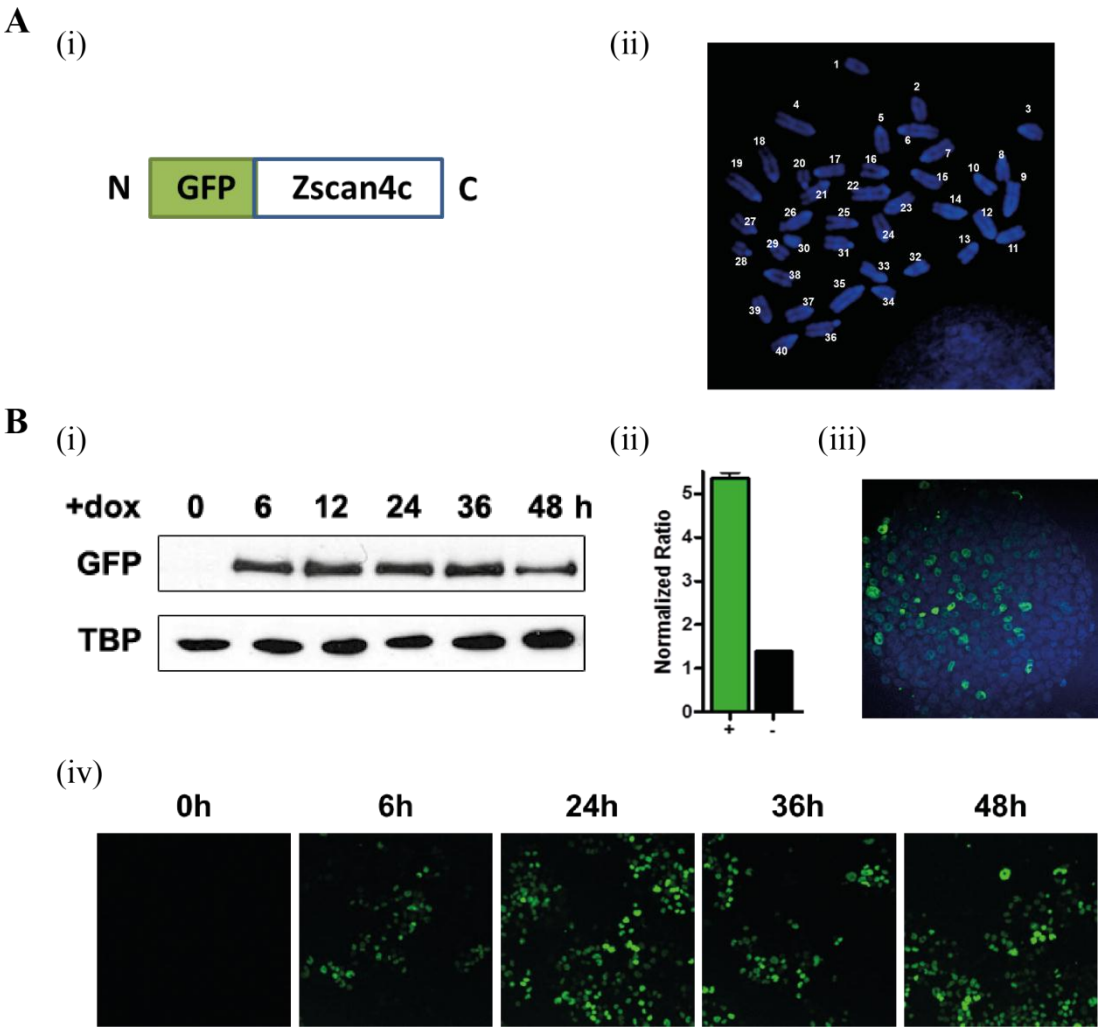

Figure 4.11 Establishment of eGFP-Zscan4c-Tet-on inducible cell lines. (A)(i) A fusion protein was generated, by cloning eGFP in frame to the N-terminus of Zscan4c. The cDNA fusion fragment was subcloned into Tet-on advanced system from Clontech (see Figure 4.4) and transfected into R1 mES cells containing the Tet-On Advanced transactivator (a kind gift of Giusi Manfredi). **(ii)** Karyotype of established clones were analysed by metaphase chromosome spreads stained with DAPI. **(B)(i)** Following induction with 1μg/ml doxycycline cells were lysed and nuclear lysates immunoblotted with an anti-GFP antibody. Blots were stripped and re-probed with an anti-TBP antibody to assess the equality of protein loading. **(ii)** Quantitative RT-PCR was used to confirm induction of Zscan4c expression. **(iii)** Confocal images of day five eGFP-Zscan4c-Tet-on colony after induction with 1μg/ml doxycycline for 48h. **(iv)** Fluorescent images showing expression of eGFP-Zscan4c (green) after addition of doxycycline as indicated.

Flow cytometry analysis was used to measure eGFP-Zscan4c fluorescence in four independent clones (clone N2, N3, N71, N73), which were screened for robust and high levels of protein expression by immunoblotting. Tet-on clones were grown in the absence or in presence of 1μg/ml doxycycline for 72h before performing flow cytometry analysis (Figure 4.12). In all four clones analysed about 40% of the cell population were GFP positive and, therefore, expressed eGFP-Zscan4c protein. The proportion of cells expressing the transgene was significantly higher in comparison to the Zscan4c-V5-Tet-off clones, but still around 60% of the population was negative. Where this heterogeneous expression arises from is not clear at present, possibly the genomic region of integration is sub-optimal for homogenous expression. But with the proportion of eGFP-Zscan4c positive cells being significantly higher than the Zscan4c expression in Tet-off clones, a downregulation by direct regulation mechanisms seems unlikely. The clones N2, N3, N71, and N73 were used in the further experiments to study effects of eGFP-Zscan4c over-expression.

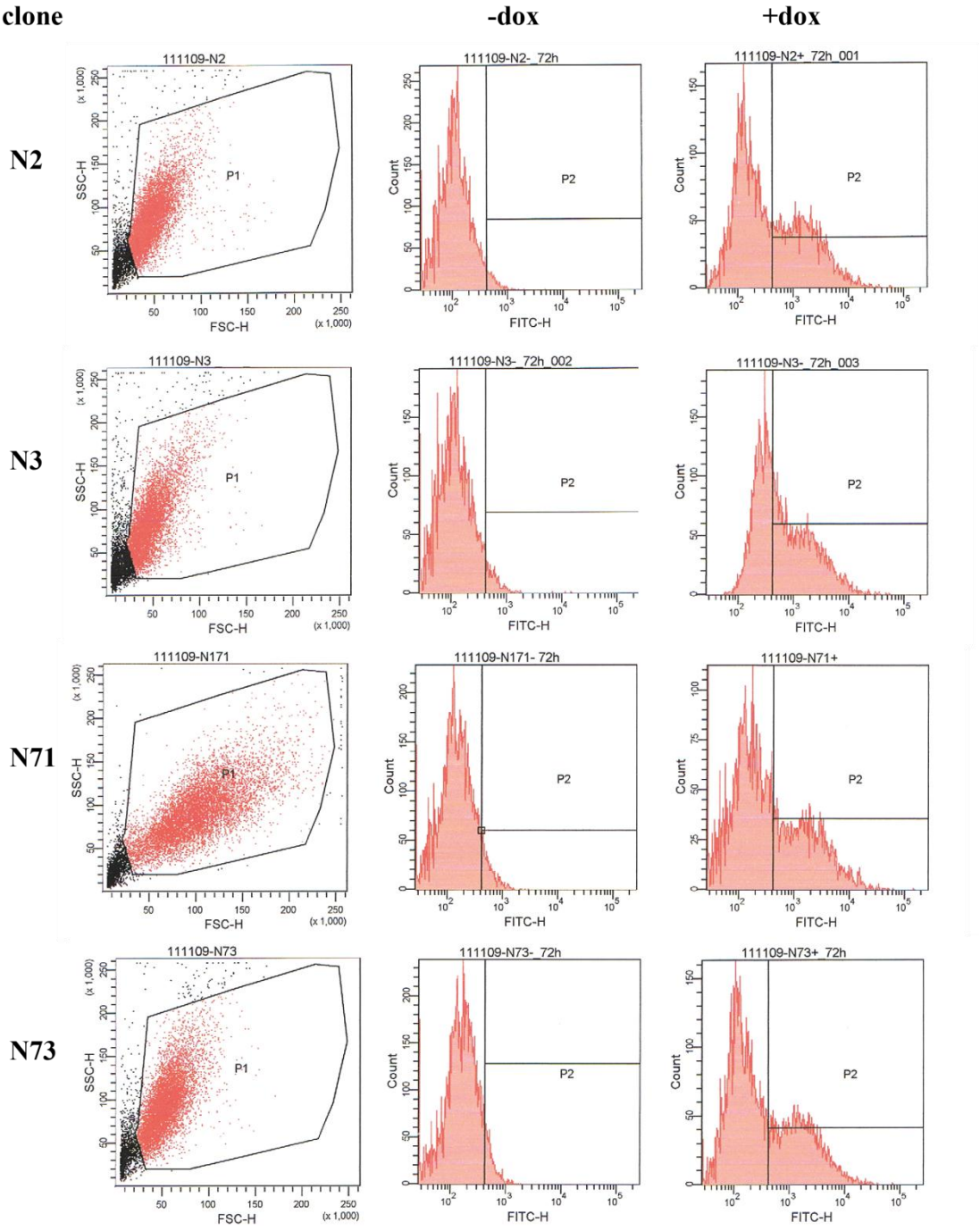

Figure 4.12 Observation of eGFP-Zscan4c expression after doxycycline induction by flow cytometry. Images show flow cytometry pictures of four independent eGFP-Zscan4c-Tet-on clones (N2, N3, N71, N73) cultured in the absence and presence of 1μg/ml doxycycline for 72h. Images in the left column show FSC/SSC plots and gating for respective clone. Images of middle and right columns show histogram plots from one experiment depicting comparative eGFP-Zscan4c expression. The Y axis represents cell number and the X axis represents fluorescent intensity.

4.4.2.2 Metabolic activity in eGFP-Zscan4c ESCs

Knockdown of Zscan4 in the two cell stage embryo delays the development of preimplantation embryos, and furthermore blastocyst outgrowth do not proliferate in in vitro culture (Falco et al., 2007). To investigate whether Zscan4c plays a role in modulating proliferation of ES cells, XTT bio-reduction assays were performed upon doxycycline-induced expression of eGFP-Zscan4c. The colourimetric XTT metabolism assay is based on the reduction of tetrazolium salts (XTT) by dehydrogenases and reductases, only present in metabolically active cells. The yellow XTT salt is metabolised to an orange, water-soluble, formazan dye product, and the colour change, reflecting the metabolic activity of the cell population, can be measured with a spectrometer at an optical density of 490nm (Mosmann, 1983; Roehm et al., 1991; Scudiero et al., 1988).

Shown in Figure 4.13 are the results of XTT bio-reducion assays performed on eGFP-Zscan4-Tet-on cells grown in absence or presence of 1μg/ml doxycycline for six days prior to the assay (2.3.7.2). Experiments shown were performed with two independent clones, but neither of them exhibited a statistically significant change in metabolic activity when eGFP-Zscan4c was expressed (Figure 4.13A). GMEM plus serum and KO medium plus KO serum replacment culture media conditions were applied to assess whether different growth environments might influence the metabolic activity (Figure 4.13B). Metabolic activity of ES cells was significantly higher in GMEM plus serum conditions, in contrast to KO medium plus serum replacement, which is probably caused by growth factors present in the Hyclone serum. Nevertheless, no differences were observed between eGFP-Zscan4c induced and non-induced cell lines, ruling out beneficial or hindering contributions of eGFP-Zscan4c on ES cell metabolism or proliferation.

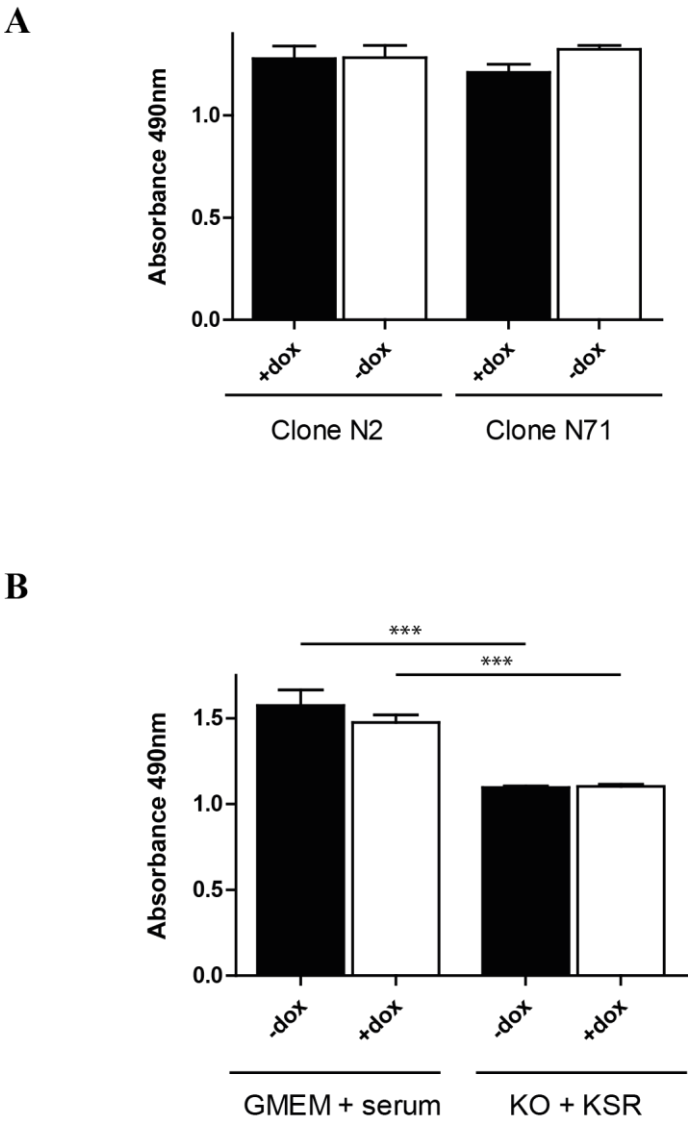

Figure 4.13 Effect of eGFP-Zscan4c doxycycline-induced expression on ESC metabolism. eGFP-Zscan4c-Tet-on mESCs were plated in 96-well plates and cultured +/- doxycycline for six days. XTT-PMS solution was added to each well and incubated for a further 4 hours. Plates were read for the absorbance of light at a wavelength of 490nm. **(A)** Graphs show comparable metabolic activity between clones, N2 and N71. **(B)** Metabolic activity of clone N2 in GMEM plus serum and KO plus Knockout serum replacement (KSR). Data are the average of a minimum of eight replicates for each condition and error bars represent s.e.m. Experiments shown are representative of three independent experiments.

4.4.2.3 Immunocytochemistry anlaysis of eGFP-Zscan4c ESCs

With the finding of Zscan4 playing a role in maintenance of ES cell self-renewal (Chapter 3), it was of interest to investigate whether there is a relationship between Zscan4 expression and the expression of other pluripotency markers. Immunocytochemistry was performed to investigate eGFP-Zscan4c co-localisation with the known pluripotency markers Nanog and Oct4. Transgenic eGFP-Zscan4c-Tet-on ES cells were cultured in the presence of doxycycline for 48h prior to immunostaining, which was performed as described in 2.3.5. Confocal images were taken and cells expressing high and low levels of eGFP-Zscan4c were analysed for Nanog or Oct4 expression levels.

The homeodomain transcription factor Nanog is itself known to be expressed in a heterogeneous fashion, both in the ICM of the blastocyst (Chazaud et al., 2006) and in embryonic stem cells (Chambers et al., 2007; Singh et al., 2007). This heterogeneous expression pattern of Nanog was also observed in the eGFP-Zscan4c-Tet-on clones (Figure 4.14). In the transgenic ES cell culture various expression levels of GFP (in green) and Nanog (in red) were detected, but no correlating trend could be observed. In Figure 4.14 one cell expressing high levels of Nanog is highlighted by a blue arrow, while a white arrow highlights a Nanog low expressing cell.

Expression of Oct4 was, homogenous in the clonal cell population, as detected by immunocytochemistry staining (Figure 4.15). This is consistent with reports of a widespread expression of Oct4 in pluripotent ES cells (Canham et al., 2010; Niwa et al., 2000; Toyooka et al., 2008). Oct4, was expressed in eGFP-Zscan4c positive cells (Figure 4.15), but was also homogeneously expressed in absence of eGFP-Zscan4c, confirming a pluripotency. These data suggest that Zscan4c is not actively driving expression of the important self-renewal core transcription factors Nanog and Oct4 (Loh et al., 2006). This might have been expected with the proposed involvement of Zscan4 in regulating ES cell self-renewal, and the predicted Zscan4c protein structure containing 4 zinc finger domains commonly associated with transcription factors (Falco et al., 2007; Storm et al., 2009).

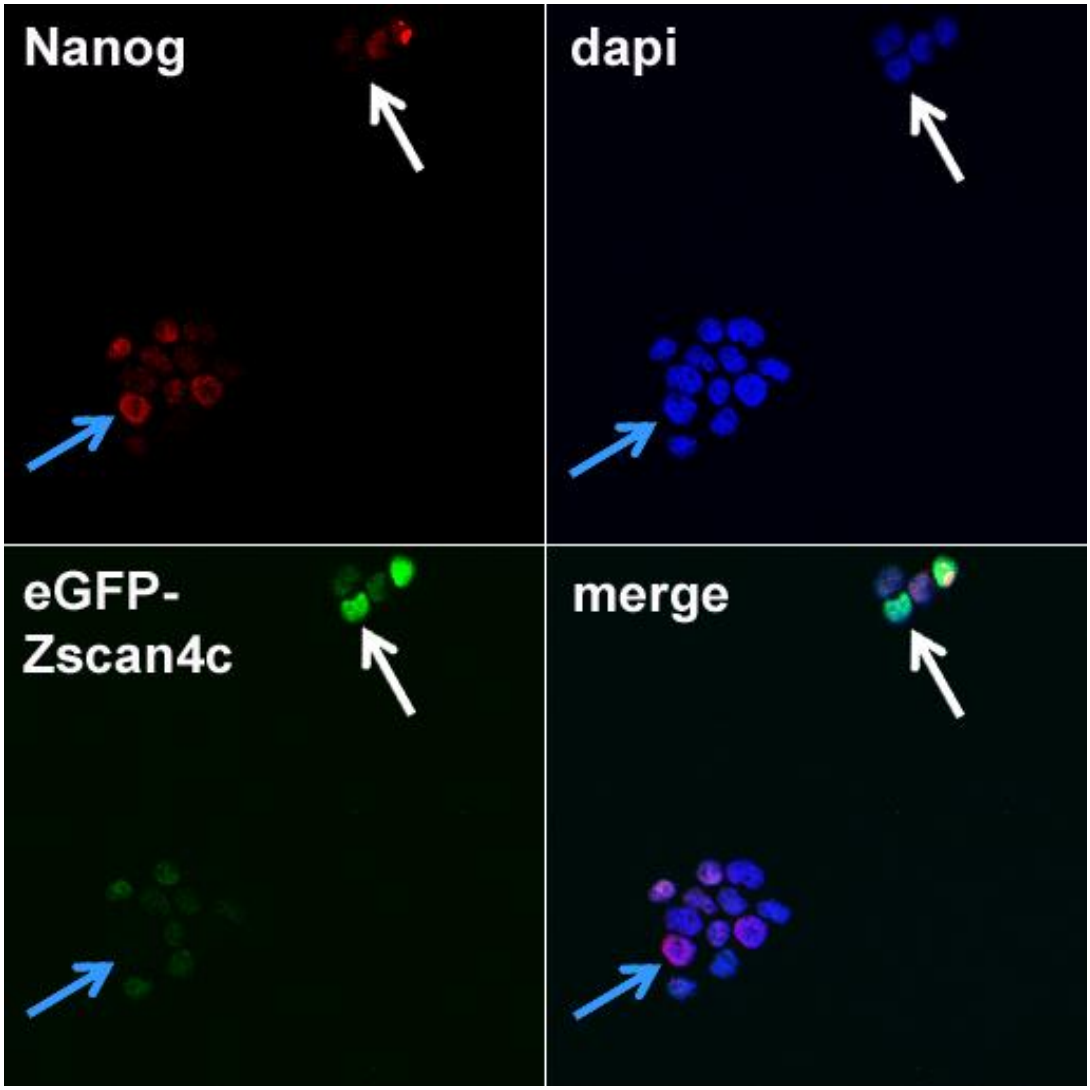

Figure 4.14 Nanog expression in eGFP-Zscan4c-Tet-on ES cells. Transgenic eGFP-Zscan4c-Tet-on ES cells were cultured in the presence of doxycycline for 48h in Lumox 24-well trays prior to immunostaining. Nanog expression was analysed by immunofluorescence (red). Light blue arrow highlights a Nanog high cell, while white arrow highlights a Nanog low cell. GFP was used as a read-out for eGFP-Zscan4c over-expression (green). Cells were counterstained with DAPI (blue) for nuclear localization.

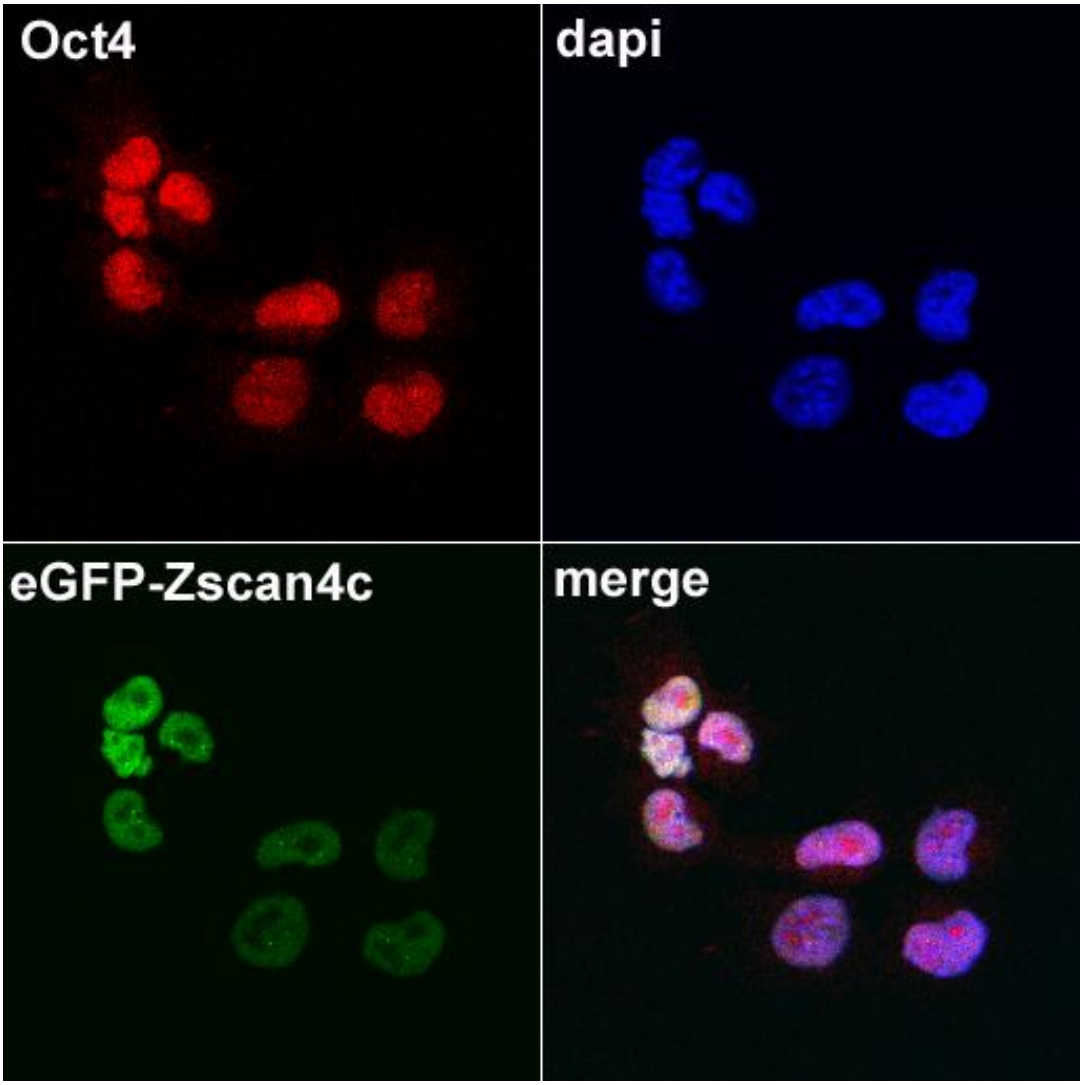

Figure 4.15 Oct4 expression in eGFP-Zscan4c-Tet-on ES cells. Transgenic eGFP-Zscan4c-Tet-on ES cells were cultured in the presence of doxycycline for 48h in Lumox 24-well trays prior to immunostaining. Oct4 expression was analysed by immunofluorescence (red). GFP was used as a read-out for eGFP-Zscan4c over-expression (green). Cells were counterstained with DAPI (blue) for nuclear localization.

When analysing confocal images, in about 30% of the GFP positive cells a focal expression was noticed (Figure 4.16). Whether these foci are random accumulations of eGFP-Zscan4c fusion proteins, or have any functional relevance is not currently clear. Typically, one or two bigger foci could be seen per cell, therefore, a potential co-localisation with the centrosomes was considered. To investigate this hypothesis, immuncytochemical staining with an anti-pericentrin antibody was performed (Figure 4.16; in red). No co-localisation of eGFP-Zscan4c foci with percentrin staining could be detected. Figure 4.16 shows a representative staining, with blue arrows marking centrosomal staining and white arrows indicating eGFP-Zscan4c foci.

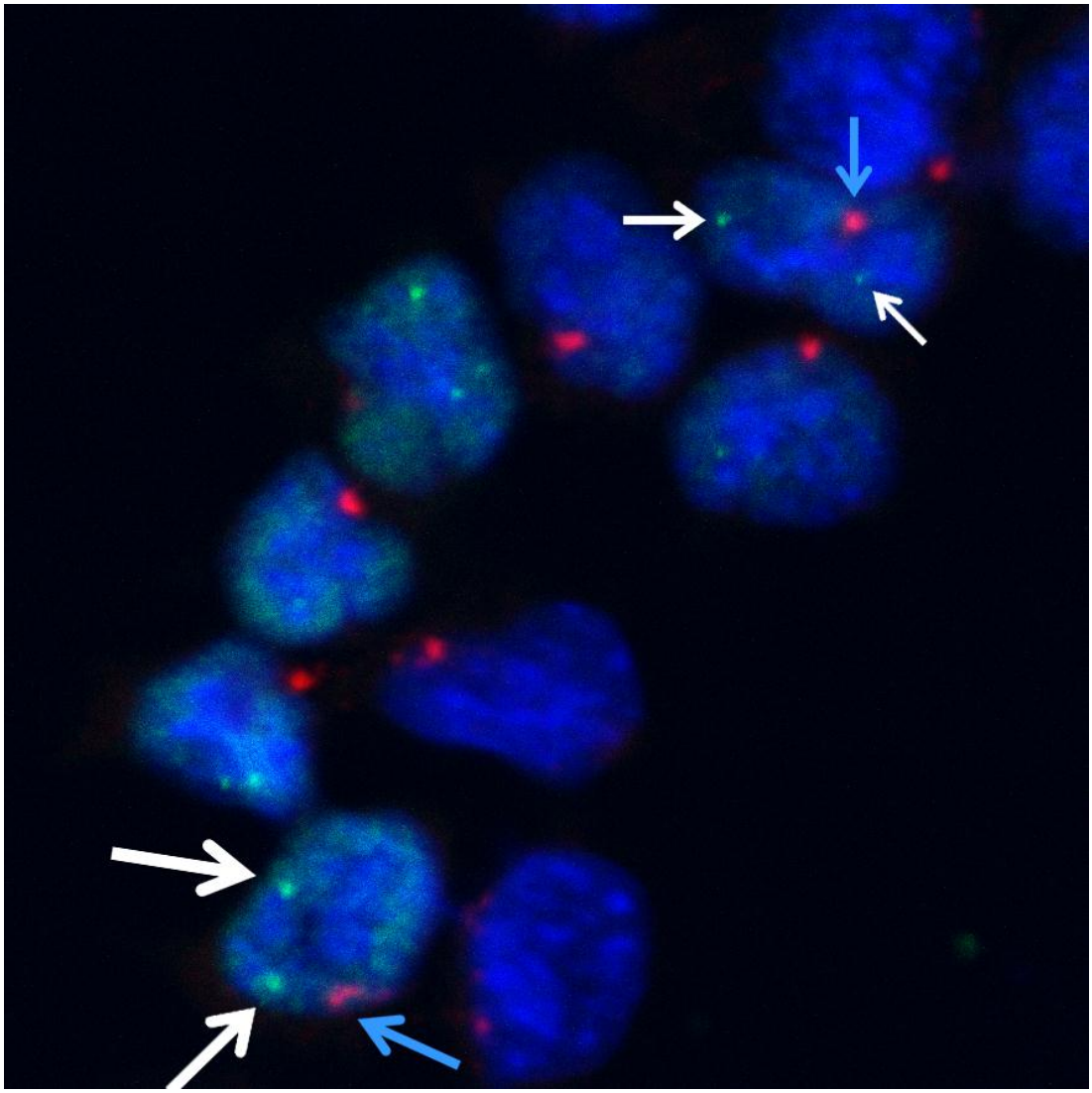

Figure 4.16 Intracellular localisation of eGFP-Zscan4c. Transgenic eGFP-Zscan4c-Tet-on ES cells (clone N3) were cultured in the presence of doxycycline for 48h in Lumox 24-well trays prior to immunostaining. eGFP-Zscan4c expression (green) was localised in the cell nucleus (blue) and a focal formation was observed in ~20% of eGFP-Zscan4c positive cells (white arrows). Centrosome localisation was assessed with α-pericentrin antibody (red; blue arrows) and colocalisation with eGFP-Zscan4c foci (white arrows) was investigated. Cells were counterstained with DAPI for nuclear localization.

4.4.3 Identification of Zscan4c Protein interactions

Understanding the molecular mechanisms by which Zscan4c functions should help to shed further light on the unique properties of its actions in embryonic stem cells. The special ES cell state of pluripotency is not solely governed at the transcriptional level, but also complex regulatory mechanisms at the protein level are important for correct function. For instance, homodimerzation of Nanog protein was demonstrated to be critical for promotion of ES cell pluripotency (Wang et al., 2008). The ES cell identity is likely to be influenced by multiprotein complexes, that can change through association and dissociation of proteins (Wang et al., 2006). Furthermore, it was shown that Nanog forms multiple protein complexes, predominantly with nuclear factors, of which many were associated with ES cell self-renwal (Wang et al., 2006). In this study it was further investigated whether Zscan4c might act as a part of such multi-protein complexes.

4.4.3.1 Size Exclusion Chromatography (Gel Filtration)

To ascertain whether Zscan4c can form protein homodimers or other protein complexes *in vivo*, size exclusion chromatography of ES cell nuclear extracts was performed to fractionate eGFP-Zscan4c-containing protein complexes. For creating nuclear extracts, eGFP-ZScan4c-Tet-on cells were grown in 175T culture flasks, and 1μg/ml doxycycline was added 48h prior to harvest for induction of eGFP-Zscan4c protein expression. Gel filtration was performed with a Superdex200 10/300 GL gel filtration column and collected fractions were tested for GFP fluorescence using a spectrometer. Results revealed three major GFP peaks, indicated as GFP1, GFP2, and GFP3 in Figure 4.17. The eGFP-Zscan4c monomer is about 100kDa in size, which would resemble the detected GFP3 peak. Interestingly, the GFP2 peak was with approximately 200kDa double the size, suggesting possible dimer formation. The GFP1 peak was far bigger than 200kDa, and must therefore arise from multiprotein complexes containing eGFP-Zscan4c. Fluorescence levels were the highest for the second GFP peak, indicating that dimerization plays an important role in the mechanisms of Zscan4c function.

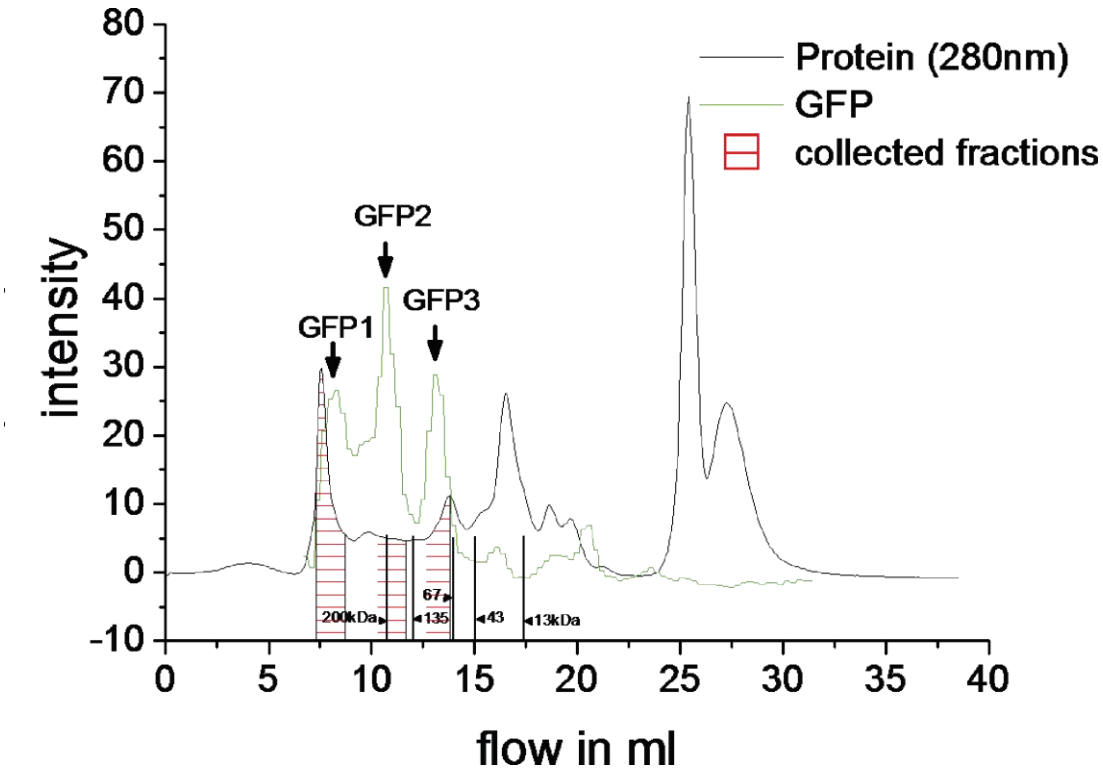

Figure 4.17 Gel filtration of nuclear protein fractions from eGFP-Zscan4c-Tet-on ESC lysates. Cells were cultured in six tissue culture 175T-flasks and expression of eGFP-Zscan4c was induced for 48h by addition of 1mg/ml doxycycline. Cytosolic and nuclear proteins were extracted and the nuclear fraction was separated with FPLC by a Superdex200 10/300 GL gel filtration column from GE Healthcare. GFP yield of collected 0.5ml fractions was determined on a fluorescent plate reader and is plotted in displayed graph (green line). Total protein was measured by FPLC at 280nm (black line). The Y axis represents intensity and the X axis represents flow in ml. Markers for 13, 43, 67, 135 and 200kDa were run through gel filtration column and are shown in graph. Three major GFP peaks, GFP1 (>200kDa), GFP2 (~200kDa), GFP3 (~100kDA) were detected.

4.4.3.2 Identification of Zscan4c binding partners

With eGFP-Zscan4c found to be bound in larger protein complexes, it was of interest to identify binding partners, as they could reveal important clues to the mechanism of action of Zscan4 proteins. To achieve this an immunoprecipitation strategy, followed by mass spectrometry analysis was chosen. Immunoprecipitation was performed using GFP-Nanotrap beads from Chromotek, which are able to very specifically bind GFP (2.3.4). The beads consist of the variable part of an camelidae antibody that binds to GFP, coupled to agarose beads (Figure 4.18A (i)). For Nanotrap immunoprecipitation cytosolic and nuclear proteins were separated as described in 2.3.3 and Figure 4.18A panel (ii) shows a scanned immunoblotting image of a representative separation, with eGFP-Zscan4c enriched in the nuclear fraction. The protein fractions were pre-cleared with hydrated agarose before performance of immunoprecipitation (Figure 4.18B (i)). For Nanotrap immunoprecipitation, the GFP-Trap®_A (Chromotek) beads were incubated on a rotator for one hour at 4°C (Figure 4.18 B ii), which was sufficient to bind ~88% of eGFP-Zscan4c protein present in the nuclear fraction. After washing, bound proteins were eluted with 200mM glycine at pH 2.5 and 1M Tris-base (pH 10.4) was added for neutralization. Eluted fractions were run on SDS-PAGE gels, which were subsequently stained with colloidal coomassie. Examples of coomassie stained gels after performance of GFP-Nanotrap affinity purification experiments are shown in Figure 4.19.

Protein bands which were only present upon eGFP-Zscan4c induction were sent to mass spectrometry facilities at the University of Bristol for sequencing. Data was compared to a mouse protein database, with a protein score threshold value of 84. Protein scores >64 are classed as significant ($p<0.05$). The over-expressed transgene, eGFP-Zscan4c, was identified by this type of analysis, proving the correct function of GFP-Nanotrap immunoprecipitation (Figure 4.20A). Further protein sequences identified by mass spectrometry were, lysine specific histone demythelase 1A (LSD1), C-terminal binding protein2 (Ctbp2), 40S ribosomal protein S7, and histidine triad nucleotide-binding protein 1 (HINT1) (all highlighted in Figure 4.20 A). Surprisingly, a protein of approximately 75kDa in size was identified as eGFP, which must result from cleavage of eGFP-Zscan4c, as eGFP alone would be smaller

in size. The reason for the shortening of eGFP-Zscan4c is not known to date, but protease and phosphatase inhibitors were included in protein lysates at all times.

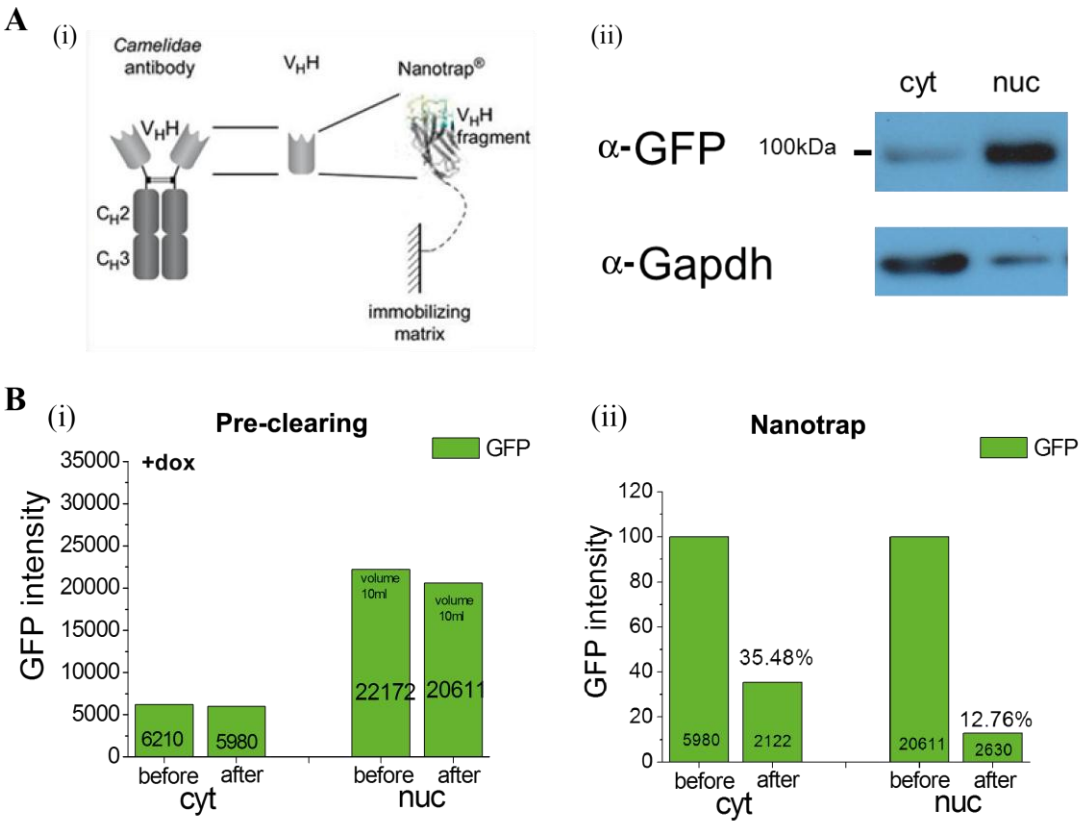

Figure 4.18 (A) Immunoaffinity purification-mass spectrometry (IP-MS) approach for identifying protein interaction partners of eGFP-Zscan4c. GFP-Nanotrap technology was used for identifying Zscan4c protein-protein interaction partners (http://www.chromotek.com). **(A) (i)** GFP-Nanotrap from Chromotek consists of a variable single domain antibody fragment, highly specific for GFP, linked to agarose beads. **(ii)** Cytosolic and nuclear extracts were prepared of eGFP-Zscan4c-Tet-on cells grown in presence of 1µg/ml doxycycline for 48 hours. Immunoblots showing eGFP-Zscan4c protein with anti-GFP antibody and Gapdh enriched in cytosolic fraction detected with anti-Gapdh antibody. **(B)** GFP intensity was measured of cytosolic and nuclear protein fractions with a fluorescent plate reader. **(i)** Graph shows GFP intensity of nuclear and cytosolic protein fractions obtained from eGFP-Zscan4c-Tet-on ESC grown in 32 tissue culture 175T-flasks for 48 hours in presence of doxycycline before and after pre-clearing with agarose beads. **(ii)** GFP intensity of cytosolic and nuclear fractions before and after incubation for 1 hour with GFP-Nanotrap beads.

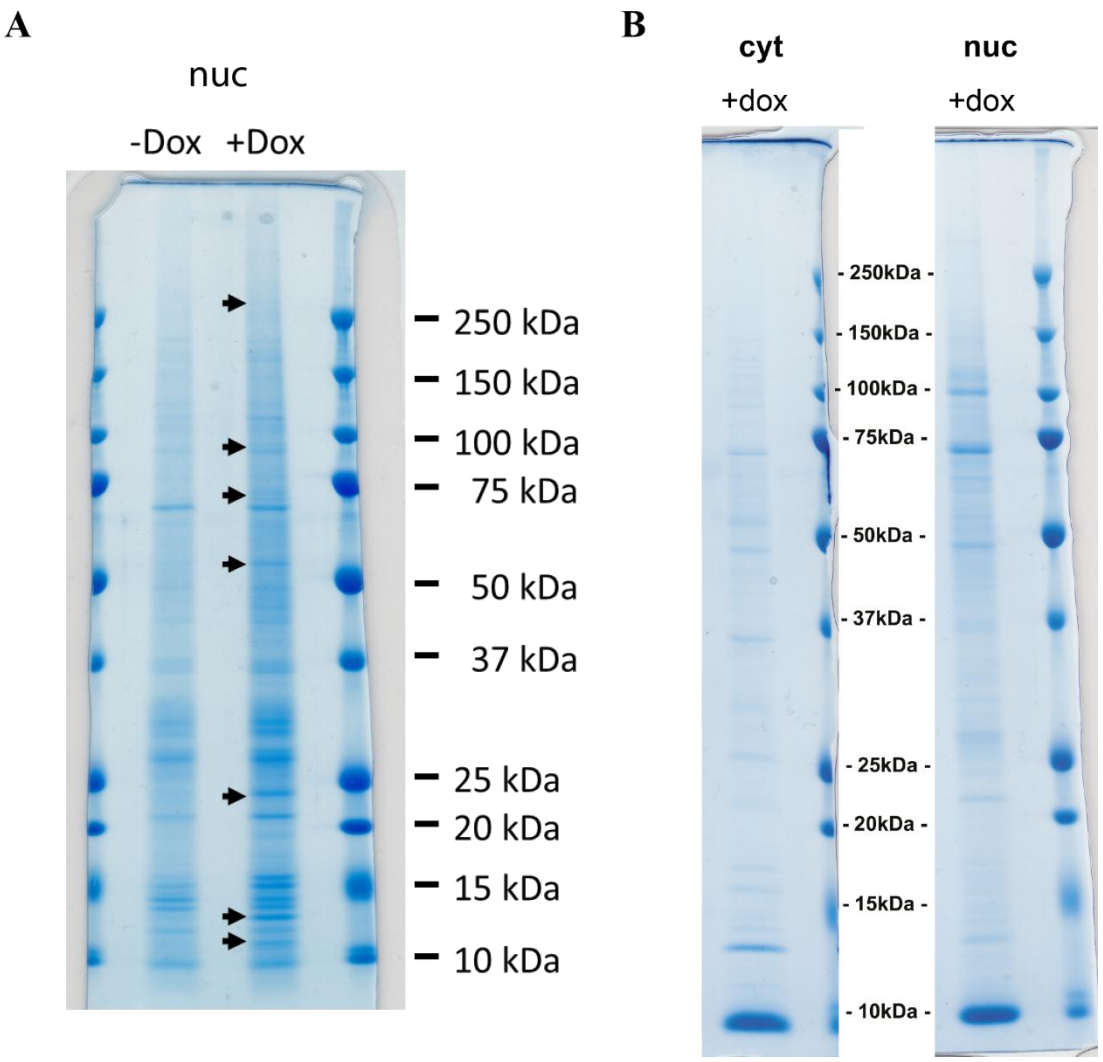

Figure 4.19 Elution of GFP Nanotrap. Colloidal coomassie stained gradient SDS-PAGE gels of GFP-Nanotrap (Chromotek) elution (cyt= cytosolic, nuc= nuclear fraction). (**A**) Nuclear protein fraction was obtained from eGFP-Zscan4c-Tet-on clone N73 lysates. ESCs were grown in 18 tissue culture 175T-flasks for 48 hours in the presence and absence of 1µg/ml doxycycline. Protein bands visible only in presence of doxycycline are highlighted by the black arrows. **(B)** Cytosolic and nuclear protein fractions were obtained from the eGFP-Zscan4c-Tet-on clone N3, grown in 32 tissue culture 175T-flasks for 48 hours in the presence of doxycycline.

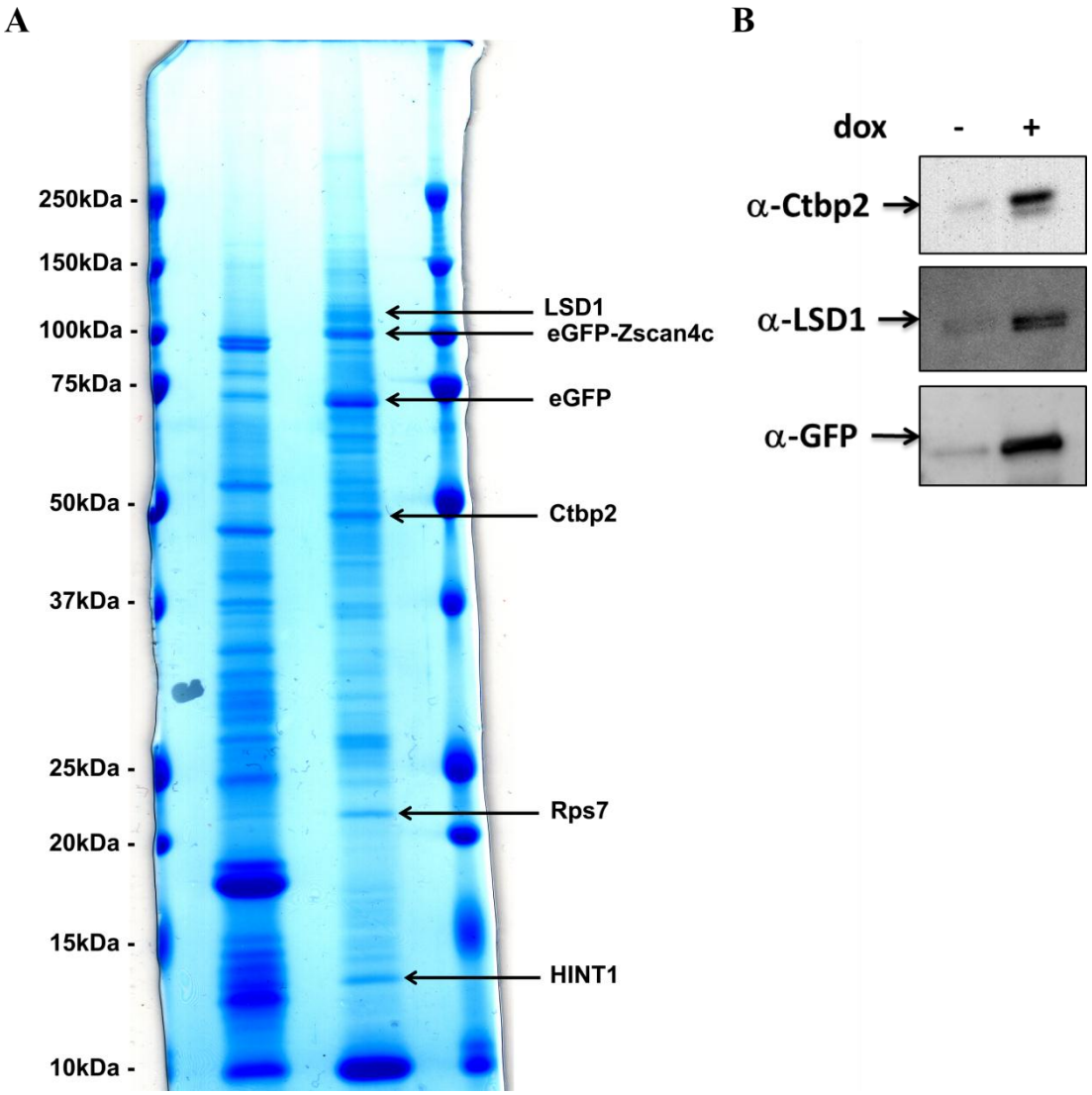

Figure 4.20 Interaction partners identified by IP-MS. (A) Colloidal coomassie stained gradient SDS-PAGE gel after immunoprecipitation of nuclear protein fraction (nuc) with GFP-Nanotrap beads. Proteins indicated were identified by mass spectrometry. Protein fractions were obtained from eGFP-Zscan4c-Tet-on clone N3 ESCs grown in 32 tissue culture 175T-flasks for 48 hours in presence of doxycycline. **(B)** GFP-Nanotrap immunoprecipitates were prepared with 60µg of nuclear extract from eGFP-Zscan4c clone N3 grown for 72h ± Dox. Immmunoblots were probed with anti-Ctbp2, anti-LSD1 or anti-GFP antibody (kindly provided by Prof. Melanie Welham).

Lysine-specific demethylase 1 (LSD1) was the first discovered protein lysine demethylase and removes methyl groups from histone H3 lysine 4, through an FAD-dependent oxidative reaction (Shi et al., 2004). It was found previously to be a component of various protein complexes containing transcriptional co-repressors and several zinc finger proteins (Hakimi et al., 2002; Lee et al., 2005; Shi et al., 2005). Interestingly, it was discovered to be associated with the transcriptional co-repressor Ctbp, which was also identified in our IP experiments (Shi et al., 2003).

C-terminal-binding protein 2 (Ctbp2) was first reported to play a role in negative modulation of oncogenic transformation by binding to the C-terminus of the adenovirus E14A proteins (Boyd et al., 1993). Ctbp was identified to exhibit important roles during development (Chinnadurai, 2003). Ctbp is recruited to DNA by transcription factors that contain a PXDLS core motif (Chinnadurai, 2002; Nibu et al., 1998), but how it acts after recruitment to the DNA is unknown. It is reassuring that Zscan4c also exhibits a PXDLS motif at position 263-268, and in fact all Zscan4 family members contain this binding domain, suggesting that each of them can bind Ctbp.

Histidine triad nucleotide-binding protein 1 (HINT1) is a haploinsufficient tumor suppressor gene with unknown molecular working mechanism (Li et al., 2006). It is involved in ionizing radiation induced DNA damage responses (Li et al., 2008a). Radiated cells respond quickly with phosphorylation of the histone variant H2AX, leading to the phosphorylated protein that is called γ-H2AX, forming distinct foci in the nucleus. γ-H2AX serves as a scaffold for other DNA repair factors to bind (Paull et al., 2000). HINT1 deficient fibroblasts ($HINT1^{-/-}$) exhibit prolonged γ-H2AX foci, and $HINT1^{-/-}$ mice, have an increased cancer risk (Li et al., 2008a; Li et al., 2006).

40S ribosomal protein S7 (Rps7) is a subunit of the ribosomes, the organelles that catalyse protein synthesis (Wool et al., 1995). Ribosomes are assembled in the nucleolus, and are exported to the cytoplasm after assembly, where they translate mRNA (Karbstein, 2011).

To this end, immunoprecipitation using GFP-Nanotrap (Figure 4.20B) and co-immunoprecipitations with murine Zscan4 antibody were performed for LSD1 and CtBP, confirming their interactions (experiments were performed by Prof. Melanie Welham).

4.5 Discussion and Summary

In this chapter experiments were performed to gain further insights into the potential action mechanisms of the Zscan4 family. To achieve this, the predominant paralogous gene Zscan4c was investigated by over-expression in mES cells.

4.5.1 Summary

- Ensembl database comparisons revealed a change in the composition of the Zscan4 family members reported by Falco et al. (Falco et al., 2007). Pseudogene two (Zscan4-ps2-201), was now found to be also full-length coding with 506aa in length. Zscan4b + e paralogous genes are in the database with 505aa, in contrast to previously reported 195aa. Furthermore, Zscan4f was found in the Ensembl database to have an additional splice variant with 77aa in size.

- Protein alignments were performed with Clone manger 9 professional, to compare sequence homologies of all paralogs.

- Episomal supertransfection was used to drive high levels of Zscan4c over-expression, which did not lead to stable cell lines.

- Zscan4c-Tet-off inducible cell lines were established.

- Nuclear accumulation of Zscan4c protein was determined by immunocytochemistry and immunoblotting of cytosolic and nuclear protein fractions.

- Tet-off clones exhibited extremely heterogeneous expression of Zscan4c-V5 protein, as detected with immunocytochemistry, despite robust expression detection by immunoblotting.

- Zscan4c protein half-life was significantly higher than half-life of Nanog protein, as determined with cycloheximide protein synthesis inhibition experiments.

- Heterogeneous expression of Zscan4c-V5 in Tet-off cell lines was cell cycle independent.

- Induced expression of Zscan4c protein in Tet-off clones could not compensate for the differentiation inducing effects of sub-optimal concentrations of LIF.

- Tet-on advanced system from Clontech Laboratories was used to establish stable mES cell lines that can be induced with doxycycline to over-express an eGFP-Zscan4c fusion protein.

- With ~40% of the population being positive for eGFP after expression induction, the induction levels were significantly higher than in Tet-off clones.

- No change in metabolic activity was observed by the XTT bio-reduction assay upon induction of eGFP-Zscan4c expression for six days.

- Immunocytochemistry experiments revealed no correlation of eGFP-Zscan4c levels with either Nanog or Oct4 expression levels. A focal accumulation of eGFP-Zscan4c protein was observed, which did not co-localize with centrosomal staining by an anti-α-pericentrin.

- Potential dimer formation of eGFP-Zscan4c, and eGFP-Zscan4c – protein interaction complexes are likely to exist, as detected by size exclusion chromatography.

- GFP-Nanotrap immunoprecipitation experiments, followed by mass spectrometry analysis revealed the potential Zscan4c binding partners: LSD1, Ctbp2, HINT1, and Rps7.

4.5.2 Discussion

The Zscan4 family was first described in 2007 and is a very novel gene family exhibiting a number of unique features (Falco et al., 2007). Originally, only three of the nine described Zscan4 paralogs were full length (506aa), whereas a further three were thought to be pseudogenes (Falco et al., 2007). Despite this early report, we were able to clone some of the pseudogenes from mES cell cDNA, indicating their transcription (Storm et al., 2009). Recent Ensembl database searches revealed that some changes had occurred since the first publication on the Zscan4 family, which is a consequence of the on-going research and updates in this area (see Table 4.1). The recent changes highlight the necessity for a consequent in-depth investigation of the Zscan4 family to rule out any misinterpretation of the data. To determine the precise function of each of the family members, with assessment of redundancy, regulation and interactions holds great benefit for the understanding of ES cell biology.

Zscan4 family members are highly similar in sequence, which has been described in the literature and could be confirmed by protein sequence alignments (Falco et al., 2007; Storm et al., 2009). Because of the very high sequence homologies, a similar function seems likely. Interestingly, Zscan4d was described to be the predominant form in the 2-cell stage, whereas Zscan4c was the most prominent in ES cells (Falco et al., 2007). How this expression regulation occurs is not known yet, but deciphering the promoter regions appears to be a helpful analysis. Attempts to map a promoter region were endeavoured, but failed due to a lack of known binding motifs. For Zscan4c a promoter region was found that, when cloned upstream of the fluorescent emerald GFP protein, mirrored the described heterogeneous expression in ES cells (Zalzman et al., 2010). It would be of interest to determine also promoter regions for other Zscan4 paralogs, which might contribute to identifying the mechanisms regulating their expression. Zscan4f-003 was only 77aa in size and might play a role in negatively regulating the function of other family members by disturbing for instance correct dimer formation.

Over-expression was chosen to shed further light into the functional mechanisms of Zscan4c. The episomal supertransfection is based on the polyoma virus replication system (Gassmann et al., 1995) and was successfully adapted to the ES cell environment (Niwa et al., 1998). This system allows high yield of target transgene expression, and was used to over-express Zscan4c. Surprisingly, when E14/T mES cells were transfected with the episomal expression vector containing Zscan4c-V5 under the CAG promoter (Niwa et al., 1991) no stable transfectants were obtained upon respective antibiotic selection. Correct expression of the transgene was detected by transient transfection, but was lost after 72 hours. ES cells might not be able to tolerate high levels of Zscan4c for a long period of time and subsequently go into crisis leading to cell death. A similar cytotoxicity was described for other pluripotency associated genes, namely Tbx3 and Klf4, which when over-expressed by the episomal expression system did not result in stable clones (Niwa et al., 2009). A tight dosage effect of these genes was postulated and this accounts most likely as well for Zscan4c.

To achieve a better control over Zscan4c expression, tetracycline inducible systems were utilized. The Tet-off system was first used for over-expressing Zscan4c protein, which was C-terminal V5-epitope tagged. An inducible expression system has many advantages, but when using the Tet-off system a highly heterogeneous expression pattern, with only a small percentage of cells in the population expressing the transgene, was encountered. Despite the limitations, transgenic Zscan4c-Tet-off cell lines were used to study Zscan4c protein localisation and stability. A nuclear accumulation of Zscan4c protein was determined by immunocytochemistry and immunoblotting of separated nuclear and cytosolic protein fractions. This suggests a predominant function in the nucleus, which fits well with the later reported function of Zscan4c in maintaining genomic stability and telomere length (Zalzman et al., 2010). Furthermore, protein domain prediction revealed four zinc fingers in the Zscan4c protein structure, which are commonly associated with DNA binding and transcription factor activity (Falco et al., 2007). Zscan4c is postulated to have multiple functions and might also act as a transcription factor, as its over-expression was reported to result in transcriptional changes (Nishiyama et al., 2009).

Zscan4c-V5 protein stability was assessed by blocking protein bio-synthesis with cycloheximide, and performing immunoblotting of subsequently harvested protein lysates over a six hour time-course. Zscan4c protein stability was found to be about two fold greater than Nanog protein stability. Zscan4f RNA was described to be extremely restricted in expression and transcribed only at the 2-cell stage of mouse embryo development, as detected with in-situ hybridization (Falco et al., 2007). There is no published protein data yet relating to how long Zscan4 protein can persist after induction at the 2-cell stage and is of considerable interest as Zscan4 function could last further if protein levels are maintained. With the novel and highly selective Zscan4 antibody recently developed in our laboratory, this kind of analysis can now be performed.

Zscan4c-Tet-off clones were used to assess the ability of Zscan4c to protect cells from differentiation-inducing environmental triggers. With the heterogeneous expression of Zscan4c in the clonal population, it was perhaps not surprising that Zscan4c was not found to shelter ES cells from differentiation upon LIF withdrawal. This is in contrast to the findings that ES cell lines, expressing Zscan4c by a constitutive active CMV promoter, had an advantage in generating undifferentiated ESC colonies, when cultured under optimal and suboptimal levels of LIF (Storm et al., 2009). With only a few cells expressing high levels of Zscan4c in the Tet-off cells, such an effect would be masked and probably not detected. On the other hand, in ESC culture Zscan4 expression is tightly regulated and long-term expression of Zscan4c might have negative impacts on ES cell identity (personal communication Minoru S. H. Ko).

To overcome the limitations encountered with the Tet-off system, I changed to the Tet-on advanced expression system from Clontech Laboratories. A fusion protein was created by fusing enhanced GFP to the N-terminus of Zscan4c and this construct was used for expression by the Tet-on system. Established eGFP-Zscan4c-Tet-on clonal cell lines exhibited a robust expression induction with around 40% of the population expressing the fusion protein. Induction proportions did not reach 100%, which might potentially arise from integration into sub-optimal locus in the genome. Such risks of sub-optimal genome integration could be bypassed in the future by directed integration into known stable genome loci, for example the ROSA26 locus

(Masui et al., 2005). It could be also that high levels of Zscan4c cannot be tolerated for long-term and therefore these cells are selected out of the population.

Metabolic activity was assessed in eGFP-Zscan4c-Tet-on clones upon induction of transgene expression by doxycycline. Therefore, the XTT bio-reduction assay was performed, on eGFP-Zscan4c-Tet-on stable cell lines, grown in presence and absence of doxycycline for six days. No negative or beneficial effects of eGFP-Zscan4c over-expression could be detected on ES cell metabolism, which is often used as a read-out for cell proliferation. A higher metabolic activity was detected when ES cells were grown in GMEM plus Serum media, compared to culture in KO DMEM media, which might be caused by cytokines present in the Serum stimulating growth. Even though there were no growth stimulating benefits observed by eGFP-Zscan4c over-expression for six days, it might be worth mentioning that occasionally an increase in colony size was observed when Zscan4c expressing clones were cultured for more than ten days and therefore the contributions might be very small and only observable after a longer time period.

The great benefit of a GFP-Zscan4c fusion protein was the possibility of tracking the fusion protein easily by fluorescence-based detection methods. Confocal image analysis commonly showed a clear nuclear localisation, consistent with previous observations and described function of maintaining genomic stability and regulation of telomere length, functions which would obviously take place in the nucleus (Zalzman et al., 2010). Correlation of Zscan4c expression with known pluripotency associated regulators, Nanog and Oct4, was investigated by immunocytochemistry analysis. No positive correlation of eGFP-Zscan4c with Nanog and Oct4 was detected on the protein level upon over-expression of eGFP-Zscan4c. GFP high cells did not exhibit higher levels of Nanog or Oct4, which rules out a direct effect on pluripotency of Zscan4c by altering their levels. Interestingly, a focal accumulation of eGFP-Zscan4c protein was observed in about 30% of the GFP positive cells. No functional effects of the foci could be observed, and co-localisation studies with α-pericentrin, marking centrosomes, were negative. Zscan4 was postulated to elongate telomere length via meiosis-specific homologous recombination mediators and to form foci at telomeres (Zalzman et al., 2010). But foci observed of the eGFP-Zscan4c protein, were smaller in number than expected for telomere foci. However, the described recombination mechanisms that account for the telomerase

independent elongation of telomeres (Zalzman et al., 2010) could be similar to the alternative lengthening of telomeres (ALT) phenomenon (Bryan et al., 1997; Bryan et al., 1995). ALT maintains telomere length in some immortalized cell lines, and in a sub-set of cancers that are negative in telomerase activity (Bryan et al., 1997; Bryan et al., 1995), but the molecular mechanisms are not yet discovered. ALT cells contain so called PML nuclear bodies (APBs), and consist of various proteins, of which telomere binding proteins, recombination proteins, and heterochromatins were described (Jiang et al., 2011). It is possible that the focal expression of eGFP-Zscan4c arises from a localisation in APBs. Their function is unknown, and they are likely to be functionally heterogeneous (Jiang et al., 2011).

The eGFP-Zscan4c-Tet-on cells were also used to understand how Zscan4c might function at the protein level by potential protein interactions. Initially, size exclusion chromatography was performed with nuclear eGFP-Zscan4c-Tet-on protein lysates to fractionate proteins by size, and individual fractions were tested for GFP fluorescence. Three GFP peaks could be detected, with the sizes of ~100kDa, ~200kDa, and >200kDa, which are likely to reflect eGFP-Zscan4c monomers, dimers, and eGFP-Zscan4c complexed with other proteins. Other important pluripotency regulators, like Nanog or Oct4, are also shown to predominantly exhibit their function as dimers or in protein complexes (van den Berg et al., 2010; Wang et al., 2008). For Oct4 an interactome of >160 proteins was reported, of which many were documented self-renewal regulating components, including chromatin-modifying complexes and transcription factors (van den Berg et al., 2010).

After establishing the possibility that Zscan4c might also act in multi-protein complexes an immunoprecipitation (IP) - mass spectrometry strategy was used to identify potential interactors, as this might give hints on the molecular mechanisms of Zscan4c action. For immunoprecipitation the GFP-Nanotrap from Chromotek, which highly specifically binds GFP protein, was used. Mass spectrometry revealed the potentially interacting proteins LSD1, Ctbp2, HINT1 and Rps7.

LSD1 (also known as Kdm1 and AOF2) is a lysine-specific demethylase, which was shown to demethylate histone H3 on lysine 4 (H3K4) and lysine 9 (H3K9) (Metzger et al., 2005; Shi et al., 2004). It was implicated to be important during mouse embryogenesis, especially for gastrulation (Wang et al., 2009). Furthermore, Wang

et al. proposed that LSD1 stabilizes Dnmt1 by demethylation and thus provides a link between histone and DNA methylation systems. Dnmt1 deficient mouse ES cells have dramatically elongated telomeres, likely to be a result of increased telomeric recombination (Gonzalo et al., 2006). Heterochromatic marks, like H3K9 and H4K20 trimethylation, remained at subtelomeric and telomeric regions of Dnmt1 deficient ES cells. Whether Zscan4 might be involved in some of these molecular processes is not known, but Zscan4c over-expression also leads to an increase in telomere length by a recombineering event (Zalzman et al., 2010). It could be speculated that high levels of Zscan4, as a result of ectopic over-expression or endogenous, through promoter activation, lead to an inactivation of LSD1 by binding to Zscan4c, which results in Dnmt1 destabilisation and subsequent alternative lengthening of telomeres. How this theory would match with the recent finding of LSD1 regulating the balance between self-renewal and differentiation in human ES cells (Adamo et al., 2011), is not clear. Knockdown of LSD1 by shRNA constructs resulted in differentiation of human ES cells through loss of control of H3K4 methylation (Adamo et al., 2011). Another mechanism of how LSD1 could act on ES cell self-renewal might be through the interaction with long intergenic noncoding RNAs (lincRNAs) (Tsai et al., 2010). LincRNAs were shown to be able to bind multiple histone modification enzymes, among them LSD1 (Tsai et al., 2010). Furthermore, loss-of function studies revealed that lincRNAs play key roles in the circuitry controlling ES cell identity (Guttman et al., 2011). If Zscan4c is interacting with LSD1, a contribution of some of these effects might be arise from either direct Zscan4c action, or by acting as a linker to recruit complexes to, for instance, telomeric regions.

Ctbp2, a 48kDa cellular phosphoprotein, was also found to associate with Zscan4c, and is likely to have bound via the PXDLS binding motif of Zscan4 (Boyd et al., 1993; Quinlan et al., 2006). Murine Ctbp1 is expressed from the embryo to the adult animal, whereas Ctbp2 is predominantly expressed during embryonic development (Furusawa et al., 1999). Ctbp1 and Ctbp2, collectively referred as Ctbp, are broadly expressed within different tissues of the developing embryo and function as transcriptional co-repressors. Ctbp forms dimers and interacts with a transcriptional repressor and a chromatin modifying protein complex comprised of enzymes such as histone deacetylases and LSD1 that suppress gene transcription (Balasubramanian et

al., 2003). The repression activity is dependent on intracellular NADH, which binds to Ctbp's dehydrogenase/NADH binding domain (Mani-Telang et al., 2007; Zhang et al., 2002). Ctbp acts as a redox sensor for regulating transcription as a consequence of the cellular metabolic environment (Fjeld et al., 2003; Zhang et al., 2006a). Interestingly, Ctbp is phosphorylated in a cell cycle dependent manner and its phosphorylation pattern suggests regulation by a cell cycle-regulated kinase (Boyd et al., 1993). Furthermore, Ctbp contain consensus DNA-PK phosphorylation sites, and were shown to interact with the Ku 70 subunit of DNA-PK, which make it possible that its activity is modulated through phosphorylation by DNA-PK or similar protein kinases (Chinnadurai, 2002; Schaeper et al., 1998; Vo et al., 2001). Regulation of Ctbp is also reported by the serine/threonine kinase HIPK2, which upon UV triggering participates in a pathway leading to ubiquitination of Ctbp and subsequently to proteasomal degradation (Zhang et al., 2005). Zscan4c might help to recruit these repressive complexes to target sites, to alter specific gene transcription. Because of the change of protein functions due to dependency on NADH and phosphorylation levels, multiple effects could arise from the specific cellular microenvironment.

The potential Zscan4c interactor HINT1 also reveals interesting properties matching some characteristics of the other identified binding partners. Homodimer formation of HINT1 protein was reported (Lima et al., 1996) and functioning in protein complexes postulated (Korsisaari and Makela, 2000; Wang et al., 2007b). HINT1 participates in ionizing radiation-induced DNA damage responses not by affecting the formation of γ-H2AX foci, but rather impairing their removal (Li et al., 2008a). It acts as a tumour suppressor, at least in part by enhancing the DNA damage response through regulating functions of γ-H2AX and ATM (Li et al., 2008a). HINT1 deficient cells exhibit prolonged γ-H2AX foci and impaired acetylation of γ-H2AX. Furthermore, MEFs deficient in HINT1 display a decrease in genomic stability accompanied by a high number of various types of chromosomal abnormalities (Li et al., 2008a). Interestingly, Zscan4c over-expression was shown to be indispensable for long-term genomic stability in mES cells (Zalzman et al., 2010). Furthermore, Zscan4 was reported to be transiently upregulated through retinoids, oxidative stress and DNA-damaging agents (Ko and Zalzman, 2011). More important, Zscan4 over-

expression can enhance survival of cells which were exposed to DNA-damaging agents like mitomycin C (MMC) and cisplatin (Ko and Zalzman, 2011).

The identified 40S ribosomal protein S7 is a subunit of the ribosome (Wool et al., 1995) and, therefore, it might be an indication that protein complexes were associated with the ribosomes, possibly an indication for active translation. The association was not further investigated by immunoprecipitations to date and in comparison with the other identified binding partners it appears less compelling in regards of unravelling the molecular mechanisms of Zscan4c action.

Zscan4 is a fascinating novel gene family with potentially a number of functions, guarding genomic stability, regulating telomere length, and protecting ES cell identity (Ko and Zalzman, 2011; Storm et al., 2009; Zalzman et al., 2010). Interestingly, the majority of potential Zscan4c interacting proteins identified are associated with functions related to transcriptional regulation and DNA damage response, all characteristics linked with Zscan4. It is not unlikely that interacting proteins like LSD1, Ctbp, and HINT1 are actively involved in enabling the full functionality of Zscan4. With this knowledge it should be now possible to address the precise working mechanisms of Zscan4.

Chapter 5: Artificial activation of Class I_A PI3K catalytic subunits in mESCs

5.1 Introduction

In embryonic stem cells, PI3K-dependent signalling has been reported to regulate cell proliferation (Hallmann et al., 2003; Jirmanova et al., 2002; Sun et al., 1999; Takahashi et al., 2003) and furthermore PI3Ks are also required for optimal self-renewal of mES cells (Niwa et al., 2009; Paling et al., 2004; Pritsker et al., 2006; Watanabe et al., 2006) In addition, expression of the well-known core pluripotency regulator Nanog and several Nanog target genes, are regulated in a PI3K-dependent manner (Storm et al., 2007). In the microarray screen introduced earlier (Chapter 3) novel regulators of mES cell self-renewal were identified downstream of PI3K signalling (Storm et al. 2009). Zscan4 was among the novel regulators and a predominant regulation via the p110α isoform was proposed. How specific PI3K isoforms couple to distinct functional responses in mES cells is of interest and was addressed in a recent study by applying a loss-of-function approach (Kingham and Welham, 2009). The p110α catalytic isoform was suggested to be mainly important for proliferation, whereas the p110β isoform appeared to exhibit some contribution to ES cell self-renewal (Kingham and Welham, 2009).

The aim of this chapter was to further investigate the function of specific PI3K isoforms in ES cells by an artificial genetic activation approach. It was of interest to determine whether constitutively activated PI3K isoforms were able to relieve the requirement of mouse ESCs for LIF.

5.2 Generation of ES cells expressing activated PI3K isoforms

Artificial activation of specific Class I_A PI3K isoforms was achieved through over-expression of myristoylated versions of the different catalytic subunit isoforms. N-myristoylation is a process catalysed by the enzyme N-myristoyl transferase (NMT), which covalently attaches myristate, a 14-carbon saturated fatty acid, to the N-terminal glycine of proteins after removal of the initial methionine residue (Figure 5.1 A) (Lindwasser and Resh, 2002). In general, N-myristoylation occurs co-translationally and is irreversible, promoting weak and reversible protein-membrane and protein-protein interactions (Murray et al., 1997; Peitzsch and McLaughlin, 1993; Towler et al., 1987; Wolven et al., 1997). Myristoylation often plays a role in signal transduction cascades by localising proteins to the intracellular membrane, triggering the activation of signalling events, and it was therefore hoped to activate the PI3K pathway, similar to work that was done with myr-Akt in mESCs (Watanabe et al., 2006).

N-myristoyl transferase requires an N-terminal recognition peptide sequence, MGSSKSKPK-, which was fused to p110α, β and δ PI3K catalytic isoform coding sequences in the pPBCAGcHAIN piggyBac vector (Figure 5.1 B). The piggyBac system is host-factor independent and only requires inverted terminal repeats at both ends of the transgene and the transient expression of the transposase enzyme, which catalyses the insertion/excision (Fraser et al., 1996). The piggyBac helper plasmid, pCAG-PBase, encoding for the transposase enzyme, was co-transfected with the piggBac vector containing the myristoylated p110 isoforms into EB5 or OCRG9 mESCs. Transcription of the myr-p110 transgenes was driven by the CAG promoter, which achieves high expression levels in eukaryotic cells (Niwa et al., 1991). Stable clonal transgenic cell lines (pPBCAG-myr-p110x) were established by selecting for G418 resistance.

Furthermore, C-terminal eGFP fusion proteins for all three myristoylated isoforms were established, to verify correct membrane localisation initiated by the myristoylation mechanism (Figure 5.2). A confocal image of an ES cell colony expressing membrane-localised myr-p110α-eGFP is shown in Figure 5.2 A, confirming function of myristoylation sequence. Correct expression of fusion proteins was determined by immunoblotting (Figure 5.2 B).

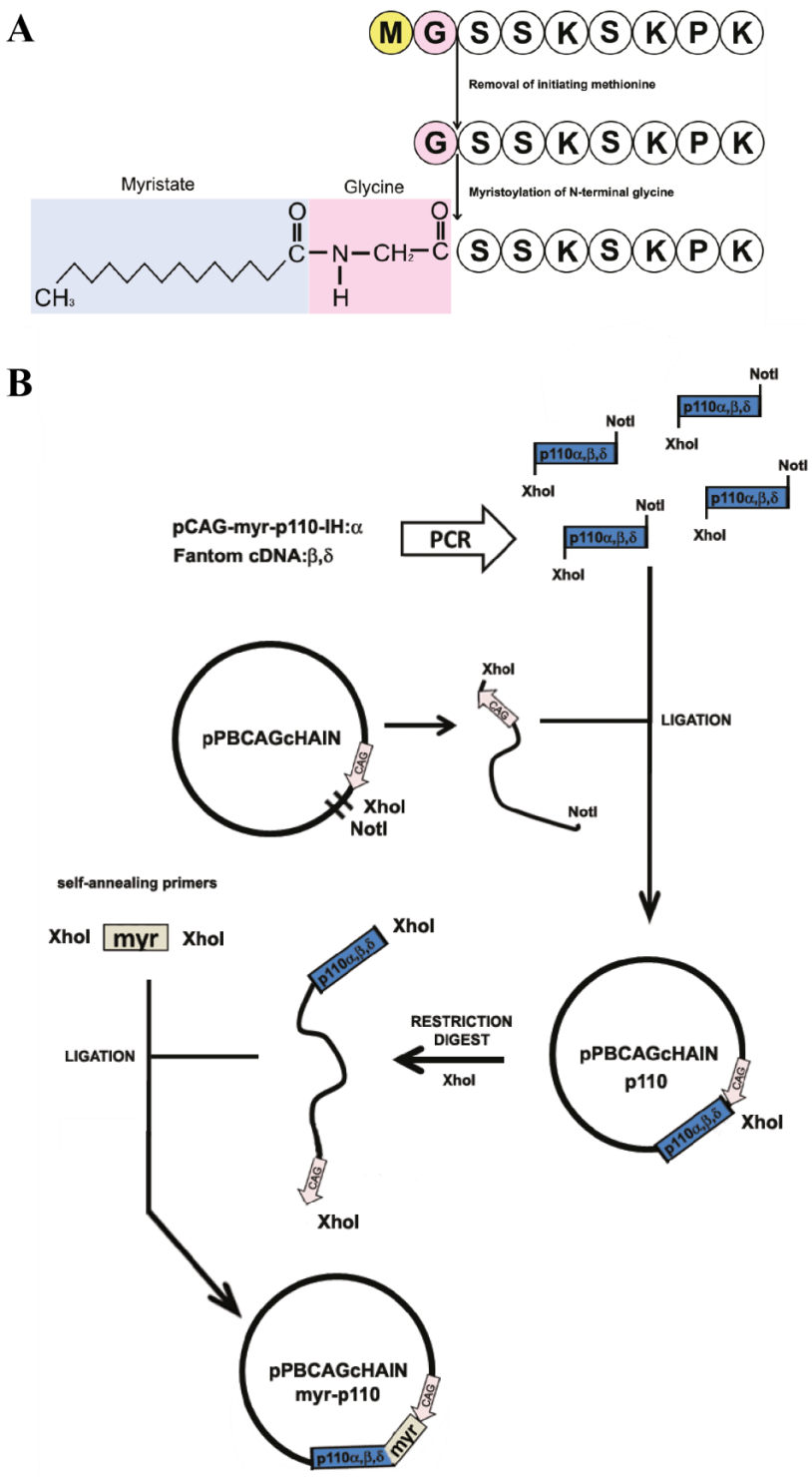

Figure 5.1 Mechanism of myristoylation and generation of myristoylated p110 piggyBac constructs. (A) Myristoyl group is covalently attached to the N-terminal glycine by the enzyme N-myristoyltransferase. (B) Schematic showing how myr tagged p110 isoforms were generated. P110β,δ were PCR amplified from RIKEN Fantom (Functional Annotation Of Mouse) cDNA clones F630002D04 and F83017C10. Fragments were ligated first into piggyBac vector pPBCAGcHAIN to add a myr tag encoding sequence in frame with the p110 coding sequences. P110α was subcloned from pCAG-myr-p110-IH vector into pPBCAGcHAIN.

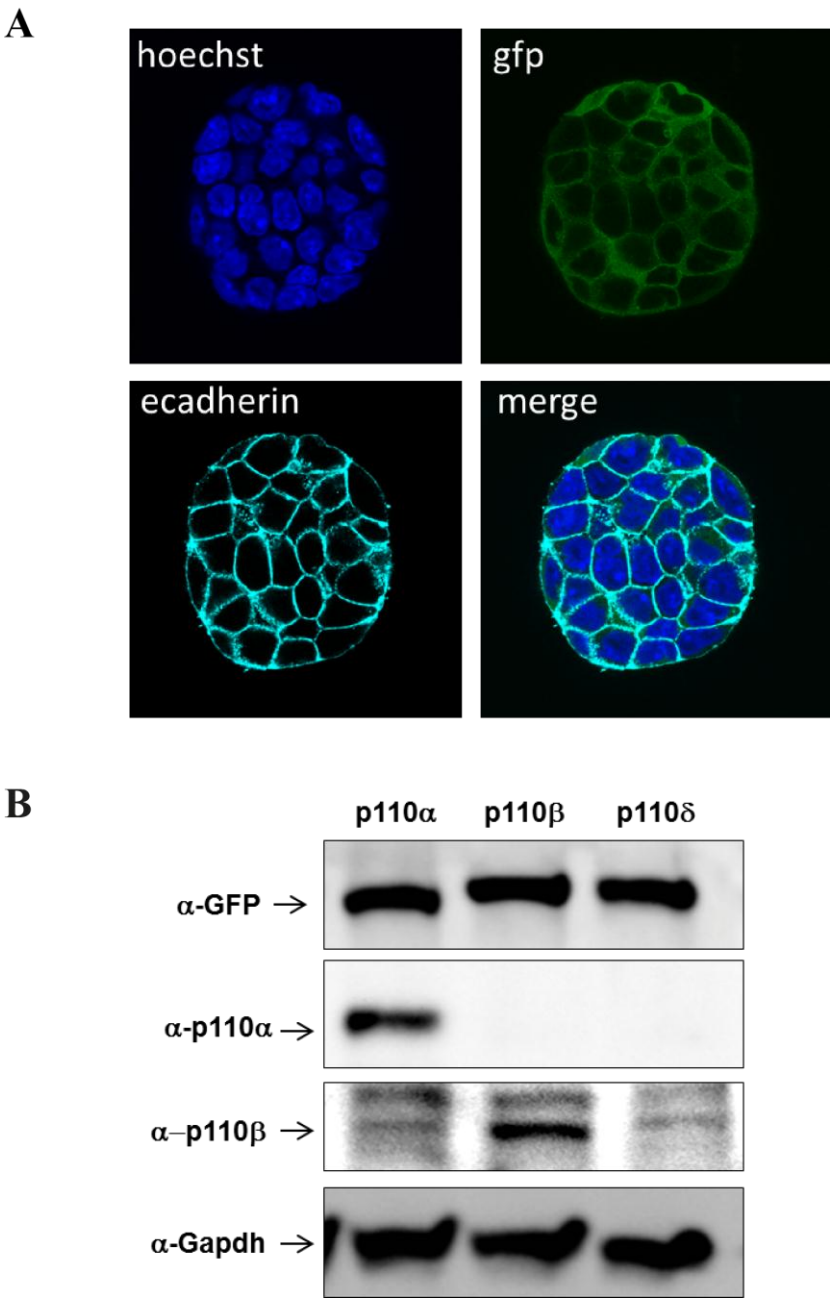

Figure 5.2 Membrane localisation of myr-p110-eGFP fusion proteins. (A) Confocal microscopic images showing myr-p110-eGFP fusion proteins and E-cadherin detected by Alexa 594. Stable cell lines were established by lipofection of myr-p110-eGFP piggyBac with the PCAGPBase helper plasmid into EB5 ES cells, and subsequent selection with G418. Cell nuclei were stained with Hoechst (blue), and E-cadherin antibody staining is shown in turquoise. Original magnification, x63. **(B)** Whole cell lysates were resolved by SDS-PAGE and immunoblotting carried out using the antibodies indicated to detect full length fusion proteins and specific p110 isoforms. The p110δ isoform was not checked by immunoblotting due to the unavailability of an antibody. Gapdh antibody was used to confirm equal loading.

5.3 Screening for LIF-independent clones

Activation of Akt signalling was previously reported to be sufficient to maintain pluripotency in mouse and primate embryonic stem cells (Watanabe et al., 2006). With activation of PI3Ks being upstream of Akt, an artificial activation of PI3Ks might potentially be enough for attaining LIF independency. To test this hypothesis, OCRG9 mES cells were transfected with the constructed piggyBac transposon vectors, resulting in transgenic cell lines over-expressing myristoylated class I_A catalytic isoforms and therefore predicted to exhibit activated PI3K-dependent signalling. OCRG9 mES cells, rather than EB5 mES cells, were chosen because selection with puromycin for Oct4 is stronger and therefore quicker than selection with blasticidin. After transfection ES cells were selected in absence of LIF but in the presence of G418 for transgene expression. Furthermore, OCRG9 cells were grown in presence of puromycin, which selects the population for Oct4 positive, self-renewing ES cells. Thus, differentiating cells, which would be expected in a culture environment without LIF, are eliminated and surviving clones will express both myr-p110 isoforms and Oct4.

Indeed, some LIF independent colonies emerged when the myr-p110α isoform was over-expressed in the OCRG9 mES cells cultured under the mentioned selection conditions. It was possible to expand these myr-p110α expressing colonies in the absence of LIF but in the presence of antibiotics, resulting in a stable clonal population. For the other p110 isoforms the results were not as clear-cut and emerging colonies did not proliferate as well and also had a more differentiated phenotype. More experiments are needed to further assess their potential to maintain ES cell self-renewal in absence of LIF. It should be noted that even myr-p110α clones did have a less stable phenotype with a more flattened morphology when grown in absence of LIF, but it was possible to maintain them in culture for more than 1 month in presence of puromycin. They still remained responsive to LIF, even after LIF starvation for one month, leading to ES cell colonies with a highly self-renewing phenotype of very tight, round and domed colonies.

To rule out that LIF independency might have arisen from potential culture artefacts because of high density culturing, LIF independent myr-p110α clones were plated at a clonal density of 10^4 cells per 10cm cell culture dish in the absence and presence of LIF (Figure 5.3). Parental OCRG9 ES cells were used as a control and puromycin

was added to cultures to select for Oct4 positive cells. Myr-p110α expressing cell lines formed colonies in the presence and absence of LIF, whereas parental OCRG9 cells only gave rise to healthy colonies in the presence of LIF. When transgenic cells were cultured in the presence of LIF a higher number of colonies formed than in absence of LIF, this might be caused by fluctuating expression of the transgene, or by the pleiotropic effect of the PI3K, leading to differentiation of a certain proportion of the population due to a sub-optimal intracellular environment.

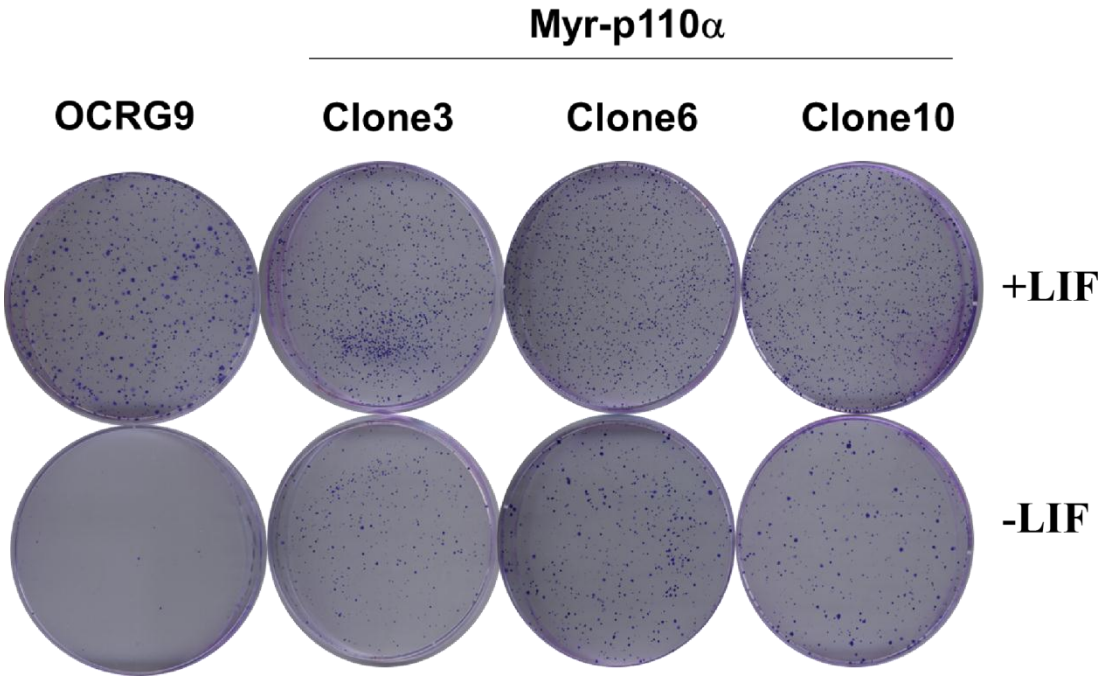

Figure 5.3 Myr-p110α supports LIF-independent self-renewal of mouse ES cells. Rex1-GFP/Oct3/4-CFP double knock-in ES cells (OCRG9) were transfected with pPBCAGcHAIN-CAG-myr-p110α and the PCAGPBase helper plasmid and clones were obtained after selected with G418 (selection for pPBCAGcHAIN) and Puromycin (selection for Oct3/4+ cells) in absence of LIF. Clones were expanded in presence of antibiotics and 10^4 cells were plated per 10cm dish +/- LIF for 7 days. Images show ESC colonies stained with Leishman stain (blue).

Autocrine signalling can contribute to ES cell self-renewal (Guo et al., 2006; Singla et al., 2008; Welham et al., 2007) and, therefore, it was important to rule out that autocrine factors might have stimulated the LIF pathway, maintaining self-renewing colonies. An inhibitor to block Janus-associated tyrosine kinases (Jak), downstream of the LIF signalling pathway, was applied to investigate complete LIF independency of myr-p110α clones. When the Jak pathway is blocked even autocrine factors are no longer able to activate the LIF signalling pathway, because the signal cannot be integrated into the core circuitry (Niwa et al., 2009). Cells were plated at $1x10^3$ cells per well of a 6-well cell culture tray and cultured for five days with the addition of a Jak pathway inhibitor (jaki) (Jak inhibitor I (Calbiochem)) at a concentration of 5, 2, 1, 0.5 and 0.1μM. Cultures contained puromycin and parental OCRG9 ES cells were used as controls. On day five, colonies were stained with Leishman's stain, to assess colony formation and morphology.

All established myr-p110α over-expressing clones formed tight round colonies when the Jak pathway was inhibited, indicating their complete relief from LIF-dependent signalling (Figure 5.4B). In contrast, the OCRG9 parental control cells only formed healthy colonies in the absence of Jak pathway inhibition, and colonies with a flattened partly differentiated appearance were observed at a low concentration (0.1μM) of Jak inhibitor (Figure 5.4A). At Jak inhibitor concentrations of between 5μM – 0.5 μM no colonies formed, because of the applied puromycin selection for Oct4 positive cells. These data suggests that myr-p110α over-expression can lead to complete LIF independency of ES cells.

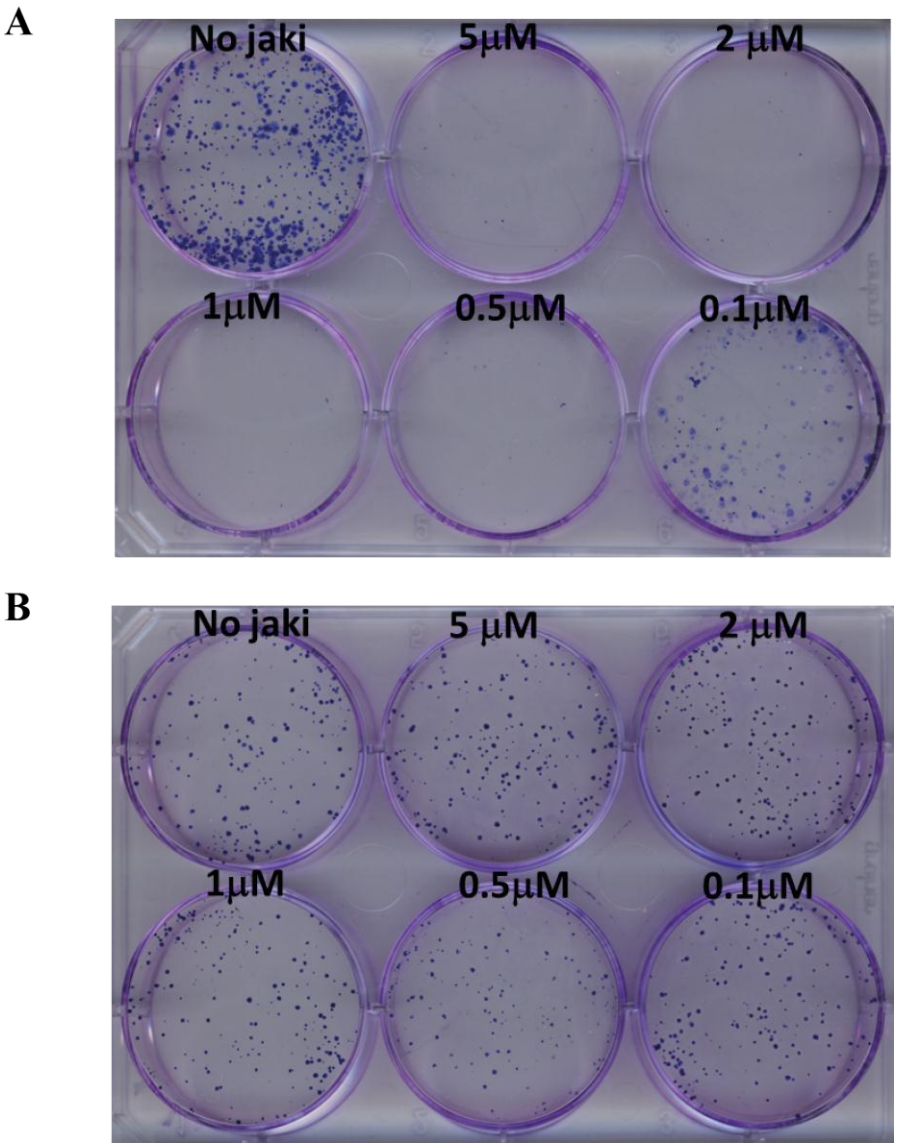

Figure 5.4 Myr-p110α transgenic ES cells were resistant to treatment with a Jak inhibitor. **(A)** OCRG9 parental cell line and **(B)** myr-p110α LIF-independent clones were grown in the presence of Jak inhibitor I (Calbiochem) at the indicated concentrations. Cells were plated at a density of 10^3 cells/well in 6-well cell culture trays and cultured for five days in the presence of puromycin. OCRG9 cells were cultured in the presence of LIF, whereas myr-p110α clones were grown without LIF. Images show Leishman stained colonies.

5.4 Characterisation of LIF-independent clones

Three LIF-independent myr-p110α clones, clone 3, 6, and 10, were further characterised for the expression of pluripotency associated genes. Rex1 is a well-known marker for pluripotency in mES cells and the OCRG9 cell line used in this study expresses an eGFP under the control of the Rex1 promoter (Toyooka et al., 2008). This makes it possible to use eGFP fluorescence as a read-out for Rex1 expression. EGFP expression was detected by flow cytometry (Figure 5.5A) and fluorescent microscopy (Figure 5.5B).

In comparison to control OCRG9 ES cells, relatively homogeneous expression levels of eGFP/Rex1 were observed by flow cytometry analyses in the established myr-p110α clones, when cultured in presence of LIF (Figure 5.5A). Furthermore, myr-p110α clones were grown in presence and absence of LIF for five days, and subsequently assessed for eGFP/Rex1 expression by fluorescent microscopy (Figure 5.5 A). OCRG9 cells were previously reported to lose GFP fluorescence within 2-3 days when cells were cultured in medium without LIF (Toyooka et al., 2008). Interestingly, eGFP/Rex1 expression was maintained, even upon LIF withdrawal, backing up the finding of their ability to self-renew in the absence of LIF.

Expression of the well established pluripotency marker Nanog, which has a functional role in maintaing self-renewal (Chambers et al., 2003; Mitsui et al., 2003), was also investigated. Nanog is heterogeneously expressed in the inner cell mass of E3.5 preimplantation blastocysts and also in embryonic stem cells (Chazaud et al., 2006; Singh et al., 2007). Surprisingly, myr-p110α over-expressing clones appeared to express Nanog homogenously in the presence of LIF, as assessed with immunocytochemistry (Figure 5.6). Some differences in Nanog expresseion were observed between the analysed clones. Clone3 (Figure 5.6A) and clone10 (not shown), exhibited a heterogenous expression of Nanog in absence of LIF, whereas clone 6 also expressed Nanog at high levels in the absence of LIF (Figure 5.6B). It is unclear at the moment why there is a difference in Nanog expression between the clones, one possible reason might be the integration site of the transgene. This highlights the importance of analysing multiple clones to reduce the risk of characterising artefacts as a result of the genetic engineering process.

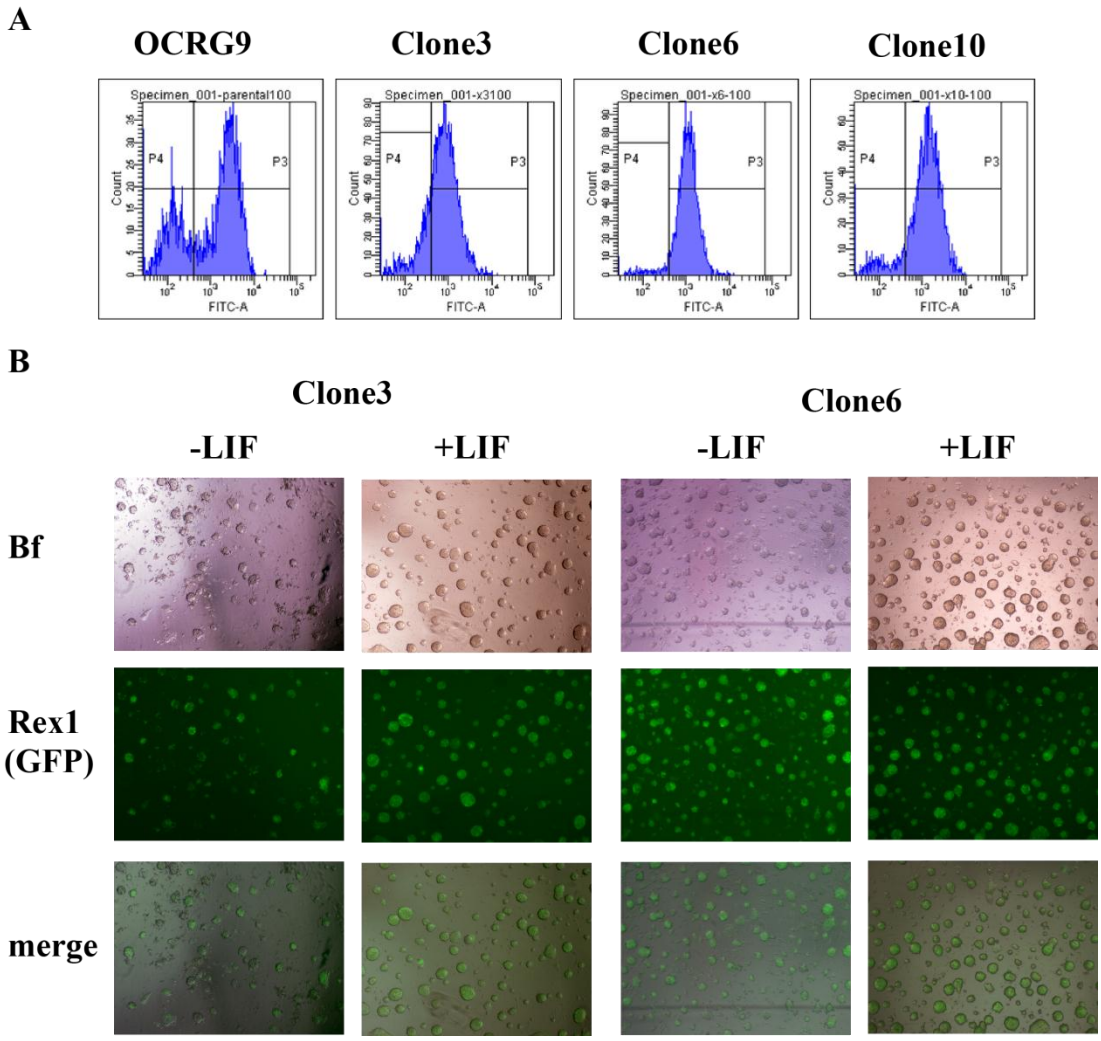

Figure 5.5 Observation of myr-p110α-OCRG9 clones by flow cytometry and microscopy. (A) Result of analysis of control OCRG9 mES cells and myr-p110α-OCRG9 clones by flow cytometry. Cells were cultured in the presence of serum and LIF and GFP-Rex1 was detected (FITC on x-axes). **(B)** Morphology and fluorescence of myr-p110α-OCRG9 colonies under puromycin selection (selection for cells expressing Oct3/4) after day 5 of culture in the presence of serum +/- LIF. Bf (bright field) and Rex1-GFP fluorescence was detected by fluorescent microscopy with low magnification.

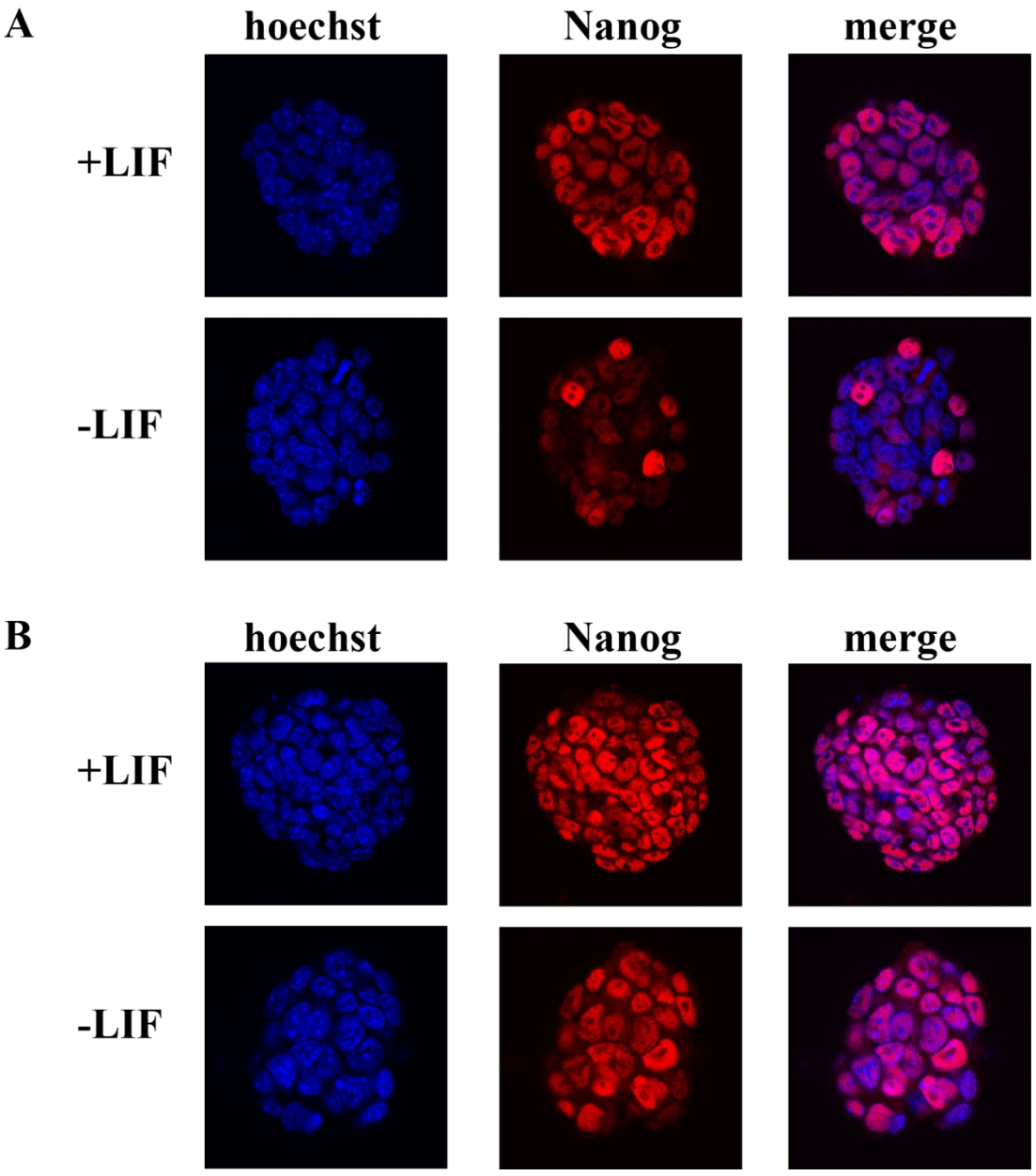

Figure 5.6 Confocal microscopic images of immunostained myr-p110α-OCRG9 ES cells. Cells were cultured in serum, +/- LIF and immunostained for Nanog. Images show untypical homogenous Nanog protein expression in the presence of LIF. Nanog was detected by Alexa 594 and nuclei were stained by hoechst. **(A)** Shows confocal images of clone 3, and **(B)** images of clone 6. Original magnification, x63.

To gain further insights into the molecular mechanisms that might be involved in establishing LIF independency in myr-p110α over-expressing clones, levels of known pluripotency regulators were assessed. Relative expression levels of the pluripotency associated genes, Tbx-3, Nanog, Klf4, Zscan4 and Oct4, were assessed by quantitative RT-PCR in myr-p110α clones. LIF independent myr-p110α clones (clone 3, 6, and 10) were plated in multi-well cell culture trays in the absence or with the addition of LIF for 4 days, before RNA was harvested. Quantitative RT-PCR revealed that all pluripotency marker genes assessed in the three selected clones were elevated in the absence of LIF in comparison to parental control OCRG9 cells grown without LIF for four days (Figure 5.7). This indicates their enhanced self-renewal ability, as a result of transgene over-expression. Interestingly, Tbx-3 and Oct4 expression levels were also elevated in the presence of LIF, when compared to control cells grown with LIF, highlighting a beneficial effect of myr-p110α over-expression also under standard culture conditions (Figure 5.7A & D). Furthermore, clones 6 and 10 also showed elevated Nanog and Klf4 levels compared to control, whereas with clone 3 expression reached the same levels as measured in control cells (Figure 5.7B &C). The higher responsiveness of Tbx-3 expression to PI3K activation by myr-p110α over-expression, in contrast to Nanog, might reflect the hierarchy in the functions of these transcription factors. Tbx3 was postulated to be upstream, whereas Nanog is placed downstream of Tbx3, supporting activation of Oct4 expression required for proper self-renewal (Niwa et al., 2009). As described earlier, Zscan4 levels were also strongly upregulated in myr-p110α clones, both in the presence and absence of LIF (Chapter 3, Figure 3.12), which might be another contributing factor to the self-renewing phenotype observed. Taking these data together, ES cell clones with activated PI3K signalling appear to have a clear self-renewal advantage over control ES cells, which was supported by this evidence of pluripotency gene expression at the transcriptional level.

Immunoblotting was used to examine protein expression of Nanog and p110α in myr-p110α clones 3, 6, and 10, grown for three days with or without LIF. In accordance with the immunocytochemistry results, Nanog protein levels are high in the presence of LIF in all of the clones analysed (Figure 5.8). In addition, Nanog

protein levels in the absence of LIF were also higher compared to levels seen in control ESCs. Consistent with the cytochemistry observations, clone 6 also showed a higher expression of Nanog in absence of LIF, in comparison to clone 3 and 10 (Figure 5.8).

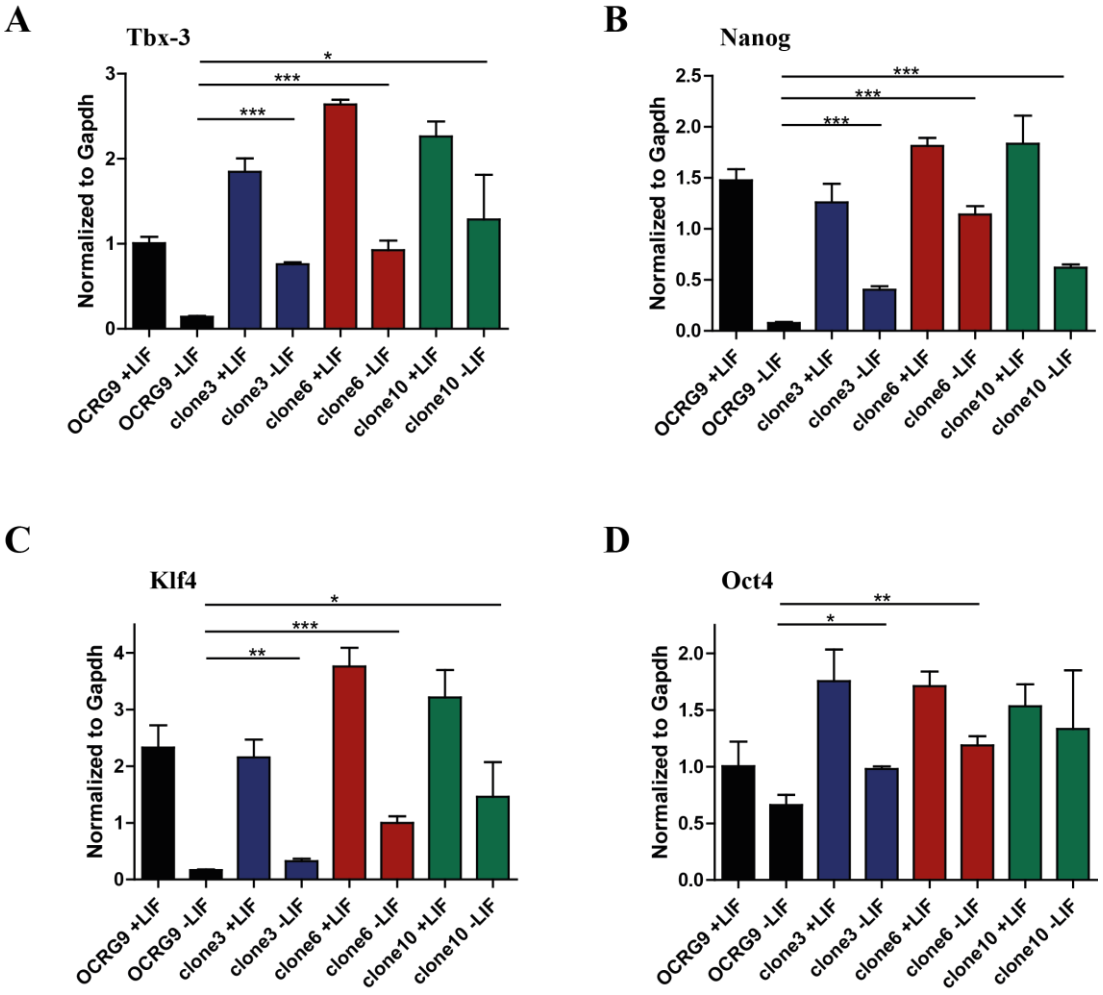

Figure 5.7 Expression of pluripotency-associated transcription factors in LIF-independent ES cell lines. Transgenic myr-p110α ES cell clones (3, 6, 10) were cultured in absence of LIF and reintroduced to LIF for 4 days. Quantitative RT–PCR analysis were performed to assess the expression levels of (A) Tbx-3, (B) Nanog, (C) Klf4, and (D) Oct4. The expression levels in parental OCRG9 ES cells cultured +/- LIF for 4 days are also shown. Error bars indicate standard deviation of three independent experiments run in triplicate and expression was normalised relative to Gapdh. *, p<.05; **, p<.005, p<.0005, in a Student's t test.

Furthermore, Akt phosphorylation (S473) was assessed, as PI3K activation is known to activate Akt through phosphorylation (reviewed in (Dreesen and Brivanlou, 2007)), which in return can lead to LIF-independent self-renewal (Watanabe et al., 2006). All the clones tested show a higher level of Akt phosphorylation in the presence of LIF in comparison to parental control cells (Figure 5.8). Surprisingly, Akt phosphorylation was also increased in parental control cells when LIF was absent, suggesting that some of the randomly differentiated cells that arise following LIF withdrawal exhibited elevated p-Akt levels. A similar trend in Akt phosphorylation upon differentation of ES cells was also observed earlier by our group (Kingham and Welham, 2009).

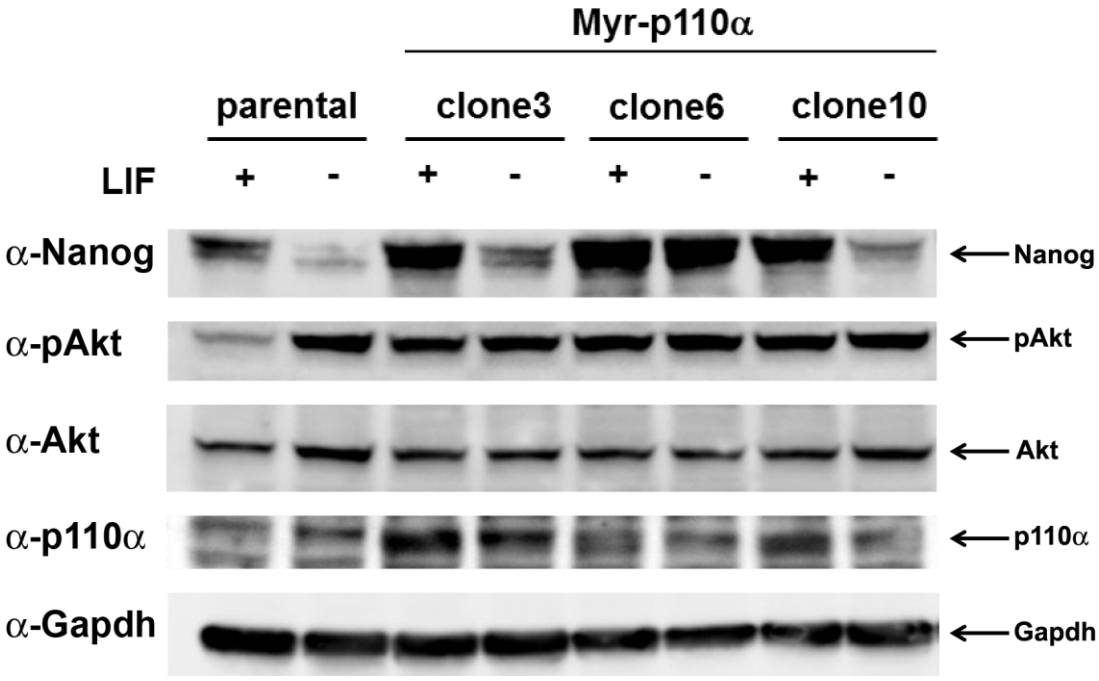

Figure 5.8 Western blot analyses of myr-p110α ES cell clones. Transgenic cells were cultured in GMEM plus serum minus LIF and reintroduced with LIF for three days. Parental cells were grown in presence of LIF and were LIF starved for three days prior of harvesting whole lysates. Immunoblotting was used to detect Nanog, p110α, and phosphorylated Akt (S473) (pAkt) protein. Immunoblots were stripped and reprobed with appropriate antibodies detecting Akt and with antibodies detecting Gapdh to confirm equal loading. The data shown are representative of two independent experiments.

5.5 Model for mechanism of LIF independency

ES cells can be propagated when Erk and GSK-3 signalling are simultaneously inhibited by pharmacological agents (Ying et al., 2008), with further beneficial effects on clonogenicity observed upon the addition of LIF (Wray et al., 2010). These culture conditions are considered optimal for mES cell self-renewal, leading to the proposed 'ground state', a basal proliferative state, without epigenetic barriers and only minimal needs for extrinsic stimulation (Wray et al., 2010). Activation of the PI3K pathway by over-expression of a myristoylated p110α catalytic isoform was shown to liberate murine ES cells from LIF dependency, but addition of LIF did increase homogeneity of Nanog in the clonal populations and furthermore clonogenicity was increased in presence of LIF. This liberation might be linked to the proposed 'ground state' by dual inhibition of Erk and GSK-3 signalling.

Zscan4c was one of 50 transcription factors that were over-expressed in ES cells to further explore the functioning of these biologically important networks (Nishiyama et al., 2009). Upon induced over-expression of Zscan4c, DNA microarray analysis was performed to assess changes in the global transcriptome (Nishiyama et al., 2009). Of more than 25000 assessed microarray probsets, Pramel7 was the most upregulated gene after induction of Zscan4c expression for 48 hours. Figure 5.9 shows the 50 most upregulated genes after over-expression of Zscan4c. Interestingly, Pramel7 was recently reported to mediate LIF/STAT3-dependent self-renewal in murine ES cells (Casanova et al., 2011). This group reported that over-expression of Pramel7 is sufficient to relief ES cells from LIF dependence and to promote self-renewal when grown on LIF-knockout feeders. Under feeder- and serum-free conditions, self-renewal was impaired, but GSK-3 inhibition could restore self-renewal. Pramel7 over-expression promoted Erk dephosphorylation and this was proposed to prevent ES cells from differentiation (Casanova et al., 2011).

Over-expression of myr-p110α was also reported to result in phosphorylation of GSK-3, leading to inhibition of GSK-3 activity (Popkie et al., 2010). This dual function of activated p110α could, therefore, lead to the '2i ground state', and this could be an explanation for the LIF-independent self-renewal ability of the myr-p110α over-expressing clones (Figure 5.10).

	Zscan4c	geneSymbol	description	chr.
1	1.1449	Pramel7	preferentially expressed antigen in melanoma like 7	2
2	1.1083	Cyp2c70	cytochrome P450, family 2, subfamily c, polypeptide 70	19
3	0.9965	Pramel6	preferentially expressed antigen in melanoma like 6	2
4	0.9811	Grid2	glutamate receptor, ionotropic, delta 2	6
5	0.9176	Frk	fyn-related kinase	10
6	0.8527	Sept4	septin 4	11
7	0.811	1700013H16Rik	RIKEN cDNA 1700013H16 gene	X
8	0.7797	Btn1a1	butyrophilin, subfamily 1, member A1	13
9	0.7641	Flvcr2	feline leukemia virus subgroup C cellular receptor family, member 2	12
10	0.7571	Casp12	caspase 12	9
11	0.7562	Rgn	regucalcin	X
12	0.7511	Hmx2	H6 homeobox 2	7
13	0.7497	Pdzrn4	PDZ domain containing RING finger 4	15
14	0.7371	Agpat9	1-acylglycerol-3-phosphate O-acyltransferase 9	5
15	0.7261	1700003M02Rik	1700003M02Rik RIKEN cDNA 1700003M02 gene	4
16	0.7224	3830417A13Rik	3830417A13Rik RIKEN cDNA 3830417A13 gene	X
17	0.7129	Efemp1	epidermal growth factor-containing fibulin-like extracellular matrix protein 1	11
18	0.7102	Cxcl10	chemokine (C-X-C motif) ligand 10	5
19	0.7101	Gata3	GATA binding protein 3	2
20	0.7024	Ccrl1	chemokine (C-C motif) receptor-like 1	9
21	0.6926	Isg15	ISG15 ubiquitin-like modifier	4
22	0.6854	Plagl1	pleiomorphic adenoma gene-like 1	10
23	0.6812	4933402E13Rik	4933402E13Rik RIKEN cDNA 4933402E13 gene	X
24	0.6696	Tshb	thyroid stimulating hormone, beta subunit	3
25	0.6618	Nlrp9b	NLR family, pyrin domain containing 9B	7
26	0.6607	Amot	angiomotin	X
27	0.6601	Sdk1	sidekick homolog 1	5
28	0.6493	Ifih1	interferon induced with helicase C domain 1	2
29	0.6472	Clca3	chloride channel calcium activated 3	3
30	0.6458	Calcoco2	calcium binding and coiled-coil domain 2	11
31	0.6453	Wnt8a	wingless-related MMTV integration site 8A	18
32	0.6433	Cdx2	caudal type homeobox 2	5
33	0.6419	Grip2	glutamate receptor interacting protein 2	6
34	0.6315	Btn2a2	butyrophilin, subfamily 2, member A2	13
35	0.6278	Dkk1	dickkopf homolog 1	3
36	0.6237	1700019B21Rik	RIKEN cDNA 1700019B21 gene	X
37	0.6202	Pof1b	premature ovarian failure 1B	X
38	0.6194	Kctd12b	potassium channel tetramerisation domain containing 12b	X
39	0.619	C030003D03Rik	Tmem200a transmembrane protein 200A	10
40	0.6153	Obox6	oocyte specific homeobox 6	7
41	0.6133	Rnf212	ring finger protein 212	5
42	0.6122	9430073N08Rik	Fam162b family with sequence similarity 162, member B	10
43	0.6108	Cpeb1	cytoplasmic polyadenylation element binding protein 1	7
44	0.608	Trim30	tripartite motif-containing 30A	7
45	0.606	Heph	hephaestin	X
46	0.6036	Esx1	extraembryonic, spermatogenesis, homeobox 1	X
47	0.6019	Msx1	homeobox, msh-like 1	13
48	0.5942	Zfp677	Zfp677 zinc finger protein 677	13
49	0.5924	Nkx2-2	NK2 transcription factor related, locus 2	2
50	0.5903	Naip5	NLR family, apoptosis inhibitory protein 5	13

Figure 5.9 Top 50 upregulated genes upon overexpression of Zscan4c in mES cells. Chart shows the 50 most upregulated genes after 48h of doxycycline induced overexpression of Zscan4c (Nishiyama et al., 2009).

Whether myr-p110α exhibits this proposed dual function by two separate pathways, or solely through Akt activation, which in turn stimulates GSK-3 inhibition and Zscan4c/Pramel7 activation is not clear to date. The latter could be possible, as activated Akt alone is also able to liberate ES cell's requirement for LIF (Watanabe et al., 2006).

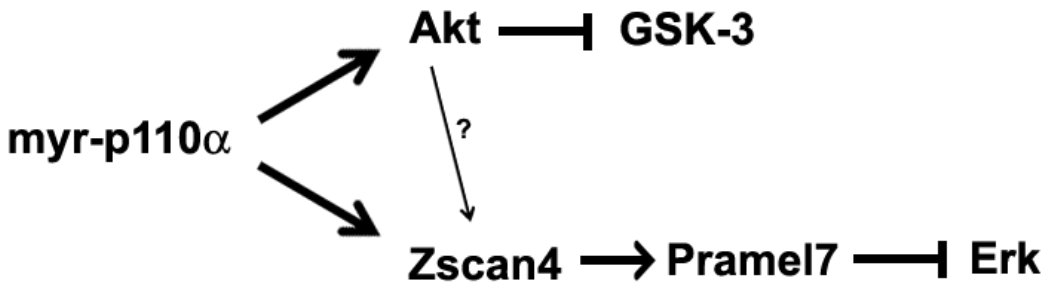

Figure 5.10 Model of activated p110α function on ES cell self-renewal. Activation of p110α is proposed to act positively on ES cell pluripotency through at least two independent mechanisms. Firstly, by activation of Akt leading to inhibition of GSK-3 and secondly by upregulating expression of Zscan4, which consequently upregulates Pramel7, which inhibits Erk. Inhibition of both Gsk-3 and Erk is sufficient to maintain ES cells in the 'ground state' of pluripotency.

5.6 Discussion and Summary

This chapter described the artificial activation of class IA PI3K catalytic subunits by myristoylation and their function on mES cell self-renewal.

5.6.1 Summary

- An N-terminal recognition peptide sequence for N-myristoyl transferase was fused to Class I_A PI3Ks catalytic subunits p110α, β, and δ (myr-p110α, β, δ).

- Myr-p110α, β, and δ were overexpressed under the contol of the CAG promoter in murine ES cell lines using the piggyBac transposon/transposase expression system.

- eGFP was fused C-terminal of myr-p110 isoforms and correct membrane localisation was determined by confocal microscopy.

- LIF independent ES cell lines could be established by over-expression of myr-p110α in OCRG9 ES cells in absence of LIF and by selection for Oct4 positive cell with puromycin.

- Liberation of LIF was confirmed by growing transgenic cell lines in the presence of a Jak inhibitor.

- Rex1/GFP expression was determined in myr-p110α OCRG9 LIF independent clones by flow cytometry and fluorescent microscopy.

- Nanog expression in the myr-p110α OCRG9 LIF independent clones was assessed by immunocytochemistry, and found to be heterogeneous in the absence of LIF and more homogenously expressed in the presence of LIF.

- Quantitative RT-PCR analysis was used to determine expression levels of pluripotency associated genes, Tbx-3, Nanog, Klf4, Zscan4, and Oct4, in myr-p110α clone. Overall, expression levels in the absence of LIF were elevated compared to control OCRG9 control ES cells grown without LIF.

- Immunoblotting confirmed elevated expression levels for Nanog on the protein level.

- Activation of the Akt signalling pathway in myr-p110α stable cell lines was also determined by immunoblotting, demonstrating activation of the PI3K signalling pathway.

- A model for the mechanism of LIF liberation in myr-p110α over-expressing cell lines was proposed. Activation of PI3K signalling might lead to the '2i ground state' through inhibition of GSK-3 by activated Akt signalling and on the other hand by stimulating Zscan4/Pramel7 expression, resulting in a decrease in Erk phosphorylation.

5.6.2 Discussion

The PI3K pathway is an important signalling pathway involved in regulating a wide range of cellular functions. However, a detailed understanding of the precise function of different isoforms, in different cell types as well as the critical substrates, and spatial dynamics of the processes, are still to be unravelled (reviewed in (Cantrell, 2001)). In murine ES cells the class I_A PI3K family of lipid kinases have been previously implicated in regulating ESC self-renewal (Kingham and Welham, 2009; Paling et al., 2004; Storm et al., 2007). Downstream signalling from PI3Ks, affecting Akt and GSK-3 activity, have also reported to be important for maintaining undifferentiated mESCs (Bone et al., 2009; Niwa et al., 2009; Pritsker et al., 2006; Sato et al., 2004). In this chapter the hypothesis tested was whether specific class I_A PI3K subunits couple to self-renewal in ES cells. A genetic activation strategy was applied by fusing a myristoylation target sequence to the p110α, β, and δ isoforms, which promotes constitutive membrane attachment and activation (Klippel et al., 1996). The piggyBac transposon system was used for over-expressing these constructs in mES cells with a CAG promoter. Myristoylation approaches for the activation of signalling pathways were previously used successfully in ES cells, and for instance myr-Akt was found to be sufficient to liberate ES cells from the

requirement of LIF (Watanabe et al., 2006). Furthermore, over-expression of activated p110α was reported to be able to rescue impaired growth and tumorigenicity in Eras (a Ras-like gene) knockout ES cells (Takahashi et al., 2003). LIF independent clones were obtained when the activated p110α isoform was over-expressed in OCRG9 ES cells and clones were selected in the absence of LIF. Selection for transgene expression was performed with G418, while Oct4 negative cells were displaced by puromycin. It should be noted, however, that LIF independent clones were rare and further experiments are necessary to rule out that potential culture artefacts or compensatory mechanisms accounted for this phenomenon. An ideal approach would be a system in which the transgene can be excised again after LIF independency was established. The Cre-Lox recombination system would be one example that could be applied (Sauer, 1987); in this system floxed transgenes can be excised by transient expression of the Cre recombinase. If ES cell self-renewal is truly dependent on myr-p110α expression, differentiation should be induced upon its excision.

For the activated p110β and δ isoforms, self-renewal in the absence of LIF was not as clear -cut, but cannot currently be ruled out. More experiments are needed to investigate the precise effects of their overexpression in ESCs. Another alternative to activation by myristoylation would be the activation by introduction of activity enhancing mutations. For instance, in human p110α two point mutations, H1047R and E545K, are described to potently activate PI3K signalling and increase oncogenic properties (Zhao et al., 2005).

LIF independency of myr-p110α cell lines was further confirmed by addition of a Jak pathway inhibitor, which did not affect their ability to self-renew, in contrast to parental control cells. This indicates that artificial stimulation of only one of the two parallel LIF integration pathways was sufficient to drive ES cell self-renewal (Niwa et al., 2009). When myr-p110α cells were reintroduced to culture conditions including LIF, they were still responsive to the cytokine, resulting in beneficial effects on self-renewal as assessed by colony morphology and ES cell marker expression. Rex1 (GFP) and Nanog expression appeared to be more homogeneous compared to OCRG9 control ES cells, when investigated with flow cytometry and immunocytochemistry. The homogeneous expression of Nanog was lost in two out

of the three analysed clones upon LIF withdrawal, and was then comparable to Nanog expression under serum plus LIF culture conditions, where Nanog is known to be heterogeneously expressed (Chambers et al., 2007; Singh et al., 2007). In one clone (clone 6) Nanog remained to be highly expressed with a homogeneous distribution even in the absence of LIF.

At the transcriptional level, pluripotency marker genes Tbx-3, Nanog, Klf4, Zscan4 and Oct4 were elevated in myr-p110α over-expressing clones compared to parental control expression, showing that activation of p110α leads to a broad shift in the transcriptional profile towards a more self-renewing signature. It is not clear yet how PI3Ks integrate their signals that influence the proliferation, self-renewal and survival of ES cells. A potential cause for the changes observed at the transcriptional level, could be the activation of Akt by myr-p110α, which was determined by immunoblotting for phosphorylated Akt (S473), and previously reported to be sufficient for ES cell self-renewal (Watanabe et al., 2006). A common upstream regulator of Akt is PDK1, and, therefore, it is somewhat surprising that ES cells in which both copies of the PDK1 gene were disrupted, did not exhibit any reported defects in proliferation or self-renewal (Williams et al., 2000). However, disruption of PDK1 did only affect Akt phosphorylation at its T-loop residue (T308), whereas phosphorylation at its hydrophobic motif (S473) was unaffected (Williams et al., 2000). Over-expression of myr-p110α resulted in an increase in S473 phosphorylation of Akt in this and in other studies (Popkie et al., 2010; Takahashi et al., 2003). This suggests that PI3Ks might have alternative pathways for regulating the hydrophobic motif of Akt, or that the PI3K/PDK1 pathway might have a supportive, but dispensable, role in self-renewal (Burdon et al., 2002). Interestingly, PDK1 null ES cells were found to have upregulated Nanog expression, which was proposed to result from compensatory alterations during either their initial derivation and/or subsequent culture (Welham et al., 2007).

Immunoblotting revealed high levels of Nanog protein in myr-p110α clones in the presence of LIF and elevated levels of Nanog in the absence of LIF in comparison to parental control ES cells. Nanog protein levels in the presence of LIF appear to be higher in myr-p110α cell lines, than expected from quantitative RT-PCR data, when compared to control. The observed uncoupling of mRNA and protein levels for

Nanog might be due to the reported inhibition of GSK-3 by the activated p110α transgene (Popkie et al., 2010). Inhibition of GSK-3 was recently found in our laboratory to positively regulate Nanog translation (Yolanda Sanchez Ripoll and Melanie Welham, unpublished data).

In one clone (clone 6) Nanog expression remained at high levels even in the absence of LIF, which must result from a difference in transgene integration or other compensatory mechanisms triggered throughout the selection process. As the results of the other two analysed clones (clone 3 and clone 10) were comparable, it is more likely that these clones reflect the real effect of the transgene expression, but further experiments are necessary to address this issue.

A homogeneous ES cell population was postulated for cells cultured under 2i conditions, by addition of small-molecule inhibitors of MEK and GSK-3, leading to the stable ground state of pluripotency (Wray et al., 2010). It is likely that ES cells over-expressing myr-p110α are also in a more stable pluripotent state, but for this reason their differentiation ability could be impaired, as even in the absence of LIF a self-renewing phenotype is maintained. A teratoma formation assay could be used to establish whether myr-p110α clones are still able to generate teratomas containing derivatives of all three germ layers. Forced over-expression of Nanog for instance was also reported to lead to LIF independent self-renewal, and these transgenic cells were still able to generate teratoma (Chambers et al., 2003). In contrast, LIF independent ES cells resulting from ectopic expression of Pramel7 did avert teratoma formation, indicating the absolute requirement for Pramel7 silencing (Casanova et al., 2011). Furthermore, it would be of interest to test whether myr-p110α LIF independent clones are able to self-renew also in serum-free condition, or if additional serum stimulation is required for maintaining the phenotype.

Over-expression of Zscan4c was found in a microarray screen to strongly upregulate Pramel7 transcription (Nishiyama et al., 2009), and Pramel7 in turn can inhibit Erk activity by promoting Erk dephosphorylation (Casanova et al., 2011). Myr-p110α LIF independent clones exhibited drastic elevated levels of Zscan4, and, therefore, it is likely that Pramel7 levels may also be elevated. Together with the reported GSK-3 inhibition by activated p110α (Popkie et al., 2010) this is proposed to lead to the

stable ground state of pluripotency (Silva and Smith, 2008; Wray et al., 2010), and might be the explanation for observed LIF independency.

Chapter 6: General discussion and future directions

6.1 General discussion and future directions

Embryonic stem (ES) cells are of enormous interest as they hold great potential to be used in regenerative medicine to treat diseases for which no curative medical treatments are currently available. This potential lies in their unique abilities to self-renew, a symmetrical cell division generating identical daughter cells without losing pluripotency and the ability to differentiate into any kind of cell. Some core elements of the molecular network governing self-renewal have already been discovered, but it is still a long way to fully understand all the signalling and regulatory elements that control these unique and very complex processes. Furthermore, the link between proliferation and pluripotency is far from being understood, but it is necessary to completely understand the whole self-renewal process in order to harness the full potential of ES cells.

The contribution of PI3Ks is known to be important for keeping ES cells in a self-renewing state (Niwa et al., 2009; Paling et al., 2004). However, precisely where PI3K-dependent signalling is placed in the regulatory network of self-renewal is still emerging and not yet completely understood. The LIF signalling pathway was found to integrate signals via two parallel pathways to the core circuit, one of which is the PI3K pathway, stimulating important pluripotency regulators like Tbx-3 and Nanog (Niwa et al., 2009; Storm et al., 2007; Storm et al., 2009). Of particular importance is determining the functional contribution of genes regulated by PI3K-dependent signalling and how they are involved in controlling ES cell identity. The aim of this study was to identify genes downstream of PI3K involved in regulating mES cell self-renewal and to characterize their molecular mechanisms of action. Furthermore, signalling pathways and the influence of specific PI3K isoforms involved in regulating expression of our genes of interest were a focus of this study.

In a microarray screen performed prior to the start of this study by M. Storm and partners of the FunGenEs consortium (www.fungenes.org), identified 646 significant (ANOVA, $p<0.05$) probe set changes following inhibition of PI3Ks in mES cells. Subsequent hierarchical clustering of these 646 probe sets and final k-means clustering into $k=12$ groups helped to differentiate expression changes between the different conditions. Loss-of-function experiments were set up to characterize the role of selected candidate genes, identified by the microarray screen, in mES cell self-renewal. In a previous loss-of-function strategy similar to ours it was possible to

identify four genes with previously unrecognized roles in mES cell self-renewal (Ivanova et al., 2006).

In this study, Zscan4 was found to be a mediator of mES cell self-renewal, affecting stem cell fate when knocked-down by siRNA-based approaches. A significant change to a more differentiated phenotype upon transient Zscan4 knock-down was detected based on assessment of colony morphology, loss of alkaline phosphatase activity and expression of pluripotency marker genes. Zscan4 is a novel family of zinc finger proteins, of which Zscan4c is the predominantly transcribed member in mES cells (Falco et al., 2007). Recent Ensembl database comparisons revealed a change in the composition of the Zscan4 family members reported by Falco et al. (Falco et al., 2007). The most apparent changes were that the Zscan4b and e paralogous genes are now, with 505aa, almost full-length coding (506aa), and the previous pseudogene two (ps2) is now also reported to encode full-length protein of 506 amino acids. The earlier reported pseudogenes ps1 and ps3 could no longer be retrieved from the Ensembl database, but are still present in the NCBI database. As the Zscan4 family is a very novel gene family future changes might still occur with progression of our understanding. Structural prediction data suggests that Zscan4c contains a SCAN domain, which is a leucine-rich motif of approximately 60aa that often mediates protein-protein interaction (Edelstein and Collins, 2005; Falco et al., 2007). In addition, Zscan4c contains 4 zinc finger motifs (Falco et al. 2007), which are associated with DNA binding and control of transcriptional targets. Therefore, it is quite likely that Zscan4c might act as a transcription factor, a possibility that was further strengthened by the finding that over-expression of Zscan4c leads to approximately 500 significant up- and downregulated gene changes in ES cells (Nishiyama et al., 2009).

Zscan4 RNA and protein are both present in undifferentiated mES cells. When ES cells were induced to differentiate by the embryoid body formation assay or LIF withdrawal, Zscan4 expression was shown to drop rapidly. Interestingly, Zscan4 expression appeared to be as, or even more sensitive to, differentiation than Nanog expression, an early marker of differentiation when compared to, for instance, Oct4 (Brill et al., 2009). Many molecular changes are triggered by the differentiation of ES cells and some major disparities between ES cells and differentiated cells lie in the cell cycle. Cell cycle regulation is unique in ES cells and the molecular

mechanisms regulating proliferation are still largely undiscovered. Murine ES cells grow rapidly in culture in the presence of LIF, due to their short cell cycle (11-16h). A reduced duration of G1 phase is the main cause of this characteristic (Burdon et al., 2002). In contrast to somatic cells, which exhibit periodically peaking cyclin E-CDK2 activity at the G1 to S transition in cell cycle, mES cells have constitutive cyclin E-CDK2 activity. The constant E-CDK2 activity of self-renewing mES cells bypasses the restriction point and, therefore, omits the early G1 phase (White et al., 2005). Recent findings have linked Nanog regulation to the cell cycle dependent histone H3 lysine 27 (H3K27) methyltransferase Ezh2, opening up the possibility that cell cycle-dependent epigenetic mechanisms can influence ES cell self-renewal (Villasante et al., 2011). Although the precise mechanisms still remain largely unknown, posttranslational modification of chromatin regulators during the G2/M phase are critical for the control of cell fate during self-renewal and development, remaining under investigation for several decades (reviewed in (Budirahardja and Gonczy, 2009; Sharif et al., 2011)). With the described mosaic expression of Zscan4 and the precise control of its expression at the 2-cell stage of embryonic development, cell-cycle mechanisms could also contribute to regulation of Zscan4 (Falco et al., 2007; Zalzman et al., 2010). Furthermore, when transiently knocked-down at the 2-cell stage, transition to the 4-cell stage was delayed for approximately 24 hours (Falco et al., 2007). Strikingly, blastocyst development was also impaired, suggesting a more complex action of Zscan4.

In a recent report, retinoids were found to transiently upregulate Zscan4 expression, with a peak at 48 hours after addition (Ko and Zalzman, 2011). Four different retinoids were tested, all-trans retinoic acid (atRA), 9-cis RA, 13-cis RA, and Vitamin A. Zscan4 positive cells peaked for all for retinoids at 48 hours, and a secondary increase was observed only for 13-cis RA, and Vitamin A within seven days, with Vitamin A resulting in the largest Zscan4 increase. It was proposed that this might partially relate to effects of these retinoids on proliferation, atRA and 9-cis RA almost completely stopped proliferation, 13-cis reduced proliferation moderately, whereas Vitamin A did not negatively affect proliferation. Retinoids are generally associated with differentiation processes (Mark et al., 2006), therefore, it is surprising that they are able to transiently increase Zscan4 expression, a gene marking self-renewal of ES cells. Interestingly, Vitamin A, which resulted in the

strongest increase of Zscan4 expression, was reported to enhance mES cell self-renewal through stimulating the PI3K/Akt pathway and upregulation of Nanog (Chen and Khillan, 2008; Chen and Khillan, 2010; Chen et al., 2007). This finding fits well with our discovery that Zscan4 is regulated downstream of PI3Ks (Storm et al., 2009). Furthermore, evidence presented in this thesis suggests regulation of Zscan4 via the p110α PI3K catalytic isoform, shown by the use of the pharmacological inhibitors PIK-75 and Compound 15e as well as over-expression of a myristoylated p110α isoform, which led to increased expression of Zscan4 family members.

It is of interest that Zscan4c was also recently reported to be involved in regulating telomere length and genomic stability (Zalzman et al., 2010). Telomere elongation occurred in mES cells with high levels of Zscan4c, or upon induced over-expression of Zscan4c, leading to rapid telomere extension, most probably by a telomere recombination mechanism. This might be due to the proposed function of Zscan4 as a transcription factor, and consequent upregulation of meiosis-specific homologous recombination genes, but possibly also through direct mechanisms, as Zscan4c was found to be in close proximity to telomeres (Zalzman et al., 2010). Spo11 catalyses meiosis-specific DNA double-strand breaks (Keeney et al., 1997) and was one of the reported upregulated genes (Zalzman et al., 2010), but it is curious that in their earlier performed microarray screen over-expression of Zscan4c did not upregulate transcription of Spo11 (Nishiyama et al., 2009). In the microarray screen over-expression of Zscan4c rather resulted in downregulation of Spo11, but where the differences arise from is unclear. Despite this discrepancy, Spo11, as well as Dmc1, a RecA homologue recombinase required for meiotic recombination (Reinholdt and Schimenti, 2005), were co-localised with Zscan4 foci at the telomeres. Homologous recombination during meiotic recombination requires the introduction of DNA double strand breaks (DSBs), which are enclosed in γ-H2AX foci (Mahadevaiah et al., 2001), and γ-H2AX foci were co-localised to a high degree (>90%) with Zscan4 foci on telomeres (Zalzman et al., 2010). Interestingly, γ-H2AX foci were observed by immunostaining from G1-S phase to G2 phase of the cell cycle, but during the metaphase γ-H2AX foci were absent, indicating the repair of DSBs. Furthermore, no Spo11, γ-H2AX, or DMC1 foci were detected in Zscan4 negative cells (Zalzman et al., 2010). Zscan4 foci were also found to co-localise with telomere repeat binding

factor 1 (TRF1) (Zalzman et al., 2010), which has a protective function for telomeres (Blasco et al., 1995; de Lange, 2005) and is also reported to be involved in telomere regulation (Munoz et al., 2009; van Steensel and de Lange, 1997). Levels of TRF1 were described to correlate with that of different pluripotency markers, and a link of chromosome stability with pluripotency was proposed (Varela et al., 2011). Interestingly, ES cells expanded *in vitro* were found to have acquired longer telomeres than their *in vivo* counterparts, cells of the inner cell mass of the blastocyst (Varela et al., 2011). During the process of ES cell establishment a loss of heterochromatic marks was described, which might facilitate the elongation of telomeres (Varela et al., 2011). It is possible that Zscan4 may play a role in some of the described functions of telomere elongation, during early stages of ES cell establishment and/or during prolonged culture of ES cells. It is also worth mentioning that iPS cells regained the ability to express Zscan4 (Zalzman et al., 2010), but whether that is a direct and essential process during reprogramming, or a secondary cause during expansion of iPS clones remains to be investigated.

Creation of murine ES cell lines with an inducible eGFP-Zscan4c fusion protein was used for identifying potential protein binding partners by a combined immunoprecipitation - mass spectrometry strategy. Identification of binding partners can help to unravel potential molecular mechanisms of action of proteins of interest. Four potential binding partners were identified in this study, lysine specific histone demethylase 1 A (LSD1), C-terminal binding protein2 (Ctbp2), histidine triad nucleotide-binding protein 1 (HINT1) and 40S ribosomal protein S7 (Rps7). Interestingly, most of these proteins are associated with functions related to transcriptional regulation and DNA damage responses, functions that Zscan4 has also been reported to be involved with (as discussed above). LSD1 is able to maintain global DNA methylation and can demethylate non-histone substrates like p53, DNA (cytosine-5)-methyltransferase and E2F1 (Huang et al., 2007; Kontaki and Talianidis, 2010; Wang et al., 2009). Furthermore, LSD1 has been shown to regulate processes for gene activation through demethylation of H3K9me1/me2 (Metzger et al., 2005; Wissmann et al., 2007) and was recently reported to play an important role in human embryonic stem cell self-renewal by maintaining the proper balance between H3K4me2/me3 and H3K27me3 at target developmental genes (Adamo et al., 2011). Mouse ES cells in which LSD1 was conditionally knocked-out

appeared to be pluripotent, but exhibited severe growth and differentiation defects with an increase in apoptosis (Wang et al., 2009). LSD1 could contribute to establish the right epigenetic environment to allow full function of Zscan4 and its partners, for instance a loss of heterochromatic marks at telomeres occurring before telomere elongation (Varela et al., 2011).

Ctbp2 was also found to associate with Zscan4c, probably by binding to the known Ctbp PXDLS binding motif (Boyd et al., 1993; Quinlan et al., 2006), which is present in all Zscan4 members. Ctbp1 and Ctbp2, collectively referred as Ctbp, function as transcriptional co-repressors, and they are reported to act in protein complexes which can be comprised of LSD1 and other zinc finger proteins (Balasubramanian et al., 2003; Wang et al., 2007a). This fits well with our finding that Zscan4c, a zinc finger protein, and LSD1 were isolated in the same screen. Furthermore, Ctbp might be involved in adding complexity to the regulation possibilities of the multi-functional role of Zscan4, as there are different layers of Ctbp regulation mechanisms reported. The activity of Ctbp is dependent on intracellular NADH, which binds to Ctbp's dehydrogenase/NADH binding domain (Mani-Telang et al., 2007; Zhang et al., 2002). Ctbp was proposed to act as a redox sensor for regulating transcription as a consequence of the cellular metabolic environment (Fjeld et al., 2003; Zhang et al., 2006a). Also the cell cycle is involved in regulating Ctbp, as phosphorylation of Ctbp occurs in a cell cycle-dependent manner and its phosphorylation pattern suggests regulation by a cell cycle-regulated kinase (Boyd et al., 1993). Phosphorylation of Ctbp might also take place at a DNA-PK consensus phosphorylation site, and Ctbp could, therefore, be the substrate of DNA-PK or related kinases (Chinnadurai, 2002; Schaeper et al., 1998; Vo et al., 2001). Furthermore, UV light triggers proteasomal degradation of Ctbp through activation mechanisms leading to its ubiquitination (Zhang et al., 2005).

These features of Ctbp proteins are interesting as another potential Zscan4c interacting protein, HINT1, participates in ionizing radiation-induced DNA damage responses involved in regulation of γ-H2AX foci (Li et al., 2008a). MEFs deficient in HINT1 were shown to be more genetically unstable than their wild-type counterparts, exhibiting various types of chromosomal abnormalities (Li et al., 2008a). Zscan4c function has been implicated in regulation of genomic stability and cells high in Zscan4c were shown to have features associated with a higher genomic

stability (Zalzman et al., 2010). In addition, Zscan4 was reported to be transiently upregulated in response to oxidative stress and DNA-damaging agents (Ko and Zalzman, 2011), probably administrating protecting functions, enhancing survival of cells that were exposed to damaging events (Ko and Zalzman, 2011). It might be that Zscan4 in combination with HINT1 accomplish this protective function, but how and what function each of them contributes needs to be established.

Carefully carried out, over-expression, knock-down, interaction, labelling and functional assays need to be performed to shed further light on these mechanisms. Time-lapse experiments with tagged Zscan4 and tagged interacting proteins might reveal their temporal and spatial expression, and from there it might be possible to draw conclusions on their individual functions. Furthermore, LSD1 DKO ES cells could be used to study if functions of Zscan4c over-expression are dependent on presence of LSD1.

In another aspect of this study, the effects of artificial activation of Class IA PI3K catalytic isoforms in mES cells were investigated. A genetic activation strategy was applied by fusing a myristoylation target sequence to the p110α, β, and δ isoforms, which promotes constitutive membrane attachment and activation (Klippel et al., 1996). The piggyBac transposon system was used for over-expressing these constructs in mES cells with a CAG promoter. Myristoylation approaches for the activation of signalling pathways were previously used successfully in ES cells and, for instance, myr-Akt was found to be sufficient to liberate ES cells from the requirement of LIF (Watanabe et al., 2006). Furthermore, over-expression of activated p110α was reported to be able to rescue impaired growth and tumorigenicity in Eras (a Ras-like gene) knockout ES cells (Takahashi et al., 2003). In this study over-expression of myr-p110α in OCRG9 mES cells, was found to be able to lead to LIF independency. For the activated p110β and δ isoforms, self-renewal in the absence of LIF was not as clear-cut, but cannot currently be ruled out. Possibly, activation of the beta and delta catalytic isoforms could also result in LIF independency, which might be triggered by elevated PIP_3 levels activating downstream signalling pathways. To test whether myristoylation of the different isoforms resulted in a comparable elevation of intracellular PIP_3 levels, biochemical

assays need to be performed, as described in other studies (Jirmanova et al., 2002; Klippel et al., 1996). Cells were also placed under some selective pressure by selecting for Oct4 positive cells with puromycin and by the selection for transgene expression with G418. Furthermore, LIF withdrawal might have caused additional cellular stress which might have triggered expression of stress response genes contributing to the observed phenotype. For instance, Zscan4 levels were reported to be elevated when ES cells were exposed to oxidative stress (Ko and Zalzman, 2011). Differences in the behaviour and expression of pluripotency marker genes have been observed between LIF independent clones, especially one clone (clone 6) exhibited higher levels of Nanog expression in absence of LIF, accompanied by an increased self-renewing phenotype, in comparison to other observed clones. Where this difference arises from is not clear yet, and needs to be further addressed. It might that the transgene integrated in very close proximity to the endogenous Nanog gene, driving its expression by the strong CAG promoter (Niwa et al., 1991). Also some culture adaptation might have occurred during selection and, for instance, epigenetic changes could have led to the permanent activation of pluripotency genes. It would be necessary to further characterise these clones to solve this puzzle, and localisation of transgene integration sites might help to understand the described differences. Immunostaining for p110α and measuring of PIP_3 levels could also help to determine differences in activity or expression levels between clones.

A model for the possible working mechanisms of activated PI3K-dependent signalling was proposed. This model is based on the pluripotency 'ground state' theory, which in brief describes that inhibition of GSK-3 and Erk activity is sufficient to keep ES cells in a basal proliferative state with only minimal required external stimuli (Wray et al., 2010; Ying et al., 2008). However, additional stimulation with LIF has beneficial effects on clonogenicity, which in fact was also observed in the system used for the studies presented in this thesis. In this model myr-p110α is proposed to stimulate Zscan4, either directly or indirectly through Akt, which leads to upregulation of Zscan4 expression, which in turn stimulates transcription of Pramel7, reported to be able to reduce Erk activity (Casanova et al., 2011; Nishiyama et al., 2009). On the other hand, myr-p110α over-expression can result in GSK-3 inactivation by stimulating Akt activity (Popkie et al., 2010). Therefore, myr-p110α over-expression is able to block activity of both, GSK-3 and

Erk, establishing the 'ground state' of pluripotency. This working model is not yet thoroughly tested and a number of experiments would be still necessary to add further weight to it. For instance, upregulation of Pramel7 was not tested, and also phosphorylation levels of Erk need to be checked by immunoblotting. Also, Akt phosphorylation needs to be checked on both phosphorylation sites, T308 and S473, to ensure its correct activation. Furthermore, GSK-3 phosphorylation needs to be also confirmed by immunoblotting and kinase assays, to ensure its inactivated status. It would also be of interest to determine whether activated p110α ES cells, with higher levels of Zscan4, show a higher rate of telomeric recombination events, and as such would place PI3K signalling as an important player in regulation of telomeres in ES cells. In summary, more work is required to completely assess the detailed effects of activated PI3Ks signalling in ESCs.

6.2 Concluding remarks

Zscan4 is a novel ES cell master regulator important for maintaining ES cell identity, genomic stability, and telomere length. This study has provided further insights into Zscan4 regulation, by placing it downstream of the PI3K signalling pathway, in particular of the p110α catalytic isoform. Furthermore, Zscan4 function was linked to self-renewal, which might be a direct effect of Zscan4 activity or an indirect effect caused by a loss of genomic stability. The identification of potential binding partners might help to contribute to the further understanding of the multi-functional mechanisms of Zscan4. Many questions remain unanswered. How Zscan4 is precisely regulated, whether it is an essential part in ES cell or iPS cell generation, how it elongates telomeres, how it is linked with pluripotency or the cell cycle, and whether it might be involved in immortalisation or contribute to cancers, will be some of the challenges that have to be addressed in future studies.

References

Aasen, T., A. Raya, M.J. Barrero, E. Garreta, A. Consiglio, F. Gonzalez, R. Vassena, J. Bilic, V. Pekarik, G. Tiscornia, M. Edel, S. Boue, and J.C. Izpisua Belmonte. 2008. Efficient and rapid generation of induced pluripotent stem cells from human keratinocytes. *Nat Biotechnol*. 26:1276-1284.

Aberle, H., A. Bauer, J. Stappert, A. Kispert, and R. Kemler. 1997. beta-catenin is a target for the ubiquitin-proteasome pathway. *EMBO J*. 16:3797-3804.

Adamo, A., B. Sese, S. Boue, J. Castano, I. Paramonov, M.J. Barrero, and J.C. Belmonte. 2011. LSD1 regulates the balance between self-renewal and differentiation in human embryonic stem cells. *Nat Cell Biol*.

Alessi, D.R., M. Andjelkovic, B. Caudwell, P. Cron, N. Morrice, P. Cohen, and B.A. Hemmings. 1996. Mechanism of activation of protein kinase B by insulin and IGF-1. *EMBO J*. 15:6541-6551.

Alessi, D.R., S.R. James, C.P. Downes, A.B. Holmes, P.R. Gaffney, C.B. Reese, and P. Cohen. 1997. Characterization of a 3-phosphoinositide-dependent protein kinase which phosphorylates and activates protein kinase Balpha. *Curr Biol*. 7:261-269.

Anderson, K.E., J. Coadwell, L.R. Stephens, and P.T. Hawkins. 1998. Translocation of PDK-1 to the plasma membrane is important in allowing PDK-1 to activate protein kinase B. *Curr Biol*. 8:684-691.

Anton, R., H.A. Kestler, and M. Kuhl. 2007. Beta-catenin signaling contributes to stemness and regulates early differentiation in murine embryonic stem cells. *FEBS Lett*. 581:5247-5254.

Aoi, T., K. Yae, M. Nakagawa, T. Ichisaka, K. Okita, K. Takahashi, T. Chiba, and S. Yamanaka. 2008. Generation of pluripotent stem cells from adult mouse liver and stomach cells. *Science*. 321:699-702.

Armstrong, L., O. Hughes, S. Yung, L. Hyslop, R. Stewart, I. Wappler, H. Peters, T. Walter, P. Stojkovic, J. Evans, M. Stojkovic, and M. Lako. 2006. The role of PI3K/AKT, MAPK/ERK and NFkappabeta signalling in the maintenance of human embryonic stem cell pluripotency and viability highlighted by transcriptional profiling and functional analysis. *Hum Mol Genet*. 15:1894-1913.

Attisano, L., and J.L. Wrana. 2002. Signal transduction by the TGF-beta superfamily. *Science*. 296:1646-1647.

Balasubramanian, P., L.J. Zhao, and G. Chinnadurai. 2003. Nicotinamide adenine dinucleotide stimulates oligomerization, interaction with adenovirus E1A and an intrinsic dehydrogenase activity of CtBP. *FEBS Lett*. 537:157-160.

Balendran, A., A. Casamayor, M. Deak, A. Paterson, P. Gaffney, R. Currie, C.P. Downes, and D.R. Alessi. 1999. PDK1 acquires PDK2 activity in the presence of a synthetic peptide derived from the carboxyl terminus of PRK2. *Curr Biol*. 9:393-404.

Balla, T. 2006. Phosphoinositide-derived messengers in endocrine signaling. *J Endocrinol*. 188:135-153.

Barrero, M.J., and J.C. Izpisua Belmonte. 2011. iPS cells forgive but do not forget. *Nat Cell Biol*. 13:523-525.

Belham, C., S. Wu, and J. Avruch. 1999. Intracellular signalling: PDK1--a kinase at the hub of things. *Curr Biol*. 9:R93-96.

Ben-Shushan, E., J.R. Thompson, L.J. Gudas, and Y. Bergman. 1998. Rex-1, a gene encoding a transcription factor expressed in the early embryo, is regulated via Oct-3/4 and Oct-6 binding to an octamer site and a novel protein, Rox-1, binding to an adjacent site. *Mol Cell Biol*. 18:1866-1878.

Benezra, R. 2001. Role of Id proteins in embryonic and tumor angiogenesis. *Trends Cardiovasc Med*. 11:237-241.

Berge, D.T., D. Kurek, T. Blauwkamp, W. Koole, A. Maas, E. Eroglu, R.K. Siu, and R. Nusse. 2011. Embryonic stem cells require Wnt proteins to prevent differentiation to epiblast stem cells. *Nat Cell Biol*.

Bernstein, E., A.A. Caudy, S.M. Hammond, and G.J. Hannon. 2001. Role for a bidentate ribonuclease in the initiation step of RNA interference. *Nature*. 409:363-366.

Berridge, M.J., and R.F. Irvine. 1984. Inositol trisphosphate, a novel second messenger in cellular signal transduction. *Nature*. 312:315-321.

Berridge, M.J., and R.F. Irvine. 1989. Inositol phosphates and cell signalling. *Nature*. 341:197-205.

Bi, L., I. Okabe, D.J. Bernard, A. Wynshaw-Boris, and R.L. Nussbaum. 1999. Proliferative defect and embryonic lethality in mice homozygous for a deletion in the p110alpha subunit of phosphoinositide 3-kinase. *J Biol Chem*. 274:10963-10968.

Blackburn, E.H. 2001. Switching and signaling at the telomere. *Cell*. 106:661-673.

Blackburn, E.H., and J.G. Gall. 1978. A tandemly repeated sequence at the termini of the extrachromosomal ribosomal RNA genes in Tetrahymena. *J Mol Biol*. 120:33-53.

Blasco, M.A., W. Funk, B. Villeponteau, and C.W. Greider. 1995. Functional characterization and developmental regulation of mouse telomerase RNA. *Science*. 269:1267-1270.

Blasco, M.A., M. Serrano, and O. Fernandez-Capetillo. 2011. Genomic instability in iPS: time for a break. *EMBO J*. 30:991-993.

Bochar, D.A., J. Savard, W. Wang, D.W. Lafleur, P. Moore, J. Cote, and R. Shiekhattar. 2000. A family of chromatin remodeling factors related to Williams syndrome transcription factor. *Proc Natl Acad Sci U S A*. 97:1038-1043.

Bodnar, A.G., M. Ouellette, M. Frolkis, S.E. Holt, C.P. Chiu, G.B. Morin, C.B. Harley, J.W. Shay, S. Lichtsteiner, and W.E. Wright. 1998. Extension of life-span by introduction of telomerase into normal human cells. *Science*. 279:349-352.

Boeuf, H., C. Hauss, F.D. Graeve, N. Baran, and C. Kedinger. 1997. Leukemia inhibitory factor-dependent transcriptional activation in embryonic stem cells. *J Cell Biol*. 138:1207-1217.

Boiani, M., and H. Schöler. 2005. Regulatory networks in embryo-derived pluripotent stem cells. *Nat Rev Mol Cell Biol*. 6:872-884.

Bone, H., U. Dechert, F. Jirik, J.W. Schrader, and M.J. Welham. 1997. SHP1 and SHP2 protein-tyrosine phosphatases associate with betac after interleukin-3-induced receptor tyrosine phosphorylation. Identification of potential binding sites and substrates. *J Biol Chem*. 272:14470-14476.

Bone, H.K., T. Damiano, S. Bartlett, A. Perry, J. Letchford, Y.S. Ripoll, A.S. Nelson, and M.J. Welham. 2009. Involvement of GSK-3 in regulation of murine embryonic stem cell self-renewal revealed by a series of bisindolylmaleimides. *Chem Biol*. 16:15-27.

Bone, H.K., A.S. Nelson, C.E. Goldring, D. Tosh, and M.J. Welham. 2011. A novel chemically directed route for the generation of definitive endoderm from human embryonic stem cells based on inhibition of GSK-3. *J Cell Sci*.

Boulton, T.G., N. Stahl, and G.D. Yancopoulos. 1994. Ciliary neurotrophic factor/leukemia inhibitory factor/interleukin 6/oncostatin M family of cytokines induces tyrosine phosphorylation of a common set of proteins overlapping those induced by other cytokines and growth factors. *J Biol Chem*. 269:11648-11655.

Boyd, J.M., T. Subramanian, U. Schaeper, M. La Regina, S. Bayley, and G. Chinnadurai. 1993. A region in the C-terminus of adenovirus 2/5 E1a protein is required for association with a cellular phosphoprotein and important for the negative modulation of T24-ras mediated transformation, tumorigenesis and metastasis. *EMBO J*. 12:469-478.

Boyer, L., T. Lee, M. Cole, S. Johnstone, S. Levine, J. Zucker, M. Guenther, R. Kumar, H. Murray, R. Jenner, D. Gifford, D. Melton, R. Jaenisch, and R. Young. 2005. Core

transcriptional regulatory circuitry in human embryonic stem cells. *Cell*. 122:947-956.

Brachmann, S.M., K. Ueki, J.A. Engelman, R.C. Kahn, and L.C. Cantley. 2005. Phosphoinositide 3-kinase catalytic subunit deletion and regulatory subunit deletion have opposite effects on insulin sensitivity in mice. *Mol Cell Biol*. 25:1596-1607.

Bradford, M.M. 1976. A rapid and sensitive method for the quantitation of microgram quantities of protein utilizing the principle of protein-dye binding. *Anal Biochem*. 72:248-254.

Bradley, A., M. Evans, M.H. Kaufman, and E. Robertson. 1984. Formation of germ-line chimaeras from embryo-derived teratocarcinoma cell lines. *Nature*. 309:255-256.

Brill, L.M., W. Xiong, K.B. Lee, S.B. Ficarro, A. Crain, Y. Xu, A. Terskikh, E.Y. Snyder, and S. Ding. 2009. Phosphoproteomic analysis of human embryonic stem cells. *Cell Stem Cell*. 5:204-213.

Brinster, R.L. 1974. The effect of cells transferred into the mouse blastocyst on subsequent development. *J Exp Med*. 140:1049-1056.

Brons, I.G., L.E. Smithers, M.W. Trotter, P. Rugg-Gunn, B. Sun, S.M. Chuva de Sousa Lopes, S.K. Howlett, A. Clarkson, L. Ahrlund-Richter, R.A. Pedersen, and L. Vallier. 2007. Derivation of pluripotent epiblast stem cells from mammalian embryos. *Nature*. 448:191-195.

Brook, F.A., and R.L. Gardner. 1997. The origin and efficient derivation of embryonic stem cells in the mouse. *Proc Natl Acad Sci U S A*. 94:5709-5712.

Brown, E.J., P.A. Beal, C.T. Keith, J. Chen, T.B. Shin, and S.L. Schreiber. 1995. Control of p70 s6 kinase by kinase activity of FRAP in vivo. *Nature*. 377:441-446.

Bryan, T.M., A. Englezou, L. Dalla-Pozza, M.A. Dunham, and R.R. Reddel. 1997. Evidence for an alternative mechanism for maintaining telomere length in human tumors and tumor-derived cell lines. *Nat Med*. 3:1271-1274.

Bryan, T.M., A. Englezou, J. Gupta, S. Bacchetti, and R.R. Reddel. 1995. Telomere elongation in immortal human cells without detectable telomerase activity. *EMBO J*. 14:4240-4248.

Budirahardja, Y., and P. Gonczy. 2009. Coupling the cell cycle to development. *Development*. 136:2861-2872.

Buecker, C., H.H. Chen, J.M. Polo, L. Daheron, L. Bu, T.S. Barakat, P. Okwieka, A. Porter, J. Gribnau, K. Hochedlinger, and N. Geijsen. 2010. A murine ESC-like state facilitates transgenesis and homologous recombination in human pluripotent stem cells. *Cell Stem Cell*. 6:535-546.

Buehr, M., S. Meek, K. Blair, J. Yang, J. Ure, J. Silva, R. McLay, J. Hall, Q.L. Ying, and A. Smith. 2008. Capture of authentic embryonic stem cells from rat blastocysts. *Cell*. 135:1287-1298.

Burdon, T., I. Chambers, C. Stracey, H. Niwa, and A. Smith. 1999a. Signaling mechanisms regulating self-renewal and differentiation of pluripotent embryonic stem cells. *Cells Tissues Organs*. 165:131-143.

Burdon, T., A. Smith, and P. Savatier. 2002. Signalling, cell cycle and pluripotency in embryonic stem cells. *Trends Cell Biol*. 12:432-438.

Burdon, T., C. Stracey, I. Chambers, J. Nichols, and A. Smith. 1999b. Suppression of SHP-2 and ERK signalling promotes self-renewal of mouse embryonic stem cells. *Dev Biol*. 210:30-43.

Cadinanos, J., and A. Bradley. 2007. Generation of an inducible and optimized piggyBac transposon system. *Nucleic Acids Res*. 35:e87.

Canham, M.A., A.A. Sharov, M.S. Ko, and J.M. Brickman. 2010. Functional heterogeneity of embryonic stem cells revealed through translational amplification of an early endodermal transcript. *PLoS Biol*. 8:e1000379.

Cantrell, D.A. 2001. Phosphoinositide 3-kinase signalling pathways. *J Cell Sci*. 114:1439-1445.

Cartwright, P., C. McLean, A. Sheppard, D. Rivett, K. Jones, and S. Dalton. 2005. LIF/STAT3 controls ES cell self-renewal and pluripotency by a Myc-dependent mechanism. *Development*. 132:885-896.

Casanova, E.A., O. Shakhova, S.S. Patel, I.N. Asner, P. Pelczar, F.A. Weber, U. Graf, L. Sommer, K. Burki, and P. Cinelli. 2011. Pramel7 mediates LIF/STAT3-dependent self-renewal in embryonic stem cells. *Stem Cells*. 29:474-485.

Cervantes, R.B., J.R. Stringer, C. Shao, J.A. Tischfield, and P.J. Stambrook. 2002. Embryonic stem cells and somatic cells differ in mutation frequency and type. *Proc Natl Acad Sci U S A*. 99:3586-3590.

Chambers, I., D. Colby, M. Robertson, J. Nichols, S. Lee, S. Tweedie, and A. Smith. 2003. Functional expression cloning of Nanog, a pluripotency sustaining factor in embryonic stem cells. *Cell*. 113:643-655.

Chambers, I., J. Silva, D. Colby, J. Nichols, B. Nijmeijer, M. Robertson, J. Vrana, K. Jones, L. Grotewold, and A. Smith. 2007. Nanog safeguards pluripotency and mediates germline development. *Nature*. 450:1230-1234.

Chaussade, C., G.W. Rewcastle, J.D. Kendall, W.A. Denny, K. Cho, L.M. Gronning, M.L. Chong, S.H. Anagnostou, S.P. Jackson, N. Daniele, and P.R. Shepherd. 2007. Evidence for functional redundancy of class IA PI3K isoforms in insulin signalling. *Biochem J*. 404:449-458.

Chazaud, C., Y. Yamanaka, T. Pawson, and J. Rossant. 2006. Early lineage segregation between epiblast and primitive endoderm in mouse blastocysts through the Grb2-MAPK pathway. *Dev Cell*. 10:615-624.

Chen, L., and J.S. Khillan. 2008. Promotion of feeder-independent self-renewal of embryonic stem cells by retinol (vitamin A). *Stem Cells*. 26:1858-1864.

Chen, L., and J.S. Khillan. 2010. A novel signaling by vitamin A/retinol promotes self renewal of mouse embryonic stem cells by activating PI3K/Akt signaling pathway via insulin-like growth factor-1 receptor. *Stem Cells*. 28:57-63.

Chen, L., M. Yang, J. Dawes, and J.S. Khillan. 2007. Suppression of ES cell differentiation by retinol (vitamin A) via the overexpression of Nanog. *Differentiation*. 75:682-693.

Chen, S., J.T. Do, Q. Zhang, S. Yao, F. Yan, E.C. Peters, H.R. Scholer, P.G. Schultz, and S. Ding. 2006. Self-renewal of embryonic stem cells by a small molecule. *Proc Natl Acad Sci U S A*. 103:17266-17271.

Cheng, A.M., T.M. Saxton, R. Sakai, S. Kulkarni, G. Mbamalu, W. Vogel, C.G. Tortorice, R.D. Cardiff, J.C. Cross, W.J. Muller, and T. Pawson. 1998. Mammalian Grb2 regulates multiple steps in embryonic development and malignant transformation. *Cell*. 95:793-803.

Chinnadurai, G. 2002. CtBP, an unconventional transcriptional corepressor in development and oncogenesis. *Mol Cell*. 9:213-224.

Chinnadurai, G. 2003. CtBP family proteins: more than transcriptional corepressors. *Bioessays*. 25:9-12.

Chou, Y.F., H.H. Chen, M. Eijpe, A. Yabuuchi, J.G. Chenoweth, P. Tesar, J. Lu, R.D. McKay, and N. Geijsen. 2008. The growth factor environment defines distinct pluripotent ground states in novel blastocyst-derived stem cells. *Cell*. 135:449-461.

Clayton, E., G. Bardi, S.E. Bell, D. Chantry, C.P. Downes, A. Gray, L.A. Humphries, D. Rawlings, H. Reynolds, E. Vigorito, and M. Turner. 2002. A crucial role for the

p110delta subunit of phosphatidylinositol 3-kinase in B cell development and activation. *J Exp Med*. 196:753-763.

Clevers, H. 2006. Wnt/beta-catenin signaling in development and disease. *Cell*. 127:469-480.

Conrad, S., M. Renninger, J. Hennenlotter, T. Wiesner, L. Just, M. Bonin, W. Aicher, H.J. Buhring, U. Mattheus, A. Mack, H.J. Wagner, S. Minger, M. Matzkies, M. Reppel, J. Hescheler, K.D. Sievert, A. Stenzl, and T. Skutella. 2008. Generation of pluripotent stem cells from adult human testis. *Nature*. 456:344-349.

Cowan, C.A., J. Atienza, D.A. Melton, and K. Eggan. 2005. Nuclear reprogramming of somatic cells after fusion with human embryonic stem cells. *Science*. 309:1369-1373.

Crabbe, T., M.J. Welham, and S.G. Ward. 2007. The PI3K inhibitor arsenal: choose your weapon! *Trends Biochem Sci*. 32:450-456.

Currie, R.A., K.S. Walker, A. Gray, M. Deak, A. Casamayor, C.P. Downes, P. Cohen, D.R. Alessi, and J. Lucocq. 1999. Role of phosphatidylinositol 3,4,5-trisphosphate in regulating the activity and localization of 3-phosphoinositide-dependent protein kinase-1. *Biochem J*. 337 (Pt 3):575-583.

Dagia, N.M., G. Agarwal, D.V. Kamath, A. Chetrapal-Kunwar, R.D. Gupte, M.G. Jadhav, S.S. Dadarkar, J. Trivedi, A.A. Kulkarni-Almeida, F. Kharas, L.C. Fonseca, S. Kumar, and M.R. Bhonde. 2010. A preferential p110alpha/gamma PI3K inhibitor attenuates experimental inflammation by suppressing the production of proinflammatory mediators in a NF-kappaB-dependent manner. *Am J Physiol Cell Physiol*. 298:C929-941.

Daheron, L., S.L. Opitz, H. Zaehres, M.W. Lensch, P.W. Andrews, J. Itskovitz-Eldor, and G.Q. Daley. 2004. LIF/STAT3 signaling fails to maintain self-renewal of human embryonic stem cells. *Stem Cells*. 22:770-778.

de Lange, T. 2005. Shelterin: the protein complex that shapes and safeguards human telomeres. *Genes Dev*. 19:2100-2110.

Dhand, R., I. Hiles, G. Panayotou, S. Roche, M.J. Fry, I. Gout, N.F. Totty, O. Truong, P. Vicendo, K. Yonezawa, and et al. 1994. PI 3-kinase is a dual specificity enzyme: autoregulation by an intrinsic protein-serine kinase activity. *EMBO J*. 13:522-533.

Diwan, S.B., and L.C. Stevens. 1976. Development of teratomas from the ectoderm of mouse egg cylinders. *J Natl Cancer Inst*. 57:937-942.

Doble, B.W., S. Patel, G.A. Wood, L.K. Kockeritz, and J.R. Woodgett. 2007. Functional redundancy of GSK-3alpha and GSK-3beta in Wnt/beta-catenin signaling shown by using an allelic series of embryonic stem cell lines. *Dev Cell*. 12:957-971.

Dravid, G., Z. Ye, H. Hammond, G. Chen, A. Pyle, P. Donovan, X. Yu, and L. Cheng. 2005. Defining the role of Wnt/beta-catenin signaling in the survival, proliferation, and self-renewal of human embryonic stem cells. *Stem Cells*. 23:1489-1501.

Dreesen, O., and A.H. Brivanlou. 2007. Signaling pathways in cancer and embryonic stem cells. *Stem Cell Rev*. 3:7-17.

Edelstein, L.C., and T. Collins. 2005. The SCAN domain family of zinc finger transcription factors. *Gene*. 359:1-17.

Egozi, D., M. Shapira, G. Paor, O. Ben-Izhak, K. Skorecki, and D.D. Hershko. 2007. Regulation of the cell cycle inhibitor p27 and its ubiquitin ligase Skp2 in differentiation of human embryonic stem cells. *FASEB J*. 21:2807-2817.

Elbashir, S.M., J. Harborth, W. Lendeckel, A. Yalcin, K. Weber, and T. Tuschl. 2001. Duplexes of 21-nucleotide RNAs mediate RNA interference in cultured mammalian cells. *Nature*. 411:494-498.

Embi, N., D.B. Rylatt, and P. Cohen. 1980. Glycogen synthase kinase-3 from rabbit skeletal muscle. Separation from cyclic-AMP-dependent protein kinase and phosphorylase kinase. *Eur J Biochem*. 107:519-527.

Engelman, J.A., J. Luo, and L.C. Cantley. 2006. The evolution of phosphatidylinositol 3-kinases as regulators of growth and metabolism. *Nat Rev Genet*. 7:606-619.

Era, T., and O.N. Witte. 2000. Regulated expression of P210 Bcr-Abl during embryonic stem cell differentiation stimulates multipotential progenitor expansion and myeloid cell fate. *Proc Natl Acad Sci U S A*. 97:1737-1742.

Evans, M.J., and M.H. Kaufman. 1981. Establishment in culture of pluripotential cells from mouse embryos. *Nature*. 292:154-156.

Falco, G., S.L. Lee, I. Stanghellini, U.C. Bassey, T. Hamatani, and M.S. Ko. 2007. Zscan4: a novel gene expressed exclusively in late 2-cell embryos and embryonic stem cells. *Dev Biol*. 307:539-550.

Fan, Q.W., Z.A. Knight, D.D. Goldenberg, W. Yu, K.E. Mostov, D. Stokoe, K.M. Shokat, and W.A. Weiss. 2006. A dual PI3 kinase/mTOR inhibitor reveals emergent efficacy in glioma. *Cancer Cell*. 9:341-349.

Fernandez, N.J., and B.A. Kidney. 2007. Alkaline phosphatase: beyond the liver. *Vet Clin Pathol*. 36:223-233.

Filippa, N., C.L. Sable, B.A. Hemmings, and E. Van Obberghen. 2000. Effect of phosphoinositide-dependent kinase 1 on protein kinase B translocation and its subsequent activation. *Mol Cell Biol*. 20:5712-5721.

Fire, A., S. Xu, M.K. Montgomery, S.A. Kostas, S.E. Driver, and C.C. Mello. 1998. Potent and specific genetic interference by double-stranded RNA in Caenorhabditis elegans. *Nature*. 391:806-811.

Fjeld, C.C., W.T. Birdsong, and R.H. Goodman. 2003. Differential binding of NAD+ and NADH allows the transcriptional corepressor carboxyl-terminal binding protein to serve as a metabolic sensor. *Proc Natl Acad Sci U S A*. 100:9202-9207.

Folkes, A.J., K. Ahmadi, W.K. Alderton, S. Alix, S.J. Baker, G. Box, I.S. Chuckowree, P.A. Clarke, P. Depledge, S.A. Eccles, L.S. Friedman, A. Hayes, T.C. Hancox, A. Kugendradas, L. Lensun, P. Moore, A.G. Olivero, J. Pang, S. Patel, G.H. Pergl-Wilson, F.I. Raynaud, A. Robson, N. Saghir, L. Salphati, S. Sohal, M.H. Ultsch, M. Valenti, H.J. Wallweber, N.C. Wan, C. Wiesmann, P. Workman, A. Zhyvoloup, M.J. Zvelebil, and S.J. Shuttleworth. 2008. The identification of 2-(1H-indazol-4-yl)-6-(4-methanesulfonyl-piperazin-1-ylmethyl)-4-morpholin -4-yl-thieno[3,2-d]pyrimidine (GDC-0941) as a potent, selective, orally bioavailable inhibitor of class I PI3 kinase for the treatment of cancer. *J Med Chem*. 51:5522-5532.

Foukas, L.C., M. Claret, W. Pearce, K. Okkenhaug, S. Meek, E. Peskett, S. Sancho, A.J. Smith, D.J. Withers, and B. Vanhaesebroeck. 2006. Critical role for the p110alpha phosphoinositide-3-OH kinase in growth and metabolic regulation. *Nature*. 441:366-370.

Fraser, M.J., T. Ciszczon, T. Elick, and C. Bauser. 1996. Precise excision of TTAA-specific lepidopteran transposons piggyBac (IFP2) and tagalong (TFP3) from the baculovirus genome in cell lines from two species of Lepidoptera. *Insect Mol Biol*. 5:141-151.

Fuchs, U., C. Damm-Welk, and A. Borkhardt. 2004. Silencing of disease-related genes by small interfering RNAs. *Curr Mol Med*. 4:507-517.

Furusawa, T., H. Moribe, H. Kondoh, and Y. Higashi. 1999. Identification of CtBP1 and CtBP2 as corepressors of zinc finger-homeodomain factor deltaEF1. *Mol Cell Biol*. 19:8581-8590.

Gadue, P., T.L. Huber, P.J. Paddison, and G.M. Keller. 2006. Wnt and TGF-beta signaling are required for the induction of an in vitro model of primitive streak formation using embryonic stem cells. *Proc Natl Acad Sci U S A*. 103:16806-16811.

Gardner, R.L., and R.S. Beddington. 1988. Multi-lineage 'stem' cells in the mammalian embryo. *J Cell Sci Suppl*. 10:11-27.

Gassmann, M., G. Donoho, and P. Berg. 1995. Maintenance of an extrachromosomal plasmid vector in mouse embryonic stem cells. *Proc Natl Acad Sci U S A*. 92:1292-1296.

Geering, B., P.R. Cutillas, and B. Vanhaesebroeck. 2007. Regulation of class IA PI3Ks: is there a role for monomeric PI3K subunits? *Biochem Soc Trans*. 35:199-203.

Gharbi, S.I., M.J. Zvelebil, S.J. Shuttleworth, T. Hancox, N. Saghir, J.F. Timms, and M.D. Waterfield. 2007. Exploring the specificity of the PI3K family inhibitor LY294002. *Biochem J*. 404:15-21.

Gingras, A.C., S.P. Gygi, B. Raught, R.D. Polakiewicz, R.T. Abraham, M.F. Hoekstra, R. Aebersold, and N. Sonenberg. 1999. Regulation of 4E-BP1 phosphorylation: a novel two-step mechanism. *Genes Dev*. 13:1422-1437.

Gonzalez, F., M. Barragan Monasterio, G. Tiscornia, N. Montserrat Pulido, R. Vassena, L. Batlle Morera, I. Rodriguez Piza, and J.C. Izpisua Belmonte. 2009. Generation of mouse-induced pluripotent stem cells by transient expression of a single nonviral polycistronic vector. *Proc Natl Acad Sci U S A*. 106:8918-8922.

Gonzalo, S., I. Jaco, M.F. Fraga, T. Chen, E. Li, M. Esteller, and M.A. Blasco. 2006. DNA methyltransferases control telomere length and telomere recombination in mammalian cells. *Nat Cell Biol*. 8:416-424.

Gossen, M., and H. Bujard. 1992. Tight control of gene expression in mammalian cells by tetracycline-responsive promoters. *Proc Natl Acad Sci U S A*. 89:5547-5551.

Guan, K., K. Nayernia, L.S. Maier, S. Wagner, R. Dressel, J.H. Lee, J. Nolte, F. Wolf, M. Li, W. Engel, and G. Hasenfuss. 2006. Pluripotency of spermatogonial stem cells from adult mouse testis. *Nature*. 440:1199-1203.

Guo, G., J. Yang, J. Nichols, J.S. Hall, I. Eyres, W. Mansfield, and A. Smith. 2009. Klf4 reverts developmentally programmed restriction of ground state pluripotency. *Development*. 136:1063-1069.

Guo, Y., B. Graham-Evans, and H.E. Broxmeyer. 2006. Murine embryonic stem cells secrete cytokines/growth modulators that enhance cell survival/anti-apoptosis and stimulate colony formation of murine hematopoietic progenitor cells. *Stem Cells*. 24:850-856.

Gurdon, J.B., T.R. Elsdale, and M. Fischberg. 1958. Sexually mature individuals of Xenopus laevis from the transplantation of single somatic nuclei. *Nature*. 182:64-65.

Guttman, M., J. Donaghey, B.W. Carey, M. Garber, J.K. Grenier, G. Munson, G. Young, A.B. Lucas, R. Ach, L. Bruhn, X. Yang, I. Amit, A. Meissner, A. Regev, J.L. Rinn, D.E. Root, and E.S. Lander. 2011. lincRNAs act in the circuitry controlling pluripotency and differentiation. *Nature*. 477:295-300.

Hakimi, M.A., D.A. Bochar, J. Chenoweth, W.S. Lane, G. Mandel, and R. Shiekhattar. 2002. A core-BRAF35 complex containing histone deacetylase mediates repression of neuronal-specific genes. *Proc Natl Acad Sci U S A*. 99:7420-7425.

Hallmann, D., K. Trümper, H. Trusheim, K. Ueki, C. Kahn, L. Cantley, D. Fruman, and D. Hörsch. 2003. Altered signaling and cell cycle regulation in embryonal stem cells with a disruption of the gene for phosphoinositide 3-kinase regulatory subunit p85alpha. *J Biol Chem*. 278:5099-5108.

Hamazaki, T., S.M. Kehoe, T. Nakano, and N. Terada. 2006. The Grb2/Mek pathway represses Nanog in murine embryonic stem cells. *Mol Cell Biol*. 26:7539-7549.

Han, D.W., B. Greber, G. Wu, N. Tapia, M.J. Arauzo-Bravo, K. Ko, C. Bernemann, M. Stehling, and H.R. Scholer. 2011. Direct reprogramming of fibroblasts into epiblast stem cells. *Nat Cell Biol*. 13:66-71.

Hanada, M., J. Feng, and B.A. Hemmings. 2004. Structure, regulation and function of PKB/AKT--a major therapeutic target. *Biochim Biophys Acta*. 1697:3-16.

Hanna, J., A.W. Cheng, K. Saha, J. Kim, C.J. Lengner, F. Soldner, J.P. Cassady, J. Muffat, B.W. Carey, and R. Jaenisch. 2010. Human embryonic stem cells with biological and epigenetic characteristics similar to those of mouse ESCs. *Proc Natl Acad Sci U S A*. 107:9222-9227.

Hanna, J., K. Saha, B. Pando, J. van Zon, C.J. Lengner, M.P. Creyghton, A. van Oudenaarden, and R. Jaenisch. 2009. Direct cell reprogramming is a stochastic process amenable to acceleration. *Nature*. 462:595-601.

Hao, J., T.G. Li, X. Qi, D.F. Zhao, and G.Q. Zhao. 2006. WNT/beta-catenin pathway up-regulates Stat3 and converges on LIF to prevent differentiation of mouse embryonic stem cells. *Dev Biol*. 290:81-91.

Harkin, D.P., J.M. Bean, D. Miklos, Y.H. Song, V.B. Truong, C. Englert, F.C. Christians, L.W. Ellisen, S. Maheswaran, J.D. Oliner, and D.A. Haber. 1999. Induction of GADD45 and JNK/SAPK-dependent apoptosis following inducible expression of BRCA1. *Cell*. 97:575-586.

Harley, C.B., A.B. Futcher, and C.W. Greider. 1990. Telomeres shorten during ageing of human fibroblasts. *Nature*. 345:458-460.

Hart, A.H., L. Hartley, M. Ibrahim, and L. Robb. 2004. Identification, cloning and expression analysis of the pluripotency promoting Nanog genes in mouse and human. *Dev Dyn*. 230:187-198.

Hawkins, P.T., K.E. Anderson, K. Davidson, and L.R. Stephens. 2006. Signalling through Class I PI3Ks in mammalian cells. *Biochem Soc Trans*. 34:647-662.

Hayakawa, M., H. Kaizawa, H. Moritomo, T. Koizumi, T. Ohishi, M. Okada, M. Ohta, S. Tsukamoto, P. Parker, P. Workman, and M. Waterfield. 2006. Synthesis and biological evaluation of 4-morpholino-2-phenylquinazolines and related derivatives as novel PI3 kinase p110alpha inhibitors. *Bioorg Med Chem*. 14:6847-6858.

Hayflick, L. 1965. The Limited in Vitro Lifetime of Human Diploid Cell Strains. *Exp Cell Res*. 37:614-636.

Hayflick, L., and P.S. Moorhead. 1961. The serial cultivation of human diploid cell strains. *Exp Cell Res*. 25:585-621.

Hennessy, B.T., D.L. Smith, P.T. Ram, Y. Lu, and G.B. Mills. 2005. Exploiting the PI3K/AKT pathway for cancer drug discovery. *Nat Rev Drug Discov*. 4:988-1004.

Henson, J.D., A.A. Neumann, T.R. Yeager, and R.R. Reddel. 2002. Alternative lengthening of telomeres in mammalian cells. *Oncogene*. 21:598-610.

Hers, I. 2007. Insulin-like growth factor-1 potentiates platelet activation via the IRS/PI3Kalpha pathway. *Blood*. 110:4243-4252.

Hiyama, E., and K. Hiyama. 2007. Telomere and telomerase in stem cells. *Br J Cancer*. 96:1020-1024.

Ho, Y., A. Gruhler, A. Heilbut, G.D. Bader, L. Moore, S.L. Adams, A. Millar, P. Taylor, K. Bennett, K. Boutilier, L. Yang, C. Wolting, I. Donaldson, S. Schandorff, J. Shewnarane, M. Vo, J. Taggart, M. Goudreault, B. Muskat, C. Alfarano, D. Dewar, Z. Lin, K. Michalickova, A.R. Willems, H. Sassi, P.A. Nielsen, K.J. Rasmussen, J.R. Andersen, L.E. Johansen, L.H. Hansen, H. Jespersen, A. Podtelejnikov, E. Nielsen, J. Crawford, V. Poulsen, B.D. Sorensen, J. Matthiesen, R.C. Hendrickson, F. Gleeson, T. Pawson, M.F. Moran, D. Durocher, M. Mann, C.W. Hogue, D. Figeys, and M. Tyers. 2002. Systematic identification of protein complexes in Saccharomyces cerevisiae by mass spectrometry. *Nature*. 415:180-183.

Hosler, B.A., G.J. LaRosa, J.F. Grippo, and L.J. Gudas. 1989. Expression of REX-1, a gene containing zinc finger motifs, is rapidly reduced by retinoic acid in F9 teratocarcinoma cells. *Mol Cell Biol*. 9:5623-5629.

Hosono, K., T. Sasaki, S. Minoshima, and N. Shimizu. 2004. Identification and characterization of a novel gene family YPEL in a wide spectrum of eukaryotic species. *Gene*. 340:31-43.

Hresko, R.C., H. Murata, and M. Mueckler. 2003. Phosphoinositide-dependent kinase-2 is a distinct protein kinase enriched in a novel cytoskeletal fraction associated with adipocyte plasma membranes. *J Biol Chem*. 278:21615-21622.

Huang, J., R. Sengupta, A.B. Espejo, M.G. Lee, J.A. Dorsey, M. Richter, S. Opravil, R. Shiekhattar, M.T. Bedford, T. Jenuwein, and S.L. Berger. 2007. p53 is regulated by the lysine demethylase LSD1. *Nature*. 449:105-108.

Irvine, R.F. 1992. Inositol lipids in cell signalling. *Curr Opin Cell Biol*. 4:212-219.

Ivanova, N., R. Dobrin, R. Lu, I. Kotenko, J. Levorse, C. DeCoste, X. Schafer, Y. Lun, and I. Lemischka. 2006. Dissecting self-renewal in stem cells with RNA interference. *Nature*. 442:533-538.

Jackson, S.P., A. ROBERTSON, D., V. KENCHE, P. THOMPSON, H. PRABAHARAN, K. ANDERSON, B. ABBOTT, I. GONCALVES, W. NESBITT, S. SCHOENWAELDER, and D. SAYLIK. 2004. Inhibition of phosphoinositide 3-kinase beta. *WO/2004/016607*.

Jackson, S.P., S.M. Schoenwaelder, I. Goncalves, W.S. Nesbitt, C.L. Yap, C.E. Wright, V. Kenche, K.E. Anderson, S.M. Dopheide, Y. Yuan, S.A. Sturgeon, H. Prabaharan, P.E. Thompson, G.D. Smith, P.R. Shepherd, N. Daniele, S. Kulkarni, B. Abbott, D. Saylik, C. Jones, L. Lu, S. Giuliano, S.C. Hughan, J.A. Angus, A.D. Robertson, and H.H. Salem. 2005. PI 3-kinase p110beta: a new target for antithrombotic therapy. *Nat Med*. 11:507-514.

Jiang, J., Y.S. Chan, Y.H. Loh, J. Cai, G.Q. Tong, C.A. Lim, P. Robson, S. Zhong, and H.H. Ng. 2008. A core Klf circuitry regulates self-renewal of embryonic stem cells. *Nat Cell Biol*. 10:353-360.

Jiang, W.Q., A. Nguyen, Y. Cao, A.C. Chang, and R.R. Reddel. 2011. HP1-mediated formation of alternative lengthening of telomeres-associated PML bodies requires HIRA but not ASF1a. *PLoS One*. 6:e17036.

Jirmanova, L., M. Afanassieff, S. Gobert-Gosse, S. Markossian, and P. Savatier. 2002. Differential contributions of ERK and PI3-kinase to the regulation of cyclin D1 expression and to the control of the G1/S transition in mouse embryonic stem cells. *Oncogene*. 21:5515-5528.

Johnson, L.V., P.G. Calarco, and M.L. Siebert. 1977. Alkaline phosphatase activity in the preimplantation mouse embryo. *J Embryol Exp Morphol*. 40:83-89.

Jones, M.H., N. Hamana, J. Nezu, and M. Shimane. 2000. A novel family of bromodomain genes. *Genomics*. 63:40-45.

Jorgensen, R.A., R.G. Atkinson, R.L. Forster, and W.J. Lucas. 1998. An RNA-based information superhighway in plants. *Science*. 279:1486-1487.

Jou, S.T., N. Carpino, Y. Takahashi, R. Piekorz, J.R. Chao, D. Wang, and J.N. Ihle. 2002. Essential, nonredundant role for the phosphoinositide 3-kinase p110delta in signaling by the B-cell receptor complex. *Mol Cell Biol*. 22:8580-8591.

Kaji, K., K. Norrby, A. Paca, M. Mileikovsky, P. Mohseni, and K. Woltjen. 2009. Virus-free induction of pluripotency and subsequent excision of reprogramming factors. *Nature*. 458:771-775.

Kanatsu-Shinohara, M., K. Inoue, J. Lee, M. Yoshimoto, N. Ogonuki, H. Miki, S. Baba, T. Kato, Y. Kazuki, S. Toyokuni, M. Toyoshima, O. Niwa, M. Oshimura, T. Heike, T. Nakahata, F. Ishino, A. Ogura, and T. Shinohara. 2004. Generation of pluripotent stem cells from neonatal mouse testis. *Cell*. 119:1001-1012.

Kanatsu-Shinohara, M., N. Ogonuki, K. Inoue, H. Miki, A. Ogura, S. Toyokuni, and T. Shinohara. 2003. Long-term proliferation in culture and germline transmission of mouse male germline stem cells. *Biol Reprod*. 69:612-616.

Kanatsu-Shinohara, M., and T. Shinohara. 2006. The germ of pluripotency. *Nat Biotechnol*. 24:663-664.

Karbstein, K. 2011. Inside the 40S ribosome assembly machinery. *Curr Opin Chem Biol*.

Katan, M., and V.L. Allen. 1999. Modular PH and C2 domains in membrane attachment and other functions. *FEBS Lett*. 452:36-40.

Kauffman, S. 2004. A proposal for using the ensemble approach to understand genetic regulatory networks. *J Theor Biol*. 230:581-590.

Kawase, E., H. Suemori, N. Takahashi, K. Okazaki, K. Hashimoto, and N. Nakatsuji. 1994. Strain difference in establishment of mouse embryonic stem (ES) cell lines. *Int J Dev Biol*. 38:385-390.

Keeney, S., C.N. Giroux, and N. Kleckner. 1997. Meiosis-specific DNA double-strand breaks are catalyzed by Spo11, a member of a widely conserved protein family. *Cell*. 88:375-384.

Keller, G., M. Kennedy, T. Papayannopoulou, and M.V. Wiles. 1993. Hematopoietic commitment during embryonic stem cell differentiation in culture. *Mol Cell Biol*. 13:473-486.

Kennedy, M., M. Firpo, K. Choi, C. Wall, S. Robertson, N. Kabrun, and G. Keller. 1997. A common precursor for primitive erythropoiesis and definitive haematopoiesis. *Nature*. 386:488-493.

Kim, D., C.H. Kim, J.I. Moon, Y.G. Chung, M.Y. Chang, B.S. Han, S. Ko, E. Yang, K.Y. Cha, R. Lanza, and K.S. Kim. 2009a. Generation of human induced pluripotent stem cells by direct delivery of reprogramming proteins. *Cell Stem Cell*. 4:472-476.

Kim, J., J. Chu, X. Shen, J. Wang, and S.H. Orkin. 2008. An extended transcriptional network for pluripotency of embryonic stem cells. *Cell*. 132:1049-1061.

Kim, J.E., P.R. Shepherd, and C. Chaussade. 2009b. Investigating the role of class-IA PI 3-kinase isoforms in adipocyte differentiation. *Biochem Biophys Res Commun*. 379:830-834.

Kingham, E., and M. Welham. 2009. Distinct roles for isoforms of the catalytic subunit of class-IA PI3K in the regulation of behaviour of murine embryonic stem cells. *J Cell Sci*. 122:2311-2321.

Kittler, R., G. Putz, L. Pelletier, I. Poser, A.K. Heninger, D. Drechsel, S. Fischer, I. Konstantinova, B. Habermann, H. Grabner, M.L. Yaspo, H. Himmelbauer, B. Korn, K. Neugebauer, M.T. Pisabarro, and F. Buchholz. 2004. An endoribonuclease-prepared siRNA screen in human cells identifies genes essential for cell division. *Nature*. 432:1036-1040.

Klippel, A., C. Reinhard, W.M. Kavanaugh, G. Apell, M.A. Escobedo, and L.T. Williams. 1996. Membrane localization of phosphatidylinositol 3-kinase is sufficient to activate multiple signal-transducing kinase pathways. *Mol Cell Biol*. 16:4117-4127.

Knight, Z.A., B. Gonzalez, M.E. Feldman, E.R. Zunder, D.D. Goldenberg, O. Williams, R. Loewith, D. Stokoe, A. Balla, B. Toth, T. Balla, W.A. Weiss, R.L. Williams, and K.M. Shokat. 2006. A pharmacological map of the PI3-K family defines a role for p110alpha in insulin signaling. *Cell*. 125:733-747.

Knight, Z.A., and K.M. Shokat. 2007. Chemically targeting the PI3K family. *Biochem Soc Trans*. 35:245-249.

Ko, K., M.J. Arauzo-Bravo, N. Tapia, J. Kim, Q. Lin, C. Bernemann, D.W. Han, L. Gentile, P. Reinhardt, B. Greber, R.K. Schneider, S. Kliesch, M. Zenke, and H.R. Scholer. 2010. Human adult germline stem cells in question. *Nature*. 465:E1; discussion E3.

Ko, K., N. Tapia, G. Wu, J.B. Kim, M.J. Bravo, P. Sasse, T. Glaser, D. Ruau, D.W. Han, B. Greber, K. Hausdorfer, V. Sebastiano, M. Stehling, B.K. Fleischmann, O. Brustle, M. Zenke, and H.R. Scholer. 2009. Induction of pluripotency in adult unipotent germline stem cells. *Cell Stem Cell*. 5:87-96.

Ko, M.S., Zalzman, M. 2011. Methods for enhancing genome stability and telomere elongation in embyonic stem cells. International Patent WO2011028880 (A2).

Komander, D., A. Fairservice, M. Deak, G.S. Kular, A.R. Prescott, C. Peter Downes, S.T. Safrany, D.R. Alessi, and D.M. van Aalten. 2004. Structural insights into the regulation of PDK1 by phosphoinositides and inositol phosphates. *EMBO J*. 23:3918-3928.

Kontaki, H., and I. Talianidis. 2010. Lysine methylation regulates E2F1-induced cell death. *Mol Cell*. 39:152-160.

Korsisaari, N., and T.P. Makela. 2000. Interactions of Cdk7 and Kin28 with Hint/PKCI-1 and Hnt1 histidine triad proteins. *J Biol Chem*. 275:34837-34840.

Kunath, T., M.K. Saba-El-Leil, M. Almousailleakh, J. Wray, S. Meloche, and A. Smith. 2007. FGF stimulation of the Erk1/2 signalling cascade triggers transition of pluripotent embryonic stem cells from self-renewal to lineage commitment. *Development*. 134:2895-2902.

Labosky, P.A., D.P. Barlow, and B.L. Hogan. 1994. Mouse embryonic germ (EG) cell lines: transmission through the germline and differences in the methylation imprint of insulin-like growth factor 2 receptor (Igf2r) gene compared with embryonic stem (ES) cell lines. *Development*. 120:3197-3204.

Laemmli, U.K. 1970. Cleavage of structural proteins during the assembly of the head of bacteriophage T4. *Nature*. 227:680-685.

Laurent, L.C., I. Ulitsky, I. Slavin, H. Tran, A. Schork, R. Morey, C. Lynch, J.V. Harness, S. Lee, M.J. Barrero, S. Ku, M. Martynova, R. Semechkin, V. Galat, J. Gottesfeld, J.C. Izpisua Belmonte, C. Murry, H.S. Keirstead, H.S. Park, U. Schmidt, A.L. Laslett, F.J. Muller, C.M. Nievergelt, R. Shamir, and J.F. Loring. 2011. Dynamic changes in the copy number of pluripotency and cell proliferation genes in human ESCs and iPSCs during reprogramming and time in culture. *Cell Stem Cell*. 8:106-118.

Lavial, F., H. Acloque, F. Bertocchini, D.J. Macleod, S. Boast, E. Bachelard, G. Montillet, S. Thenot, H.M. Sang, C.D. Stern, J. Samarut, and B. Pain. 2007. The Oct4 homologue PouV and Nanog regulate pluripotency in chicken embryonic stem cells. *Development*. 134:3549-3563.

Leach, B.E., J.H. Ford, and A.J. Whiffen. 1947. Actidione, an antibiotic from Streptomyces griseus. *J Am Chem Soc*. 69:474.

Lee, K.S., H.K. Lee, J.S. Hayflick, Y.C. Lee, and K.D. Puri. 2006. Inhibition of phosphoinositide 3-kinase delta attenuates allergic airway inflammation and hyperresponsiveness in murine asthma model. *FASEB J*. 20:455-465.

Lee, M.G., C. Wynder, N. Cooch, and R. Shiekhattar. 2005. An essential role for CoREST in nucleosomal histone 3 lysine 4 demethylation. *Nature*. 437:432-435.

Lengner, C.J., A.A. Gimelbrant, J.A. Erwin, A.W. Cheng, M.G. Guenther, G.G. Welstead, R. Alagappan, G.M. Frampton, P. Xu, J. Muffat, S. Santagata, D. Powers, C.B. Barrett, R.A. Young, J.T. Lee, R. Jaenisch, and M. Mitalipova. 2010. Derivation of pre-X inactivation human embryonic stem cells under physiological oxygen concentrations. *Cell*. 141:872-883.

Li, D.M., and H. Sun. 1997. TEP1, encoded by a candidate tumor suppressor locus, is a novel protein tyrosine phosphatase regulated by transforming growth factor beta. *Cancer Res*. 57:2124-2129.

Li, H., A.S. Balajee, T. Su, B. Cen, T.K. Hei, and I.B. Weinstein. 2008a. The HINT1 tumor suppressor regulates both gamma-H2AX and ATM in response to DNA damage. *J Cell Biol*. 183:253-265.

Li, H., Y. Zhang, T. Su, R.M. Santella, and I.B. Weinstein. 2006. Hint1 is a haplo-insufficient tumor suppressor in mice. *Oncogene*. 25:713-721.

Li, P., C. Tong, R. Mehrian-Shai, L. Jia, N. Wu, Y. Yan, R.E. Maxson, E.N. Schulze, H. Song, C.L. Hsieh, M.F. Pera, and Q.L. Ying. 2008b. Germline competent embryonic stem cells derived from rat blastocysts. *Cell*. 135:1299-1310.

Li, Y., J. McClintick, L. Zhong, H.J. Edenberg, M.C. Yoder, and R.J. Chan. 2005. Murine embryonic stem cell differentiation is promoted by SOCS-3 and inhibited by the zinc finger transcription factor Klf4. *Blood*. 105:635-637.

Lima, C.D., M.G. Klein, I.B. Weinstein, and W.A. Hendrickson. 1996. Three-dimensional structure of human protein kinase C interacting protein 1, a member of the HIT family of proteins. *Proc Natl Acad Sci U S A*. 93:5357-5362.

Lindsley, R.C., J.G. Gill, M. Kyba, T.L. Murphy, and K.M. Murphy. 2006. Canonical Wnt signaling is required for development of embryonic stem cell-derived mesoderm. *Development*. 133:3787-3796.

Lindwasser, O.W., and M.D. Resh. 2002. Myristoylation as a target for inhibiting HIV assembly: unsaturated fatty acids block viral budding. *Proc Natl Acad Sci U S A*. 99:13037-13042.

Liu, L., S.M. Bailey, M. Okuka, P. Munoz, C. Li, L. Zhou, C. Wu, E. Czerwiec, L. Sandler, A. Seyfang, M.A. Blasco, and D.L. Keefe. 2007. Telomere lengthening early in development. *Nat Cell Biol*. 9:1436-1441.

Loh, Y.H., Q. Wu, J.L. Chew, V.B. Vega, W. Zhang, X. Chen, G. Bourque, J. George, B. Leong, J. Liu, K.Y. Wong, K.W. Sung, C.W. Lee, X.D. Zhao, K.P. Chiu, L. Lipovich, V.A. Kuznetsov, P. Robson, L.W. Stanton, C.L. Wei, Y. Ruan, B. Lim, and H.H. Ng. 2006. The Oct4 and Nanog transcription network regulates pluripotency in mouse embryonic stem cells. *Nat Genet*. 38:431-440.

Loh, Y.H., W. Zhang, X. Chen, J. George, and H.H. Ng. 2007. Jmjd1a and Jmjd2c histone H3 Lys 9 demethylases regulate self-renewal in embryonic stem cells. *Genes Dev*. 21:2545-2557.

MacDonald, B.T., K. Tamai, and X. He. 2009. Wnt/beta-catenin signaling: components, mechanisms, and diseases. *Dev Cell*. 17:9-26.

Mahadevaiah, S.K., J.M. Turner, F. Baudat, E.P. Rogakou, P. de Boer, J. Blanco-Rodriguez, M. Jasin, S. Keeney, W.M. Bonner, and P.S. Burgoyne. 2001. Recombinational DNA double-strand breaks in mice precede synapsis. *Nat Genet*. 27:271-276.

Mani-Telang, P., M. Sutrias-Grau, G. Williams, and D.N. Arnosti. 2007. Role of NAD binding and catalytic residues in the C-terminal binding protein corepressor. *FEBS Lett*. 581:5241-5246.

Mark, M., N.B. Ghyselinck, and P. Chambon. 2006. Function of retinoid nuclear receptors: lessons from genetic and pharmacological dissections of the retinoic acid signaling pathway during mouse embryogenesis. *Annu Rev Pharmacol Toxicol*. 46:451-480.

Marone, R., V. Cmiljanovic, B. Giese, and M.P. Wymann. 2008. Targeting phosphoinositide 3-kinase: moving towards therapy. *Biochim Biophys Acta*. 1784:159-185.

Marson, A., S.S. Levine, M.F. Cole, G.M. Frampton, T. Brambrink, S. Johnstone, M.G. Guenther, W.K. Johnston, M. Wernig, J. Newman, J.M. Calabrese, L.M. Dennis, T.L. Volkert, S. Gupta, J. Love, N. Hannett, P.A. Sharp, D.P. Bartel, R. Jaenisch, and R.A. Young. 2008. Connecting microRNA genes to the core transcriptional regulatory circuitry of embryonic stem cells. *Cell*. 134:521-533.

Martin, G.R. 1981. Isolation of a pluripotent cell line from early mouse embryos cultured in medium conditioned by teratocarcinoma stem cells. *Proc Natl Acad Sci U S A*. 78:7634-7638.

Martin, G.R., and M.J. Evans. 1975. Differentiation of clonal lines of teratocarcinoma cells: formation of embryoid bodies in vitro. *Proc Natl Acad Sci U S A*. 72:1441-1445.

Martinez, J., A. Patkaniowska, H. Urlaub, R. Luhrmann, and T. Tuschl. 2002. Single-stranded antisense siRNAs guide target RNA cleavage in RNAi. *Cell*. 110:563-574.

Marygold, S.J., and S.J. Leevers. 2002. Growth signaling: TSC takes its place. *Curr Biol*. 12:R785-787.

Masui, S., S. Ohtsuka, R. Yagi, K. Takahashi, M.S. Ko, and H. Niwa. 2008. Rex1/Zfp42 is dispensable for pluripotency in mouse ES cells. *BMC Dev Biol*. 8:45.

Masui, S., D. Shimosato, Y. Toyooka, R. Yagi, K. Takahashi, and H. Niwa. 2005. An efficient system to establish multiple embryonic stem cell lines carrying an inducible expression unit. *Nucleic Acids Res*. 33:e43.

Matsuda, T., T. Nakamura, K. Nakao, T. Arai, M. Katsuki, T. Heike, and T. Yokota. 1999. STAT3 activation is sufficient to maintain an undifferentiated state of mouse embryonic stem cells. *EMBO J*. 18:4261-4269.

Matsui, Y., K. Zsebo, and B.L. Hogan. 1992. Derivation of pluripotential embryonic stem cells from murine primordial germ cells in culture. *Cell*. 70:841-847.

McManus, E.J., B.J. Collins, P.R. Ashby, A.R. Prescott, V. Murray-Tait, L.J. Armit, J.S. Arthur, and D.R. Alessi. 2004. The in vivo role of PtdIns(3,4,5)P3 binding to PDK1 PH domain defined by knockin mutation. *EMBO J*. 23:2071-2082.

Melton, C., R.L. Judson, and R. Blelloch. 2010. Opposing microRNA families regulate self-renewal in mouse embryonic stem cells. *Nature*. 463:621-626.

Metzger, E., M. Wissmann, N. Yin, J.M. Muller, R. Schneider, A.H. Peters, T. Gunther, R. Buettner, and R. Schule. 2005. LSD1 demethylates repressive histone marks to promote androgen-receptor-dependent transcription. *Nature*. 437:436-439.

Mikkelsen, T.S., J. Hanna, X. Zhang, M. Ku, M. Wernig, P. Schorderet, B.E. Bernstein, R. Jaenisch, E.S. Lander, and A. Meissner. 2008. Dissecting direct reprogramming through integrative genomic analysis. *Nature*. 454:49-55.

Mitsui, K., Y. Tokuzawa, H. Itoh, K. Segawa, M. Murakami, K. Takahashi, M. Maruyama, M. Maeda, and S. Yamanaka. 2003. The homeoprotein Nanog is required for maintenance of pluripotency in mouse epiblast and ES cells. *Cell*. 113:631-642.

Mora, A., D. Komander, D.M. van Aalten, and D.R. Alessi. 2004. PDK1, the master regulator of AGC kinase signal transduction. *Semin Cell Dev Biol*. 15:161-170.

Mosmann, T. 1983. Rapid colorimetric assay for cellular growth and survival: application to proliferation and cytotoxicity assays. *J Immunol Methods*. 65:55-63.

Munoz, P., R. Blanco, G. de Carcer, S. Schoeftner, R. Benetti, J.M. Flores, M. Malumbres, and M.A. Blasco. 2009. TRF1 controls telomere length and mitotic fidelity in epithelial homeostasis. *Mol Cell Biol*. 29:1608-1625.

Murray, D., N. Ben-Tal, B. Honig, and S. McLaughlin. 1997. Electrostatic interaction of myristoylated proteins with membranes: simple physics, complicated biology. *Structure*. 5:985-989.

Najm, F.J., J.G. Chenoweth, P.D. Anderson, J.H. Nadeau, R.W. Redline, R.D. McKay, and P.J. Tesar. 2011. Isolation of epiblast stem cells from preimplantation mouse embryos. *Cell Stem Cell*. 8:318-325.

Ng, H.H., and M.A. Surani. 2011. The transcriptional and signalling networks of pluripotency. *Nat Cell Biol*. 13:490-496.

Nibu, Y., H. Zhang, and M. Levine. 1998. Interaction of short-range repressors with Drosophila CtBP in the embryo. *Science*. 280:101-104.

Nichols, J., I. Chambers, T. Taga, and A. Smith. 2001. Physiological rationale for responsiveness of mouse embryonic stem cells to gp130 cytokines. *Development*. 128:2333-2339.

Nichols, J., J. Silva, M. Roode, and A. Smith. 2009. Suppression of Erk signalling promotes ground state pluripotency in the mouse embryo. *Development*. 136:3215-3222.

Nichols, J., B. Zevnik, K. Anastassiadis, H. Niwa, D. Klewe-Nebenius, I. Chambers, H. Scholer, and A. Smith. 1998. Formation of pluripotent stem cells in the mammalian embryo depends on the POU transcription factor Oct4. *Cell*. 95:379-391.

Nishiyama, A., L. Xin, A.A. Sharov, M. Thomas, G. Mowrer, E. Meyers, Y. Piao, S. Mehta, S. Yee, Y. Nakatake, C. Stagg, L. Sharova, L.S. Correa-Cerro, U. Bassey, H. Hoang, E. Kim, R. Tapnio, Y. Qian, D. Dudekula, M. Zalzman, M. Li, G. Falco, H.T. Yang, S.L. Lee, M. Monti, I. Stanghellini, M.N. Islam, R. Nagaraja, I. Goldberg, W. Wang, D.L. Longo, D. Schlessinger, and M.S. Ko. 2009. Uncovering early response of gene regulatory networks in ESCs by systematic induction of transcription factors. *Cell Stem Cell*. 5:420-433.

Niwa, H. 2007. How is pluripotency determined and maintained? *Development*. 134:635-646.

Niwa, H., T. Burdon, I. Chambers, and A. Smith. 1998. Self-renewal of pluripotent embryonic stem cells is mediated via activation of STAT3. *Genes Dev*. 12:2048-2060.

Niwa, H., S. Masui, I. Chambers, A.G. Smith, and J. Miyazaki. 2002. Phenotypic complementation establishes requirements for specific POU domain and generic transactivation function of Oct-3/4 in embryonic stem cells. *Mol Cell Biol*. 22:1526-1536.

Niwa, H., J. Miyazaki, and A.G. Smith. 2000. Quantitative expression of Oct-3/4 defines differentiation, dedifferentiation or self-renewal of ES cells. *Nat Genet*. 24:372-376.

Niwa, H., K. Ogawa, D. Shimosato, and K. Adachi. 2009. A parallel circuit of LIF signalling pathways maintains pluripotency of mouse ES cells. *Nature*. 460:118-122.

Niwa, H., K. Yamamura, and J. Miyazaki. 1991. Efficient selection for high-expression transfectants with a novel eukaryotic vector. *Gene*. 108:193-199.

Norton, J.D. 2000. ID helix-loop-helix proteins in cell growth, differentiation and tumorigenesis. *J Cell Sci*. 113 (Pt 22):3897-3905.

Obrig, T.G., W.J. Culp, W.L. McKeehan, and B. Hardesty. 1971. The mechanism by which cycloheximide and related glutarimide antibiotics inhibit peptide synthesis on reticulocyte ribosomes. *J Biol Chem*. 246:174-181.

Ogawa, K., H. Matsui, S. Ohtsuka, and H. Niwa. 2004. A novel mechanism for regulating clonal propagation of mouse ES cells. *Genes Cells*. 9:471-477.

Ogawa, K., R. Nishinakamura, Y. Iwamatsu, D. Shimosato, and H. Niwa. 2006. Synergistic action of Wnt and LIF in maintaining pluripotency of mouse ES cells. *Biochem Biophys Res Commun*. 343:159-166.

Okamoto, K., H. Okazawa, A. Okuda, M. Sakai, M. Muramatsu, and H. Hamada. 1990. A novel octamer binding transcription factor is differentially expressed in mouse embryonic cells. *Cell*. 60:461-472.

Okita, K., T. Ichisaka, and S. Yamanaka. 2007. Generation of germline-competent induced pluripotent stem cells. *Nature*. 448:313-317.

Okita, K., M. Nakagawa, H. Hyenjong, T. Ichisaka, and S. Yamanaka. 2008. Generation of mouse induced pluripotent stem cells without viral vectors. *Science*. 322:949-953.

Okkenhaug, K., A. Bilancio, G. Farjot, H. Priddle, S. Sancho, E. Peskett, W. Pearce, S.E. Meek, A. Salpekar, M.D. Waterfield, A.J. Smith, and B. Vanhaesebroeck. 2002. Impaired B and T cell antigen receptor signaling in p110delta PI 3-kinase mutant mice. *Science*. 297:1031-1034.

Olovnikov, A.M. 1996. Telomeres, telomerase, and aging: origin of the theory. *Exp Gerontol*. 31:443-448.

Paling, N., H. Wheadon, H. Bone, and M. Welham. 2004. Regulation of embryonic stem cell self-renewal by phosphoinositide 3-kinase-dependent signaling. *J Biol Chem*. 279:48063-48070.

Parsons, D.W., T.L. Wang, Y. Samuels, A. Bardelli, J.M. Cummins, L. DeLong, N. Silliman, J. Ptak, S. Szabo, J.K. Willson, S. Markowitz, K.W. Kinzler, B. Vogelstein, C. Lengauer,

and V.E. Velculescu. 2005. Colorectal cancer: mutations in a signalling pathway. *Nature*. 436:792.

Paull, T.T., E.P. Rogakou, V. Yamazaki, C.U. Kirchgessner, M. Gellert, and W.M. Bonner. 2000. A critical role for histone H2AX in recruitment of repair factors to nuclear foci after DNA damage. *Curr Biol*. 10:886-895.

Paulson, R.F., S. Vesely, K.A. Siminovitch, and A. Bernstein. 1996. Signalling by the W/Kit receptor tyrosine kinase is negatively regulated in vivo by the protein tyrosine phosphatase Shp1. *Nat Genet*. 13:309-315.

Pease, S., P. Braghetta, D. Gearing, D. Grail, and R.L. Williams. 1990. Isolation of embryonic stem (ES) cells in media supplemented with recombinant leukemia inhibitory factor (LIF). *Dev Biol*. 141:344-352.

Peitzsch, R.M., and S. McLaughlin. 1993. Binding of acylated peptides and fatty acids to phospholipid vesicles: pertinence to myristoylated proteins. *Biochemistry*. 32:10436-10443.

Pengue, G., V. Calabro, P.C. Bartoli, A. Pagliuca, and L. Lania. 1994. Repression of transcriptional activity at a distance by the evolutionarily conserved KRAB domain present in a subfamily of zinc finger proteins. *Nucleic Acids Res*. 22:2908-2914.

Perez, E.E., J. Wang, J.C. Miller, Y. Jouvenot, K.A. Kim, O. Liu, N. Wang, G. Lee, V.V. Bartsevich, Y.L. Lee, D.Y. Guschin, I. Rupniewski, A.J. Waite, C. Carpenito, R.G. Carroll, J.S. Orange, F.D. Urnov, E.J. Rebar, D. Ando, P.D. Gregory, J.L. Riley, M.C. Holmes, and C.H. June. 2008. Establishment of HIV-1 resistance in CD4+ T cells by genome editing using zinc-finger nucleases. *Nat Biotechnol*. 26:808-816.

Plath, K., and W.E. Lowry. 2011. Progress in understanding reprogramming to the induced pluripotent state. *Nat Rev Genet*. 12:253-265.

Popkie, A.P., L.C. Zeidner, A.M. Albrecht, A. D'Ippolito, S. Eckardt, D.E. Newsom, J. Groden, B.W. Doble, B. Aronow, K.J. McLaughlin, P. White, and C.J. Phiel. 2010. Phosphatidylinositol 3-kinase (PI3K) signaling via glycogen synthase kinase-3 (Gsk-3) regulates DNA methylation of imprinted loci. *J Biol Chem*. 285:41337-41347.

Pritsker, M., N. Ford, H. Jenq, and I. Lemischka. 2006. Genomewide gain-of-function genetic screen identifies functionally active genes in mouse embryonic stem cells. *Proc Natl Acad Sci U S A*. 103:6946-6951.

Qi, X., T.G. Li, J. Hao, J. Hu, J. Wang, H. Simmons, S. Miura, Y. Mishina, and G.Q. Zhao. 2004. BMP4 supports self-renewal of embryonic stem cells by inhibiting mitogen-activated protein kinase pathways. *Proc Natl Acad Sci U S A*. 101:6027-6032.

Qu, C.K., and G.S. Feng. 1998. Shp-2 has a positive regulatory role in ES cell differentiation and proliferation. *Oncogene*. 17:433-439.

Quinlan, K.G., A. Verger, A. Kwok, S.H. Lee, J. Perdomo, M. Nardini, M. Bolognesi, and M. Crossley. 2006. Role of the C-terminal binding protein PXDLS motif binding cleft in protein interactions and transcriptional repression. *Mol Cell Biol*. 26:8202-8213.

Reinholdt, L.G., and J.C. Schimenti. 2005. Mei1 is epistatic to Dmc1 during mouse meiosis. *Chromosoma*. 114:127-134.

Resnick, J.L., L.S. Bixler, L. Cheng, and P.J. Donovan. 1992. Long-term proliferation of mouse primordial germ cells in culture. *Nature*. 359:550-551.

Riley, J.K., M.O. Carayannopoulos, A.H. Wyman, M. Chi, C.K. Ratajczak, and K.H. Moley. 2005. The PI3K/Akt pathway is present and functional in the preimplantation mouse embryo. *Dev Biol*. 284:377-386.

Robertson, A.D., S. JACKSON, V. KENCHE, C. YAIP, H. PARBAHARAN, and P. THOMPSON. 2001. Therapeutic morpholino-substituted compounds. *Pat., WO/2001/053266.*

Rodriguez-Viciana, P., P.H. Warne, R. Dhand, B. Vanhaesebroeck, I. Gout, M.J. Fry, M.D. Waterfield, and J. Downward. 1994. Phosphatidylinositol-3-OH kinase as a direct target of Ras. *Nature*. 370:527-532.

Roehm, N.W., G.H. Rodgers, S.M. Hatfield, and A.L. Glasebrook. 1991. An improved colorimetric assay for cell proliferation and viability utilizing the tetrazolium salt XTT. *J Immunol Methods*. 142:257-265.

Rogers, M.B., B.A. Hosler, and L.J. Gudas. 1991. Specific expression of a retinoic acid-regulated, zinc-finger gene, Rex-1, in preimplantation embryos, trophoblast and spermatocytes. *Development*. 113:815-824.

Rommel, C., M. Camps, and H. Ji. 2007. PI3K delta and PI3K gamma: partners in crime in inflammation in rheumatoid arthritis and beyond? *Nat Rev Immunol*. 7:191-201.

Rosner, M.H., M.A. Vigano, K. Ozato, P.M. Timmons, F. Poirier, P.W. Rigby, and L.M. Staudt. 1990. A POU-domain transcription factor in early stem cells and germ cells of the mammalian embryo. *Nature*. 345:686-692.

Rossant, J., and P.P. Tam. 2004. Emerging asymmetry and embryonic patterning in early mouse development. *Dev Cell*. 7:155-164.

Rubinfeld, B., I. Albert, E. Porfiri, C. Fiol, S. Munemitsu, and P. Polakis. 1996. Binding of GSK3beta to the APC-beta-catenin complex and regulation of complex assembly. *Science*. 272:1023-1026.

Ruckle, T., M.K. Schwarz, and C. Rommel. 2006. PI3Kgamma inhibition: towards an 'aspirin of the 21st century'? *Nat Rev Drug Discov*. 5:903-918.

Ruzinova, M.B., and R. Benezra. 2003. Id proteins in development, cell cycle and cancer. *Trends Cell Biol*. 13:410-418.

Ryan, A.K., and M.G. Rosenfeld. 1997. POU domain family values: flexibility, partnerships, and developmental codes. *Genes Dev*. 11:1207-1225.

Sadhu, C., K. DICK, J. TREIBERG, C. SOWELL, Gregor, E. KESICKI, A., and A. OLIVER. 2001. Inhibitors of human phosphatidyl-inositol 3-kinase delta. *Pat., WO/2001/081346.*

Sadhu, C., B. Masinovsky, K. Dick, C.G. Sowell, and D.E. Staunton. 2003. Essential role of phosphoinositide 3-kinase delta in neutrophil directional movement. *J Immunol*. 170:2647-2654.

Saez, E., D. No, A. West, and R.M. Evans. 1997. Inducible gene expression in mammalian cells and transgenic mice. *Curr Opin Biotechnol*. 8:608-616.

Samuels, Y., Z. Wang, A. Bardelli, N. Silliman, J. Ptak, S. Szabo, H. Yan, A. Gazdar, S.M. Powell, G.J. Riggins, J.K. Willson, S. Markowitz, K.W. Kinzler, B. Vogelstein, and V.E. Velculescu. 2004. High frequency of mutations of the PIK3CA gene in human cancers. *Science*. 304:554.

Sato, N., L. Meijer, L. Skaltsounis, P. Greengard, and A.H. Brivanlou. 2004. Maintenance of pluripotency in human and mouse embryonic stem cells through activation of Wnt signaling by a pharmacological GSK-3-specific inhibitor. *Nat Med*. 10:55-63.

Sauer, B. 1987. Functional expression of the cre-lox site-specific recombination system in the yeast Saccharomyces cerevisiae. *Mol Cell Biol*. 7:2087-2096.

Savatier, P., S. Huang, L. Szekely, K.G. Wiman, and J. Samarut. 1994. Contrasting patterns of retinoblastoma protein expression in mouse embryonic stem cells and embryonic fibroblasts. *Oncogene*. 9:809-818.

Savatier, P., H. Lapillonne, L. Jirmanova, L. Vitelli, and J. Samarut. 2002. Analysis of the cell cycle in mouse embryonic stem cells. *Methods Mol Biol*. 185:27-33.

Schaeper, U., T. Subramanian, L. Lim, J.M. Boyd, and G. Chinnadurai. 1998. Interaction between a cellular protein that binds to the C-terminal region of adenovirus E1A (CtBP) and a novel cellular protein is disrupted by E1A through a conserved PLDLS motif. *J Biol Chem*. 273:8549-8552.

Scholer, H.R., A.K. Hatzopoulos, R. Balling, N. Suzuki, and P. Gruss. 1989. A family of octamer-specific proteins present during mouse embryogenesis: evidence for germline-specific expression of an Oct factor. *EMBO J*. 8:2543-2550.

Scholer, H.R., S. Ruppert, N. Suzuki, K. Chowdhury, and P. Gruss. 1990. New type of POU domain in germ line-specific protein Oct-4. *Nature*. 344:435-439.

Scudiero, D.A., R.H. Shoemaker, K.D. Paull, A. Monks, S. Tierney, T.H. Nofziger, M.J. Currens, D. Seniff, and M.R. Boyd. 1988. Evaluation of a soluble tetrazolium/formazan assay for cell growth and drug sensitivity in culture using human and other tumor cell lines. *Cancer Res*. 48:4827-4833.

Scutt, A., and P. Bertram. 1999. Basic fibroblast growth factor in the presence of dexamethasone stimulates colony formation, expansion, and osteoblastic differentiation by rat bone marrow stromal cells. *Calcif Tissue Int*. 64:69-77.

Seandel, M., D. James, S.V. Shmelkov, I. Falciatori, J. Kim, S. Chavala, D.S. Scherr, F. Zhang, R. Torres, N.W. Gale, G.D. Yancopoulos, A. Murphy, D.M. Valenzuela, R.M. Hobbs, P.P. Pandolfi, and S. Rafii. 2007. Generation of functional multipotent adult stem cells from GPR125+ germline progenitors. *Nature*. 449:346-350.

Sharif, J., M. Endoh, and H. Koseki. 2011. Epigenetic memory meets G2/M: to remember or to forget? *Dev Cell*. 20:5-6.

Shi, Y., F. Lan, C. Matson, P. Mulligan, J.R. Whetstine, P.A. Cole, and R.A. Casero. 2004. Histone demethylation mediated by the nuclear amine oxidase homolog LSD1. *Cell*. 119:941-953.

Shi, Y., and J. Massague. 2003. Mechanisms of TGF-beta signaling from cell membrane to the nucleus. *Cell*. 113:685-700.

Shi, Y., J. Sawada, G. Sui, B. Affar el, J.R. Whetstine, F. Lan, H. Ogawa, M.P. Luke, and Y. Nakatani. 2003. Coordinated histone modifications mediated by a CtBP co-repressor complex. *Nature*. 422:735-738.

Shi, Y.J., C. Matson, F. Lan, S. Iwase, T. Baba, and Y. Shi. 2005. Regulation of LSD1 histone demethylase activity by its associated factors. *Mol Cell*. 19:857-864.

Silva, J., O. Barrandon, J. Nichols, J. Kawaguchi, T.W. Theunissen, and A. Smith. 2008. Promotion of reprogramming to ground state pluripotency by signal inhibition. *PLoS Biol*. 6:e253.

Silva, J., J. Nichols, T.W. Theunissen, G. Guo, A.L. van Oosten, O. Barrandon, J. Wray, S. Yamanaka, I. Chambers, and A. Smith. 2009. Nanog is the gateway to the pluripotent ground state. *Cell*. 138:722-737.

Silva, J., and A. Smith. 2008. Capturing pluripotency. *Cell*. 132:532-536.

Singh, A.M., T. Hamazaki, K.E. Hankowski, and N. Terada. 2007. A heterogeneous expression pattern for Nanog in embryonic stem cells. *Stem Cells*. 25:2534-2542.

Singla, D.K., D.J. Schneider, M.M. LeWinter, and B.E. Sobel. 2006. wnt3a but not wnt11 supports self-renewal of embryonic stem cells. *Biochem Biophys Res Commun*. 345:789-795.

Singla, D.K., R.D. Singla, and D.E. McDonald. 2008. Factors released from embryonic stem cells inhibit apoptosis in H9c2 cells through PI3K/Akt but not ERK pathway. *Am J Physiol Heart Circ Physiol*. 295:H907-913.

Smith, A., J. Heath, D. Donaldson, G. Wong, J. Moreau, M. Stahl, and D. Rogers. 1988. Inhibition of pluripotential embryonic stem cell differentiation by purified polypeptides. *Nature*. 336:688-690.

Smith, A., Ying Qi-Long. 2009. CULTURE MEDIUM CONTAINING KINASE INHIBITOR, AND USE THEREOF. *United States Patent Application Publication*. US 2009/0130759 A1.

Smith, A.G. 2001. Embryo-derived stem cells: of mice and men. *Annu Rev Cell Dev Biol*. 17:435-462.

Solter, D., N. Skreb, and I. Damjanov. 1970. Extrauterine growth of mouse egg-cylinders results in malignant teratoma. *Nature*. 227:503-504.

Stadtfeld, M., K. Brennand, and K. Hochedlinger. 2008a. Reprogramming of pancreatic beta cells into induced pluripotent stem cells. *Curr Biol*. 18:890-894.

Stadtfeld, M., M. Nagaya, J. Utikal, G. Weir, and K. Hochedlinger. 2008b. Induced pluripotent stem cells generated without viral integration. *Science*. 322:945-949.

Stahl, M., P.F. Dijkers, G.J. Kops, S.M. Lens, P.J. Coffer, B.M. Burgering, and R.H. Medema. 2002. The forkhead transcription factor FoxO regulates transcription of p27Kip1 and Bim in response to IL-2. *J Immunol*. 168:5024-5031.

Stambolic, V., A. Suzuki, J.L. de la Pompa, G.M. Brothers, C. Mirtsos, T. Sasaki, J. Ruland, J.M. Penninger, D.P. Siderovski, and T.W. Mak. 1998. Negative regulation of PKB/Akt-dependent cell survival by the tumor suppressor PTEN. *Cell*. 95:29-39.

Stavridis, M.P., J.S. Lunn, B.J. Collins, and K.G. Storey. 2007. A discrete period of FGF-induced Erk1/2 signalling is required for vertebrate neural specification. *Development*. 134:2889-2894.

Stephens, L., K. Anderson, D. Stokoe, H. Erdjument-Bromage, G.F. Painter, A.B. Holmes, P.R. Gaffney, C.B. Reese, F. McCormick, P. Tempst, J. Coadwell, and P.T. Hawkins. 1998. Protein kinase B kinases that mediate phosphatidylinositol 3,4,5-trisphosphate-dependent activation of protein kinase B. *Science*. 279:710-714.

Stevens, L.C. 1970. Experimental production of testicular teratomas in mice of strains 129, A/He, and their F1 hybrids. *J Natl Cancer Inst*. 44:923-929.

Stewart, C.L., P. Kaspar, L.J. Brunet, H. Bhatt, I. Gadi, F. Kontgen, and S.J. Abbondanzo. 1992. Blastocyst implantation depends on maternal expression of leukaemia inhibitory factor. *Nature*. 359:76-79.

Stiles, B., V. Gilman, N. Khanzenzon, R. Lesche, A. Li, R. Qiao, X. Liu, and H. Wu. 2002. Essential role of AKT-1/protein kinase B alpha in PTEN-controlled tumorigenesis. *Mol Cell Biol*. 22:3842-3851.

Storm, M., H. Bone, C. Beck, P. Bourillot, V. Schreiber, T. Damiano, A. Nelson, P. Savatier, and M. Welham. 2007. Regulation of Nanog expression by phosphoinositide 3-kinase-dependent signaling in murine embryonic stem cells. *J Biol Chem*. 282:6265-6273.

Storm, M., B. Kumpfmueller, B. Thompson, R. Kolde, J. Vilo, O. Hummel, H. Schulz, and M. Welham. 2009. Characterization of the phosphoinositide 3-kinase-dependent transcriptome in murine embryonic stem cells: identification of novel regulators of pluripotency. *Stem Cells*. 27:764-775.

Strumpf, D., C.A. Mao, Y. Yamanaka, A. Ralston, K. Chawengsaksophak, F. Beck, and J. Rossant. 2005. Cdx2 is required for correct cell fate specification and differentiation of trophectoderm in the mouse blastocyst. *Development*. 132:2093-2102.

Suda, Y., M. Suzuki, Y. Ikawa, and S. Aizawa. 1987. Mouse embryonic stem cells exhibit indefinite proliferative potential. *J Cell Physiol*. 133:197-201.

Sun, H., R. Lesche, D.M. Li, J. Liliental, H. Zhang, J. Gao, N. Gavrilova, B. Mueller, X. Liu, and H. Wu. 1999. PTEN modulates cell cycle progression and cell survival by regulating phosphatidylinositol 3,4,5,-trisphosphate and Akt/protein kinase B signaling pathway. *Proc Natl Acad Sci U S A*. 96:6199-6204.

Taapken, S.M., B.S. Nisler, M.A. Newton, T.L. Sampsell-Barron, K.A. Leonhard, E.M. McIntire, and K.D. Montgomery. 2011. Karotypic abnormalities in human induced pluripotent stem cells and embryonic stem cells. *Nat Biotechnol*. 29:313-314.

Tada, M., Y. Takahama, K. Abe, N. Nakatsuji, and T. Tada. 2001. Nuclear reprogramming of somatic cells by in vitro hybridization with ES cells. *Curr Biol*. 11:1553-1558.

Takahashi, K. 2010. Direct reprogramming 101. *Dev Growth Differ*. 52:319-333.

Takahashi, K., K. Mitsui, and S. Yamanaka. 2003. Role of ERas in promoting tumour-like properties in mouse embryonic stem cells. *Nature*. 423:541-545.

Takahashi, K., M. Murakami, and S. Yamanaka. 2005. Role of the phosphoinositide 3-kinase pathway in mouse embryonic stem (ES) cells. *Biochem Soc Trans*. 33:1522-1525.

Takahashi, K., K. Tanabe, M. Ohnuki, M. Narita, T. Ichisaka, K. Tomoda, and S. Yamanaka. 2007. Induction of pluripotent stem cells from adult human fibroblasts by defined factors. *Cell*. 131:861-872.

Takahashi, K., and S. Yamanaka. 2006. Induction of pluripotent stem cells from mouse embryonic and adult fibroblast cultures by defined factors. *Cell*. 126:663-676.

Tchieu, J., E. Kuoy, M.H. Chin, H. Trinh, M. Patterson, S.P. Sherman, O. Aimiuwu, A. Lindgren, S. Hakimian, J.A. Zack, A.T. Clark, A.D. Pyle, W.E. Lowry, and K. Plath. 2010. Female human iPSCs retain an inactive X chromosome. *Cell Stem Cell*. 7:329-342.

Tesar, P.J., J.G. Chenoweth, F.A. Brook, T.J. Davies, E.P. Evans, D.L. Mack, R.L. Gardner, and R.D. McKay. 2007. New cell lines from mouse epiblast share defining features with human embryonic stem cells. *Nature*. 448:196-199.

Thomson, J.A., J. Itskovitz-Eldor, S.S. Shapiro, M.A. Waknitz, J.J. Swiergiel, V.S. Marshall, and J.M. Jones. 1998. Embryonic stem cell lines derived from human blastocysts. *Science*. 282:1145-1147.

Towler, D.A., S.P. Adams, S.R. Eubanks, D.S. Towery, E. Jackson-Machelski, L. Glaser, and J.I. Gordon. 1987. Purification and characterization of yeast myristoyl CoA:protein N-myristoyltransferase. *Proc Natl Acad Sci U S A*. 84:2708-2712.

Toyooka, Y., D. Shimosato, K. Murakami, K. Takahashi, and H. Niwa. 2008. Identification and characterization of subpopulations in undifferentiated ES cell culture. *Development*. 135:909-918.

Tsai, M.C., O. Manor, Y. Wan, N. Mosammaparast, J.K. Wang, F. Lan, Y. Shi, E. Segal, and H.Y. Chang. 2010. Long noncoding RNA as modular scaffold of histone modification complexes. *Science*. 329:689-693.

Urlinger, S., U. Baron, M. Thellmann, M.T. Hasan, H. Bujard, and W. Hillen. 2000. Exploring the sequence space for tetracycline-dependent transcriptional activators: novel mutations yield expanded range and sensitivity. *Proc Natl Acad Sci U S A*. 97:7963-7968.

Urnov, F.D., E.J. Rebar, M.C. Holmes, H.S. Zhang, and P.D. Gregory. 2010. Genome editing with engineered zinc finger nucleases. *Nat Rev Genet*. 11:636-646.

van den Berg, D.L., T. Snoek, N.P. Mullin, A. Yates, K. Bezstarosti, J. Demmers, I. Chambers, and R.A. Poot. 2010. An Oct4-centered protein interaction network in embryonic stem cells. *Cell Stem Cell*. 6:369-381.

van Steensel, B., and T. de Lange. 1997. Control of telomere length by the human telomeric protein TRF1. *Nature*. 385:740-743.

Vanhaesebroeck, B., K. Ali, A. Bilancio, B. Geering, and L.C. Foukas. 2005. Signalling by PI3K isoforms: insights from gene-targeted mice. *Trends Biochem Sci*. 30:194-204.

Vanhaesebroeck, B., J. Guillermet-Guibert, M. Graupera, and B. Bilanges. 2010. The emerging mechanisms of isoform-specific PI3K signalling. *Nat Rev Mol Cell Biol*. 11:329-341.

Vanhaesebroeck, B., S.J. Leevers, K. Ahmadi, J. Timms, R. Katso, P.C. Driscoll, R. Woscholski, P.J. Parker, and M.D. Waterfield. 2001. Synthesis and function of 3-phosphorylated inositol lipids. *Annu Rev Biochem*. 70:535-602.

Vanhaesebroeck, B., S.J. Leevers, G. Panayotou, and M.D. Waterfield. 1997. Phosphoinositide 3-kinases: a conserved family of signal transducers. *Trends Biochem Sci*. 22:267-272.

Vanhaesebroeck, B., and M.D. Waterfield. 1999. Signaling by distinct classes of phosphoinositide 3-kinases. *Exp Cell Res*. 253:239-254.

Varela, E., R.P. Schneider, S. Ortega, and M.A. Blasco. 2011. Different telomere-length dynamics at the inner cell mass versus established embryonic stem (ES) cells. *Proc Natl Acad Sci U S A*. 108:15207-15212.

Villasante, A., D. Piazzolla, H. Li, G. Gomez-Lopez, M. Djabali, and M. Serrano. 2011. Epigenetic regulation of Nanog expression by Ezh2 in pluripotent stem cells. *Cell Cycle*. 10:1488-1498.

Vlahos, C.J., W.F. Matter, K.Y. Hui, and R.F. Brown. 1994. A specific inhibitor of phosphatidylinositol 3-kinase, 2-(4-morpholinyl)-8-phenyl-4H-1-benzopyran-4-one (LY294002). *J Biol Chem*. 269:5241-5248.

Vo, N., C. Fjeld, and R.H. Goodman. 2001. Acetylation of nuclear hormone receptor-interacting protein RIP140 regulates binding of the transcriptional corepressor CtBP. *Mol Cell Biol*. 21:6181-6188.

von Dassow, G., E. Meir, E.M. Munro, and G.M. Odell. 2000. The segment polarity network is a robust developmental module. *Nature*. 406:188-192.

von Zglinicki, T. 2000. Role of oxidative stress in telomere length regulation and replicative senescence. *Ann N Y Acad Sci*. 908:99-110.

Walker, E.H., M.E. Pacold, O. Perisic, L. Stephens, P.T. Hawkins, M.P. Wymann, and R.L. Williams. 2000. Structural determinants of phosphoinositide 3-kinase inhibition by wortmannin, LY294002, quercetin, myricetin, and staurosporine. *Mol Cell*. 6:909-919.

Wang, D., D. Manali, T. Wang, N. Bhat, N. Hong, Z. Li, L. Wang, Y. Yan, R. Liu, and Y. Hong. 2011. Identification of pluripotency genes in the fish medaka. *Int J Biol Sci*. 7:440-451.

Wang, J., S. Hevi, J.K. Kurash, H. Lei, F. Gay, J. Bajko, H. Su, W. Sun, H. Chang, G. Xu, F. Gaudet, E. Li, and T. Chen. 2009. The lysine demethylase LSD1 (KDM1) is required for maintenance of global DNA methylation. *Nat Genet*. 41:125-129.

Wang, J., D.N. Levasseur, and S.H. Orkin. 2008. Requirement of Nanog dimerization for stem cell self-renewal and pluripotency. *Proc Natl Acad Sci U S A*. 105:6326-6331.

Wang, J., S. Rao, J. Chu, X. Shen, D.N. Levasseur, T.W. Theunissen, and S.H. Orkin. 2006. A protein interaction network for pluripotency of embryonic stem cells. *Nature*. 444:364-368.

Wang, J., K. Scully, X. Zhu, L. Cai, J. Zhang, G.G. Prefontaine, A. Krones, K.A. Ohgi, P. Zhu, I. Garcia-Bassets, F. Liu, H. Taylor, J. Lozach, F.L. Jayes, K.S. Korach, C.K. Glass, X.D. Fu, and M.G. Rosenfeld. 2007a. Opposing LSD1 complexes function in developmental gene activation and repression programmes. *Nature*. 446:882-887.

Wang, L., Y. Zhang, H. Li, Z. Xu, R.M. Santella, and I.B. Weinstein. 2007b. Hint1 inhibits growth and activator protein-1 activity in human colon cancer cells. *Cancer Res*. 67:4700-4708.

Wang, Z.X., J.L. Kueh, C.H. Teh, M. Rossbach, L. Lim, P. Li, K.Y. Wong, T. Lufkin, P. Robson, and L.W. Stanton. 2007c. Zfp206 is a transcription factor that controls pluripotency of embryonic stem cells. *Stem Cells*. 25:2173-2182.

Ware, C.B., M.C. Horowitz, B.R. Renshaw, J.S. Hunt, D. Liggitt, S.A. Koblar, B.C. Gliniak, H.J. McKenna, T. Papayannopoulou, B. Thoma, and et al. 1995. Targeted disruption of the low-affinity leukemia inhibitory factor receptor gene causes placental, skeletal, neural and metabolic defects and results in perinatal death. *Development*. 121:1283-1299.

Watanabe, S., H. Umehara, K. Murayama, M. Okabe, T. Kimura, and T. Nakano. 2006. Activation of Akt signaling is sufficient to maintain pluripotency in mouse and primate embryonic stem cells. *Oncogene*. 25:2697-2707.

Watson, J.D. 1972. Origin of concatemeric T7 DNA. *Nat New Biol*. 239:197-201.

Welham, M.J., E. Kingham, Y. Sanchez-Ripoll, B. Kumpfmueller, M. Storm, and H. Bone. 2011. Controlling embryonic stem cell proliferation and pluripotency: the role of PI3K- and GSK-3-dependent signalling. *Biochem Soc Trans*. 39:674-678.

Welham, M.J., M.P. Storm, E. Kingham, and H.K. Bone. 2007. Phosphoinositide 3-kinases and regulation of embryonic stem cell fate. *Biochem Soc Trans*. 35:225-228.

Whang, Y.E., X. Wu, and C.L. Sawyers. 1998. Identification of a pseudogene that can masquerade as a mutant allele of the PTEN/MMAC1 tumor suppressor gene. *J Natl Cancer Inst*. 90:859-861.

White, J., E. Stead, R. Faast, S. Conn, P. Cartwright, and S. Dalton. 2005. Developmental activation of the Rb-E2F pathway and establishment of cell cycle-regulated cyclin-dependent kinase activity during embryonic stem cell differentiation. *Mol Biol Cell*. 16:2018-2027.

Wiesinger, D., H.U. Gubler, W. Haefliger, and D. Hauser. 1974. Antiinflammatory activity of the new mould metabolite 11-desacetoxy-wortmannin and of some of its derivatives. *Experientia*. 30:135-136.

Williams, A.J., L.M. Khachigian, T. Shows, and T. Collins. 1995. Isolation and characterization of a novel zinc-finger protein with transcription repressor activity. *J Biol Chem*. 270:22143-22152.

Williams, M.R., J.S. Arthur, A. Balendran, J. van der Kaay, V. Poli, P. Cohen, and D.R. Alessi. 2000. The role of 3-phosphoinositide-dependent protein kinase 1 in activating AGC kinases defined in embryonic stem cells. *Curr Biol*. 10:439-448.

Williams, R.L., D.J. Hilton, S. Pease, T.A. Willson, C.L. Stewart, D.P. Gearing, E.F. Wagner, D. Metcalf, N.A. Nicola, and N.M. Gough. 1988. Myeloid leukaemia inhibitory factor maintains the developmental potential of embryonic stem cells. *Nature*. 336:684-687.

Wilmut, I., A.E. Schnieke, J. McWhir, A.J. Kind, and K.H. Campbell. 1997. Viable offspring derived from fetal and adult mammalian cells. *Nature*. 385:810-813.

Wissmann, M., N. Yin, J.M. Muller, H. Greschik, B.D. Fodor, T. Jenuwein, C. Vogler, R. Schneider, T. Gunther, R. Buettner, E. Metzger, and R. Schule. 2007. Cooperative demethylation by JMJD2C and LSD1 promotes androgen receptor-dependent gene expression. *Nat Cell Biol*. 9:347-353.

Woltjen, K., I.P. Michael, P. Mohseni, R. Desai, M. Mileikovsky, R. Hamalainen, R. Cowling, W. Wang, P. Liu, M. Gertsenstein, K. Kaji, H.K. Sung, and A. Nagy. 2009. piggyBac transposition reprograms fibroblasts to induced pluripotent stem cells. *Nature*. 458:766-770.

Wolven, A., H. Okamura, Y. Rosenblatt, and M.D. Resh. 1997. Palmitoylation of p59fyn is reversible and sufficient for plasma membrane association. *Mol Biol Cell*. 8:1159-1173.

Woodgett, J.R. 2001. Judging a protein by more than its name: GSK-3. *Sci STKE*. 2001:re12.

Woodgett, J.R., and P. Cohen. 1984. Multisite phosphorylation of glycogen synthase. Molecular basis for the substrate specificity of glycogen synthase kinase-3 and casein kinase-II (glycogen synthase kinase-5). *Biochim Biophys Acta*. 788:339-347.

Wool, I.G., Y.L. Chan, and A. Gluck. 1995. Structure and evolution of mammalian ribosomal proteins. *Biochem Cell Biol*. 73:933-947.

Wray, J., T. Kalkan, S. Gomez-Lopez, D. Eckardt, A. Cook, R. Kemler, and A. Smith. 2011. Inhibition of glycogen synthase kinase-3 alleviates Tcf3 repression of the pluripotency network and increases embryonic stem cell resistance to differentiation. *Nat Cell Biol*. 13:838-845.

Wray, J., T. Kalkan, and A.G. Smith. 2010. The ground state of pluripotency. *Biochem Soc Trans*. 38:1027-1032.

Wu, D., and W. Pan. 2010. GSK3: a multifaceted kinase in Wnt signaling. *Trends Biochem Sci*. 35:161-168.

Wymann, M.P., G. Bulgarelli-Leva, M.J. Zvelebil, L. Pirola, B. Vanhaesebroeck, M.D. Waterfield, and G. Panayotou. 1996. Wortmannin inactivates phosphoinositide 3-

kinase by covalent modification of Lys-802, a residue involved in the phosphate transfer reaction. *Mol Cell Biol*. 16:1722-1733.

Wymann, M.P., and L. Pirola. 1998. Structure and function of phosphoinositide 3-kinases. *Biochim Biophys Acta*. 1436:127-150.

Xu, X.Y., Z. Zhang, W.H. Su, Y. Zhang, C. Feng, H.M. Zhao, Z.H. Zong, C. Cui, and B.Z. Yu. 2009. Involvement of the p110 alpha isoform of PI3K in early development of mouse embryos. *Mol Reprod Dev*. 76:389-398.

Yamaguchi, S., H. Kimura, M. Tada, N. Nakatsuji, and T. Tada. 2005. Nanog expression in mouse germ cell development. *Gene Expr Patterns*. 5:639-646.

Yart, A., S. Roche, R. Wetzker, M. Laffargue, N. Tonks, P. Mayeux, H. Chap, and P. Raynal. 2002. A function for phosphoinositide 3-kinase beta lipid products in coupling beta gamma to Ras activation in response to lysophosphatidic acid. *J Biol Chem*. 277:21167-21178.

Yin, D.X., L. Zhu, and R.T. Schimke. 1996. Tetracycline-controlled gene expression system achieves high-level and quantitative control of gene expression. *Anal Biochem*. 235:195-201.

Ying, Q.L., J. Nichols, I. Chambers, and A. Smith. 2003. BMP induction of Id proteins suppresses differentiation and sustains embryonic stem cell self-renewal in collaboration with STAT3. *Cell*. 115:281-292.

Ying, Q.L., J. Wray, J. Nichols, L. Batlle-Morera, B. Doble, J. Woodgett, P. Cohen, and A. Smith. 2008. The ground state of embryonic stem cell self-renewal. *Nature*. 453:519-523.

Yoshida, K., I. Chambers, J. Nichols, A. Smith, M. Saito, K. Yasukawa, M. Shoyab, T. Taga, and T. Kishimoto. 1994. Maintenance of the pluripotential phenotype of embryonic stem cells through direct activation of gp130 signalling pathways. *Mech Dev*. 45:163-171.

Yoshida, K., T. Taga, M. Saito, S. Suematsu, A. Kumanogoh, T. Tanaka, H. Fujiwara, M. Hirata, T. Yamagami, T. Nakahata, T. Hirabayashi, Y. Yoneda, K. Tanaka, W.Z. Wang, C. Mori, K. Shiota, N. Yoshida, and T. Kishimoto. 1996. Targeted disruption of gp130, a common signal transducer for the interleukin 6 family of cytokines, leads to myocardial and hematological disorders. *Proc Natl Acad Sci U S A*. 93:407-411.

Yoshikawa, T., Y. Piao, J. Zhong, R. Matoba, M.G. Carter, Y. Wang, I. Goldberg, and M.S. Ko. 2006. High-throughput screen for genes predominantly expressed in the ICM of mouse blastocysts by whole mount in situ hybridization. *Gene Expr Patterns*. 6:213-224.

Yu, H.B., G. Kunarso, F.H. Hong, and L.W. Stanton. 2009a. Zfp206, Oct4, and Sox2 are integrated components of a transcriptional regulatory network in embryonic stem cells. *J Biol Chem*. 284:31327-31335.

Yu, J., K. Hu, K. Smuga-Otto, S. Tian, R. Stewart, Slukvin, II, and J.A. Thomson. 2009b. Human induced pluripotent stem cells free of vector and transgene sequences. *Science*. 324:797-801.

Yu, J., M.A. Vodyanik, K. Smuga-Otto, J. Antosiewicz-Bourget, J.L. Frane, S. Tian, J. Nie, G.A. Jonsdottir, V. Ruotti, R. Stewart, Slukvin, II, and J.A. Thomson. 2007. Induced pluripotent stem cell lines derived from human somatic cells. *Science*. 318:1917-1920.

Zalzman, M., G. Falco, L.V. Sharova, A. Nishiyama, M. Thomas, S.L. Lee, C.A. Stagg, H.G. Hoang, H.T. Yang, F.E. Indig, R.P. Wersto, and M.S. Ko. 2010. Zscan4 regulates telomere elongation and genomic stability in ES cells. *Nature*. 464:858-863.

Zenklusen, D., P. Vinciguerra, J.C. Wyss, and F. Stutz. 2002. Stable mRNP formation and export require cotranscriptional recruitment of the mRNA export factors Yra1p and Sub2p by Hpr1p. *Mol Cell Biol*. 22:8241-8253.

Zhang, Q., A. Nottke, and R.H. Goodman. 2005. Homeodomain-interacting protein kinase-2 mediates CtBP phosphorylation and degradation in UV-triggered apoptosis. *Proc Natl Acad Sci U S A*. 102:2802-2807.

Zhang, Q., D.W. Piston, and R.H. Goodman. 2002. Regulation of corepressor function by nuclear NADH. *Science*. 295:1895-1897.

Zhang, Q., S.Y. Wang, A.C. Nottke, J.V. Rocheleau, D.W. Piston, and R.H. Goodman. 2006a. Redox sensor CtBP mediates hypoxia-induced tumor cell migration. *Proc Natl Acad Sci U S A*. 103:9029-9033.

Zhang, W., E. Walker, O.J. Tamplin, J. Rossant, W.L. Stanford, and T.R. Hughes. 2006b. Zfp206 regulates ES cell gene expression and differentiation. *Nucleic Acids Res*. 34:4780-4790.

Zhang, Z., A. Jones, C.-W. Sun, C. Li, C.-W. Chang, H.-Y. Joo, Q. Dai, M.R. Mysliwiec, L.-C. Wu, Y. Guo, W. Yang, K. Liu, K.M. Pawlik, H. Erdjument-Bromage, P. Tempst, Y. Lee, J. Min, T.M. Townes, and H. Wang. 2011. PRC2 Complexes with JARID2, MTF2, and esPRC2p48 in ES Cells to Modulate ES Cell Pluripotency and Somatic Cell Reprograming. *Stem Cells*. 29:229-240.

Zhao, J.J., Z. Liu, L. Wang, E. Shin, M.F. Loda, and T.M. Roberts. 2005. The oncogenic properties of mutant p110alpha and p110beta phosphatidylinositol 3-kinases in human mammary epithelial cells. *Proc Natl Acad Sci U S A*. 102:18443-18448.

Zhao, X.Y., W. Li, Z. Lv, L. Liu, M. Tong, T. Hai, J. Hao, C.L. Guo, Q.W. Ma, L. Wang, F. Zeng, and Q. Zhou. 2009. iPS cells produce viable mice through tetraploid complementation. *Nature*. 461:86-90.

Zhou, H., S. Wu, J.Y. Joo, S. Zhu, D.W. Han, T. Lin, S. Trauger, G. Bien, S. Yao, Y. Zhu, G. Siuzdak, H.R. Scholer, L. Duan, and S. Ding. 2009. Generation of induced pluripotent stem cells using recombinant proteins. *Cell Stem Cell*. 4:381-384.

Zwaka, T.P., and J.A. Thomson. 2005. A germ cell origin of embryonic stem cells? *Development*. 132:227-233.